

ACIS-I observations of NGC 2264. Membership and X-ray properties of PMS stars[★]

E. Flaccomio, G. Micela, and S. Sciortino

INAF - Osservatorio Astronomico di Palermo Giuseppe S. Vaiana, Palazzo dei Normanni, 90134 Palermo, Italy
e-mail: [ettoref;giusi;sciorti]@astropa.inaf.it

Received 24 February 2006 / Accepted 5 April 2006

ABSTRACT

Aims. This paper's goal is to improve the member census of the NGC 2264 star-forming region and study the origin of X-ray activity in young PMS stars.

Methods. We analyze a deep, 100 ks long, Chandra ACIS observation covering a $17' \times 17'$ field in NGC 2264. The preferential detection in X-rays of low-mass PMS stars gives strong indications of their membership. We study X-ray activity as a function of stellar and circumstellar characteristics by correlating the X-ray luminosities, temperatures, and absorptions with optical and near-infrared data from the literature.

Results. We detect 420 X-ray point sources. Optical and NIR counterparts are found in the literature for 85% of the sources. We argue that more than 90% of these counterparts are NGC 2264 members, thereby significantly increasing the known low-mass cluster population by about 100 objects. Among the sources without counterpart, about 50% are probably associated with members, several of which we expect to be previously unknown protostellar objects. With regard to activity we confirm several previous findings: X-ray luminosity is related to stellar mass, although with a large scatter; L_X/L_{bol} is close to, but almost invariably below, the saturation level, 10^{-3} , especially when considering the *quiescent* X-ray emission. A comparison between CTTS and WTTS shows several differences: CTTS have, at any given mass, activity levels that are both lower and more scattered than WTTS; emission from CTTS may also be more time variable and is on average slightly harder than for WTTS. However, we find evidence in some CTTS of extremely cool, ~ 0.1 – 0.2 keV, plasma which we speculate is heated by accretion shocks.

Conclusions. Activity in low-mass PMS stars, while generally similar to that of saturated MS stars, may be significantly affected by mass accretion in several ways: accretion is probably responsible for very soft X-ray emission directly produced in the accretion shock; it may reduce the average energy output of solar-like coronae, at the same time making them hotter and more dynamic. We briefly speculate on a physical scenario that can explain these observations.

Key words. stars: activity – stars: coronae – stars: pre-main sequence – open clusters and associations: individual: NGC 2264 – X-rays: stars

1. Introduction

The collapse of molecular cores and the early evolution of pre-main sequence (PMS) stars+disk systems involve a variety of complex phenomena leading to the formation of main sequence (MS) stars and planetary systems. Most of these phenomena, and their influence on the outcome of the formation process, are not yet fully understood.

The X-ray observations of star-forming regions have proved an invaluable tool for star formation studies. On one hand, because of the much higher luminosity of PMS stars in the X-ray band with respect to older field stars, deep imaging observations are one of the few effective means of selecting unbiased samples of members comprising both classical T-Tauri stars (CTTS) and, most importantly, the otherwise hard to distinguish weak-line T-Tauri stars (WTTS). Selection of a complete member sample is of paramount importance for any star formation study, such as those focused on the initial mass function (Salpeter 1955), the star formation history (e.g. Palla & Stahler 2000), the evolution of circumstellar disks and planetary systems (e.g. Haisch et al. 2005), and binarity (e.g. Lada 2006). On the other hand, the conspicuous X-ray activity of PMS stars is one of the aspects of

the PMS stellar evolution that are not yet well understood, both with respect to its physical origin and to its consequences for the stellar/planetary formation process. Indeed, the ionization and heating caused by the penetrating X-ray emission might have a significant impact on the evolution of star/disk systems (Igea & Glassgold 1999; Glassgold et al. 2004), as well as on that of the star forming cloud as a whole (Lorenzani & Palla 2001).

The high X-ray activity levels of PMS stars (e.g. Preibisch et al. 2005) have often been attributed to a “scaled up” solar-like corona formed by active regions. This is the same picture proposed for MS stars, for which the X-ray activity is related to the stellar rotation (e.g. Pizzolato et al. 2003), evidence that a stellar dynamo is responsible for the creation and heating of coronae. For most non-accreting PMS stars (WTTS), the fractional X-ray luminosity, L_X/L_{bol} , is indeed close to the saturation level, 10^{-3} , seen on rapidly rotating MS stars (Flaccomio et al. 2003b; Preibisch et al. 2005; Pizzolato et al. 2003). This might suggest a common physical mechanism for the emission of X-rays in WTTS and MS stars or, at least, for its saturation. However, the analogy with the Sun and MS stars may not be fully valid, because: i) the relation between activity and rotation is not observed in the PMS (Preibisch et al. 2005; Rebull et al. 2006); ii) with respect to the Sun at the *maximum* of its activity cycle, saturated WTTS have $L_X/L_{bol} \sim 1000$ times greater and plasma temperatures that are also significantly higher.

[★] Tables 1, 3, 4 and 6 are only available in electronic form at <http://www.edpsciences.org>

The X-ray emission of CTTS, PMS stars that are still undergoing mass accretion, is even more puzzling. With their circumstellar disks and magnetically regulated matter inflows and outflows, CTTS are complex systems. With respect to their X-ray activity, the bulk of the observational evidence points toward phenomena similar to those occurring on WTTS. However, CTTS have significantly lower and unsaturated values of L_X and L_X/L_{bol} (Damiani & Micela 1995; Flaccomio et al. 2003a,b; Preibisch et al. 2005). In apparent contradiction to this latter result, high-resolution X-ray spectra of two observed CTTS, TW Hydrae (Kastner et al. 2002; Stelzer & Schmitt 2004) and BP Tau (Schmitt et al. 2005), have indicated that soft X-rays may also be produced in accretion shocks at the base of magnetic funnels. Moreover, magnetic loops connecting the stellar surface with the inner parts of a circumstellar disk may produce some of the strongest and longer-lasting flares observed on PMS stars (Favata et al. 2005). The recent detection of X-ray rotational modulation (Flaccomio et al. 2005), however, implies that emitting structures are generally compact, so that these long loops cannot dominate the quiescent X-ray emission.

NGC 2264 is a ~ 3 Myr-old star-forming region located at ~ 760 pc (Sung et al. 1997) in the Monoceros. Compared to the Orion Nebula Cluster (ONC) and Taurus, NGC 2264 has intermediate stellar density and total population, making it an interesting target for investigating the dependence of star formation on the environment. It is on average older than the ONC (~ 1 Myr), but star formation is still active inside the molecular cloud in at least two sites where a number of protostars and prestellar clumps have been detected (Young et al. 2006; Peretto et al. 2006). It is therefore a useful target for the study of the formation and time evolution of young stars. Its study is eased by the presence of an optically thick background cloud, effectively obscuring unrelated background objects, and by the low and uniform extinction of the foreground population (Walker 1956; Rebull et al. 2002). Despite being the first star forming region ever identified as such, the low-mass population of NGC 2264 is still not well characterized: proper motion studies (Vasilevskis et al. 1965) have been restricted to high mass objects; several studies have identified the CTTS population using disk and accretion indicators (Park et al. 2000; Rebull et al. 2002; Lamm et al. 2004), but have missed WTTS; past X-ray observations with *ROSAT* (Flaccomio et al. 2000) have been useful in identifying the WTTS population, but have not been sensitive enough to detect low-mass ($M \leq 0.3 M_\odot$) and embedded stars. We present here results from the analysis of a deep *Chandra* observation of the region. Another similar observation of a region just to the north of the one considered here has been analyzed by Ramírez et al. (2004a). The X-ray properties of NGC 2264 members derived in the present paper and by Ramírez et al. (2004a), augmented with similar data for the Orion Flaking Fields (Ramírez et al. 2004b) are studied by Rebull et al. (2006) in comparison with the results of the COUP survey (Getman et al. 2005). Results from the same *Chandra* observation analyzed here on the peculiar binary system KH 15D have been presented by Herbst & Moran (2005). Finally, the properties of three embedded X-ray sources near Allen's source, observed with *XMM-Newton*, have been recently presented by Simon & Dahm (2005).

The paper is organized as follows. We begin (Sect. 2) with the presentation of the X-ray data, its reduction, source detection, and photon extraction. In Sect. 3 we then introduce the optical and near infrared data used to complement the X-ray observation. In Sect. 4 we present the temporal and spectral analysis of X-ray sources and derive X-ray luminosities. Sections 5 and 6



Fig. 1. Digitized Sky Survey image of NGC 2264. The field of view of the *Chandra*-ACIS observation discussed in this paper is shown as a white square. The famous Cone Nebula is visible toward the bottom of the image and the O7 star S Mon is close to the upper edge.

then discuss our results with respect to cluster membership and the origin of X-ray activity on PMS stars. We finally summarize and draw our conclusions in Sect. 7.

2. X-ray data and preparatory analysis

We obtained a 97 ks long ACIS-I exposure of NGC 2264 on 28 Oct. 2002 (Obs. Id. 2540; GO proposal PI S. Sciortino). The $17' \times 17'$ field of view (FOV) of ACIS is shown in Fig. 1, superimposed on the Digitized Sky Survey image of the region. It was centered on RA $6^h40^m58\rlap{.}^s7$, Dec $9^\circ34'14''$ (roll angle: 79°). Figure 2 shows a color rendition of the spatial and spectral information we obtained. ACIS was operated in FAINT mode with CCD 0, 1, 2, 3, 6, and 7 turned on. Data obtained with CCD 6 and 7, part of the ACIS-S array, will not be discussed in the following because of the very degraded point-spread function (PSF) and effective area resulting from their large distance from the optical axis.

2.1. Data preparation

Data reduction, starting from the level 1 event file, was performed in a standard fashion, using the CIAO 2.3 package and following the threads provided by the *Chandra X-ray Center*¹. Several IDL custom programs were also employed. First, we corrected the degradation in the spectral response due to the charge transfer inefficiency (CTI), which occurred in particular during the first months of the *Chandra* mission, using the ACIS_PROCESS_EVENTS CIAO task. We then produced a level 2 event file by retaining only events with grade = 0, 2, 3, 4, 6 and status = 0. Finally we corrected the data for the time dependence of the energy gain using the CORR_TGAIN utility.

The X-ray stellar sources have, on average, a different spectrum with respect to the ACIS background. The total signal-to-noise ratio (SNR) of sources can therefore be maximized by filtering out events with energy outside a suitable spectral

¹ See cxc.harvard.edu

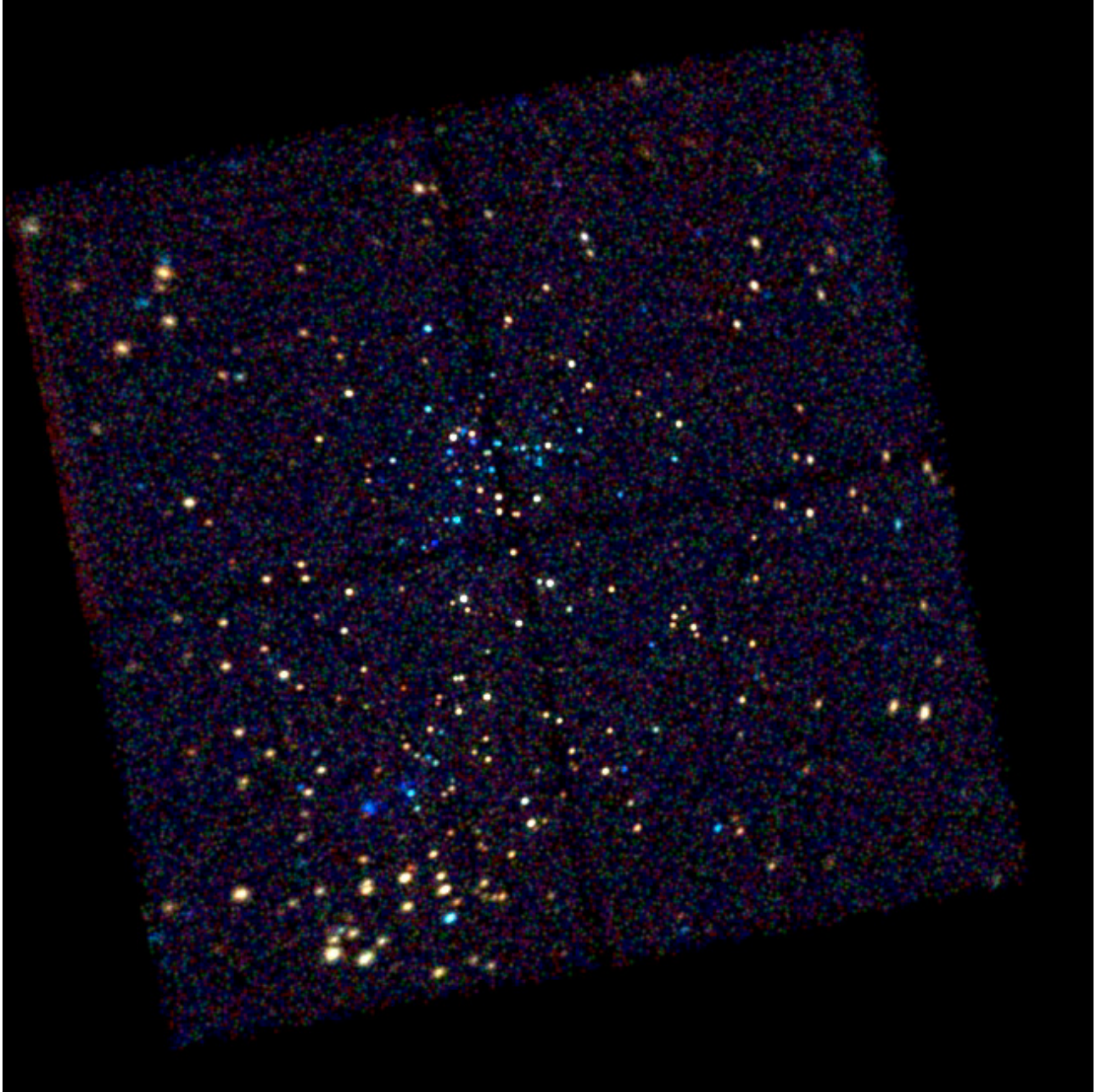


Fig. 2. NGC 2264 as seen in X-rays by ACIS. The true color (RGB) image is constructed from images in three energy bands: [200:1150] eV (red), [1150:1900] (green), and [1900:7000] (blue). Red therefore indicates soft and unabsorbed sources, blue hard and/or absorbed sources.

band: we first performed a preliminary source detection as discussed in Sect. 2.2 on the whole event list. We then defined a radius, R_{97} , for each source such that 97% of the PSF counts fall within this radius (Sect. 2.3). We extracted source photons for all sources from circles with $R = 0.5 \times R_{97}$ and background photons from a single background region that excludes photons from all sources within their respective R_{97} (a sort of “Swiss cheese” image with the sources carved out). We then computed the total SNR of sources² for a fine grid of minimum and maximum energy cuts. The highest source SNR was obtained for

$E_{\min} = 200$ eV and $E_{\max} = 7000$ eV. With these cuts, the number of photons in the source extraction area (including background photons) is reduced to 96% of the total, while the background is reduced to 28% of the total. We checked that consistent results are obtained by maximizing the SNR of faint sources only (<20 net counts), which may have a different average spectrum and are the ones we are most interested in for the purpose of detection.

After filtering in energy, the time-integrated background is 0.07 counts per arcsec², consistent with nominal values. The background was constant in time except for a small flare with a peak reaching about twice the quiescent rate. The flare starts 13 ks after the beginning of the observation and lasts ~ 1 ks. The effect of the background flare on source light curves is negligible however, even for faint sources, i.e. those most affected by the background. This is confirmed by the negative results of

² $SNR_{\text{tot}} = \sum (S^i - \alpha_i B) / \sqrt{\sum (S^i + \alpha_i B)}$ where $\alpha_i = A_s^i / A_b$; S_i and A_s^i are the number of counts in the i th source region and its area, respectively. B and A_b are the background counts and relative extraction area, respectively. The background was taken for the present purpose as uniform within the FOV.

Kolmogorov-Smirnov variability tests (see Sect. 4.1) performed on the background extraction regions relative to each source. In the study of source lightcurves (Sect. 4.1), we will therefore assume a constant background.

2.2. Source detection

We detected sources using the PWDetect code (Damiani et al. 1997)³. The significance threshold was set to 4.6σ . According to extensive simulations of source-free fields with the background level of our observation, this threshold corresponds to an expectancy of 10 spurious sources in the whole FOV. PWDetect reports 423 sources. Upon careful inspection we removed three entries relative to sources that were detected twice, leaving a total of 420 distinct sources. Twenty eight of these are below the 5.0σ significance threshold, corresponding to the more conservative criteria of one expected spurious source in the FOV. Background-subtracted source counts in the 0.2–7 keV band are derived by PWDetect directly from the wavelet transform of the data. Effective exposure times at the source positions, averaged over the PSF, are also computed by PWDetect from an exposure map created with standard CIAO tools assuming an input energy of 2.0 keV⁴. Detected sources are listed in Table 1. In the first eight columns we report source number, sky positions with uncertainty, distance from the *Chandra* optical axis, source net counts (in the 0.2–7 keV band), effective exposure time, and the statistical significance of the detection.

2.3. Photon extraction

Source and background photon extraction for spectral and timing analysis was performed using CIAO and custom IDL software. We first determined the expected PSF for each source using the CIAO MKPSF tool, assuming a monochromatic source spectrum ($E = 1.5$ keV). We thus determined the expected encircled energy fraction as a function of distance from the source. Photons' extraction circles were defined so as to contain 90% of the PSF, save for 28 sources for which the encircled PSF fractions were reduced to values ranging from 74% to 89% to avoid overlap with neighboring sources. The local background for each source was determined from annuli whose inner radii exclude 97% of the PSF and whose outer radii are twice as large. In order to eliminate contamination of the background regions due to the emission of neighboring sources, we excluded from these annuli all the intersections with the 97% encircled counts circles of other sources. The area of background extraction regions were computed through a mask in which we *drilled* regions outside the detector boundaries and circles containing 97% of the PSF photons from all sources.

For sources with at least 50 photons, source and background spectra suited to the XSPEC spectral fitting package were then created using standard CIAO tools. Corresponding response matrices and effective areas (RMF and ARF files, respectively) were also produced with CIAO. For spectral analysis, spectra were energy binned so that each bin contains a fixed number of photons, depending on net source counts N_{src} : 15 photons per bin for $N_{\text{src}} > 200$, 10 photons for $100 < N_{\text{src}} < 200$, and

5 photons for $N_{\text{src}} < 100$. Because spectral analysis (Sect. 4.2) was restricted to energies >0.5 keV, the first energy bin was forced to begin at that energy.

3. Ancillary data

In this section we discuss the non-X-ray data that we collected from the literature on the known objects in the FOV of our ACIS observation, and in particular on the detected X-ray sources. We first describe the cross-identifications with spatially complete optical, NIR, and X-ray catalogs (Sect. 3.1) and the informations we collected and/or derived from these catalogs (Sect. 3.2). We then briefly discuss the identifications of our X-ray sources with spatially incomplete mid-IR and millimeter catalogs (Sect. 3.3).

3.1. Cross-identifications – optical/NIR/X-ray catalogs

We cross-identified our X-ray source list with catalogs from the following optical/NIR surveys covering the whole area of our ACIS field: 2Mass (NIR photometry), Walker (1956, optical photometry + spectroscopy), Rebull et al. (2002, optical/NIR photometry + low resolution optical spectroscopy)⁵, Lamm et al. (2004, optical photometry + variability), Dahm & Simon (2005, optical photometry + spectroscopy), Flaccomio et al. (2000, X-ray sources). The seven cross-identified catalogs are listed in the first column of Table 2. In the 2nd column, we indicate the number of objects within the ACIS FOV and, in the third, the number of objects identified with ACIS sources and of those for which the identification is unique. Adopted positional tolerances for cross-identifications are reported in the 4th column, either as a single figure for the whole catalog or as a range when defined for each individual object (see the table footnotes). They are based on the uncertainties quoted for each catalog.

Among the catalogs considered here, the deepest photometric surveys are 2Mass in the NIR (JHK_s)⁶ and Lamm et al. (2004) in the optical (VR_cI_c). A comparison with the isochrones of Siess et al. (2000, hereafter SDF) in the optical and NIR color-magnitude diagrams (Figs. 3 and 4) indicates that at the distance of NGC 2264, 2Mass reaches down to about $0.1 M_\odot$ for 10 Myr old stars, i.e. the oldest expected in the region, while Lamm et al. (2004) reaches slightly deeper for unabsorbed stars, but is obviously less sensitive to highly absorbed ones. Within the ACIS FOV, spectral types are given for 7 stars by Walker (1956), for 87 stars by Rebull et al. (2002), for 150 stars by Lamm et al. (2004), and for 157 stars by Dahm & Simon (2005).

We created a master list of cross-identified objects following a step-by-step procedure. In the first step we matched ACIS sources with 2Mass objects: first we registered the ACIS coordinates to the 2Mass ones by iteratively cross-identifying the two catalogs and shifting the ACIS coordinates by the mean offset of uniquely identified source pairs. Identification radii were chosen as the quadrature sum of the position tolerances defined above (Table 2). We then created a joint catalog of objects containing all matched and unmatched ACIS and 2Mass objects, assigning them coordinates from 2MASS when available. In the following step we repeated the above process using the ACIS+2Mass catalog as reference and matching it with the Rebull et al. (2002) one. We then repeated the process with the Flaccomio et al. (2000),

³ Available at:

http://www.astropa.unipa.it/progetti_ricerca/PWDetect

⁴ The choice of energy is not crucial: the ratio between the effective area at the source position and on the optical axis, which is the quantity we use to define the effective exposure time, has only a small dependence on energy.

⁵ The Rebull et al. (2002), catalog was updated following private communication from L. Rebull.

⁶ Note that in the following we neglect the small differences among NIR photometric systems and, in particular, that between the 2MASS K_s and the standard K bands.

Table 2. Catalogs used for cross-identification

Catalog	N_{obj}	$N_{\text{det}}/N_{\text{unique}}$	Id.Rad. ["]	ΔRA ["]	ΔDec ["]	$\text{Off}_{50\%}$ ["]
ACIS	420		1.0–12.6 ^a	-0.09	-0.09	0.24
2Mass	1098	346/344	0.5–1.4 ^b	0.00	0.00	–
Walker (1956)	67	52/52	1.0	-0.45	0.08	0.47
Rebull et al. (2002)	511	236/235	1.5	0.73	-0.03	0.73
Lamm et al. (2004)	1598	305/299	1.0	-0.13	0.45	0.47
Dahm & Simon (2005)	229	183/183	1.0	-0.16	0.18	0.36
Flaccomio et al. (2000)	84	80/80	8.1–42.8 ^c	-0.85	1.49	3.70

^a $\max[2\sigma_{rd}, 1"]$. Mean/median: 1.74"/1.25".

^b $\max[2(\sigma_{\text{RA}}^2 + \sigma_{\text{Dec}}^2)^{1/2}, 0.5"]$. Mean/median: 0.54"/0.50".

^c 85% point source encircled energy radii (Flaccomio et al. 2000). Mean/median: 12.0"/9.2".

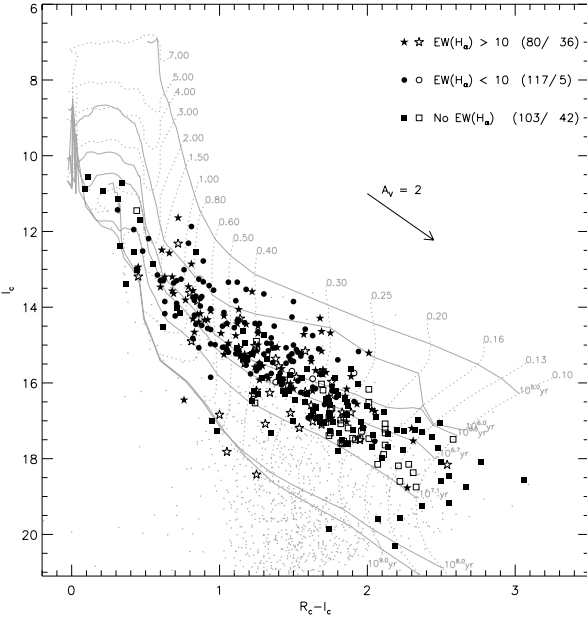


Fig. 3. Optical color-magnitude diagram of all the objects in the ACIS field of view. Larger symbols indicate X-ray sources or likely NGC 2264 members as defined in Sect. 3.2. Filled symbols refer to ACIS detected objects. As indicated in the legend, when possible we distinguish between CTTS and WTTS as defined by the EW of their H_{α} line. The number of detected and undetected objects in each class is indicated in the legend. The grid shows the SDF evolutionary tracks and isochrones transformed to colors and magnitudes using the conversion table in Kenyon & Hartmann (1995).

X-ray source list, then with the Lamm et al. (2004), Dahm & Simon (2005), and Walker (1956) catalogs. The coordinate shifts of all catalogs with respect to the 2Mass system are given in Table 2 (Cols. 5 and 6), along with the median offsets between object positions and the reference 2Mass catalog. After each step, identified source pairs and unidentified objects were checked individually and a small fraction of the identifications (<1%) were modified. In the first step, for example, five identifications between four ACIS and five 2Mass sources were added: in two cases (sources #64 and #404), 2Mass sources were only slightly more distant with respect to the identification radii. In another case, the X-ray source, #102, was situated at the edge of the detector, and its position was therefore more uncertain than the formal error indicated. In the last case the X-ray source, #237, was detected between two nearby 2Mass objects and an identification was forced with both.

Table 3 lists, for the 1888 distinct objects in the ACIS FOV, consolidated coordinates and cross-identifications numbers for

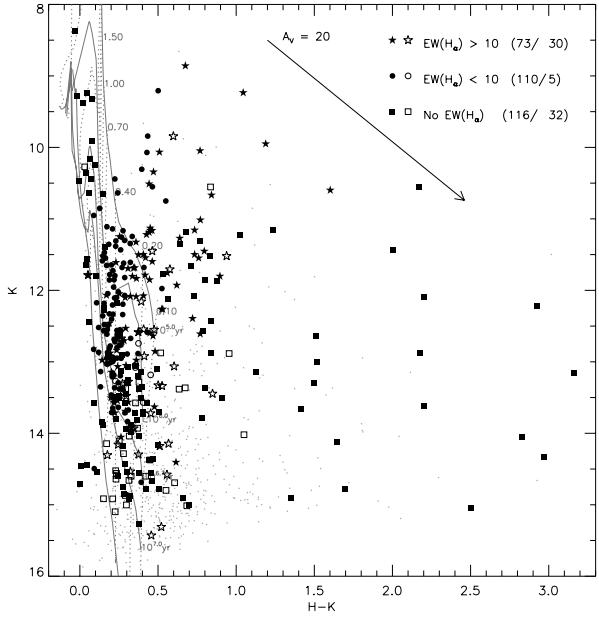


Fig. 4. Near-IR color magnitude diagram for the objects in the ACIS FOV. Symbols and tracks as in Fig. 3.

each of the seven catalogs. 425 rows refer to objects related to one of the 420 ACIS sources: 351 are identified with a single optical/NIR counterpart, two are identified with 5 and 2 counterparts respectively, and 67 do not have any optical or near-infrared identification. The other 1463 rows in Table 3 refer to non ACIS-detected objects. For these latter we computed upper limits to the ACIS count rate using PW Detect and the same event file used for source detection. Measured count rates, repeated from Table 1, and upper limits are reported in Col. 12 of Table 3.

Focusing on the identification of ACIS sources with optical/NIR catalogs, given the relatively large number objects in the field of view, we can wonder how many of the identifications are due to chance alignment and not to a true physical association. We can constrain the number of chance identifications by assuming that positions in the two lists are fully uncorrelated. Because this is definitively not the case for our full X-ray source catalog, our estimate can only be considered a loose upper limit. Furthermore, limiting our X-ray sample to the 28 sources with significance below 5.0σ , 9 of which are expected to be spurious and whose positions will indeed be random, we can place an upper limit on the fraction of spurious sources associated with an optical object. This value is of interest when studying the X-ray

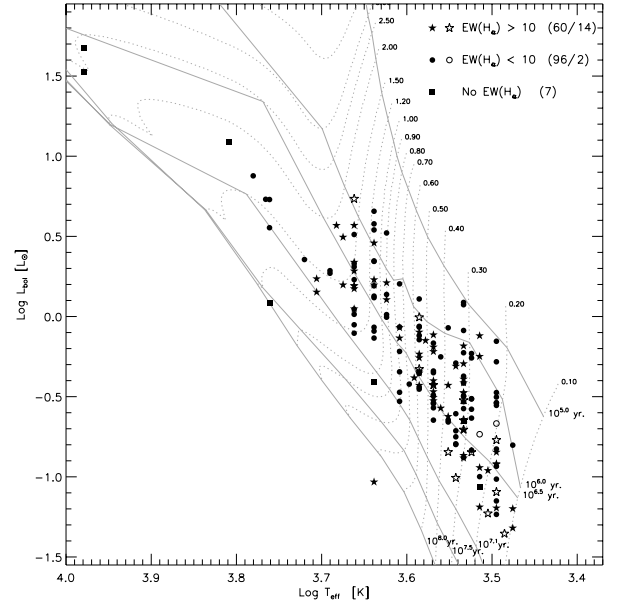
properties of optically/NIR selected samples. In order to estimate the number of spurious identifications assuming uncorrelated positions, we proceeded as follows: for each X-ray source we considered optical objects within a circular neighborhood of area A_{nei} , within which source density is assumed uniform. We then estimated the fraction of A_{nei} covered by identification circles. The sum of these fractions is our upper limit to the number of chance identifications. We repeated the calculation for radii of the neighborhood circle from $1.0'$ to $4.0'$. The upper limit to the number of chance identifications for the full sample of ACIS sources ranges from 13 to 15. For the 28 source with significance $<5.0\sigma$, we instead estimated no more than 2.5 chance identifications. If we assume that, out of the 28 sources, only the nine spurious detections have positions that are indeed uncorrelated with optical objects, we can scale this result and conclude that ~ 1 spurious X-ray source will be identified by chance with an optical object. Conversely, we can most likely locate spurious sources among the 15 sources whose detection significance is below 5.0σ and that are not identified with optical/NIR catalogs.

3.2. Characterization of stars in the FOV

We collected optical and NIR data from the literature for all the stars in the master catalog assembled in the previous section. In Table 4 we report photometry and spectral types for our X-ray sources with unique optical identification. A total of 300 X-ray detected stars were assigned both R_c and I_c magnitudes and are plotted in Fig. 3 as filled symbols; 299 have H and K magnitudes and are plotted in Fig. 4 (264 of these also appear in Fig. 3). In both color-magnitude diagrams (CMDs), we also show SDF tracks and isochrones for reference, transformed to colors and magnitudes using the conversion table given by Kenyon & Hartmann (1995) and shifted along the reddening vectors by the median extinction of known members ($A_V = 0.44$) and vertically by the distance modulus corresponding to the adopted distance. The extinction law was adopted from Rieke & Lebofsky (1985). For stars with spectral types, we derived effective temperatures, T_{eff} , bolometric corrections, BC_I , and intrinsic colors, $(R - I)$, using the relations compiled by Kenyon & Hartmann (1995) and, for the temperatures of M stars, the intermediate-gravity scale of Luhman (1999). Using the available R_c and I_c photometry, we then derived extinction values ($A_V = 4.46 \times E(R - I)$, where $E(R - I) = (R - I)_0 - (R - I)$) and bolometric luminosities ($L_{\text{bol}} = -0.4 \times [I_c - BC_I - A_V/1.63 - DM(760 \text{ pc})]$). Finally we estimated masses and ages from the theoretical HR diagram, Fig. 5, through interpolation of the SDF evolutionary tracks. In summary, out of the 351 X-ray sources with a unique optical/NIR identification, we estimated T_{eff} for 165 X-ray sources, A_V and L_{bol} for 163, masses and ages for 161.

Other than the sample of X-ray detected stars, that are likely cluster members, as discussed in Sect. 5, we also consider another sample of 83 X-ray undetected likely cluster members. These, plotted with empty symbols in Figs. 3–5, were chosen according to their position in the I vs. $R - I$ diagram, the strength of the H_α line (measured either spectroscopically or photometrically) and optical variability: first, we defined a *cluster locus* in the I vs. $R - I$ diagram using the SDF tracks and the observed concentration of X-ray sources. The cluster locus was defined as the area either above the $10^{7.1}$ Myr isochrone or to the left of the $0.8 M_\odot$ evolutionary track⁷. We then considered the following as

⁷ This latter condition was required by the convergence of the isochrones at higher masses and by the observed spread of stars in the “cluster locus”, at least in part due to uncertainties.



surveys target very young and/or embedded objects and are therefore ideal for checking the nature of X-ray sources with no optical/NIR counterpart. They are, however, limited in area coverage: T06 lists Class I/0 sources detected with *SPITZER* in a $\sim 3 \times 3$ arcmin 2 region close to IRS 2, Y06 lists all *SPITZER* detected objects in a dense but even smaller $\sim 2 \times 2$ arcmin 2 region slightly south-east of IRS 2, P06 list the pre/protostellar cores detected at 1.2 mm in both the IRS 1 and IRS 2 regions.

Within the area of Y06, the only MIR work available so far that lists all the objects detected in the surveyed region, we find MIR counterparts for 2 out of 4 X-ray sources lacking optical/NIR counterparts. In total, 4 of the 67 unidentified X-ray sources were assigned new counterparts: #145 was associated with source 12 of T06, a Class I/0 source; #228 was associated with the D-MM 15 mm core, indicated by P06 as probably starless; #244 was associated with source 43 in Y06 and is, judging from its spectral energy distribution (SED), an absorbed class II/III PMS star that is relatively bright in *K*-band ($K = 12.15$, Y06)⁸; finally, #274 was associated with the D-MM 10 mm core, indicated as starless by P06, with source 1656 in Y06 and source 15 in T06 (characterized by a steeply rising MIR SED).

Among the X-ray sources with optical/NIR counterparts, 17 in the region covered by Y06 were identified with *SPITZER* sources, of which one, #281, is a likely Class I source (Y06's source 62). Three more X-ray sources were identified with Class I/0 sources in the list of T06: #150 and #242 also having NIR counterparts, and #194 (see also Sect. 6.3) with both NIR and optical ($I = 19.89$) counterpart. As for the P06 mm-cores, identifications are made uncertain by the limited spatial resolution of the mm data (cf. P06). The core D-MM 14, classified as protostellar by P06, is probably associated with ACIS source #89 (offset: 1.2''), an optically faint ($V = 20.91$) and NIR bright ($K = 10.6$) star with intense H_α emission: $EW(H_\alpha) = 458$. Quite similarly, C-MM 1, also indicated as a protostellar core by P06, is offset by 1.3'' from the ACIS source #361, an optically visible source with strong H_α ($V = 18.55$, $K = 11.85$, $EW(H_\alpha) = 231$)⁹ and it is therefore likely to be associated with it. Finally, C-MM 5, classified by P06 as a protostellar core, might be associated with ACIS # 305 (offset: 1.9''). This ACIS source is in turn most likely associated with IRS 1 (offset: 0.8'', Schreyer et al. 2003). Note, however, that P06 suggests that C-MM 5 may not be associated with IRS 1. A more detailed analysis of the X-ray properties of young protostars in NGC 2264 will be the subject of a future paper.

4. Analysis

In this section we analyze the X-ray properties of our ACIS sources as indicated by their ACIS lightcurves (Sect. 4.1) and spectra (Sect. 4.2). The results of the spectral analysis are then used in Sect. 4.3 to estimate X-ray luminosities.

4.1. Temporal analysis

Source variability was characterized through the Kolmogorov-Smirnov test. Column 9 of Table 1 reports the resulting probability that the distribution of photon arrival times is not compatible with a constant count-rate. Given the sample size (420 sources), a value below 0.1% (obtained for 72 sources)

⁸ Note that the source is missed by 2MASS because, at the 2MASS spatial resolution, it is blended with a nearby source.

⁹ Although Y06 report that C-MM 1 has no NIR counterpart, we associate it with 2MASS source 06411792+0929011 (offset = 1.5'').

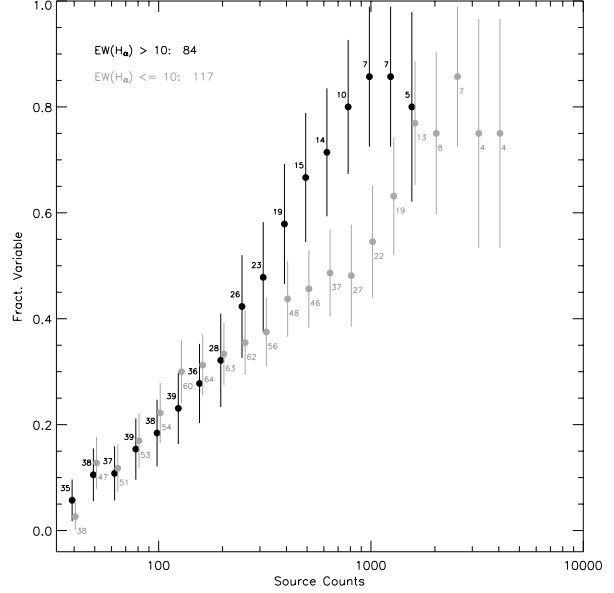


Fig. 6. Fraction of variable stars as a function of count statistics for stars with H_α EW greater and smaller than 10 (i.e. CTTS and WTTS). Note that counts bin are centered at the plot symbol and are 0.8 dex wide, so that successive bins are not independent. Error bars are based on binomial statistics. Symbols referring to the two subsamples are slightly shifted in the horizontal direction with respect to each other so to avoid confusion. The total numbers of objects in the subsamples are given in the legend, while the numbers of objects from which each variability fraction is computed are shown beside the plotting symbols.

indicates the light-curve is almost certainly variable, while a $<1\%$ value (87 sources) indicates probable variability, although up to ~ 4 ($= 420 \times 0.01$) of the *variable* sources might actually be constant. If we are not interested in the individual sources but in the overall fraction of variable sources, we can place a lower limit on this quantity by computing the minimum number of variable sources as a function of probability threshold, P_{th} : $N_{min} = N(P_{KS} < P_{th}) - 420 \times P_{th}$. The maximum N_{min} is obtained for $P_{th} = 15\%$, for which $N(P_{KS} < P_{th}) = 189$ and $N_{min} = 126$. We conclude that within our observation *at least* 30% (126/420) of the lightcurves are statistically inconsistent with constancy. This fraction is certainly a lower limit to the true number of variable sources, as our ability to tell a variable source from a constant one is influenced by photon statistics. This is clearly indicated by the dependence of the fraction of variable sources on source counts. If for example, we restrict the above analysis to sources with more than 100(500) counts, a total of 145(33) sources, we find that at least 54%(73%) of these are variable.

We next investigated whether different kinds of stars, classified from optical data, showed different variability fractions. From the previous discussion, it is clear that for a meaningful comparison, source statistics must be taken into account. Figure 6 shows the variability fraction, $f(P_{KS} < 1\%)$, as a function of source counts for CTTS and WTTS, as distinguished by their H_α equivalent width. Variability fractions are computed for sources with counts in intervals spanning 0.8 dex (because in the figure points are spaced by 0.1 dex, only one point every eighth is independent). Error bars on the variability fractions are estimated by assuming binomial statistics: $\delta f = [f \times (1-f)/N_{src}]^{1/2}$, where N_{src} is the number of sources in each count bin. In addition to the expected increase in the variability fraction with source statistics, we note that CTTS appear to be more variable with respect to WTTS, at least when considering stars with

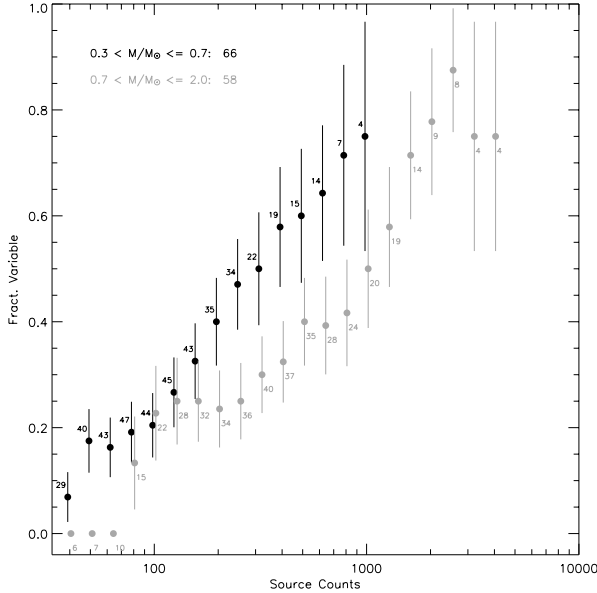


Fig. 7. Fraction of variable stars as a function of count statistics for stars in two different mass ranges: $0.3 < M/M_{\odot} < 0.7$ and $0.7 < M/M_{\odot} < 2.0$. Symbols and legend as in Fig. 6.

more than ~ 200 counts. Figure 7 shows a similar comparison for two mass segregated sub-samples: $0.3 < M/M_{\odot} < 0.7$ and $0.7 < M/M_{\odot} < 2.0$. Lower mass stars appear to be more variable, and again this difference is noticeable only for stars that are bright enough. We quantified the differences between variability fractions, by testing, for each count bin, the null hypothesis that the two samples are drawn from the same parent population. We chose the difference of the two observed variability fractions, Δf , as statistics. We then numerically computed the probability that a Δf equal or larger than the observed one is obtained by randomly drawing pairs of numbers from binomial distributions appropriate to the two sample sizes but characterized by the same probability of observing a variable source, i.e. the variability fraction. Because this number is not well constrained, we conservatively took as our confidence level the minimum that is obtained varying this fraction between 0 and 1. The results of these tests indicate that the differences in the variability fractions are statistically not highly significant: in the bin centered at ~ 400 counts, the low mass stars are more variable than higher mass stars with a 94% confidence, and CTTS are more variable than WTTS with a 92% confidence and in the bin centered at ~ 800 counts. We thus consider these results as tentative. However we note that the significance of the difference between CTTS and WTTS in NGC 2264 is strengthened by the fact that a similar result, with a similar confidence, was also obtained by Flaccomio et al. (2000) using totally independent ROSAT data.

4.2. Spectral analysis

We have analyzed the X-ray spectra of the 199 sources with more than 50 detected photons. Spectral fits were performed with XSPEC 11.3 and with several shell and TCL scripts to automate the process. For each source we fit the data in the [0.5–7.0] keV energy interval¹⁰ with several model spectra: one and two isothermal components (APEC), subject to photoelectric

Table 5. Initial conditions for XSPEC models.

Model name	N_{H} [cm $^{-2}$]	kT_1/kT_2	Abund.
1T	0.0, 10^{22}	0.5/–, 1.0/–, 2.0/–, 10.0/–	0.3
2T	0.0, 10^{22}	0.4/1.0, 1.0/3.0, 0.5/2.0	0.3
2Tab	0.0, 10^{22}	0.4/1.0, 1.0/3.0, 0.5/2.0	0.3
1T _{Av}	$1.6 \times 10^{21} \text{Av}$	0.5/–, 1.0/–, 2.0/–, 10.0/–	0.3
2T _{Av}	$1.6 \times 10^{21} \text{Av}$	0.4/1.0, 1.0/3.0, 0.5/2.0	0.3
2Tab _{Av}	$1.6 \times 10^{21} \text{Av}$	0.4/1.0, 1.0/3.0, 0.5/2.0	0.3

Multiple values indicate that all combinations of initial values were adopted. Values in italic indicate that fit parameters were fixed to those values.

absorption from interstellar and circumstellar material (WABS). Plasma abundances for one-temperature (1T) models were fixed at 0.3 times the solar abundances (Wilms et al. 2000), while they were both fixed at that value and treated as a free parameter for two-temperature (2T) models. The absorbing column densities, N_{H} , were both left as a free parameter and fixed at values corresponding to the optically/NIR determined extinctions, when available: $N_{\text{H}} = 1.6 \times 10^{21} \text{Av}$ (Vuong et al. 2003). A total of three or six models were thus fit for each source depending on the availability of optical extinction values. For each model, spectral fits were performed starting from several initial conditions for the fit parameters as indicated in Table 5. For example for isothermal models with free N_{H} , two values of N_{H} and four values of kT were adopted as initial conditions, for a total of eight distinct fits. For each model the adopted fit parameter set was chosen from the model fit that minimizes the χ^2 . This procedure was adopted in order to reduce the risk that the χ^2 minimization algorithm used by XSPEC finds a relative minimum.

Next, we considered which of the available model fits for each source (three or six, reference model names are given in Table 5) was the most representative of the true source spectrum, and thus the one to be adopted for the following considerations. The goal was twofold: to characterize the emitting plasma, in order to investigate its origin, and to determine accurate intrinsic band-integrated X-ray luminosities. Crucial for this latter step is to determine extinction (N_{H} , see Sect. 4.3). Generally speaking, models must have enough components to yield statistically acceptable fits according to the χ^2 or, equivalently, the null probabilities (n.p.) that the observed spectra are described by the models. However, models with too many free parameters with respect to the spectra statistics, while formally yielding good fits, will not be constrained by the data and will yield limited physical information. A particularly severe problem with CCD-quality (ACIS) low-statistic spectra is the degeneracy between absorption and temperature: an equally good fit can be often obtained with a cool plasma model with a large emission measure but suffering high absorption, or with a warmer temperature and a lower extinction. It is therefore desirable to check the N_{H} obtained from the fits with independent information from optical/NIR data. Figures 8 and 9 show the cumulative distribution of the n.p. for spectral fits performed with four different models, respectively for faint and bright sources ($50 < \text{cnts} < 300$, $\text{cnts} > 300$). The models are 1T, 2T, and, for sources with independent N_{H} estimates, 1T_{Av} and 2T_{Av}. In this kind of plot the distribution for a perfectly adequate spectral model should follow the diagonal, that for an oversimplified model should fall below the diagonal, and that for an over-specified model should lie above. For faint sources, 1T model appears perfectly adequate. Fixing the N_{H} to the optically determined value worsens the agreement somewhat but still results in fits that are, when

¹⁰ Events with energies below 0.5 keV were not used because of uncertainties in the calibration resulting from the time-dependent degradation of the ACIS quantum efficiency at low energies.

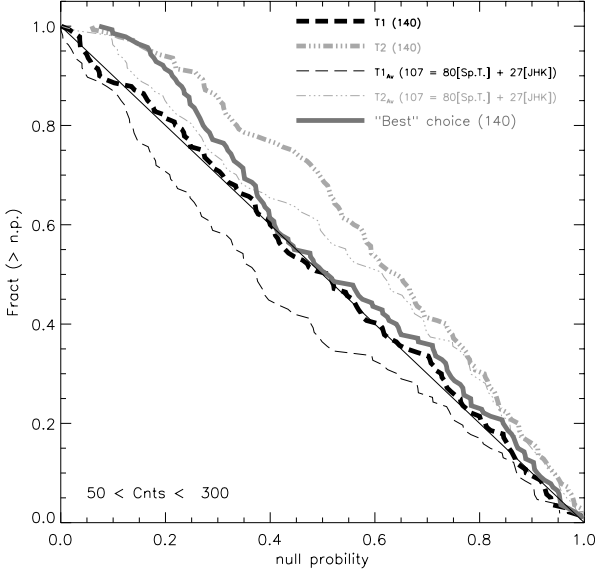


Fig. 8. Cumulative distribution of null probabilities resulting from X-ray spectral fits. The curves refer here to X-ray sources with more than 50 counts (the minimum for which we performed spectral fits) and less than 300 counts. The different lines refer to different physical models (one and two temperature, with free or fixed N_{H}) as indicated in the legend, along with the number of sources that enter in each distribution. For the models with fixed N_{H} , we also indicate the number of N_{H} derived from optical spectral types + photometry and of those derived from 2MASS J , H , and K photometry. The gray thick line refers to the “best” choice of models described in Sect. 4.2.

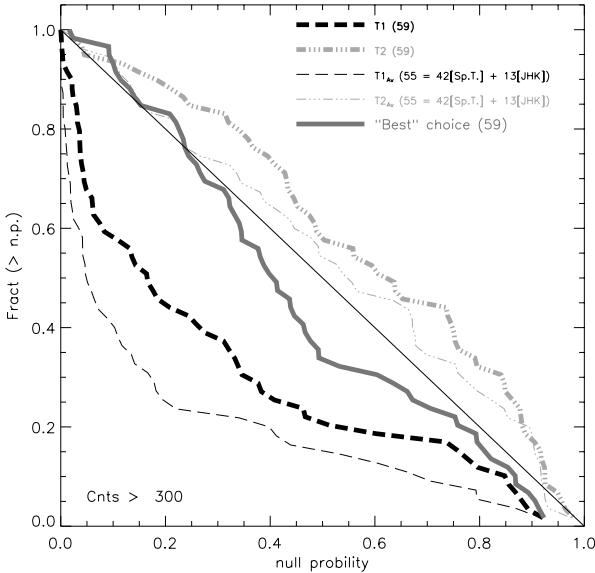


Fig. 9. Same as Fig. 8 for sources with more than 300 counts.

considered individually, acceptable for the most part. A 2T model with free N_{H} appears to be too complicated (and therefore unconstrained), while a 2T model with fixed N_{H} is more acceptable, but still on average too sophisticated for the quality of these low-statistic spectra. For brighter sources we notice instead that 1T models are on average not favored, while 2T models are still not always needed.

For most sources more than one spectral model is statistically acceptable. We choose a best-guess model as the simplest that still gives a statistically acceptable fit. The compelling reason to choose this approach is the mentioned degeneracy

between temperature and absorption. Note for example that, from Fig. 8, one could be tempted to always choose 1T models with free N_{H} for faint sources, as these models appear to be statistically perfectly adequate for representing the spectra. However, when examined individually, many of these 1T spectral fits have rather degenerate fit solutions, i.e. large and correlated uncertainties on the N_{H} and kT values, also implying large uncertainties on unabsorbed fluxes. This degeneracy can be broken by using the additional information on absorption coming from optical/NIR data, when available and compatible with the X-ray spectra.

After some experimenting, we chose our best-guess model according to the following empirical scheme: if $\text{n.p.}(1T_{A_{\text{v}}}) > 20\%$ we chose the $1T_{A_{\text{v}}}$ model. Otherwise, if $\text{n.p.}(1T) > 20\%$ we chose the 1T model (with free N_{H}). If both of the previous tests for isothermal models failed, we tried with two temperature models, this time lowering our n.p. threshold to 5%. First we tried the $2T_{A_{\text{v}}}$ model ($\text{n.p.}(2T_{A_{\text{v}}}) > 5\%$) and then the 2T model ($\text{n.p.}(2T) > 5\%$). As a last resort, in case none of the previous models could be adopted, we chose the $2T_{\text{Ab}}$ model (free N_{H} , free abundances). Although the above scheme was designed so as to favor simple models, the different n.p. thresholds resulted in four cases (sources #257, #275, #280, and #300) in adopting $2T_{\text{Ab}}$ models that were either statistically worse or comparable to simpler 1T, $1T_{A_{\text{v}}}$, or $2T_{A_{\text{v}}}$ models. We therefore adopted these latter. After careful examination of individual fits, the spectral models adopted for four more sources (#97, #104, #127, and #241) were modified. In these cases the automatic choice would result in unphysical, unusual, or unconstrained temperatures and absorptions, whereas our adopted models are both statistically and physically acceptable¹¹.

The solid gray lines in Figs. 8 and 9 refer to the final choice of best-guess models. Table 6 lists the end result of our spectral analysis: we report the adopted model, the source of the adopted N_{H} , the null probability, the plasma temperature(s) and normalization(s), the observed and absorption corrected fluxes in the [0.5–7] keV band.

In summary, out of the 199 sources with more than 50 counts, we adopted isothermal models in 147 cases and two component models in the remaining 52 cases. For 138 sources we adopted a spectral fit in which the N_{H} was fixed, in 101 cases to the value estimated from the optically determined A_{V} and in 37 cases from NIR photometry. In the remaining 61 cases, N_{H} was treated as a free fit parameter. Out of these 61 cases, independent estimates of extinction were available from optical and NIR data in 21 and 3 cases respectively, but our algorithm (or, for sources #97 and #127, our choice) preferred the spectral fit with free N_{H} . We examine these cases more in detail to assess the ambiguities in the model fits and the consequences on the derived X-ray fluxes.

Figure 10 illustrates one such case: source #375. Here the extinction determined from the 1T ($kT = 1.3$ keV) spectral fit (90% confidence interval: $N_{\text{H}} < 2 \times 10^{20} \text{ cm}^{-2}$) is lower than that estimated from the A_{V} ($9 \times 10^{20} \text{ cm}^{-2}$). Fixing the N_{H} to that

¹¹ For source #241 we changed the 2T model ($\text{n.p.} = 32\%$, $kT_1 = 0.057_{-0.022}^{+0.078}$ keV, $kT_2 = 0.57_{-0.30}^{+1.30}$ keV, $N_{\text{H}} = 13_{-1.8}^{+21} \times 10^{21} \text{ cm}^{-2}$) to a 1T model ($\text{n.p.} = 17\%$, $kT = 0.60_{-0.38}^{+0.84}$ keV, $N_{\text{H}} = 3.3_{-0.0}^{+6.5} \times 10^{21} \text{ cm}^{-2}$). For source #104 we changed the 1T model ($\text{n.p.} = 40\%$, $kT = 0.43_{-0.29}^{+0.73}$ keV, $N_{\text{H}} = 3.0_{-0.78}^{+5.6} \times 10^{21} \text{ cm}^{-2}$) to a $2T_{A_{\text{v}}}$ model ($\text{n.p.} = 32\%$, $N_{\text{H}}(A_{\text{v}}) = 0.0 \text{ cm}^{-2}$ and reasonable temperatures). For sources #97 and #127 we changed from $1T_{A_{\text{v}}}$ models ($p = 68\%$ and $p = 21\%$, $kT = 54$ keV and $kT = 19$ keV, both with unconstrained uncertainties) to 1T models ($p = 97\%$ and $p = 56\%$, $kT = 4.7$ keV and $kT = 3.5$ keV).

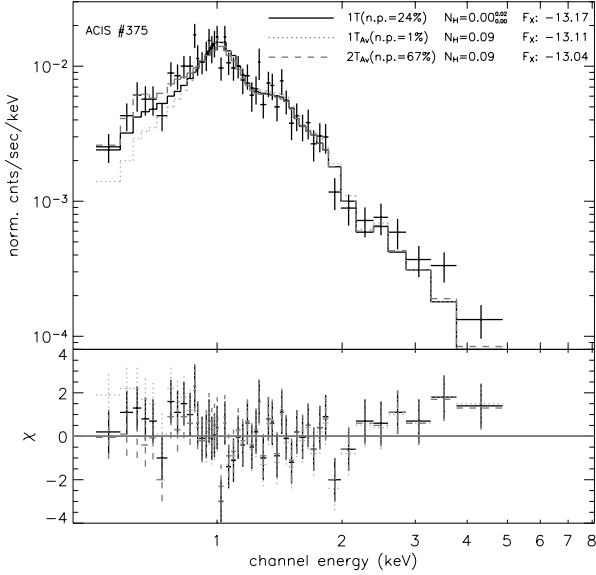


Fig. 10. *Upper panel:* spectrum of source #375 with overlaid three different spectral models, 1T with both free and fixed N_{H} (solid and dotted lines, respectively) and 2T with fixed N_{H} (dashed line). Null probabilities, N_{H} values (in units of 10^{22} cm^{-1}), and unabsorbed fluxes for each model are given in the legend. Note that the 1T and $2T_{\text{Av}}$ models are both statistically acceptable. *Lower panel:* residuals for the three models in terms of sigmas (error bars all of unit size).

value yields an unsatisfactory isothermal fit. However, adding a second cool isothermal component to the spectral model ($kT = 0.25$ keV), a good fit can be obtained even when fixing the N_{H} . This is quite a typical example of the degeneracy in the fitting of sources with low/moderate statistics. We can estimate the uncertainty in the X-ray unabsorbed fluxes derived from the spectral fits due to this degeneracy, as the difference between the fluxes derived from the two acceptable fits: for source #375, for example, this is 0.14 dex. More generally, acceptable fits with N_{H} fixed to the optical/NIR values could be obtained in 22 of the 24 cases in which our procedure preferred the spectral fit with free N_{H} . In five cases¹², among which the one described above, in order to reconcile the observed spectra with the optical extinction, an additional cool thermal component ($kT = 0.22\text{--}0.34$) would be required to compensate for the higher N_{H} . If for these five sources the true N_{H} were the optically derived ones, we are underestimating the unabsorbed fluxes by 0.14–0.37 dex (mean 0.2dex) by choosing the 1T fit with free (lower) N_{H} . For the other 17 sources, fixing the N_{H} would not require an additional component: reasonable fits (n.p. > 5%) were obtained even with the same models (1T in 16 cases, 2Tab for source #187). In 10 of these 17 cases the adopted fits with free N_{H} lead to smaller absorptions and slightly hotter (0.2–0.3 keV) temperatures (the cool temperature for #187), while the opposite happens in the 7 other cases. Had we fixed the N_{H} to the optical values in these 17 cases, we would have obtained unabsorbed fluxes on average ~ 0.03 dex larger and always within 0.20 dex (in either direction) of the adopted ones.

From this discussion of the 22 cases with most ambiguous extinctions ($\sim 14\%$ of the sources for which we have optical/NIR N_{H}), we conclude that (i) typical uncertainties in the unabsorbed flux are less than 0.2 dex and that (ii) individual X-ray fluxes corrected using an N_{H} from spectral fits can be as wrong as

¹² Sources #190, #340, #352, #375, #391.

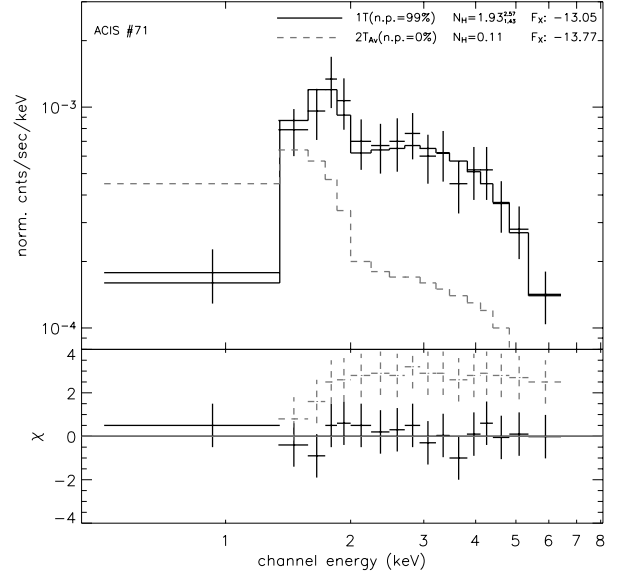


Fig. 11. Some as Fig. 10 for source #71. In this case we plot the 1T model with free N_{H} and the 2T model with N_{H} fixed to the optical value. Note how even adding a second component, it is impossible to reconcile the observed spectrum with the N_{H} implied by the optical absorption and a standard absorption law.

~ 0.4 dex, if the cool temperature is altogether missed by the spectral fit with a consequent underestimation of the N_{H} .

Two more sources have incompatible X-ray and optical extinctions according to our choice of *best* model. Source #234 did not enter into the previous discussion because it has the least acceptable fits of the whole sample, at most n.p. = 1.6% for a 2T model with free N_{H} (note, however, that with an adequate spectral model, we would expect three sources out of 199 to have lower n.p.). Adopting the optical N_{H} (1.8×10^{21}) would result in an unabsorbed flux that is only 0.07dex larger with respect to the one obtained leaving N_{H} as a free fit parameter ($N_{\text{H}} = 0.59_{-0.16}^{0.78} \times 10^{21}$). Source #71 is a more interesting case. Figure 11 shows its spectrum, with spectral fits obtained with free and fixed N_{H} . The X-ray-derived extinction ($N_{\text{H}} = 19_{-14}^{26} \times 10^{21}$) is about 17 times larger than estimated from the optical reddening ($N_{\text{H}} = 1.1 \times 10^{21}$)¹³. The discrepancy is highly significant and independent of the considered spectral model. We note that the detected emission from this source is dominated by a powerful flare, with a peak count rate ~ 100 times what it was before and after the flare. A possible scenario to explain the high absorption might involve a solar-like coronal mass ejection associated with the flare, providing the additional absorbing material. This hypothesis has been formulated by Favata & Schmitt (1999) to explain a more modest increase in N_{H} during a powerful flare observed on Algol. Further discussion of the physical interpretation of spectral fit results is deferred to Sect. 6.

¹³ For this source we adopted the spectral type (K2) from Dahm & Simon (2005) and the photometry ($R_{\text{c}} - I_{\text{c}} = 0.62$) from Lamm et al. (2004). Independent photometry and spectral types are available from Rebull et al. (2002), Lamm et al. (2004), and Dahm & Simon (2005). The $R_{\text{c}} - I_{\text{c}}$ color ranges between 0.55 and 0.62 and spectral types between G9 and K2. The possible range in $N_{\text{H}} = 1.6 \times 10^{21} \text{ Av}$ is thus $0.57\text{--}1.64 \times 10^{21}$, i.e. between ~ 9 and ~ 46 times the value derived from the X-ray spectrum, considering its 90% confidence interval.

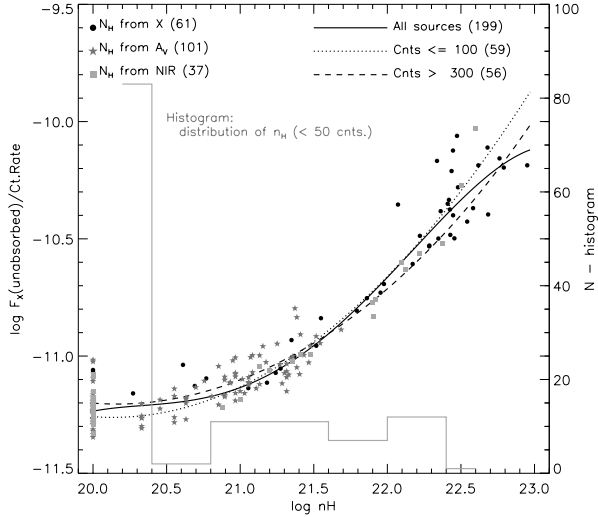


Fig. 12. Count-rate to unabsorbed flux conversion factor as a function of N_{H} as derived from spectral fits. Circles refer to the spectral fits in which N_{H} was treated as a free parameter, star-symbols and squares to fits to sources for which N_{H} was fixed to the values derived from the optical A_V or from the NIR photometry, respectively. The three curves indicate polynomial fits to the data obtained for the whole sample of 199 sources and for subsamples of sources with less than 100 counts (59 sources) or more than 300 counts (56 sources). The gray histogram (vertical scale on the right hand side) shows the distribution of absorption values, derived from the A_V or the NIR CCD, of X-ray sources with less than 50 counts, for which count-rate to flux conversion factor was determined using the polynomial fit to faint sources (<100 counts, dotted curve).

4.3. X-ray luminosities

Extinction-corrected X-ray luminosities in the [0.5–7.0] keV band were estimated for all sources for which an indication of extinction was available. For the 199 sources with more than 50 counts and for which spectral fits were performed, we computed L_X from the $F_X[u]$ (unabsorbed fluxes) column in Table 6, adopting a distance of 760 pc, adequate for NGC 2264 members. For the fainter sources, for which spectral fits were not performed, we derived a count-rate to unabsorbed flux conversion factors using the results of the spectral fits for the brighter stars. Figure 12 shows the run of the flux/rate ratio vs. N_{H} for this sample. Different symbols indicate different origins of the absorption values (see previous section). We then performed polynomial fits to the data points for the whole sample, for the 56 sources with more than 300 counts, and for the 59 sources with less than 100 counts. Results are shown in Fig. 12. Because the sources for which we want to determine fluxes have <50 counts, we adopt the latter fit as our relation between N_{H} and the conversion factor:

$$\log \frac{F_X(u)}{\text{Ct.Rate}} = 58.62 - 6.942 \times \log N_{\text{H}} + 0.1724 \times (\log N_{\text{H}})^2 \quad (1)$$

where the units are ergs cm^{-2} . The 1σ dispersion of the data-points around this relation is 0.1 dex, which can be taken as an upper limit to the error on the source flux introduced by ignoring the spectral shape of faint sources. From the observed count-rates, we thus estimated fluxes for 127 X-ray sources with <50 counts and with N_{H} estimates coming from either the A_V or the JHK photometry. The gray histogram in figure 12 shows the distribution of N_{H} for these sources. Results are reported in Table 1. Note that we do not quote X-ray fluxes for faint sources without an independent extinction estimate. Upper limit fluxes for 425 X-ray undetected stars in the ACIS FOV and with an

absorption estimate (out of a total of 1463) were similarly computed from the upper-limits to the count rates.

5. Results – membership

In this section we define a sample of 491 likely NGC 2264 members within the FOV of our ACIS observation. The X-ray sources account for 408 objects while the remaining 83 are selected on the basis of the strength of H_{α} line and of optical variability as described in Sect. 3.2. The likely members are indicated in Table 3 by an asterisk following the identification number. We first consider the possibility of extragalactic contamination and then discuss the nature of X-ray sources with and without optical/NIR counterparts separately.

5.1. Extragalactic X-ray sources

Extragalactic contamination is expected only among X-ray sources that lack an optical and/or NIR counterpart. We reach this conclusion by considering the 489 ACIS sources of a probably non stellar origin detected in the *Chandra Deep Field North* (CDFN; Alexander et al. 2003; Barger et al. 2003)¹⁴. After defining random positions in our FOV for each CDFN source, we compared their observed count rates with upper limits computed from our ACIS data at those positions (see Sect. 3.1). We then selected CDFN sources that would have been detected with our exposure: a total of 139 ± 3 objects¹⁵. Next, we compared the positions of these simulated CDFN AGNs in the optical (I vs. $R - I$) and NIR (H vs. $H - K$) color-magnitude diagrams¹⁶ with those of the X-ray sources in the NGC 2264 exposure that could be placed in the same diagrams. These plots show that AGNs are considerably fainter on average than our identified X-ray sources that can be placed in either of these diagrams, and only two or three of the AGNs that we could have detected occupy positions that overlap with the loci where our X-ray sources are found. Moreover, in this comparison we have totally neglected the effect of extinction. Because of the dark cloud in our line of sight, the number of AGNs we are sensitive to is certainly much reduced with respect to the above estimate, and their optical and NIR luminosities should also be considerably reduced. We therefore conclude that the contamination of AGNs to the sample of X-ray-selected probable members with optical/NIR identification is negligible.

5.2. X-ray sources with optical/NIR counterparts

In Fig. 3 we show the optical CMD for the 300 X-ray sources that can be placed in such a diagram and for the 83 other undetected probable members discussed in Sect. 3.2. Note that the X-ray sources are found for the most part in the locus expected for NGC 2264 members (i.e. the previously defined cluster locus). However some X-ray sources lie below that locus, their position being compatible with the one expected for MS foreground stars. Very few, if any, of the X-ray sources in this diagram may be background MS stars, which are expected to lie below the 1 Gyr isochrone. In order to reduce contamination in the sample of likely members to a minimum, we excluded X-ray sources that lie outside the cluster locus, i.e. below the $10^{7.1}$ Myr

¹⁴ We excluded 14 sources identified as stars by Barger et al. (2003).

¹⁵ Mean value and 1σ uncertainty result from repeating the experiment 10 times, each time varying the position of simulated extragalactic sources.

¹⁶ The NIR photometry of the CDFN sources was taken from 2Mass.

isochrone and to the right of the $0.8 M_{\odot}$ evolutionary track, but we made an exception for two sources: (i) #305 ($I = 17.28$, $R - I = 0.98$), associated with the IRAS source IRS-1, classified as a Class I object by Margulis et al. (1989) but more recently suggested as a deeply embedded B star in a more evolved evolutionary stage (Schreyer et al. 2003)¹⁷; (ii) #309 ($I = 16.45$, $R - I = 0.76$), a known member, because indeed the peculiar and well-studied accreting binary system KH 15D (e.g. Hamilton et al. 2005; Herbst & Moran 2005; Dahm & Simon 2005). The 8 sources that lie to the right of the $0.1 M_{\odot}$ track are considered likely members, either of very low (sub)stellar mass or else very absorbed. Since we lack A_V values from optical spectra, we can check these two possibilities using our X-ray data and the JHK photometry. Out of these 8 sources, 4 (#125, #192, #251, #273) are highly absorbed as indicated by their X-ray spectra (or hardness ratios) and/or their positions in the $J - H$ vs. $H - K$ diagram. Another three sources (#215, #316, #358) however appear to have negligible absorption and are good candidates for detected brown dwarfs.

Only 10 X-ray sources (out of 300) are excluded as members because they are incompatible with our cluster locus in the optical CMD and might be associated with field stars¹⁸. Among them only one (source #258, an X-ray faint, $L_X/L_{\text{bol}} = -4.8$, and soft G5 star) could be placed in the HR diagram of Fig. 5, where it lies on the 100Myr isochrone. Although we exclude these 10 sources from our sample of likely members, some of them might actually be members.

- In Fig. 3 six very likely members, 5 undetected, and one detected CTTS, are found below the cluster locus, indicating that some members do have a position in the optical CMD that differs from expectations.
- The spatial distribution of these 10 sources (Fig. 13) is similar to that of cluster members and not uniform, as expected from foreground stars.
- The ACIS spectra and hardness ratios indicate that 5 of these sources suffer high extinction in the X-ray band, which is incompatible with foreground MS star (but not with background giants).

Our next step was to statistically estimate the number of foreground stars that, if present in our FOV and detected by ACIS, contaminate our list of 290 (=300–10) X-ray detected cluster-locus candidate members, as well as the 10 X-ray sources outside of the cluster locus. We considered the volume-limited stellar samples of the NEXXUS survey (Schmitt & Liefke 2004), extracting from it a nearly complete sample of stars of spectral types F to M within 6 pc from the Sun. These stars are well characterized optically and have known distances and X-ray luminosities as measured with *ROSAT*. We estimated the number of foreground stars, N_{fg} , in our FOV assuming that the spatial density of field stars in the direction of NGC 2264 is uniform and equal to that in the solar neighborhood¹⁹. We next randomly drew N_{fg} stars from the NEXXUS sample and assigned them random distances, d , in the range [0–760] pc, according to a uniform stellar density. With these distances and assuming an isothermal X-ray spectrum with $kT = 0.3$ keV, we converted the NEXXUS X-ray luminosities to ACIS count rates using an N_{H} -dependent conversion factor calculated with the “Portable,

¹⁷ The ACIS spectrum indicates $N_{\text{H}} = 4.8_{-3.2}^{+8.9} \times 10^{22}$ (90% confidence interval), corresponding to $A_V = 20 - 56$.

¹⁸ #7, #51, #110, #128, #130, #171, #224, #248, #258, and #267.

¹⁹ This is justified by the low equatorial longitude of NGC 2264: 2.2 deg.

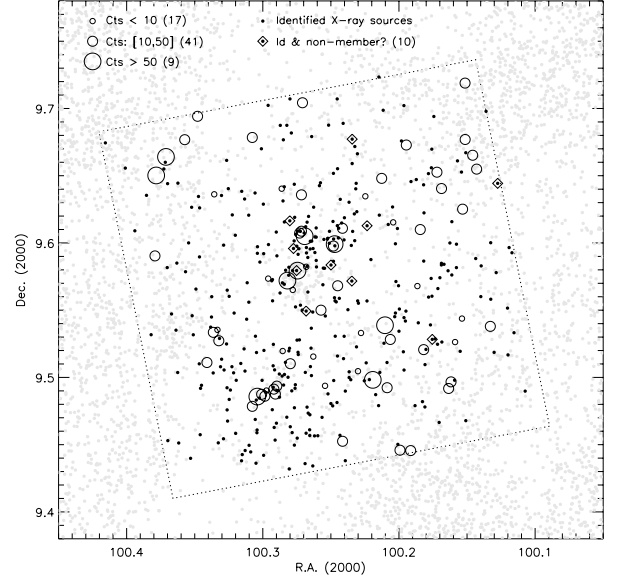


Fig. 13. Spatial distributions of sources around the ACIS FOV (the area within the dotted square). Light gray points: cataloged optical/NIR objects not detected in X-rays. Black symbols: X-ray detected objects. Squares with dots: X-ray sources that might be non-members because of their position in the optical CMD (Sect. 5). Empty circles with size indicating source statistics (see legend): unidentified X-ray sources.

Interactive Multi-Mission Simulator” (PIMMS). The hydrogen column density toward each star was estimated as $\rho \times d$, where the volume density ρ was set to 0.3 cm^{-3} and the distance is expressed in cm²⁰. We finally compared these simulated count-rates with upper limits estimated at random positions in the ACIS FOV estimated using PW Detect (Sect. 3.1). This simulation was repeated 100 times, varying the sample of NEXXUS stars and their position in space. On average, the sample of foreground stars that we would have detected counts 20 stars, 15 of which should fall in the cluster locus and 5 outside of it. About half of the 10 stars outside the cluster locus are thus expected to be cluster members, thus reinforcing the arguments given in the previous paragraph. Within the cluster locus, only 5% (15/290) of the X-ray sources are estimated to be non-members²¹. Given that eighty of the X-ray sources in the cluster locus had not been previously selected as likely members because of either their H_{α} emission or optical variability, we estimate that our sample contains ~ 65 new optically visible members.

Fifty-one more X-ray sources were identified with optical or NIR objects but could not be placed in the optical CMD (14 have I magnitudes but no R , 37 are only detected in 2MASS). Extending the previous result, and because we can exclude an extragalactic nature for these sources, we consider these stars as additional candidate members. Only four of them had previous indication of membership from their H_{α} or optical variability.

5.3. Sources with no optical/NIR counterpart

Sixty-seven ACIS sources are not identified with any object listed in the full-field optical/NIR catalogs we have

²⁰ With the chosen value of ρ , taking $N_{\text{H}}/A_V = 1.6 \times 10^{21}$ and $d = 760$ pc (the assumed distance of NGC 2264), we obtain $A_V = 0.44$, in agreement with the median of values measured for NGC 2264 members.

²¹ The fraction of non-members is expected to be higher among X-ray sources with $M/M_{\odot} > 1$ and ages $\sim 10^7$ yr.

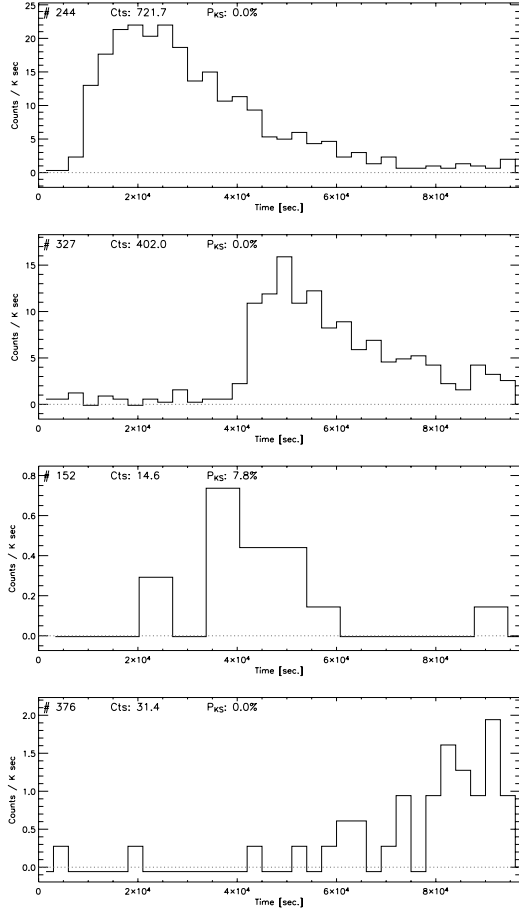


Fig. 14. Lightcurves for four “flaring” sources (#152, #244, #327, and #376) with no optical/IR counterpart. The background subtracted count rate is plotted vs. the time since the beginning of the observation. Source number, net counts, and the result of the KS variability test are given in the upper part of each panel.

considered²². None of them was detected by Flaccomio et al. (2000) with the ROSAT HRI²³. They have significantly fewer detected counts than identified sources. Fifteen of them have detection significance $<5.0\sigma$, and the 10 expected spurious detections (cf. Sect. 2.2) are most likely found in this group. Nine have more than 50 counts and were subject to spectral analysis.

Depending on the optical depth of the background cloud, a number of AGNs are expected to be detected in our FOV and will be found among the non-identified sources (Sect. 5.1). It is therefore reasonable to ask whether the characteristics of our sources without counterparts are compatible with an AGN nature. The X-ray spectra of AGNs should be rather hard and well fit by power-law models with indexes between ~ 0.9 and ~ 1.9 ²⁴. Their lightcurves should be constant or slowly varying. They should be distributed uniformly in space or anti-correlated with the cloud

²² Four of these X-ray sources were actually identified with MIR and/or mm sources in Sect. 3.3. Because these catalogs are not spatially complete, we here treat them as unidentified for uniformity.

²³ In Table 3 our ACIS source # 376 is associated with HRI source 138 due to the large uncertainty of the HRI positions; the HRI source is, however, closer to the brighter ACIS source #375, with which it is most likely associated.

²⁴ 80% interval of the power indexes reported by Alexander et al. (2003) for the sources in the CDFN that we would have detected in our ACIS data and for which the 1σ uncertainty in the index is lower than 0.1.

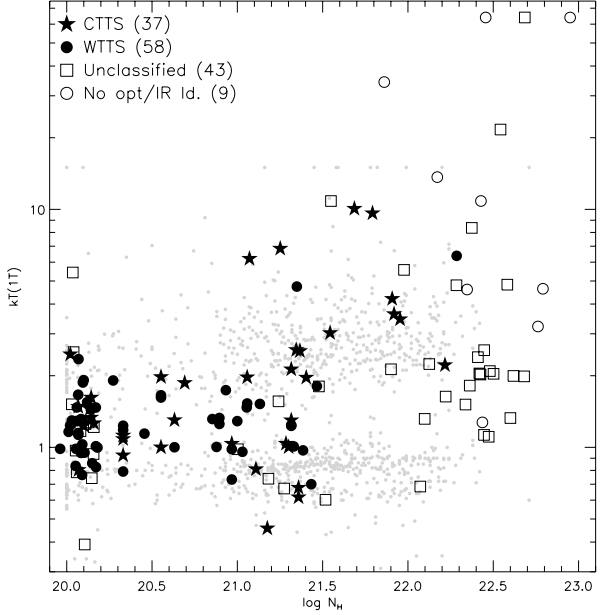


Fig. 15. Large black symbols: kT vs. N_H for NGC 2264 sources for which isothermal models were adopted. We distinguish (see legend) CTTS and WTTS, stars that are identified with optical and/or NIR sources but for which the PMS class is unknown, and X-ray sources that are not identified with any known optical/NIR object. Note that stars with $\log N_H < 20.1$ have been shifted to that value and their horizontal position slightly randomized so that the symbols do not overlap completely. The small gray circles show for comparison the two temperatures derived by Getman et al. (2005) for a sample of 566 ONC members observed by the COUP collaboration.

optical depth. With respect to this latter point, Fig. 13 shows, with different symbols, the spatial distribution of several classes of objects: X-ray sources without counterparts in three source count ranges, cross-identified X-ray sources, all the other X-ray undetected objects in our master catalog. This last group contains for the most part background field stars whose density is a good indicator of the optical depth of the molecular cloud. Note how the X-ray sources with counterparts, i.e. likely members, lie preferentially in front of or close to the cloud and have a highly structured distribution (cf., Lamm et al. 2004), with at least two concentrations in the south and toward the field center, corresponding to two well-known embedded sub-clusters roughly centered on IRS 1 (Allen’s source, e.g. Schreyer et al. 2003) and IRS 2 (e.g. Williams & Garland 2002).

We first discuss the nine unidentified sources with more than 50 counts: two of them (#244, #327), located in the IRS 1 and IRS 2 regions, show distinct long-lasting flares (Fig. 14) and are therefore most likely PMS stars or YSOs. As discussed in Sect. 3.3, source #244 is actually identified with a *SPITZER* source and, although missing in the 2MASS catalog, it is rather bright in K. The spectra of the other seven are compatible with both isothermal models and power-law models. Assuming isothermal models, they have higher extinctions and temperatures with respect to the 190 sources with counterparts and >50 counts (cf. Fig. 15): the median N_H is $2.7 \times 10^{22} \text{ cm}^{-2}$, vs. $7 \times 10^{20} \text{ cm}^{-2}$ and the median kT is 13.7 keV vs. 1.33 keV. Neither the N_H nor the kT are incompatible with those of other highly extinct X-ray sources with counterparts (cf. Fig. 15), which we have argued are most likely *not* AGNs. Due to the high extinction, the L_X of these sources (if at the distance of NGC 2264) is also high: median $\log L_X = 30.4$ vs. $\log L_X = 29.8$.

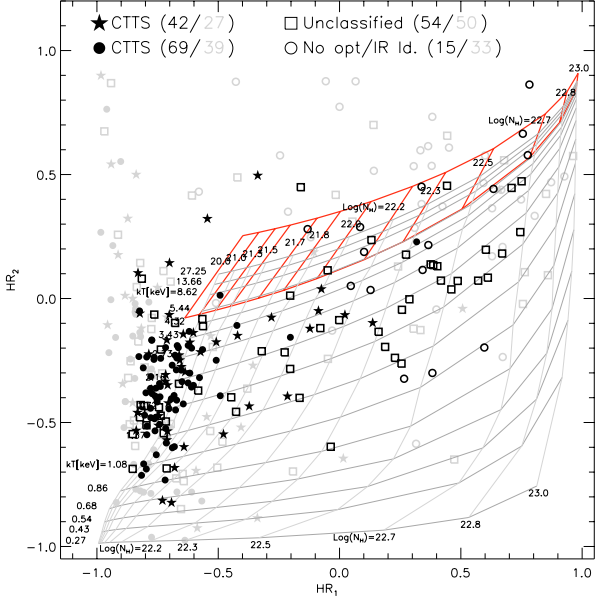


Fig. 16. $HR_1 = (M-S)/(M+S)$ vs. $HR_2 = (H-M)/(H+M)$, where H , M , and S are the photon fluxes in the [500:1700] eV, [1700:2800] eV, and [2800:7000] eV bands. Sources for which 1σ uncertainties on HR_1 and HR_2 are less than 0.3 are plotted in black and those with larger uncertainties in gray. Symbols are as in Fig. 15. The number of plotted sources in each class are given in the legend. The light gray grid indicates the expected loci of isothermal sources of a given kT absorbed by interstellar matter of varying N_H . Values of kT 's and $\log N_H$ are given on the left and top/bottom of the grid. The upper thick-line grid indicates the region expected for AGNs (power-law spectra with indexes between 0.9 and 1.9).

for identified sources. If instead we assume that the correct models are power laws, the best-fit indexes range between $0.25^{+0.9}_{-0.23}$ and $4.1^{+6.5}_{-2.5}$ (median 1.6). The two flaring sources have power indexes with 90% confidence above the range expected for AGNs, and the same is true also for source # 162 ($\Gamma = 4.1^{+6.5}_{-2.5}$), which also lies in the IRS 2 region and is therefore likely to be a star (the isothermal fit yield a rather common $kT = 1.27$ keV). Two more (# 228, # 274) of the remaining six objects, although with rather hard and absorbed spectra, are clustered around IRS 2 and are therefore also likely to be YSOs. We thus conclude that 50% (5 out of 9) or more of the unidentified sources with more than 50 counts are likely to be stars.

Turning to the remaining 58 sources with less than 50 counts, two show flares (#152 and #376, Fig. 14) and are likely to be stars. The others, although maybe a little less spatially concentrated than sources with counterparts, seem to follow a similar distribution in the sky. We conclude that, rather qualitatively, a sizable fraction (on the order of 50%) of them are associated with NGC 2264. This conclusion is corroborated by the distribution of unidentified sources in the HR_1 vs. HR_2 hardness ratio diagram, Fig. 16. We show for reference a grid of expected loci for absorbed isothermal spectra and the region where power-law sources with indexes between 0.9 and 1.9 should lie. Both grids are computed using PIMMS. We note that both HR_1 (most sensitive to N_H) and HR_2 (most sensitive to kT) are on average significantly different for sources with and without counterparts, indicating that non-identified sources are on average characterized by hotter and more absorbed emission. However, the region occupied by about half of the unidentified sources is also occupied by a number of absorbed sources with counterparts, i.e.

probable members, while the rest appear to be significantly hotter and possibly compatible with the expected AGN locus.

In conclusion, our 67 sources lacking optical/NIR counterparts are good candidates for new embedded members. Given their absorption, these are rather luminous X-ray sources. They are thus unlikely to be low-mass stars that have escaped optical/NIR detection because intrinsically fainter than the detection limit. Given the small dependency of L_X/L_{bol} on mass (Flaccomio et al. 2003a; Preibisch et al. 2005), low-mass stars are indeed usually faint in X-rays. Non-identified sources might be embedded protostars (class I and class 0 objects), medium/high-mass very obscured PMS members of NGC 2264 or extragalactic objects shining through the background molecular cloud. They certainly deserve to be followed up with more sensitive IR observations.

6. Results – X-ray activity

Our data indicate that the source of X-ray emission in NGC 2264 low-mass members is hot (0.3–10 keV) thermal plasma. The X-ray emission is highly variable in time, the most prominent phenomena being impulsive flares due to magnetic reconnection events. These observations fit well with a solar-like picture of coronal emission and are quite usual for PMS stars. They are, for example, in qualitative agreement with those recently reported for the ~ 1 Myr old stars in the ONC by the COUP collaboration (Preibisch et al. 2005). The spectral and temporal characteristics of PMS stars are, broadly speaking, also similar to those of active MS stars, e.g. in the young Pleiades cluster.

The most striking differences with respect to MS stars are the X-ray luminosities and the plasma temperatures, both of which are usually found to be higher. As for L_X , we note that the fractional X-ray luminosities (L_X/L_{bol}) of PMS stars are comparable or smaller than those of saturated MS stars. Therefore, the higher L_X can be explained by the almost saturated emission of PMS stars and by their larger bolometric luminosities. The higher temperatures might instead indicate a difference in the heating mechanism and/or, a larger contribution to the average flux of flares with hard spectra. At least three questions remain open. First and foremost, the nature of the ultimate mechanism that sustains PMS coronae. While for partially convective MS stars this is identified with the $\alpha - \omega$ dynamo thanks to the observed relation between activity and stellar rotation, no such evidence is available for PMS stars (Flaccomio et al. 2003a; Preibisch et al. 2005; Rebull et al. 2006). Second, the extent and geometry of coronae and, in particular, the possibility of interactions of plasma-filled magnetic structures and circumstellar disks (Favata et al. 2005; Jardine et al. 2006). Third, the role of accretion and outflows: soft X-ray emission has been inferred to originate both at the interface between the accretion flow and the photosphere and within the stellar jets (Kastner et al. 2002; Bally et al. 2003). In this section we now use our data to statistically investigate the dependence of activity, in terms of emission level, variability, and spectra, on the stellar and circumstellar characteristics. First, however, we discuss the results of our X-ray spectral analysis in more detail, with respect to plasma temperatures and absorption values.

Figure 15 shows the plasma temperature as a function of absorption for all the sources with spectral fits and for which we adopted isothermal models. Figure 17 similarly shows the two best-fit plasma temperatures of sources for which we adopted 2T models. First of all we observe that 2T models were required only for $\log N_H < 21.5$, probably because higher column densities absorb the cool component to the extent that it becomes

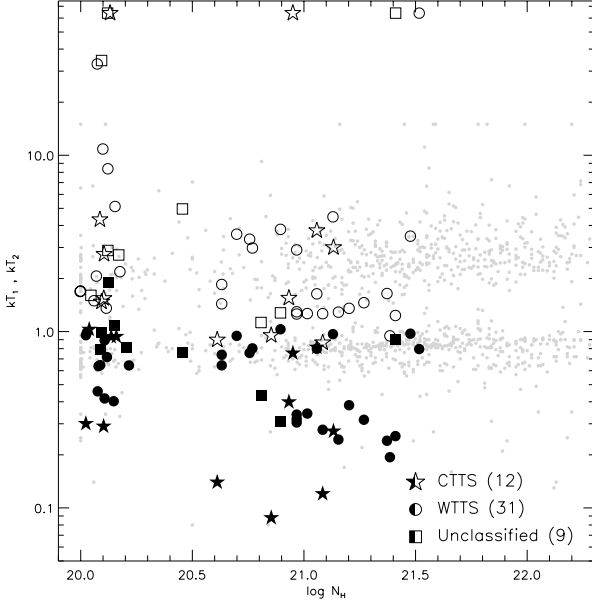


Fig. 17. kT_1 and kT_2 as a function of N_H for sources for which 2T spectral fits were adopted. The results for NGC 2264 presented in this paper are shown as larger symbols, filled ones for the cool component temperature and empty ones for the hot component. Stars, circles, and squares indicate CTTS, WTTS, and unclassified stars, respectively. The small gray circles show for comparison the two temperatures derived by Getman et al. (2005) for a sample of 566 ONC members observed by the COUP collaboration.

unobservable. Moreover, in the N_H range covered by both models, 2T models were statistically favored in sources with higher statistics while low-statistic sources were in most cases successfully fit with a single plasma component with temperature roughly intermediate between those of the two components in 2T models. For 1T models we also note a certain correlation between kT and N_H (Fig. 15). While a positive slope of the lower envelope of the datapoints is easily explained as a selection effect, this is not the case for the upper envelope. The paucity of sources with low N_H and high kT indicates that the X-ray emitting plasma of highly extinct sources is intrinsically hotter than that of optically revealed PMS stars. These hot, highly extinct sources are good candidates for embedded Class 0/I protostars, which have already been suggested to have harder X-ray spectra (Imanishi et al. 2001).

Figure 18 shows the run of kT_1 and kT_2 with stellar mass for 2T models. As for the two previously discussed plots, we also show for reference the temperatures obtained by the COUP collaboration (Preibisch et al. 2005) for ~ 1 Myr old stars in the ONC²⁵. With respect to the ONC, temperatures in NGC 2264 appear to be lower on average. This could indicate that at ~ 3 Myr the hot flaring component of the X-ray emission has become less important. It could also result from a lower fraction of CTTSs given that CTTS tend to have slightly higher plasma temperatures than WTTS (see Sect. 6.1).

We also note that the temperatures of the two isothermal components show a larger scatter in the NGC 2264 stars than in the COUP data. This could be due to: i) larger uncertainties in the NGC 2264 results because of the shorter exposure time and

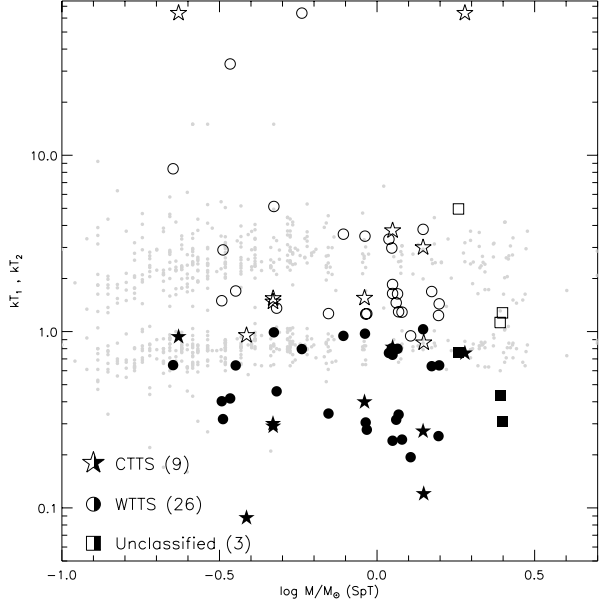


Fig. 18. kT_1 and kT_2 as a function of stellar mass for sources that are both placed in the theoretical HR diagram and for which we adopted a 2T spectral model. Symbols and legend as in Fig. 17.

longer distance with respect to the ONC; ii) the shorter exposure time resulting in a stronger influence of spectral time variability on the time-averaged spectra; iii) a real evolutionary effect (e.g. most ONC stars are CTTS, while in NGC 2264 we observe a more varied mixture of CTTS and WTTS); iv) the existence of an additional thermal component that is only sometimes present and/or revealed by the spectral fitting process. In this respect Figs. 17 and 18 indicate, for sources fit with 2T models, an interesting feature: an apparent separation of the temperatures into two branches, more evident for the cool isothermal component. Taking $kT_1 = 0.5$ keV as the dividing line between the two branches, we have 23 and 29 sources in the *cool* and *hot* branches, respectively. The hot branch has median kT_1 and kT_2 of 0.8 and 3.6 keV, respectively, roughly coincident with the temperatures of most COUP sources. The cool branch has median kT_1 and kT_2 of 0.3 and 1.3 keV, respectively. Since this latter median kT_2 is similar to the temperatures found for sources that were successfully fit by 1T models, it is reasonable to hypothesize that the EM distributions of these sources have three peaks: one corresponding to the cool ~ 0.3 keV component that is not present and/or visible for sources in the hot branch, and two peaks at hotter temperatures (i.e. ~ 0.8 and ~ 3.6 keV) that are, however, well-represented by an isothermal component with intermediate temperature. Given the limited statistics of our sources, three component spectral models are not needed, although physically reasonable, and would therefore remain unconstrained by the data.

As for the physical origin of the two branches, we note that, with respect to the hot branch, stars in the cool branch have lower counts (median counts 270 vs. 630), are significantly less variable according to the KS test (variability fraction 30% vs. 66%, at the 1% confidence level), and are slightly more likely to be CTTS (CTTS fraction: 33% vs. 23%). We note that the difference in variability fractions is unlikely to be explained by statistics alone (cf. Figs. 6 and 7). If the $kT_2 \sim 3$ keV component is due to flaring, it is then possible that the $kT_1 \sim 0.3$ keV component becomes detectable preferentially when flaring is absent, so that the hot component is suppressed. This soft emission

²⁵ Note that the COUP observation, obtained with *Chandra* ACIS, was 850 ks long. The temperatures are thus derived from a spectrum that has been integrated in time over a period that is 8.5 times longer than that of our NGC 2264 observation.

might be physically assimilated to the X-ray emission from the solar corona, which would indeed show temperatures similar to 0.3 keV if analyzed with *ASCA* SIS (cf. Table 1 in Orlando et al. 2001), an instrument with a response similar to ACIS. The emission measures we derive for the ~ 0.3 keV component of our NGC 2264 sources (3.1×10^{52} – $1.6 \times 10^{54} \text{ cm}^{-3}$), although much larger than those estimated for the Sun, could still be explained by much larger filling factors (~ 1) and/or larger scale heights of the densest structures (i.e. active region cores).

6.1. Activity in CTTS and WTTS

Comparing the plasma temperatures of CTTS and WTTS that are well fit by a single temperature model (37 CTTS, 58 WTTS), we learn that the former are statistically hotter, with a median kT of 1.5 keV vs. 1.3 keV (K-S test probability that the two distributions are compatible: 0.2%). A similar comparison for the two plasma temperatures of stars that required a 2T spectral model (12 CTTS and 31 WTTS) is inconclusive, possibly because of the lower number of stars. However, we have noted above that CTTS appear to be more common among stars with low values of kT_1 (Fig. 17). In particular, the three stars with the lowest kT_1 are all CTTS. Figure 19 shows the ACIS spectra for these three sources, #17, #111, and #183. The two thermal components of the best-fit models are shown separately, and the temperatures and absorptions are reported from Table 6. The most striking case appears to be source #183, which has the highest kT_1 (0.14 keV) and shows a clear double-peaked spectrum. The emission measure (EM) of the cool plasma is estimated to be $5.7 \times 10^{53} \text{ cm}^{-3}$. The other two sources have lower kT and higher EMs (#17: $kT_1 = 0.09$ keV, $EM = 2.3 \times 10^{54} \text{ cm}^{-3}$; #111: $kT_1 = 0.12$ keV, $EM = 1.2 \times 10^{54} \text{ cm}^{-3}$). We also note that among the three sources #183 has the largest H_α line equivalent width: 27.9 vs. 10.9 and 18.2 for #17 and #111.

As noted in the previous section, low kT_1 values are usually associated with low kT_2 . For the three CTTS just discussed, for example, the kT_2 values, 0.87–0.95 keV, are among the lowest observed and are very similar to the cool component for the majority of PMS stars. This suggests that the ultra-cold component is present and/or observable with our spectra only when $kT = 2$ –4 keV plasma is absent.

A similar trend can be observed for 1T fits (Fig. 15): among the six lowest kT s ($kT < 0.68$ keV), the $EW(H_\alpha)$ is known for three stars, and it indicates accretion (i.e. a CTTS) in all cases. CTTS thus appear to possess both warmer and cooler plasma than WTTS. If this result is confirmed with more statistical significance by further observations, it could imply that the accretion process results, on one hand, in more frequent/energetic flares and, on the other, in a very cool X-ray plasma produced in the accretion shock (cf. the cases of TW Hydreae and BP Tau: Kastner et al. 2002; Stelzer & Schmitt 2004; Schmitt et al. 2005).

We now investigate the X-ray activity levels (L_X and L_X/L_{bol}) as a function of bolometric luminosity, stellar mass, and accretion properties for the subsample of stars for which stellar masses were derived by placement in the theoretical HR diagram (Fig. 5) and interpolation of the SDF tracks (160 X-ray detected stars, excluding one possible non-member and two stars outside the tracks). For this investigation we also include upper limits for 16 X-ray undetected likely members. Note that a more exhaustive account of the relation between activity and stellar properties, using the X-ray data presented here in conjunction with those of Ramírez et al. (2004a) for another field in NGC 2264 and those of Ramírez et al. (2004b) for the “Orion Flanking Fields”, can be found in Rebull et al. (2006). In that

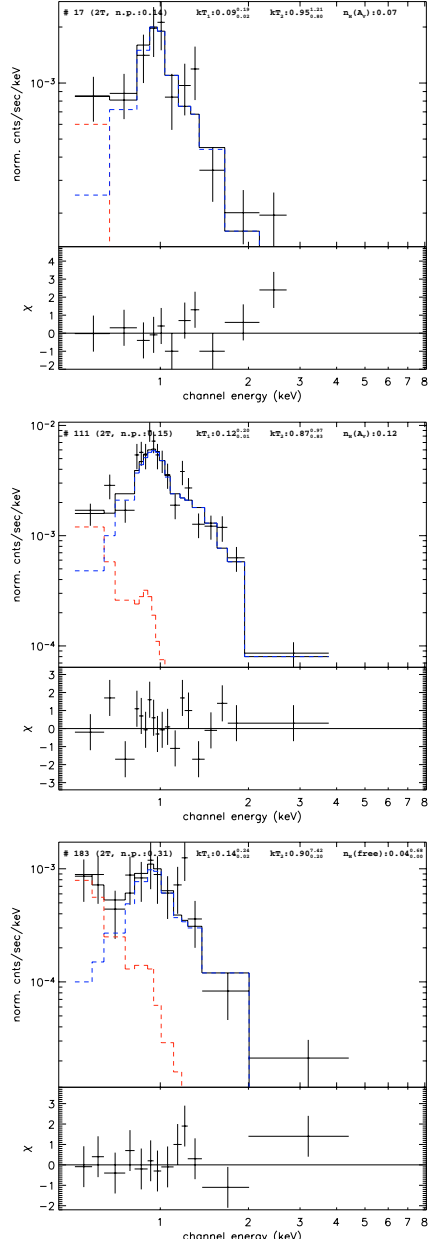


Fig. 19. ACIS spectra of three CTTS with a very low kT_1 . At the top of each panel, we report the source number, fit model, goodness of fit (null probability), kT_1 , kT_2 , and N_H values, in units of 10^{22} cm^{-2} . For these, we also indicate in parenthesis their origin, “ A_V ”, or, for source #183, “free”, i.e. derived from the X-ray spectral fitting.

paper the samples for each cluster included many more stars than we have here, but with more uncertain stellar parameters on average. Here we take a different approach, focusing only on the NGC 2264 members in our FOV that are well characterized optically.

Our L_X -mass scatter plot is shown in Fig. 20. We observe the commonly found mass- L_X correlation (e.g. Rebull et al. 2006), although with a large spread. The position of upper limits indicates that our sensitivity limit is $\log L_X \sim 29$ ergs/s, which appears to correspond to a completeness limit in mass at about 0.3 – $0.4 M_\odot$. Moreover we note that, at each stellar mass for which our sample is reasonably complete, CTTS are on average fainter and more scattered with respect to WTTS, confirming the results obtained for ONC stars (Flaccomio et al. 2003a;

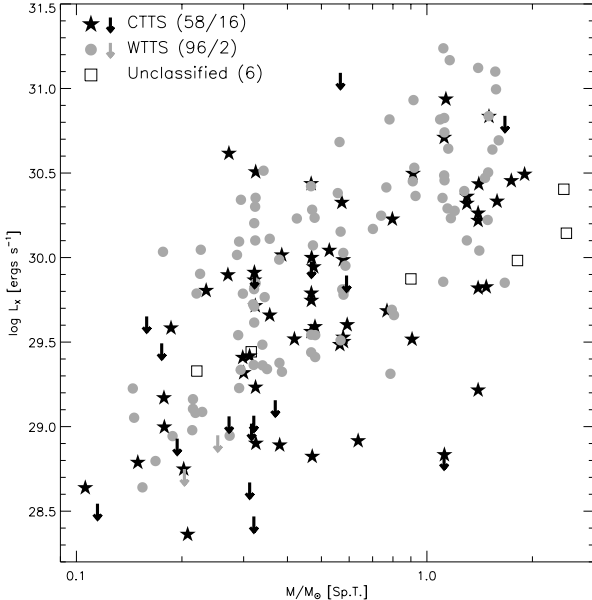


Fig. 20. $\log L_X$ vs. mass for likely members placed in the theoretical HR diagram. Black stars and arrows indicate CTTSs (detections and upper limits, respectively). Gray circles and arrows indicate WTTSs. Squares indicate detections of unclassified PMS class. The legend gives the number of detections and upper limits for each of the three subsamples.

Preibisch et al. 2005). A similar plot is shown for L_X/L_{bol} in Fig. 21. L_X/L_{bol} appears to be generally high, roughly between 10^{-4} and the saturation level $\sim 10^{-3.0}$. Twenty-two sources actually have measured L_X/L_{bol} above the saturation level. However, a large fraction of these, 73%, are variable, a significantly higher variability fraction than among sources below the saturation threshold (16%). Moreover, most of the sources with the highest values of L_X/L_{bol} show large flares, which if excluded would bring them close to or below the saturation level. Flaccomio et al. (2003a) found evidence for ONC stars of a decrease in L_X/L_{bol} at the very lowest masses. Our sample of stars with mass estimates is not complete enough at those masses to study this effect in detail. However, consistent with these results, we do note a decrease in the upper envelope of the L_X/L_{bol} vs. mass relation for $M/M_{\odot} \lesssim 0.3$. Considering CTTS and WTTS separately, the difference in activity is less striking in this plot compared to the L_X -mass one. However, Fig. 22 shows, separately for the two PMS classes, the distributions of L_X/L_{bol} , both for the whole mass range and for the subsample with $M > 0.6 M_{\odot}$. As noted above this latter sample should be almost complete, according to the L_X -mass relation. All the distributions take into account upper limits via the Kaplan-Meier estimator. For both samples, and in particular for the mass-restricted one, we observe that CTTS are less active than WTTS. Median $\log L_X/L_{\text{bol}}$ values differ by 0.32 and 0.41 dex for the two subsamples. The statistical significance of the difference is confirmed by the five two-sample tests in the ASURV package (Feigelson & Nelson 1985), giving probabilities that the $\log L_X/L_{\text{bol}}$ distributions of CTTS and WTTS are taken from the same parent distribution of $<0.02\%$ for the whole stellar sample and of $<0.3\%$ for the mass-restricted one. We note that this latter result differs from that of Preibisch et al. (2005), who find a statistically significant difference in the activity levels of CTTS and WTTS in the ONC only for stars in the $0.2-0.5 M_{\odot}$ mass range.

Finally we used our data to repeat the correlation analysis between L_X and L_{bol} performed by Preibisch et al. (2005) for ONC

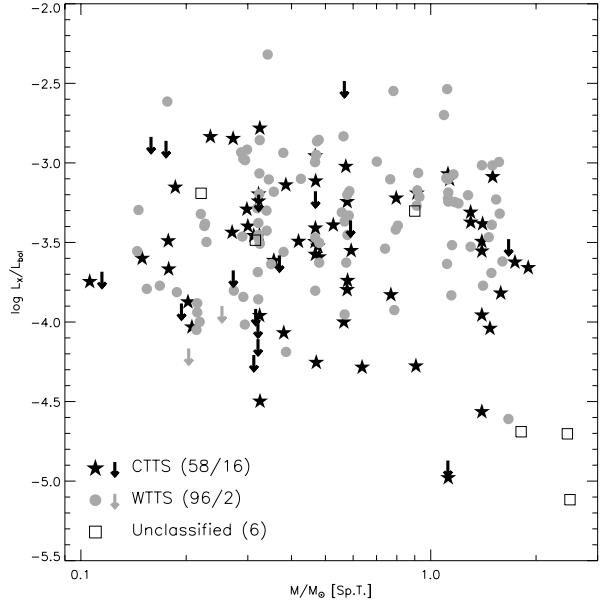


Fig. 21. $\log L_X/L_{\text{bol}}$ vs. mass for the same stars as in Fig. 20.

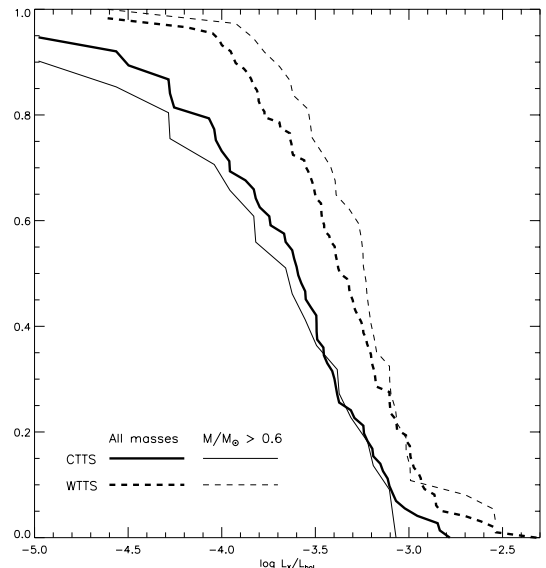


Fig. 22. Distribution of $\log L_X/L_{\text{bol}}$ for WTTS and CTTS (solid and dashed lines, respectively). The thick lines refer to the whole sample of stars depicted in Fig. 21; the thin lines to stars more massive than $0.6 M_{\odot}$. Note how in both cases CTTS are on average less active than WTTS.

stars classified as CTTS and WTTS. Using the estimation maximization (EM) algorithm in the ASURV package, we found very nearly linear correlations between L_X and L_{bol} for the two classes of stars: $\log L_X = (1.02 \pm 0.09) \log L_{\text{bol}} + 30.21 \pm 0.05$ for WTTS (1σ dispersion: 0.4 dex) and $\log L_X = (1.02 \pm 0.12) \log L_{\text{bol}} + 29.92 \pm 0.07$ for CTTS (1σ dispersion: 0.5 dex). As in the ONC case, accreting stars in NGC 2264 thus appear to be fainter on average than non accreting ones with the same L_{bol} (in this case by a factor of 2) and to have slightly more scattered L_X values. However, we note that the power-law slope derived by Preibisch et al. (2005) for accreting stars in the ONC (0.6 ± 0.1) is significantly shallower than the one derived here and that the 1σ dispersion of points with respect to the best-fit relations appear to be larger in the ONC: 0.5 vs. 0.4 dex for WTTS and 0.7 vs. 0.5

for CTTS. The differences might be interpreted as an evolutionary effect, given that the ONC is younger than NGC 2264 (~ 1 vs. ~ 3 Myr) and that accretion disks are expected to have evolved significantly in the older cluster (Flaccomio et al. 2003c). We note, however, that the comparison between the effects of accretion on X-ray activity in the two regions is made uncertain by the different accretion indicators used in the two cases, the H_α and the Ca II equivalent widths for NGC 2264 and the ONC, respectively.

6.2. KH 15D

The peculiar binary system KH 15D has been the subject of many investigations. Herbst & Moran (2005), in particular, analyzed the same X-ray data discussed here to conclude that the system is a very weak source of X-ray emission for its mass and age. They tentatively attribute the low X-ray emission to the high eccentricity of the binary system and/or to the close periastron approach of the two stars, which may either disrupt the stellar magnetosphere and/or adversely affect the stellar dynamo.

The X-ray luminosity we derive for KH 15D (our source #309), based on 21.6 detected photons, is 1.3×10^{29} , lower by 0.07 dex than the value reported by Herbst & Moran (2005). This difference is small and within the uncertainties but, given that the two values are derived from the same X-ray data, we investigated the matter further. This discrepancy can be fully explained by the different estimated number of source photons, 21.6 vs. 22.5, the assumed value of interstellar absorption, 9×10^{20} vs. $2 \times 10^{20} \text{ cm}^{-2}$, and the assumed source spectrum²⁶. The 0.07 dex difference in L_X , however, is not particularly relevant for the physical conclusions regarding the low L_X of the system. KH 15D is not shown in our L_X -mass scatter plot (Fig. 20) because the system is located in the HR diagram below the grid of the evolutionary tracks (Fig. 5) and we did not derive a mass. By extrapolating the tracks one would estimate a mass of $0.6\text{--}0.7 M_\odot$, consistent with the value used by Herbst & Moran (2005), $0.6 M_\odot$. Thus placing KH 15D in the L_X -mass diagram we notice that it would fall below the bulk of the other NGC 2264 members but in an area that is populated by other CTTSs. The value of $\log L_X/L_{\text{bol}}$ we derive from our data, -3.45, is moreover perfectly in line with most of the other NGC 2264 members (cf. Fig. 21). We therefore tend to believe that, rather than being affected by the peculiar binary orbits, the low X-ray emission of KH 15D is due to the same mechanism that suppresses activity in CTTSs.

6.3. Embedded XMM-Newton sources studied by Simon & Dahm (2005)

Simon & Dahm (2005, hereafter SD05) studied three embedded X-ray sources close to IRS 1 in detail (see also Sect. 3.3) using XMM-Newton EPIC data taken in March 2002, i.e. 7 months

²⁶ Our N_{H} is based on $A_V = 0.58$, derived here from published photometry and spectral type. Herbst & Moran (2005) derive their value from $E(B - V) = 0.1$. This $E(B - V)$ should, however, imply $N_{\text{H}} = 5\text{--}6 \times 10^{20} \text{ cm}^{-2}$ assuming $A_V/E(B - V) = 3.1$ and depending on the assumed A_V/N_{H} ratio in the range $1.6\text{--}2.0 \times 10^{21}$. Herbst & Moran (2005) assume solar abundances and $kT = 2.7 \text{ keV}$, the latter based on the uncertain (due to statistics) hardness ratio. The count to flux conversion factor we used (Eq. (1)) was derived from sources with 50 to 100 counts, which were fit with APEC models with subsolar abundances and median kT of 1.0 keV. Note that our hardness ratio analysis (cf. Fig. 16) actually indicates a very cool spectrum, $kT \sim 0.3 \text{ keV}$, with large uncertainties.

before our ACIS exposure. All three sources are retrieved in our data and we now compare the results with respect to spectral characteristics, variability, and average X-ray luminosities.

EPIC source #26 (our source #194) was the stablest of the three sources. The lightcurves were constant in both observations; the absorption was identical, $N_{\text{H}} = 2.6 \times 10^{22} \text{ cm}^{-2}$; and the kT was also the same within uncertainties²⁷: $2.09 \pm 0.23 \text{ keV}$ (EPIC) vs. $kT = 2.4^{4.8}_{1.5} \text{ keV}$ (ACIS). The X-ray luminosity, however, when corrected for the different energy band used by SD05 (1–10 keV vs. our 0.5–7 keV) and for the different assumed distance ($d = 800 \text{ pc}$, vs. our 760 pc), seems to have dropped by a factor ~ 2 between the two observations.

The EPIC source #10 (our source #141) showed a dramatic flare toward the end of SD05's exposure with the peak count rate reaching ~ 100 times brighter than the quiescent emission before the flare. Our lightcurve is instead compatible with constant emission. SD05 have analyzed the spectrum during the flare, while we report results for the average spectrum, which is, however, built from only ~ 65 photons. There is no evidence of variation in the absorption: SD05 find $N_{\text{H}} = 2.26 \pm 0.16 \times 10^{22} \text{ cm}^{-2}$ vs. our $2.6^{4.3}_{1.5} \times 10^{22} \text{ cm}^{-2}$. The temperatures are, however, very different owing to the bright flare in the EPIC data: $kT = 12.94 \pm 3.30 \text{ keV}$ vs. $kT = 2.0^{6.1}_{1.0} \text{ keV}$. The X-ray luminosities are also very different, with the SD05 value ($L_X = 32.37$) about 2 dex larger than the value obtained from our analysis and corrected for the different bands and distances. It is, therefore, likely that we observed the source in a state similar to the pre-flare state in the SD05 data.

Finally, the lightcurve of EPIC source #1 (our source #296) showed a remarkable rise in count rate during the XMM exposure, by a factor ≥ 7 in about 8 ks, and then began what appears a slow decay for the remaining 30 ks of the observation. An isothermal spectral fit gave a very high absorption, $N_{\text{H}} = 9.32 \pm 0.15 \times 10^{22} \text{ cm}^{-2}$, temperature, $kT = 10.38 \pm 0.54 \text{ keV}$, and total luminosity $L_X = 1.1 \times 10^{33} \text{ erg s}^{-1}$ (in the 1–10 keV band). From our ACIS data we derive a two order-of-magnitude lower luminosity $L_X = 1.1 \times 10^{31}$, a somewhat colder plasma, $kT = 4.8^{9.6}_{3.0} \text{ keV}$ and a 5-fold lower absorption $N_{\text{H}} = 1.9^{2.4}_{1.6} \times 10^{22} \text{ cm}^{-2}$. The lightcurve indicates a roughly linear decay of the count rate during the 100 ks of our observation from $\sim 6 \text{ cts ks}^{-1}$ to $\sim 2 \text{ cts ks}^{-1}$. We note that our value of N_{H} (90% confidence interval corresponding to $A_V = 10\text{--}15$) agrees roughly with the absorption SD05 derived for the source from NIR spectroscopy ($A_V = 15\text{--}20$) and, contrary to the value observed during the *XMM-Newton* exposure, does not imply a higher gas-to-dust ratio than in the interstellar medium. We speculate that the high absorption seen by SD05 was due to a solar-like CME associated with the flare as we have also speculated for our source #71 in Sect. 4.2.

7. Summary and conclusions

We observed NGC 2264 with *Chandra*-ACIS for 97 ks, detecting a total of 420 X-ray point sources. We identified 85% of the X-ray sources with known optical and NIR objects, while 67 sources remain with no counterparts in the considered optical/NIR catalogs. More than 90% of the 353 X-ray sources with counterparts are expected to be members of NGC 2264. Using H_α and optical variability data from the literature we selected a further sample of 83 X-ray undetected likely members in the FOV of our ACIS observation, bringing the census of likely

²⁷ In this section uncertainties quoted for quantities derived by SD05 are 1σ , while for our results we quote 90% confidence intervals.

members with optical/NIR counterparts to more than 400 stars. Taking the small estimated contamination from field stars into account, we have thus increased the known member census of the region by about 100 objects, mostly very low-mass stars, and including some candidate brown dwarfs. A further group of 10 X-ray sources, excluded from the member sample because their position in the optical CMD is discrepant with the cluster locus, is also likely to include members. Moreover, among the 67 sources with no optical/NIR counterparts, we argue that about half are previously unrecognized embedded members and good candidates for X-ray detected Class 0/I sources. The other half are instead likely associated with extragalactic objects. The coming *SPITZER* data will be very useful for clarifying the nature of each source and will allow a systematic study of X-ray activity in the protostellar phase.

We determined X-ray unabsorbed fluxes and luminosities for 326 sources for which absorption could be estimated, either from the X-ray spectra, from optical spectral types and photometry (Av), or from NIR photometry. With the aim of shedding light on PMS X-ray activity, we then performed a detailed study of X-ray lightcurves and spectra and studied the relation between the properties of X-ray emitting plasma and stellar/circumstellar characteristics. We confirm several previous findings: X-ray luminosity is related to bolometric luminosity and to stellar mass; L_X/L_{bol} is on average high and fairly independent of mass, other than for a possible drop at $\sim 2 M_\odot$ and a shallow decrease for $M/M_\odot \lesssim 0.3$. The mass- L_X relation appears to be better defined for WTTS than for CTTS, and CTTS have on average lower activity levels at any given bolometric luminosity and mass. We found tentative evidence that CTTS are more time variable with respect to WTTS, which might be related to the time-variable nature of the accretion process if it plays a role in the X-ray emission. With respect to spectral characteristics, the plasma on CTTS is on average slightly hotter than on WTTS, a finding possibly related to the higher variability of CTTS. However, we also observe that the sources with the coolest plasma are preferentially CTTS. Three CTTSs in particular appear to have plasma at ~ 0.1 – 0.2 keV, i.e. comparable to the temperatures expected for plasma heated by accretion shocks, as observed on TW Hydrea ($kT \sim 0.25$ keV, Kastner et al. 2002; Stelzer & Schmitt 2004). The estimated emission measures of this cool plasma are between 4 and 17 times larger than on TW Hydrea ($EM = 1.3 \times 10^{53} \text{ cm}^{-3}$), maybe as a result of the expected higher accretion rates of NGC 2264 stars. These results, taken as a whole, reinforce the mounting evidence that activity in low-mass PMS stars, while generally similar to that of saturated MS stars, is significantly affected by mass accretion. This influence has at least two aspects: accretion is, on one hand, a positive source of very soft X-ray emission produced in the accretion shock. On the other hand, it reduces the average energy output of coronae and makes the emission more time variable. Preibisch et al. (2005) discuss several possible explanations for the suppression of activity. They favor the idea that accretion modifies the magnetic field geometry and results in the “mass-loading” of field lines, thus hampering the heating of plasma to X-ray temperatures. It is at the same time conceivable that the resulting magnetic field structure will be less stable because of the the temporal variability of the mass accretion rate, as well as the rotational shear at the inner edge of the circumstellar disk. To tackle the so-far elusive activity-accretion relation, a better characterization of the circumstellar/accretion properties, e.g. measures of mass

accretion rates, is essential. Particularly useful in this respect would be contemporary observations in the X-ray band and in accretion/outflow sensitive optical/NIR lines.

Acknowledgements. The authors wish to thank the anonymous referee for comments that helped to improve this work and acknowledge financial support from the *Ministero dell’Istruzione dell’Università e della Ricerca*, PRIN-INAF and contract ASI-INAF I/023/05/0.

References

Alexander, D. M., Bauer, F. E., Brandt, W. N., et al. 2003, AJ, 126, 539
 Bally, J., Feigelson, E., & Reipurth, B. 2003, ApJ, 584, 843
 Barger, A. J., Cowie, L. L., Capak, P., et al. 2003, AJ, 126, 632
 Dahm, S. E., & Simon, T. 2005, AJ, 129, 829
 Damiani, F., Maggio, A., Micela, G., & Sciortino, S. 1997, ApJ, 483, 350
 Damiani, F., & Micela, G. 1995, ApJ, 446, 341
 Favata, F., & Schmitt, J. H. M. 1999, A&A, 350, 900
 Favata, F., Flaccomio, E., Reale, et al., ApJS, 160, 469
 Feigelson, E. D., & Nelson, P. I. 1985, ApJ, 293, 192
 Flaccomio, E., Micela, G., Sciortino, S., et al. 2000, A&A, 355, 651
 Flaccomio, E., Damiani, F., Micela, G., et al. 2003a, ApJ, 582, 398
 Flaccomio, E., Micela, G., & Sciortino, S. 2003b, A&A, 397, 611
 Flaccomio, E., Micela, G., & Sciortino, S. 2003c, A&A, 402, 277
 Flaccomio, E., Micela, G., Sciortino, S., et al. 2005, ApJS, 160, 450
 Getman, K. V., Flaccomio, E., Broos, P. S., et al. 2005, ApJS, 160, 319
 Glassgold, A. E., Najita, J., & Igea, J. 2004, ApJ, 615, 972
 Haisch, K. E., Jayawardhana, R., & Alves, J. 2005, ApJ, 627, L57
 Hamilton, C. M., Herbst, W., Vrba, F. J., et al. 2005, AJ, 130, 1896
 Herbst, W., & Moran, E. C. 2005, ApJ, 630, 400
 Igea, J., & Glassgold, A. E. 1999, ApJ, 518, 848
 Imanishi, K., Koyama, K., & Tsuboi, Y. 2001, ApJ, 557, 747
 Jardine, M., Collier Cameron, A., Donati, J., Gregory, S. G., & Wood, K. 2006, [arXiv:astro-ph/0601213]
 Kastner, J. H., Huenemoerder, D. P., Schulz, N. S., Canizares, C. R., & Weintraub, D. A. 2002, ApJ, 567, 434
 Kenyon, S. J., & Hartmann, L. 1995, ApJS, 101, 117
 Lada, C. J. 2006, [arXiv:astro-ph/0601375]
 Lamm, M. H., Bailer-Jones, C. A. L., Mundt, R., Herbst, W., & Scholz, A. 2004, A&A, 417, 557
 Lorenzani, A., & Palla, F. 2001, From Darkness to Light: Origin and Evolution of Young Stellar Clusters, ASP Conf. Ser., 243, 745
 Luhman, K. L. 1999, ApJ, 525, 466
 Margulies, M., Lada, C. J., & Young, E. T. 1989, ApJ, 345, 906
 Meyer, M. R., Calvet, N., & Hillenbrand, L. A. 1997, AJ, 114, 288
 Orlando, S., Peres, G., & Reale, F. 2001, ApJ, 560, 499
 Palla, F., & Stahler, S. W. 2000, ApJ, 540, 255
 Park, B., Sung, H., Bessell, M. S., & Kang, Y. H. 2000, AJ, 120, 894
 Peretto, N., André, P., & Belloche, A. 2006, A&A, 445, 979
 Pizzolato, N., Maggio, A., Micela, G., Sciortino, S., & Ventura, P. 2003, A&A, 397, 147
 Preibisch, T., Kim, Y.-C., Favata, Fabio, et al. 2005, ApJS, 160, 401
 Ramírez, S. V., Rebull, L., Stauffer, J., et al. 2004a, AJ, 127, 2659
 Ramírez, S. V., Rebull, L., Stauffer, J., et al. 2004b, AJ, 128, 787
 Rebull, L. M., Makidon, R. B., Strom, S. E., et al. 2002, AJ, 123, 1528
 Rebull, L. M., Stauffer, J. R., Ramirez, S. V., et al. 2006, [arXiv:astro-ph/0603027]
 Rieke, G. H., & Lebofsky, M. J. 1985, ApJ, 288, 618
 Salpeter, E. E. 1955, ApJ, 121, 16
 Schreyer, K., Stecklum, B., Linz, H., & Henning, T. 2003, ApJ, 599, 335
 Schmitt, J. H. M. M., & Liefke, C. 2004, A&A, 417, 651
 Schmitt, J. H. M. M., Robrade, J., Ness, J.-U., Favata, F., & Stelzer, B. 2005, A&A, 432, L35
 Siess, L., Dufour, E., & Forestini, M. 2000, A&A, 358, 593
 Simon, T., & Dahm, S. E. 2005, ApJ, 618, 795
 Stelzer, B., & Schmitt, J. H. M. M. 2004, A&A, 418, 687
 Sung, H., Bessell, M. S., & Lee, S.-W. 1997, AJ, 114, 2644
 Teixeira, P. S., et al. 2006, [arXiv:astro-ph/0511732]
 Vasilevskis, S., Sanders, W. L., Balz, A. G. A. J. 1965, AJ, 70, 797
 Vuong, M. H., Montmerle, T., Grossi, et al. 2003, A&A, 408, 581
 Walker, M. F. 1956, ApJS, 2, 365
 Williams, J. P., & Garland, C. A. 2002, ApJ, 568, 259
 Wilms, J., Allen, A., & McCray, R. 2000, ApJ, 542, 914
 Young, E. T., et al. 2006, [arXiv:astro-ph/0601300]

Online Material

Table 1. Catalog of X-ray ACIS detections.

N	RA [h m s]	Dec. [d m s.]	δ_{rd} ["]	Offax [']	Net Cts.	Exp. T. [s]	Signif	P_{KS}	n_H [10^{22}cm^{-2}]	n_H (Ref)	Mod	F_X [u] [ergs/s/cm^2]
1	6:40:25.8	9:29:24.0	3.14	9.5	25.1	80579	6.1	0.088	1.59	JHK	—	-14.03
2	6:40:27.7	9:32:00.1	1.52	8.0	81.2	82888	16.2	0.262	0.00	Av	1T	-14.35
3	6:40:28.1	9:35:33.7	1.37	7.7	44.7	81810	9.0	0.032	0.00	Av	—	-14.52
4	6:40:28.6	9:35:47.3	1.22	7.6	186.6	64151	29.6	0.000	0.10	Av	1T	-13.69
5	6:40:28.8	9:30:59.6	0.59	8.1	1222.2	82889	70.2	0.000	0.26	Av	2T	-12.74
6	6:40:28.8	9:33:05.3	0.80	7.5	111.0	83404	17.7	0.579	0.00	Av	1T	-14.12
7	6:40:30.6	9:38:37.7	1.84	8.2	11.1	82255	4.7	0.724	—	—	—	—
8	6:40:30.9	9:34:40.4	0.92	6.9	179.1	83958	25.7	0.001	0.62	X	1T	-13.48
9	6:40:31.2	9:31:07.0	0.71	7.5	506.4	84042	45.7	0.093	0.09	Av	2T	-13.31
10	6:40:31.7	9:33:28.9	1.64	6.7	18.9	84683	6.0	0.045	0.00	JHK	—	-14.91
11	6:40:31.8	9:36:00.6	0.90	6.9	180.4	65959	27.9	0.171	0.10	JHK	1T	-13.75
12	6:40:31.9	9:32:16.6	1.42	6.9	35.1	84807	9.3	0.262	—	—	—	—
13	6:40:32.9	9:41:51.3	2.49	9.9	81.1	74590	10.6	0.096	1.66	X	1T	-13.45
14	6:40:33.5	9:34:58.6	0.86	6.3	67.9	84974	14.4	0.007	0.00	Av	1T	-14.43
15	6:40:33.6	9:33:36.2	0.73	6.2	34.0	82415	10.0	0.327	0.00	JHK	—	-14.64
16	6:40:34.3	9:39:17.6	1.60	7.9	26.4	82947	7.2	0.845	—	—	—	—
17	6:40:34.5	9:35:18.0	0.72	6.1	140.7	84911	21.8	0.466	0.07	Av	2T	-13.82
18	6:40:35.0	9:39:54.8	2.17	8.2	29.0	82369	7.0	0.700	—	—	—	—
19	6:40:36.2	9:40:01.6	1.60	8.0	78.3	82640	14.6	0.116	0.00	X	1T	-14.31
20	6:40:36.3	9:28:04.2	2.17	8.3	34.8	83176	7.2	0.697	0.00	JHK	—	-14.64
21	6:40:36.3	9:40:36.9	4.46	8.4	19.8	81817	4.9	0.320	—	—	—	—
22	6:40:36.3	9:43:07.9	3.31	10.5	22.8	76153	4.8	0.189	—	—	—	—
23	6:40:36.8	9:37:30.4	1.27	6.3	18.9	80653	6.0	0.836	—	—	—	—
24	6:40:36.9	9:32:37.5	0.76	5.6	2.6	86958	4.9	0.829	—	—	—	—
25	6:40:37.0	9:39:09.7	0.90	7.3	185.5	82420	27.3	0.000	0.14	Av	1T	-13.77
26	6:40:37.2	9:31:09.8	0.65	6.1	157.2	86607	26.9	0.562	0.16	JHK	2T	-13.80
27	6:40:37.7	9:39:39.5	1.12	7.5	86.7	81358	17.2	0.418	0.07	Av	1T	-14.18
28	6:40:37.8	9:41:23.9	6.32	8.8	14.1	80327	5.0	0.053	—	—	—	—
29	6:40:37.8	9:35:56.5	0.43	5.4	303.4	85489	32.9	0.000	0.00	X	2T	-13.51
30	6:40:37.9	9:34:54.1	0.34	5.2	651.1	86838	54.4	0.000	0.00	Av	1T	-13.33
31	6:40:38.1	9:31:34.6	0.98	5.7	6.7	87213	5.4	0.277	—	—	—	—
32	6:40:38.2	9:29:52.5	0.91	6.7	47.2	82997	13.0	0.376	0.06	Av	—	-14.43
33	6:40:38.7	9:36:56.9	0.59	5.6	99.5	84957	17.0	0.989	0.00	Av	1T	-14.22
34	6:40:38.7	9:34:35.3	0.95	5.0	13.8	87525	5.9	0.968	0.00	JHK	—	-15.06
35	6:40:38.8	9:29:48.0	0.88	6.6	14.5	81981	6.1	0.915	—	—	—	—
36	6:40:39.0	9:35:59.7	0.67	5.2	131.6	82279	25.5	0.381	0.02	Av	1T	-14.06
37	6:40:39.2	9:29:30.4	0.96	6.7	17.9	78920	5.8	0.133	—	—	—	—
38	6:40:39.3	9:34:45.9	0.70	4.8	32.3	87604	10.4	0.228	0.40	Av	—	-14.32
39	6:40:40.1	9:35:02.9	0.41	4.7	256.6	87545	34.5	0.251	0.00	X	1T	-13.80
40	6:40:40.4	9:31:34.1	0.72	5.2	9.7	81618	6.0	0.022	0.00	JHK	—	-15.19
41	6:40:40.5	9:35:05.5	0.61	4.6	18.5	87679	7.4	0.586	—	—	—	—
42	6:40:40.5	9:38:25.6	1.11	6.1	19.6	84592	7.8	0.190	—	—	—	—
43	6:40:40.5	9:35:00.5	0.52	4.6	18.2	87764	6.6	0.988	—	—	—	—
44	6:40:40.8	9:34:26.4	0.54	4.4	4.2	88477	5.4	0.514	0.00	JHK	—	-15.59
45	6:40:40.9	9:27:59.3	0.76	7.6	120.4	84578	19.8	0.000	0.00	Av	1T	-14.05
46	6:40:41.1	9:33:57.6	0.74	4.3	7.7	88601	5.4	0.372	0.00	JHK	—	-15.32
47	6:40:41.2	9:31:28.2	0.74	5.1	7.2	84892	5.5	0.136	—	—	—	—
48	6:40:41.3	9:39:09.4	1.07	6.5	30.5	80858	9.2	0.149	—	—	—	—
49	6:40:41.6	9:31:43.7	0.66	4.9	18.3	84535	6.5	0.425	0.11	Av	—	-14.79
50	6:40:41.8	9:41:37.9	2.10	8.5	37.4	81767	7.5	0.289	0.00	JHK	—	-14.60
51	6:40:42.1	9:31:42.1	0.75	4.8	29.5	88745	9.6	0.609	0.00	JHK	—	-14.74
52	6:40:42.2	9:33:37.5	0.33	4.1	166.0	86733	27.1	0.145	0.00	Av	1T	-13.99
53	6:40:42.2	9:40:11.1	0.74	7.2	412.4	78154	42.1	0.000	0.00	Av	1T	-13.51
54	6:40:42.3	9:39:20.9	0.62	6.5	630.7	83614	59.7	0.000	0.00	JHK	2T	-13.30
55	6:40:42.3	9:34:25.0	0.51	4.1	87.5	83977	22.6	0.000	0.00	JHK	1T	-14.28
56	6:40:42.4	9:32:20.4	0.30	4.4	257.7	87293	34.9	0.000	0.09	Av	2T	-13.61
57	6:40:42.8	9:33:35.2	0.45	4.0	26.6	85404	8.2	0.148	0.21	Av	—	-14.53
58	6:40:42.8	9:39:05.8	1.26	6.2	12.4	86213	5.8	0.764	—	—	—	—
59	6:40:43.2	9:31:14.8	0.39	4.9	295.0	88980	40.4	0.000	0.09	Av	2T	-13.49
60	6:40:43.4	9:30:34.3	0.70	5.3	37.2	88511	10.8	0.136	0.29	Av	—	-14.34

Table 1. (Continued)

N	RA [h m s]	Dec. [d m s].	$\delta_{r,d}$ ["]	Offax ['']	Net Cts.	Exp. T. [s]	Signif	P_{KS}	n_H [10^{22}cm^{-2}]	n_H (Ref)	Mod	$F_X[\text{u}]$ [ergs/s/cm^2]
61	6:40:43.4	9:28:40.7	0.92	6.7	148.9	86266	26.3	0.725	0.00	X	1T	-14.03
62	6:40:43.6	9:37:20.1	0.84	4.9	17.7	82740	7.5	0.446	0.00	JHK	-	-14.93
63	6:40:43.6	9:31:14.3	1.04	4.8	16.5	89123	5.0	0.691	-	-	-	-
64	6:40:43.7	9:35:10.2	0.29	3.8	6.7	37810	5.3	0.276	0.00	JHK	-	-15.01
65	6:40:43.7	9:38:35.5	0.54	5.7	326.4	87242	40.5	0.000	0.00	JHK	2T	-13.58
66	6:40:43.8	9:28:55.2	1.36	6.5	33.9	86733	9.7	0.345	0.00	JHK	-	-14.67
67	6:40:44.2	9:36:35.8	0.53	4.3	12.7	85869	5.6	0.589	-	-	-	-
68	6:40:44.6	9:32:26.2	0.43	3.9	65.4	90018	16.5	0.136	0.04	Av	1T	-14.42
69	6:40:44.7	9:34:04.5	0.41	3.5	8.3	90100	5.1	0.784	-	-	-	-
70	6:40:45.0	9:38:49.3	0.86	5.7	16.4	79465	7.0	0.325	-	-	-	-
71	6:40:45.2	9:28:44.5	0.58	6.4	291.4	86894	34.9	0.000	1.93	X	1T	-13.00
72	6:40:45.9	9:38:44.3	0.94	5.5	17.4	81482	6.1	0.585	0.00	JHK	-	-14.93
73	6:40:45.9	9:26:44.1	2.63	8.1	9.6	80056	4.6	0.222	-	-	-	-
74	6:40:46.7	9:40:22.2	1.35	6.8	38.0	73992	11.0	0.912	-	-	-	-
75	6:40:46.9	9:32:30.9	0.36	3.4	95.6	90968	22.6	0.328	0.00	Av	1T	-14.30
76	6:40:46.9	9:33:01.1	2.38	3.2	4.0	91067	5.1	0.590	1.80	JHK	-	-14.84
77	6:40:47.1	9:30:20.0	1.02	4.8	6.3	89567	4.7	0.394	0.00	JHK	-	-15.41
78	6:40:47.1	9:32:40.0	0.23	3.3	571.0	91121	58.7	0.004	0.00	Av	2T	-13.40
79	6:40:47.1	9:42:08.5	1.89	8.4	15.1	74097	5.0	0.919	0.01	Av	-	-14.95
80	6:40:47.2	9:31:08.9	0.64	4.2	13.3	90300	6.7	0.494	0.00	Av	-	-15.09
81	6:40:47.6	9:40:33.5	1.35	6.9	15.8	82215	5.2	0.233	0.00	JHK	-	-14.97
82	6:40:47.8	9:26:45.1	1.31	8.0	47.1	84535	11.2	0.581	-	-	-	-
83	6:40:47.9	9:33:03.0	0.27	2.9	98.4	91483	20.6	0.013	0.00	JHK	1T	-14.16
84	6:40:48.0	9:32:03.2	0.57	3.4	6.9	91185	4.7	0.682	0.00	JHK	-	-15.38
85	6:40:48.1	9:34:05.4	0.56	2.6	10.8	91488	5.1	0.037	0.00	JHK	-	-15.19
86	6:40:48.1	9:27:01.1	1.48	7.7	26.9	84955	8.1	0.330	0.00	Av	-	-14.76
87	6:40:48.3	9:36:38.5	0.23	3.5	538.7	87849	54.9	0.000	0.00	X	1T	-13.42
88	6:40:48.5	9:34:16.6	0.61	2.5	15.4	91546	7.4	0.875	0.00	JHK	-	-15.03
89	6:40:48.6	9:35:57.4	0.24	3.0	150.3	92107	25.8	0.232	1.65	JHK	1T	-13.35
90	6:40:48.6	9:32:52.3	0.21	2.8	246.1	91775	33.8	0.000	0.10	Av	2T	-13.67
91	6:40:48.8	9:32:42.5	0.23	2.9	165.9	91786	28.7	0.135	0.27	Av	1T	-13.74
92	6:40:49.0	9:36:55.1	0.99	3.6	7.9	91255	4.9	0.426	-	-	-	-
93	6:40:49.1	9:37:36.2	0.57	4.1	27.3	86242	9.3	0.740	0.17	JHK	-	-14.55
94	6:40:49.5	9:31:41.5	0.77	3.4	16.9	84088	8.9	0.554	-	-	-	-
95	6:40:49.9	9:36:49.2	0.35	3.4	114.7	91665	23.9	0.776	0.19	Av	1T	-14.02
96	6:40:50.1	9:29:32.4	1.63	5.2	14.2	89256	6.1	0.272	-	-	-	-
97	6:40:50.1	9:30:39.7	0.36	4.2	121.1	90500	23.5	0.000	0.22	X	1T	-13.81
98	6:40:50.5	9:32:19.6	0.27	2.8	100.1	88572	20.8	0.297	2.68	X	1T	-13.43
99	6:40:50.6	9:31:31.1	0.51	3.4	8.9	91357	6.0	0.842	0.00	JHK	-	-15.27
100	6:40:50.8	9:41:55.9	1.20	7.9	27.5	83075	7.4	0.718	0.00	JHK	-	-14.74
101	6:40:51.0	9:38:52.8	0.74	5.0	38.6	88762	10.0	0.532	-	-	-	-
102	6:40:51.3	9:43:19.2	2.24	9.3	88.2	76964	5.5	0.034	0.09	Av	1T	-14.01
103	6:40:51.4	9:30:13.4	0.58	4.4	22.6	90340	8.5	0.160	0.00	Av	-	-14.86
104	6:40:51.5	9:37:14.2	0.38	3.5	78.5	91576	20.2	0.026	0.00	Av	2T	-14.30
105	6:40:51.6	9:28:44.5	0.57	5.8	267.5	88272	35.7	0.189	0.23	Av	1T	-13.52
106	6:40:52.1	9:29:13.8	0.53	5.3	105.6	89254	21.2	0.280	0.00	Av	2T	-14.03
107	6:40:52.6	9:29:53.4	0.51	4.6	113.6	90240	22.4	0.423	2.86	X	1T	-13.40
108	6:40:52.9	9:35:15.2	0.25	1.8	107.2	90348	23.8	0.031	2.80	X	1T	-13.33
109	6:40:53.2	9:29:54.3	0.67	4.5	6.7	90369	5.8	0.070	0.00	JHK	-	-15.39
110	6:40:53.6	9:36:45.6	0.47	2.8	9.6	87693	6.4	0.617	0.00	JHK	-	-15.22
111	6:40:53.6	9:33:24.6	0.18	1.5	365.2	93281	45.8	0.016	0.12	Av	2T	-13.40
112	6:40:53.8	9:30:38.8	0.30	3.8	195.2	91356	32.2	0.777	0.03	Av	2T	-13.86
113	6:40:53.9	9:38:04.8	0.58	4.0	1.7	90692	5.2	0.002	-	-	-	-
114	6:40:54.1	9:29:51.0	0.31	4.5	726.9	90475	66.7	0.000	0.00	JHK	2T	-13.28
115	6:40:54.7	9:31:58.9	0.55	2.5	6.1	93115	4.8	0.027	-	-	-	-
116	6:40:55.2	9:33:18.6	0.45	1.3	10.7	93618	6.8	0.790	0.00	Av	-	-15.20
117	6:40:55.2	9:30:16.6	0.69	4.1	7.8	91188	5.4	0.070	-	-	-	-
118	6:40:55.3	9:33:24.6	0.32	1.2	18.5	93618	8.2	0.007	0.00	JHK	-	-14.96
119	6:40:55.3	9:39:59.0	0.72	5.8	110.1	87488	21.5	0.040	0.20	Av	1T	-13.97
120	6:40:55.4	9:37:23.4	0.26	3.3	362.5	92186	44.2	0.170	0.12	Av	2T	-13.48

Table 1. (Continued)

N	RA [h m s]	Dec. [d m s.]	$\delta_{r,d}$ ["]	Offax ['']	Net Cts.	Exp. T. [s]	Signif	P_{KS}	n_H [10^{22}cm^{-2}]	n_H (Ref)	Mod	F_x [u] [ergs/s/cm^2]
121	6:40:55.5	9:31:21.8	0.57	3.0	14.2	92455	8.2	0.773	0.00	JHK	—	-15.07
122	6:40:55.5	9:38:38.7	0.92	4.5	11.9	86476	6.0	0.000	0.00	JHK	—	-15.12
123	6:40:55.6	9:38:24.5	0.48	4.2	19.8	86203	6.8	0.144	0.02	Av	—	-14.89
124	6:40:55.8	9:40:18.0	0.52	6.1	426.1	86940	42.9	0.000	0.00	Av	2T	-13.33
125	6:40:55.8	9:36:05.8	0.48	2.0	8.2	94475	6.5	0.047	—	—	—	—
126	6:40:55.9	9:37:17.4	0.36	3.1	35.9	92447	11.2	0.370	0.00	Av	—	-14.67
127	6:40:56.2	9:36:30.7	0.22	2.4	207.3	93839	32.1	0.040	0.90	X	1T	-13.39
128	6:40:56.2	9:40:37.6	1.35	6.4	9.0	86359	5.0	0.905	0.00	JHK	—	-15.24
129	6:40:56.3	9:39:33.1	2.22	5.3	12.1	84741	6.0	0.850	0.07	Av	—	-15.02
130	6:40:56.3	9:34:17.9	0.30	0.6	49.5	93507	16.9	0.985	0.00	JHK	—	-14.53
131	6:40:56.4	9:35:53.1	0.42	1.7	16.4	93022	8.5	0.101	0.44	Av	—	-14.62
132	6:40:56.5	9:29:53.6	0.69	4.4	30.3	90643	11.4	0.895	0.00	Av	—	-14.73
133	6:40:56.8	9:30:14.8	0.42	4.0	194.5	91106	32.9	0.006	0.00	X	1T	-13.91
134	6:40:56.8	9:29:59.4	0.64	4.3	14.4	75335	6.8	0.625	0.11	Av	—	-14.84
135	6:40:56.8	9:37:48.9	0.21	3.6	839.4	91676	66.2	0.000	0.11	Av	2T	-13.13
136	6:40:57.0	9:33:01.2	0.17	1.3	150.3	93963	26.3	0.907	0.29	Av	1T	-13.82
137	6:40:57.5	9:29:23.4	0.89	4.9	42.0	37661	13.5	0.481	0.00	JHK	—	-14.21
138	6:40:57.5	9:26:16.6	1.64	8.0	15.2	82088	6.4	0.563	0.00	JHK	—	-14.99
139	6:40:57.6	9:37:07.1	0.29	2.9	14.7	91165	6.0	0.876	0.00	Av	—	-15.05
140	6:40:57.7	9:31:50.0	0.29	2.4	21.6	93553	9.2	0.129	0.00	Av	—	-14.90
141	6:40:57.7	9:36:08.0	0.27	1.9	70.6	90901	19.7	0.145	2.62	X	1T	-13.44
142	6:40:57.8	9:30:50.3	0.22	3.4	244.2	55899	31.1	0.444	0.21	Av	1T	-13.42
143	6:40:57.9	9:41:20.0	1.71	7.1	48.5	80975	11.6	0.923	0.10	Av	—	-14.35
144	6:40:57.9	9:27:09.0	1.70	7.1	13.3	84375	5.4	0.146	—	—	—	—
145	6:40:58.0	9:36:39.2	0.55	2.4	11.8	89724	5.4	0.192	—	—	—	—
146	6:40:58.1	9:36:52.8	0.31	2.6	26.2	89301	8.7	0.258	0.33	JHK	—	-14.46
147	6:40:58.3	9:37:56.6	0.36	3.7	34.9	89715	10.3	0.395	0.00	JHK	—	-14.67
148	6:40:58.4	9:27:24.9	1.20	6.8	51.7	85243	13.4	0.049	0.00	JHK	—	-14.48
149	6:40:58.5	9:33:31.6	0.10	0.7	3194.7	94186	147.2	0.000	0.00	JHK	2T	-12.55
150	6:40:58.6	9:36:39.2	0.49	2.4	7.3	90740	6.0	0.360	—	—	—	—
151	6:40:58.7	9:36:13.0	0.15	2.0	781.5	94749	66.1	0.000	0.04	Av	1T	-13.22
152	6:40:58.8	9:34:05.3	0.41	0.1	16.3	94144	8.9	0.078	—	—	—	—
153	6:40:58.8	9:42:24.6	1.49	8.2	10.0	78820	4.7	0.951	0.00	JHK	—	-15.16
154	6:40:58.8	9:30:57.1	0.23	3.3	205.4	43709	27.2	0.732	0.09	Av	2T	-13.35
155	6:40:58.8	9:39:18.4	0.46	5.1	202.2	86462	28.1	0.055	0.00	X	1T	-13.85
156	6:40:58.9	9:36:46.0	0.36	2.5	28.8	89311	11.2	0.234	—	—	—	—
157	6:40:58.9	9:28:52.8	0.62	5.4	43.8	88230	14.1	0.224	0.07	JHK	—	-14.47
158	6:40:59.1	9:33:22.2	0.97	0.9	8.1	94226	4.8	0.309	—	—	—	—
159	6:40:59.2	9:31:50.4	0.34	2.4	14.1	40232	6.6	0.954	0.67	JHK	—	-14.22
160	6:40:59.3	9:33:25.5	0.50	0.8	7.9	94258	5.6	0.501	—	—	—	—
161	6:40:59.3	9:35:52.2	0.22	1.6	161.4	95208	30.4	0.772	2.37	JHK	1T	-13.29
162	6:40:59.3	9:35:56.8	0.28	1.7	63.1	95135	18.1	0.362	2.73	X	1T	-13.39
163	6:40:59.4	9:33:33.2	0.16	0.7	205.9	94283	31.5	0.062	0.30	JHK	1T	-13.65
164	6:40:59.5	9:29:51.5	0.49	4.4	40.1	89447	11.9	0.058	0.00	Av	—	-14.61
165	6:40:59.5	9:36:10.2	0.24	1.9	127.1	94907	26.6	0.157	3.02	X	1T	-13.15
166	6:40:59.5	9:39:06.2	0.57	4.9	10.8	80058	5.1	0.739	0.19	JHK	—	-14.91
167	6:40:59.5	9:35:10.7	0.14	1.0	1067.6	95643	83.0	0.486	0.30	Av	2T	-12.91
168	6:40:59.5	9:35:51.7	0.45	1.6	11.1	95228	7.1	0.297	—	—	—	—
169	6:40:59.6	9:36:57.5	0.50	2.7	10.0	93518	5.9	0.296	0.01	Av	—	-15.23
170	6:40:59.7	9:28:43.3	0.84	5.5	23.1	89213	7.9	0.370	0.22	JHK	—	-14.60
171	6:40:60.0	9:35:00.7	0.28	0.8	4.0	91008	5.0	0.419	—	—	—	—
172	6:40:60.0	9:28:50.1	0.30	5.4	1122.7	86974	69.8	0.000	0.05	Av	2T	-13.02
173	6:41:00.2	9:36:30.9	0.67	2.3	9.2	94348	5.4	0.416	2.17	JHK	—	-14.44
174	6:41:00.3	9:35:58.9	0.33	1.8	39.3	95166	13.0	0.337	—	—	—	—
175	6:41:00.4	9:41:15.5	0.99	7.0	9.2	83011	5.3	0.660	0.00	JHK	—	-15.21
176	6:41:00.5	9:29:15.9	0.30	5.0	879.5	88795	66.9	0.122	0.23	X	1T	-13.00
177	6:41:00.5	9:36:12.2	0.38	2.0	27.1	94913	10.5	0.489	1.41	JHK	—	-14.11
178	6:41:00.6	9:36:09.9	0.25	2.0	115.9	94978	24.5	0.237	0.35	X	1T	-13.75
179	6:41:01.0	9:32:44.4	0.15	1.6	835.4	95245	73.3	0.000	0.13	JHK	2T	-13.10
180	6:41:01.0	9:29:37.4	0.59	4.6	4.4	89533	4.8	0.200	—	—	—	—

Table 1. (Continued)

N	RA [h m s]	Dec. [d m s].	$\delta_{r,d}$ ["]	Offax [']	Net Cts.	Exp. T. [s]	Signif	P_{KS}	n_H [10^{22}cm^{-2}]	n_H (Ref)	Mod	$F_X[\text{u}]$ [ergs/s/cm^2]
181	6:41:01.1	9:34:52.1	0.22	0.9	147.1	49970	30.0	0.435	0.00	X	1T	-13.80
182	6:41:01.2	9:36:09.2	0.29	2.0	67.0	92952	17.8	0.002	2.97	X	1T	-13.20
183	6:41:01.3	9:34:52.5	0.26	0.9	80.9	36893	22.7	0.432	0.04	X	2T	-13.70
184	6:41:01.4	9:34:08.1	0.18	0.7	333.0	49310	44.8	0.556	0.04	Av	2T	-13.35
185	6:41:01.6	9:28:13.2	0.59	6.1	226.4	88904	33.2	0.070	0.08	Av	2T	-13.70
186	6:41:01.7	9:32:60.0	0.26	1.4	15.9	87754	6.8	0.555	—	—	—	—
187	6:41:01.8	9:38:40.7	0.37	4.5	380.9	90472	43.5	0.248	0.00	X	2Tab	-13.62
188	6:41:02.0	9:38:32.9	0.72	4.4	25.5	90706	10.8	0.199	—	—	—	—
189	6:41:02.3	9:27:23.7	0.67	6.9	198.1	87370	26.1	0.002	0.19	X	1T	-13.70
190	6:41:02.5	9:34:55.6	0.16	1.2	614.0	82782	61.2	0.073	0.00	X	1T	-13.37
191	6:41:02.6	9:36:39.7	0.38	2.6	19.2	47017	10.0	0.247	0.00	JHK	—	-14.65
192	6:41:02.6	9:36:15.3	0.24	2.2	140.9	41221	25.3	0.110	2.17	X	1T	-12.63
193	6:41:02.6	9:35:12.9	0.15	1.4	794.4	65563	69.2	0.000	0.06	Av	2T	-13.02
194	6:41:02.8	9:36:16.0	0.26	2.3	114.0	26949	22.5	0.034	2.57	X	1T	-12.72
195	6:41:02.8	9:35:34.5	0.50	1.7	10.9	60549	5.7	0.016	—	—	—	—
196	6:41:02.9	9:27:23.4	0.86	6.9	89.9	87361	15.6	0.352	0.00	JHK	1T	-14.24
197	6:41:03.0	9:37:36.0	0.58	3.5	55.7	56589	16.9	0.377	0.49	Av	1T	-13.89
198	6:41:03.1	9:30:55.6	0.74	3.5	5.1	93271	4.6	0.685	—	—	—	—
199	6:41:03.1	9:35:44.7	0.22	1.9	211.7	80125	32.5	0.338	3.17	JHK	1T	-12.85
200	6:41:03.2	9:26:03.0	1.02	8.3	126.5	79331	20.4	0.000	0.21	Av	1T	-13.89
201	6:41:03.2	9:32:55.0	0.38	1.7	19.8	92136	10.1	0.580	0.00	JHK	—	-14.93
202	6:41:03.4	9:36:04.6	0.28	2.2	87.2	72148	19.6	0.239	0.22	Av	1T	-13.93
203	6:41:03.4	9:40:44.6	1.32	6.6	116.1	86490	22.7	0.597	0.00	Av	1T	-14.05
204	6:41:03.4	9:30:05.0	0.40	4.3	240.6	92050	37.8	0.000	0.00	JHK	1T	-13.79
205	6:41:03.4	9:32:11.7	0.28	2.4	64.9	92215	18.3	0.003	0.00	JHK	1T	-14.24
206	6:41:03.5	9:31:18.4	0.12	3.2	2022.9	93781	99.8	0.027	0.04	Av	2T	-12.84
207	6:41:03.6	9:30:29.0	0.25	3.9	147.6	92621	23.5	0.941	0.23	JHK	1T	-13.82
208	6:41:03.6	9:36:04.3	0.32	2.2	55.2	88076	13.3	0.057	1.18	X	1T	-13.56
209	6:41:03.6	9:35:43.4	0.27	1.9	9.3	89314	6.2	0.677	—	—	—	—
210	6:41:03.7	9:28:20.1	0.71	6.0	37.7	89118	11.0	0.985	0.20	Av	—	-14.40
211	6:41:03.7	9:27:24.4	1.49	6.9	39.1	87375	8.5	0.000	—	—	—	—
212	6:41:03.7	9:27:39.8	0.84	6.7	215.0	87862	32.2	0.113	0.24	Av	2T	-13.45
213	6:41:03.9	9:37:11.0	0.42	3.2	54.0	50872	16.2	0.132	1.43	JHK	—	-13.53
214	6:41:04.0	9:28:24.5	0.68	6.0	53.3	89246	12.0	0.055	0.00	JHK	—	-14.48
215	6:41:04.1	9:33:48.6	0.36	1.4	27.1	93012	11.4	0.411	—	—	—	—
216	6:41:04.1	9:35:21.0	0.20	1.7	279.0	94048	40.7	0.516	0.00	Av	2T	-13.73
217	6:41:04.2	9:34:57.1	0.32	1.5	47.2	94252	15.7	0.147	0.00	JHK	—	-14.56
218	6:41:04.2	9:28:40.6	0.72	5.7	36.2	89741	10.6	0.004	0.00	JHK	—	-14.65
219	6:41:04.2	9:36:55.4	0.41	3.0	19.5	86457	8.4	0.756	0.00	JHK	—	-14.91
220	6:41:04.3	9:35:33.1	0.51	1.9	8.0	93908	5.4	0.000	0.85	JHK	—	-14.78
221	6:41:04.3	9:35:47.5	0.31	2.1	46.1	93673	15.3	0.000	0.14	Av	—	-14.40
222	6:41:04.3	9:34:56.1	0.29	1.5	6.4	94256	4.8	0.947	—	—	—	—
223	6:41:04.4	9:27:30.1	1.13	6.9	29.3	81902	7.6	0.029	0.00	JHK	—	-14.71
224	6:41:04.4	9:32:57.3	0.48	1.9	8.7	95281	6.3	0.992	—	—	—	—
225	6:41:04.4	9:36:43.1	0.46	2.9	19.3	87411	7.2	0.431	0.00	JHK	—	-14.92
226	6:41:04.5	9:30:13.4	0.37	4.3	99.7	92221	21.9	0.331	0.00	JHK	1T	-14.24
227	6:41:04.6	9:26:09.5	1.45	8.2	110.0	83905	18.9	0.019	0.04	Av	1T	-14.05
228	6:41:04.6	9:36:18.0	0.27	2.5	276.8	92907	40.1	0.000	6.18	X	1T	-12.72
229	6:41:04.7	9:36:26.5	0.18	2.7	505.5	92660	47.6	0.016	0.06	Av	2T	-13.44
230	6:41:05.0	9:42:15.3	1.22	8.2	16.1	83504	7.3	0.367	—	—	—	—
231	6:41:05.1	9:33:00.2	0.16	2.0	200.1	95369	30.0	0.068	0.08	Av	1T	-13.85
232	6:41:05.2	9:36:31.5	0.51	2.8	11.9	92482	5.8	0.784	—	—	—	—
233	6:41:05.2	9:38:08.7	0.89	4.2	13.7	83965	6.6	0.496	—	—	—	—
234	6:41:05.4	9:33:13.4	0.11	1.9	2972.0	95370	136.8	0.000	0.06	X	2Tab	-12.60
235	6:41:05.4	9:36:30.6	0.26	2.8	118.6	92469	21.4	0.659	4.79	X	1T	-13.00
236	6:41:05.5	9:36:26.4	0.42	2.8	24.4	92575	8.0	0.026	—	—	—	—
237	6:41:05.5	9:34:08.0	0.49	1.7	9.3	40322	5.9	0.107	—	—	—	—
238	6:41:05.5	9:31:40.5	0.21	3.1	228.5	94022	33.1	0.538	0.11	Av	1T	-13.74
239	6:41:05.6	9:35:44.3	0.35	2.3	36.1	93578	11.6	0.259	—	—	—	—
240	6:41:05.7	9:31:01.3	0.18	3.7	565.1	93179	48.4	0.192	0.24	Av	2T	-13.01

Table 1. (Continued)

N	RA [h m s]	Dec. [d m s.]	$\delta_{r,d}$ ["]	Offax ['']	Net Cts.	Exp. T. [s]	Signif	P_{KS}	n_H [10^{22}cm^{-2}]	n_H (Ref)	Mod	F_X [u] [ergs/s/cm^2]
241	6:41:05.8	9:36:31.9	0.32	2.9	62.7	92395	14.8	0.001	0.33	X	1T	-14.12
242	6:41:05.8	9:35:29.3	0.22	2.1	195.5	93851	29.8	0.000	3.98	JHK	1T	-12.71
243	6:41:05.8	9:31:07.2	0.57	3.6	22.9	93296	9.0	0.048	—	—	—	—
244	6:41:05.9	9:34:45.8	0.15	1.8	807.5	94328	65.4	0.000	2.22	X	1T	-12.57
245	6:41:05.9	9:27:17.7	1.00	7.2	115.2	85076	20.8	0.004	0.09	Av	1T	-14.03
246	6:41:06.0	9:31:39.8	0.23	3.1	185.5	93948	29.0	0.000	0.17	X	1T	-13.78
247	6:41:06.0	9:35:51.3	0.54	2.4	17.1	93359	8.7	0.882	0.00	JHK	—	-15.00
248	6:41:06.1	9:34:46.1	0.20	1.9	131.0	94325	19.0	0.308	2.30	X	1T	-13.24
249	6:41:06.2	9:36:22.8	0.17	2.8	2175.5	92576	117.6	0.000	0.08	Av	2T	-12.72
250	6:41:06.2	9:33:08.8	0.25	2.1	100.4	95303	24.7	0.513	0.00	Av	1T	-14.26
251	6:41:06.2	9:29:40.1	0.74	4.9	27.0	87393	9.9	0.125	1.34	JHK	—	-14.09
252	6:41:06.3	9:29:30.9	0.52	5.1	107.4	87559	22.2	0.066	0.21	Av	1T	-13.99
253	6:41:06.3	9:37:07.8	0.43	3.4	21.3	91322	8.3	0.059	—	—	—	—
254	6:41:06.4	9:28:38.9	0.59	5.9	78.5	89488	16.8	0.518	0.02	Av	1T	-14.32
255	6:41:06.4	9:26:58.9	0.57	7.5	1299.4	84665	75.7	0.000	0.95	X	1T	-12.51
256	6:41:06.5	9:38:37.2	0.60	4.8	19.2	88794	7.8	0.000	—	—	—	—
257	6:41:06.5	9:36:05.2	0.19	2.7	389.8	92966	39.8	0.000	3.82	X	1T	-12.75
258	6:41:06.6	9:35:45.0	0.41	2.5	19.0	93372	8.8	0.477	0.00	Av	—	-14.95
259	6:41:06.7	9:33:54.2	0.41	2.0	5.1	91547	4.7	0.877	—	—	—	—
260	6:41:06.7	9:34:45.8	0.27	2.0	82.8	94300	20.2	0.316	0.81	JHK	1T	-13.89
261	6:41:06.8	9:27:32.2	0.53	7.0	1472.9	84815	87.4	0.000	0.00	JHK	2T	-12.94
262	6:41:06.9	9:40:54.0	1.85	7.0	13.8	47475	5.8	0.672	0.10	JHK	—	-14.66
263	6:41:06.9	9:29:23.8	0.58	5.2	73.4	89616	17.2	0.949	0.21	Av	1T	-14.24
264	6:41:07.1	9:30:36.6	0.47	4.2	46.2	88779	13.3	0.000	—	—	—	—
265	6:41:07.2	9:27:47.8	0.50	6.8	534.2	86916	47.4	0.082	0.00	Av	1T	-13.46
266	6:41:07.2	9:42:24.1	2.25	8.4	19.1	38497	4.7	0.240	0.00	JHK	—	-14.56
267	6:41:07.3	9:36:59.4	0.31	3.5	1.6	91451	4.6	0.324	—	—	—	—
268	6:41:07.3	9:31:18.0	0.36	3.6	98.1	87202	21.8	0.000	0.00	JHK	1T	-14.28
269	6:41:07.3	9:25:55.1	1.00	8.6	435.7	84465	43.2	0.383	0.24	Av	1T	-13.34
270	6:41:07.4	9:34:54.7	0.52	2.2	9.7	94096	5.3	0.619	—	—	—	—
271	6:41:07.4	9:31:10.9	0.46	3.7	42.5	89025	13.1	0.097	0.07	Av	—	-14.50
272	6:41:07.4	9:34:33.4	0.40	2.2	5.7	94226	4.6	0.156	0.01	Av	—	-15.48
273	6:41:07.6	9:30:00.6	0.53	4.8	91.2	91521	19.7	0.062	1.25	JHK	1T	-13.60
274	6:41:07.7	9:34:19.1	0.21	2.2	260.3	80631	34.4	0.000	8.92	X	1T	-12.68
275	6:41:07.7	9:41:14.6	0.91	7.3	67.4	78717	13.6	0.023	0.04	Av	1T	-14.33
276	6:41:07.8	9:28:13.7	0.54	6.4	350.0	88664	39.1	0.057	0.02	Av	1T	-13.61
277	6:41:08.0	9:34:46.9	0.53	2.3	21.7	93998	9.8	0.180	0.92	JHK	—	-14.32
278	6:41:08.0	9:30:40.2	0.30	4.2	229.4	92319	32.2	0.453	0.14	Av	2T	-13.56
279	6:41:08.2	9:30:07.6	0.41	4.7	78.3	89617	17.2	0.028	2.66	X	1T	-13.43
280	6:41:08.2	9:36:55.9	0.28	3.6	305.2	91378	38.5	0.000	1.33	JHK	1T	-13.11
281	6:41:08.2	9:34:09.6	0.49	2.3	5.9	44438	5.7	0.050	0.58	JHK	—	-14.68
282	6:41:08.2	9:38:30.3	0.49	4.9	430.5	88826	49.1	0.000	0.83	JHK	1T	-13.07
283	6:41:08.3	9:29:39.6	0.64	5.1	10.2	88980	6.5	0.734	—	—	—	—
284	6:41:08.4	9:40:35.7	1.04	6.8	40.5	84970	9.8	0.546	0.00	JHK	—	-14.58
285	6:41:08.4	9:37:52.4	0.43	4.4	61.6	89842	16.0	0.133	0.00	JHK	1T	-14.41
286	6:41:08.5	9:31:10.6	0.49	3.9	8.7	92789	5.9	0.168	—	—	—	—
287	6:41:08.5	9:34:13.0	0.29	2.4	64.9	61899	17.4	0.528	2.79	X	1T	-13.10
288	6:41:08.6	9:30:03.4	0.95	4.8	10.2	89454	5.8	0.409	0.00	Av	—	-15.20
289	6:41:08.7	9:38:25.2	0.90	4.8	10.6	88916	5.7	0.638	—	—	—	—
290	6:41:08.9	9:41:14.7	1.00	7.4	425.2	83709	45.3	0.000	0.00	Av	1T	-13.49
291	6:41:09.0	9:33:46.2	0.58	2.6	13.0	93542	8.0	0.467	0.14	Av	—	-14.94
292	6:41:09.0	9:29:07.5	0.52	5.7	120.6	90074	21.1	0.000	0.80	JHK	1T	-13.64
293	6:41:09.1	9:30:09.2	0.58	4.8	69.2	91479	17.0	0.032	0.21	Av	1T	-14.15
294	6:41:09.5	9:35:25.3	0.41	2.9	58.4	92982	16.8	0.790	0.00	Av	1T	-14.52
295	6:41:09.5	9:29:36.7	0.99	5.3	34.5	90759	9.8	0.014	—	—	—	—
296	6:41:09.5	9:29:25.2	0.37	5.5	486.4	90464	42.8	0.000	1.92	X	1T	-12.80
297	6:41:09.6	9:27:57.6	0.85	6.8	81.9	87174	15.3	0.060	0.00	JHK	1T	-14.22
298	6:41:09.6	9:36:28.8	0.51	3.5	28.0	91762	10.5	0.243	1.86	JHK	—	-13.99
299	6:41:09.8	9:29:15.3	0.62	5.7	20.4	90163	6.9	0.168	—	—	—	—
300	6:41:09.8	9:27:12.2	0.67	7.5	587.0	84781	50.7	0.746	0.19	Av	2Tab	-13.20

Table 1. (Continued)

N	RA [h m s]	Dec. [d m s].	$\delta_{r,d}$ ["]	Offax [']	Net Cts.	Exp. T. [s]	Signif	P_{KS}	n_H [10^{22}cm^{-2}]	n_H (Ref)	Mod	$F_X[\text{u}]$ [ergs/s/cm^2]
301	6:41:09.9	9:30:20.1	0.43	4.8	187.8	91663	31.7	0.530	0.00	X	1T	-13.95
302	6:41:10.0	9:27:46.1	0.45	7.0	2502.2	85776	120.7	0.000	0.00	JHK	2T	-12.75
303	6:41:10.0	9:29:28.5	0.80	5.5	24.5	90448	5.0	0.296	—	—	—	—
304	6:41:10.1	9:31:28.5	0.35	3.9	41.5	92815	11.6	0.424	0.01	Av	—	-14.61
305	6:41:10.2	9:29:34.2	1.14	5.5	70.1	90572	15.7	0.000	4.84	X	1T	-13.51
306	6:41:10.2	9:30:31.0	0.76	4.7	22.6	91818	8.7	0.541	—	—	—	—
307	6:41:10.3	9:33:25.1	0.31	3.0	58.6	93784	15.0	0.595	0.01	Av	1T	-14.47
308	6:41:10.3	9:34:21.6	0.39	2.8	25.7	89525	10.0	0.052	—	—	—	—
309	6:41:10.3	9:28:33.9	0.87	6.3	21.6	85185	7.3	0.329	0.09	Av	—	-14.74
310	6:41:10.4	9:34:18.6	0.59	2.9	15.9	88925	7.9	0.163	—	—	—	—
311	6:41:11.0	9:35:55.5	0.32	3.5	184.2	85551	29.9	0.000	0.35	Av	1T	-13.61
312	6:41:11.0	9:42:08.3	2.17	8.5	27.2	81862	6.1	0.000	0.19	Av	—	-14.51
313	6:41:11.0	9:34:24.5	0.31	3.0	2.9	92906	4.7	0.115	—	—	—	—
314	6:41:11.4	9:29:24.8	0.71	5.7	6.9	88313	4.8	0.216	—	—	—	—
315	6:41:11.6	9:29:09.7	1.26	6.0	18.1	86706	5.6	0.598	—	—	—	—
316	6:41:11.8	9:31:12.3	0.55	4.4	19.1	92205	8.6	0.308	0.00	JHK	—	-14.94
317	6:41:11.8	9:35:31.2	0.72	3.5	26.5	92004	9.9	0.588	—	—	—	—
318	6:41:11.8	9:26:31.3	0.82	8.4	306.7	84729	34.3	0.024	0.00	X	1T	-13.59
319	6:41:11.9	9:37:43.8	0.86	4.8	18.8	89473	7.0	0.662	0.75	JHK	—	-14.41
320	6:41:12.2	9:29:52.2	0.62	5.5	49.2	88081	13.3	0.995	—	—	—	—
321	6:41:12.2	9:29:14.7	1.20	6.0	21.0	89659	6.7	0.130	—	—	—	—
322	6:41:12.3	9:40:12.2	1.02	6.8	16.1	85236	5.8	0.024	0.00	JHK	—	-14.98
323	6:41:12.5	9:35:08.5	0.72	3.5	23.8	92125	10.6	0.676	0.00	JHK	—	-14.85
324	6:41:12.6	9:29:03.6	0.66	6.2	119.3	89291	13.5	0.653	3.49	X	1T	-13.30
325	6:41:12.9	9:35:49.9	0.73	3.8	23.1	91457	10.3	0.907	0.00	JHK	—	-14.86
326	6:41:13.0	9:35:32.1	0.29	3.7	83.3	91693	17.7	0.146	0.00	X	1T	-14.33
327	6:41:13.0	9:29:08.6	0.68	6.2	489.0	89342	49.3	0.000	5.78	X	1T	-12.42
328	6:41:13.0	9:27:40.0	0.63	7.5	347.7	81569	29.8	0.000	0.00	X	2T	-13.44
329	6:41:13.0	9:27:32.0	0.48	7.6	867.2	79860	53.1	0.086	0.15	X	1T	-13.08
330	6:41:13.1	9:31:06.8	0.66	4.7	39.4	89350	12.8	0.936	0.00	Av	—	-14.61
331	6:41:13.1	9:28:58.8	1.03	6.3	24.6	89057	5.2	0.222	0.06	Av	—	-14.75
332	6:41:13.2	9:26:10.7	0.79	8.8	1357.2	80837	76.9	0.000	0.05	X	1T	-12.90
333	6:41:13.3	9:31:50.4	0.33	4.3	164.6	90527	26.6	0.666	0.04	Av	1T	-13.94
334	6:41:13.3	9:28:07.5	0.91	7.1	161.6	84565	26.0	0.285	0.00	X	1T	-13.98
335	6:41:13.4	9:38:13.4	0.78	5.4	25.5	84778	8.8	0.988	0.78	JHK	—	-14.25
336	6:41:13.8	9:40:42.3	2.37	7.5	17.3	84109	5.9	0.834	—	—	—	—
337	6:41:13.8	9:28:42.5	0.91	6.7	15.9	79183	6.3	0.299	—	—	—	—
338	6:41:14.1	9:26:40.7	1.09	8.5	336.1	83187	36.8	0.000	0.00	Av	2T	-13.56
339	6:41:14.4	9:26:58.5	1.53	8.2	41.1	83716	8.5	0.802	0.06	Av	—	-14.50
340	6:41:14.5	9:33:21.3	0.24	4.0	626.1	90446	53.4	0.000	0.00	X	1T	-13.38
341	6:41:14.5	9:37:14.2	0.42	4.9	681.5	89492	67.0	0.000	0.00	JHK	2T	-13.31
342	6:41:14.7	9:34:14.0	0.92	3.9	11.6	91704	6.0	0.852	0.20	Av	—	-14.92
343	6:41:14.8	9:32:35.9	0.37	4.3	347.9	92232	44.5	0.089	0.09	Av	1T	-13.54
344	6:41:15.1	9:26:44.4	0.78	8.5	134.2	83131	17.8	0.094	0.12	Av	1T	-13.80
345	6:41:15.2	9:37:57.6	0.76	5.5	84.0	88340	18.7	0.064	0.02	Av	1T	-14.28
346	6:41:15.2	9:30:16.5	0.79	5.7	9.0	84924	4.7	0.050	0.00	JHK	—	-15.23
347	6:41:15.3	9:31:16.5	0.61	5.0	47.7	91408	14.9	0.230	0.00	JHK	—	-14.54
348	6:41:15.7	9:26:33.7	0.88	8.7	360.4	82717	30.6	0.729	0.11	X	1T	-13.50
349	6:41:15.7	9:38:18.1	0.66	5.8	48.2	87696	12.3	0.842	0.00	JHK	—	-14.52
350	6:41:15.7	9:26:17.1	0.68	9.0	2334.2	84049	107.1	0.000	0.11	Av	2T	-12.67
351	6:41:15.9	9:30:37.4	0.73	5.6	14.0	84959	5.4	0.307	1.51	JHK	—	-14.32
352	6:41:16.7	9:29:52.4	0.54	6.2	356.9	87547	40.4	0.799	0.02	X	1T	-13.55
353	6:41:16.8	9:27:30.4	1.17	8.1	226.2	85889	30.4	0.001	0.14	Av	2T	-13.58
354	6:41:16.8	9:36:20.5	0.42	4.9	250.3	89845	32.3	0.019	0.00	Av	1T	-13.75
355	6:41:17.0	9:32:52.2	0.47	4.7	50.9	90913	14.0	0.124	0.04	Av	—	-14.48
356	6:41:17.2	9:30:12.1	0.93	6.1	49.1	87777	12.3	0.418	1.62	JHK	—	-13.77
357	6:41:17.4	9:30:29.0	1.31	5.9	18.5	87760	5.9	0.120	1.48	JHK	—	-14.22
358	6:41:17.5	9:37:15.3	1.40	5.5	12.0	88627	4.6	0.289	0.00	JHK	—	-15.13
359	6:41:17.7	9:29:26.3	0.57	6.7	325.9	85711	36.5	0.749	0.00	Av	2T	-13.64
360	6:41:17.9	9:33:36.9	0.41	4.8	312.8	42406	36.6	0.000	0.00	Av	1T	-13.16

Table 1. (Continued)

N	RA [h m s]	Dec. [d m s.]	$\delta_{r,d}$ ["]	Offax ['']	Net Cts.	Exp. T. [s]	Signif	P_{KS}	n_H [10^{22}cm^{-2}]	n_H (Ref)	Mod	F_x [u] [ergs/s/cm^2]
361	6:41:17.9	9:29:01.1	1.17	7.0	69.4	87910	14.8	0.000	0.25	Av	1T	-14.18
362	6:41:18.1	9:38:25.2	0.98	6.3	119.5	86898	22.7	0.000	0.00	X	1T	-14.12
363	6:41:18.2	9:28:03.8	1.95	7.8	43.9	86471	8.8	0.280	—	—	—	—
364	6:41:18.3	9:33:53.5	0.41	4.8	285.7	86669	35.1	0.474	0.13	Av	1T	-13.62
365	6:41:18.3	9:28:33.0	1.37	7.5	110.7	87176	20.9	0.000	0.33	Av	2T	-13.81
366	6:41:18.3	9:29:32.6	1.12	6.7	88.5	88477	16.5	0.000	4.15	X	1T	-13.19
367	6:41:18.4	9:39:41.1	0.82	7.3	102.0	84931	17.0	0.603	0.00	Av	2T	-14.09
368	6:41:18.4	9:31:29.8	0.50	5.6	153.4	87437	23.0	0.020	0.00	JHK	1T	-14.05
369	6:41:18.8	9:30:19.9	1.30	6.3	8.3	89111	5.6	0.752	0.00	JHK	—	-15.29
370	6:41:18.9	9:27:15.9	0.83	8.6	119.0	82751	16.2	0.341	0.00	Av	2T	-13.94
371	6:41:19.0	9:35:53.3	1.73	5.3	13.1	89545	5.6	0.450	0.00	JHK	—	-15.09
372	6:41:19.2	9:30:48.3	1.24	6.1	14.7	89452	6.5	0.427	0.00	Av	—	-15.04
373	6:41:19.3	9:38:06.9	1.87	6.4	13.7	85004	5.2	0.019	1.10	JHK	—	-14.43
374	6:41:19.4	9:30:28.8	2.44	6.3	15.9	89100	5.6	0.791	0.00	Av	—	-15.01
375	6:41:19.6	9:31:44.4	0.40	5.7	1168.4	86128	77.8	0.000	0.00	X	1T	-13.10
376	6:41:19.7	9:31:38.1	0.99	5.8	37.6	89848	6.2	0.000	—	—	—	—
377	6:41:19.9	9:27:05.1	2.23	8.9	31.2	81754	6.6	0.438	0.00	Av	—	-14.68
378	6:41:20.0	9:32:07.3	1.38	5.7	9.5	87004	4.7	0.220	—	—	—	—
379	6:41:20.6	9:38:10.2	1.78	6.7	5.2	86538	4.9	0.544	—	—	—	—
380	6:41:20.7	9:32:00.6	1.02	5.9	31.1	89711	8.9	0.523	—	—	—	—
381	6:41:20.7	9:30:12.0	0.85	6.8	215.2	88270	30.5	0.009	0.00	JHK	1T	-13.85
382	6:41:21.0	9:32:41.2	1.24	5.7	11.9	89835	6.2	0.206	0.00	JHK	—	-15.14
383	6:41:21.0	9:33:36.3	0.54	5.5	338.3	57602	40.1	0.040	0.09	Av	2T	-13.34
384	6:41:21.2	9:32:14.7	0.68	5.9	145.5	89645	24.4	0.135	0.00	Av	1T	-14.07
385	6:41:21.8	9:30:39.9	1.45	6.7	12.8	83562	4.8	0.632	—	—	—	—
386	6:41:22.8	9:29:39.2	0.72	7.5	155.3	87156	21.5	0.078	0.00	Av	1T	-13.97
387	6:41:23.0	9:29:30.6	1.30	7.6	39.1	86383	6.7	0.000	—	—	—	—
388	6:41:23.0	9:27:26.9	0.79	9.1	1324.1	84317	77.6	0.358	0.00	JHK	2T	-13.02
389	6:41:23.1	9:37:33.6	1.04	6.9	110.4	86004	20.0	0.000	0.18	Av	1T	-13.84
390	6:41:23.1	9:35:22.0	0.98	6.1	12.3	88078	5.9	0.100	0.00	JHK	—	-15.11
391	6:41:23.2	9:30:36.5	0.77	7.0	330.8	87716	39.2	0.000	0.00	X	1T	-13.60
392	6:41:23.4	9:38:04.6	1.90	7.2	31.2	84049	9.5	0.112	0.00	JHK	—	-14.69
393	6:41:23.5	9:41:39.0	3.87	9.6	42.2	79818	6.2	0.546	—	—	—	—
394	6:41:23.8	9:33:56.5	0.77	6.2	30.9	88218	9.1	0.508	0.00	JHK	—	-14.71
395	6:41:24.2	9:31:54.2	0.74	6.7	362.6	88146	42.3	0.621	0.00	JHK	1T	-13.62
396	6:41:24.4	9:32:45.5	0.81	6.5	236.5	85706	33.9	0.137	0.00	Av	1T	-13.79
397	6:41:24.5	9:37:35.5	1.33	7.2	118.6	85785	22.2	0.056	0.00	Av	1T	-14.13
398	6:41:24.9	9:26:21.9	2.44	10.2	21.6	82280	5.5	0.868	0.00	JHK	—	-14.84
399	6:41:25.0	9:36:00.1	1.34	6.7	33.8	87013	10.6	0.324	0.00	JHK	—	-14.67
400	6:41:25.6	9:34:42.8	0.81	6.6	85.0	87293	16.9	0.457	0.02	Av	1T	-14.31
401	6:41:25.8	9:40:36.4	1.55	9.2	26.2	81607	7.0	0.731	—	—	—	—
402	6:41:27.0	9:38:41.2	2.54	8.3	18.6	83756	5.2	0.171	0.00	JHK	—	-14.91
403	6:41:27.0	9:30:13.1	1.23	8.0	51.6	86173	13.4	0.073	0.15	Av	1T	-14.25
404	6:41:27.1	9:27:03.6	1.48	10.0	45.0	82702	9.3	0.727	—	—	—	—
405	6:41:27.1	9:35:06.1	0.62	7.1	800.5	86524	60.2	0.001	0.08	Av	1T	-13.20
406	6:41:27.2	9:32:06.7	1.42	7.3	28.5	87113	8.8	0.039	0.00	JHK	—	-14.74
407	6:41:28.1	9:32:50.4	1.46	7.4	91.4	84426	16.7	0.000	0.00	JHK	1T	-14.26
408	6:41:28.7	9:38:39.0	1.05	8.6	420.3	83220	41.8	0.001	0.26	JHK	2T	-13.29
409	6:41:28.8	9:27:10.7	1.41	10.2	150.0	82389	18.3	0.562	0.08	JHK	1T	-13.96
410	6:41:28.8	9:34:53.5	2.23	7.5	18.1	83812	6.2	0.684	0.14	JHK	—	-14.75
411	6:41:29.1	9:39:50.3	1.36	9.3	111.4	81697	11.9	0.449	0.73	X	1T	-13.62
412	6:41:29.2	9:39:35.7	0.92	9.2	843.4	81946	56.8	0.029	0.11	Av	1T	-13.15
413	6:41:29.4	9:39:18.0	1.16	9.1	119.7	82211	17.1	0.060	0.09	Av	1T	-14.03
414	6:41:30.8	9:39:00.6	1.54	9.2	125.5	77599	16.2	0.092	1.49	X	1T	-13.40
415	6:41:31.0	9:35:25.3	1.38	8.0	43.6	81908	9.9	0.030	—	—	—	—
416	6:41:31.7	9:31:54.1	2.54	8.5	53.2	85099	9.3	0.994	0.00	Av	—	-14.46
417	6:41:32.5	9:38:07.2	1.00	9.2	564.1	82268	45.0	0.022	0.03	Av	1T	-13.39
418	6:41:34.5	9:36:32.2	1.61	9.1	80.2	78097	13.4	0.017	0.02	Av	1T	-14.30
419	6:41:36.2	9:39:20.6	2.12	10.5	104.6	79023	15.4	0.847	0.04	Av	1T	-14.15
420	6:41:39.6	9:40:28.7	2.24	11.8	308.3	76522	25.2	0.001	0.11	Av	1T	-13.51

Table 3. Master catalogs of objects in the ACIS FOV.

N	RA [h m s]	Dec. [d m s]	Id. rad. [""]	ACIS	2Mass	Reb.+	Lamm+	Flacc+	W56	Dahm+	Ct. Rate. [$10^{-4} s^{-1}$]
1	6:40:22.4	9:28:03.2	0.54	—	06402243+0928032	—	3228	—	—	—	< 8.7
2	6:40:24.2	9:30:38.1	0.50	—	06402419+0930381	2229	—	—	—	—	< 3.3
3	6:40:24.3	9:27:44.4	0.50	—	06402425+0927443	—	—	—	—	—	< 23.5
4	6:40:24.8	9:29:39.6	0.66	—	06402475+0929395	—	—	—	—	—	< 3.4
5	6:40:24.8	9:28:42.6	0.50	—	06402482+0928425	—	—	—	—	—	< 3.3
6	6:40:24.8	9:28:59.8	0.64	—	06402482+0928597	—	—	—	—	—	< 3.5
7	6:40:25.0	9:30:00.5	1.00	—	—	—	3295	—	—	—	< 3.0
8*	6:40:25.0	9:32:08.4	0.50	—	06402504+0932084	2258	3299	—	—	—	< 4.1
9	6:40:25.1	9:29:36.9	0.50	—	06402505+0929369	2261	3300	—	—	—	< 3.4
10	6:40:25.4	9:30:26.4	1.00	—	—	—	3326	—	—	—	< 2.8
11	6:40:25.5	9:29:44.6	1.00	—	—	—	3331	—	—	—	< 3.2
12	6:40:25.5	9:29:54.4	1.00	—	—	—	3334	—	—	—	< 2.9
13	6:40:25.6	9:32:35.9	0.50	—	06402559+0932358	—	3348	—	—	—	< 2.9
14	6:40:25.7	9:33:05.7	1.00	—	—	—	3351	—	—	—	< 17.0
15	6:40:25.7	9:29:09.8	1.00	—	—	—	3352	—	—	—	< 3.4
16*	6:40:25.8	9:29:23.3	0.50	1	06402575+0929232	2284	3356	—	—	—	3.5
17	6:40:25.8	9:32:36.4	0.50	—	06402580+0932363	—	3364	—	—	—	< 2.7
18	6:40:25.8	9:30:20.5	1.00	—	—	—	3363	—	—	—	< 2.7
19	6:40:25.9	9:33:08.9	1.00	—	—	—	3371	—	—	—	< 4.5
20	6:40:26.0	9:30:23.1	0.57	—	06402604+0930231	2295	3379	—	—	—	< 2.7
21	6:40:26.2	9:30:12.2	1.00	—	—	—	3391	—	—	—	< 2.8
22	6:40:26.2	9:30:19.9	1.00	—	—	—	3393	—	—	—	< 2.7
23	6:40:26.2	9:30:47.8	0.50	—	06402621+0930477	2301	3395	—	—	—	< 2.8
24	6:40:26.2	9:32:36.3	1.00	—	—	—	3396	—	—	—	< 2.5
25	6:40:26.3	9:30:30.2	1.00	—	—	—	3398	—	—	—	< 2.7
26	6:40:26.4	9:28:44.1	0.50	—	06402635+0928440	2305	3406	—	—	—	< 3.1
27	6:40:26.4	9:33:51.6	0.50	—	06402638+0933515	2306	3409	—	—	—	< 3.0
28	6:40:26.5	9:31:48.9	0.50	—	06402648+0931488	2313	3417	—	—	—	< 2.7
29*	6:40:26.5	9:29:22.1	0.50	—	06402649+0929220	2314	3421	—	—	—	< 3.2
30	6:40:26.6	9:33:25.0	0.50	—	06402656+0933250	2317	3427	—	49	—	< 2.5
31	6:40:26.6	9:27:58.0	0.50	—	06402664+0927579	2319	3433	—	—	—	< 3.7
32	6:40:26.7	9:29:59.8	1.00	—	—	—	3434	—	—	—	< 2.8
33	6:40:26.7	9:31:38.6	1.00	—	—	—	3435	—	—	—	< 2.7
34	6:40:26.8	9:33:42.3	0.50	—	06402684+0933422	—	3449	—	—	—	< 2.4
35	6:40:26.8	9:29:48.9	1.00	—	—	—	3448	—	—	—	< 2.9
36	6:40:26.9	9:32:56.0	1.00	—	—	—	3451	—	—	—	< 2.5
37	6:40:27.1	9:32:05.0	1.00	—	—	—	3459	—	—	—	< 4.6
38	6:40:27.1	9:31:57.6	1.00	—	—	—	3463	—	—	—	< 7.5
39	6:40:27.1	9:32:31.2	0.50	—	06402710+0932311	2326	3464	—	—	—	< 2.4
40	6:40:27.1	9:29:30.0	0.50	—	06402710+0929299	2330	3462	—	—	—	< 3.1
41	6:40:27.1	9:29:00.6	1.00	—	—	—	3466	—	—	—	< 3.0
42	6:40:27.2	9:28:43.0	0.50	—	06402716+0928430	2329	3471	—	—	—	< 3.1
43	6:40:27.2	9:30:56.2	1.00	—	—	—	3474	—	—	—	< 2.9
44	6:40:27.2	9:32:26.5	0.50	—	06402724+0932264	—	3476	—	—	—	< 2.4
45	6:40:27.3	9:29:29.4	1.00	—	—	—	3478	—	—	—	< 3.1
46	6:40:27.4	9:33:54.9	14.50	—	—	—	—	11	—	—	< 2.4
47*	6:40:27.7	9:31:59.7	0.50	2	06402772+0931596	2344	3518	—	—	37	10.0
48	6:40:27.8	9:30:01.8	1.00	—	—	—	3527	—	—	—	< 2.8
49	6:40:28.0	9:32:34.1	1.00	—	—	—	3531	—	—	—	< 2.3
50	6:40:28.0	9:32:19.2	1.00	—	—	—	3535	—	—	—	< 2.4
51	6:40:28.0	9:34:57.6	0.50	—	06402802+0934575	—	3539	—	—	—	< 2.4
52	6:40:28.1	9:31:36.1	0.57	—	06402805+0931360	2350	3543	—	—	—	< 2.5
53*	6:40:28.1	9:35:33.8	0.50	3	06402807+0935337	2351	3546	—	—	—	5.2
54	6:40:28.1	9:30:58.4	0.50	—	06402810+0930584	—	3549	13†	—	—	< 2.9
55	6:40:28.2	9:32:07.8	1.00	—	—	—	3556	—	—	—	< 3.8
56	6:40:28.2	9:35:12.0	0.50	—	06402817+0935120	—	3558	—	—	—	< 2.6
57	6:40:28.3	9:31:11.2	0.75	—	06402832+0931112	—	3570	13†	—	—	< 2.7
58	6:40:28.4	9:30:24.8	1.00	—	—	—	3579	—	—	—	< 2.7
59	6:40:28.5	9:28:31.3	0.69	—	06402846+0928313	—	3580	—	—	—	< 3.0
60	6:40:28.5	9:32:55.1	0.51	—	06402847+0932551	2365	3581	—	—	—	< 2.4

Table 3. (Continued)

N	RA [h m s]	Dec. [d m s]	Id. rad. [""]	ACIS	2Mass	Reb.+	Lamm+	Flacc+	W56	Dahm+	Ct. Rate. [$10^{-4} s^{-1}$]
61	6:40:28.5	9:33:47.1	0.50	—	06402850+0933470	2368	3584	—	—	—	< 2.2
62	6:40:28.6	9:36:08.2	1.00	—	—	—	3587	—	—	—	< 3.3
63	6:40:28.6	9:30:26.0	0.50	—	06402857+0930260	2372	3590	—	—	—	< 2.6
64	6:40:28.6	9:30:57.3	1.00	—	—	—	3591	—	—	—	< 121.3
65*	6:40:28.6	9:35:47.6	0.50	4	06402858+0935476	2373	3592	12	51	—	29.1
66	6:40:28.7	9:34:49.9	0.50	—	06402866+0934498	—	3599	—	—	—	< 2.3
67	6:40:28.7	9:27:36.6	1.00	—	—	—	3600	—	—	—	< 4.5
68*	6:40:28.8	9:31:00.3	0.50	5	06402877+0931002	2378	3603	13†	—	40	153.6
69	6:40:28.8	9:33:16.0	1.00	—	—	—	3606	—	—	—	< 2.3
70*	6:40:28.8	9:31:01.8	1.00	—	—	—	3609	—	—	41	< 121.3
71*	6:40:28.9	9:33:05.6	0.50	6	06402886+0933055	2382	3612	—	—	—	14.2
72	6:40:29.0	9:28:33.9	1.00	—	—	—	3620	—	—	—	< 2.8
73	6:40:29.1	9:29:38.4	1.00	—	—	—	3622	—	—	—	< 2.7
74	6:40:29.2	9:29:29.6	0.84	—	06402919+0929296	2386	3626	—	—	—	< 2.7
75	6:40:29.2	9:29:39.2	1.00	—	—	—	3632	—	—	—	< 2.7
76	6:40:29.7	9:37:45.3	1.00	—	—	—	3664	—	—	—	< 2.7
77	6:40:29.8	9:31:58.4	1.00	—	—	—	3665	—	—	—	< 2.3
78	6:40:29.8	9:28:03.7	0.50	—	06402977+0928036	2413	3668	—	—	—	< 3.0
79	6:40:29.8	9:30:55.9	1.00	—	—	—	3672	—	—	—	< 2.9
80	6:40:29.9	9:29:15.2	1.00	—	—	—	3679	—	—	—	< 2.6
81	6:40:29.9	9:28:29.9	1.00	—	—	—	3682	—	—	—	< 2.8
82	6:40:29.9	9:32:21.9	1.00	—	—	—	3684	—	—	—	< 2.2
83	6:40:29.9	9:33:43.0	1.00	—	—	—	3686	—	—	—	< 2.0
84	6:40:30.0	9:38:07.6	1.00	—	—	—	3691	—	—	—	< 2.8
85	6:40:30.0	9:34:43.3	0.50	—	06403004+0934433	2424	3695	—	—	—	< 2.2
86	6:40:30.2	9:30:48.3	0.50	—	06403015+0930483	2428	3699	—	—	—	< 2.7
87	6:40:30.2	9:28:08.4	0.50	—	06403017+0928084	2429	3702	—	—	—	< 2.9
88	6:40:30.2	9:31:48.3	1.00	—	—	—	3708	—	—	—	< 2.2
89	6:40:30.2	9:31:51.7	1.00	—	—	—	3709	—	—	—	< 2.2
90	6:40:30.3	9:34:42.6	1.00	—	—	—	3713	—	—	—	< 2.2
91	6:40:30.3	9:30:04.4	0.50	—	06403028+0930044	2433	3715	—	—	—	< 2.5
92	6:40:30.3	9:30:57.0	1.00	—	—	—	3717	—	—	—	< 2.7
93	6:40:30.5	9:30:20.4	0.50	—	06403051+0930203	2440	3729	—	—	—	< 2.4
94	6:40:30.6	9:38:39.6	1.00	7	—	—	3733	—	—	—	2.2
95	6:40:30.6	9:30:59.4	1.00	—	—	—	3735	—	—	—	< 2.5
96	6:40:30.8	9:36:40.8	0.76	—	06403077+0936408	—	3742	—	—	—	< 2.1
97	6:40:30.8	9:35:37.1	0.50	—	06403081+0935370	—	3747	—	—	—	< 2.2
98*	6:40:30.9	9:34:40.6	0.50	8	06403086+0934405	2456	3748	—	55	49	19.0
99	6:40:30.9	9:36:16.5	0.50	—	06403088+0936165	—	3755	—	—	—	< 2.2
100	6:40:30.9	9:30:29.0	1.00	—	—	—	3754	—	—	—	< 2.3
101	6:40:31.0	9:33:59.5	0.50	—	06403104+0933594	2461	3762	—	—	—	< 1.9
102	6:40:31.1	9:35:40.2	0.50	—	06403106+0935401	2462	3763	—	—	—	< 2.6
103	6:40:31.1	9:34:46.6	0.50	—	06403108+0934465	—	—	—	—	—	< 12.3
104	6:40:31.1	9:30:16.1	1.00	—	—	—	3765	—	—	—	< 2.4
105*	6:40:31.1	9:31:08.1	1.00	—	—	—	3766	—	—	—	< 43.7
106	6:40:31.2	9:27:26.3	1.00	—	—	—	3771	—	—	—	< 6.1
107	6:40:31.2	9:31:02.6	1.00	—	—	—	3773	—	—	—	< 43.7
108*	6:40:31.2	9:31:07.1	0.50	9	06403123+0931071	2465	3778	16	56	51	58.1
109	6:40:31.3	9:29:43.0	0.52	—	06403128+0929430	—	3779	—	—	—	< 2.5
110	6:40:31.3	9:39:12.4	1.00	—	—	—	3781	—	—	—	< 2.7
111	6:40:31.3	9:35:29.6	0.50	—	06403129+0935296	2468	3780	—	—	—	< 2.0
112	6:40:31.3	9:33:44.1	1.00	—	—	—	3783	—	—	—	< 1.9
113	6:40:31.4	9:32:52.6	0.50	—	06403135+0932525	2470	3786	—	—	—	< 1.9
114	6:40:31.4	9:32:59.4	0.50	—	06403135+0932594	—	3787	—	—	—	< 1.9
115	6:40:31.4	9:30:10.9	0.50	—	06403142+0930109	—	3790	—	—	—	< 2.4
116	6:40:31.5	9:27:55.4	1.00	—	—	—	3796	—	—	—	< 2.7
117	6:40:31.6	9:40:22.4	1.00	—	—	—	3801	—	—	—	< 17.5
118*	6:40:31.6	9:36:15.8	0.50	—	06403158+0936157	2472	3803	—	—	—	< 2.1
119	6:40:31.6	9:31:41.9	1.00	—	—	—	3804	—	—	—	< 2.0
120	6:40:31.6	9:40:21.9	1.00	—	—	—	3806	—	—	—	< 13.7

Table 3. (Continued)

N	RA [h m s]	Dec. [d m s]	Id. rad. ['"]	ACIS	2Mass	Reb.+	Lamm+	Flacc+	W56	Dahm+	Ct. Rate. [$10^{-4} s^{-1}$]
121	6:40:31.7	9:27:30.7	1.00	—	—	—	3810	—	—	—	< 3.7
122	6:40:31.7	9:30:08.4	1.00	—	—	—	3817	—	—	—	< 2.4
123	6:40:31.7	9:38:26.9	1.00	—	—	—	3821	—	—	—	< 2.4
124	6:40:31.8	9:37:58.9	0.50	—	06403175+0937588	2480	3825	—	—	—	< 2.4
125	6:40:31.8	9:32:03.4	1.00	—	—	—	3827	—	—	—	< 2.0
126*	6:40:31.8	9:33:29.4	0.50	10	06403181+0933293	2482	3828	—	—	—	2.1
127*	6:40:31.8	9:36:00.6	0.50	11	06403183+0936006	2484	3829	—	—	—	26.8
128	6:40:31.9	9:38:55.8	0.67	—	06403186+0938557	2486	—	—	—	—	< 2.5
129*	6:40:31.9	9:32:16.7	2.84	12	—	—	—	—	—	—	3.8
130	6:40:31.9	9:32:02.6	0.84	—	06403191+0932026	—	3836	—	—	—	< 2.0
131	6:40:31.9	9:28:42.1	1.00	—	—	—	3841	—	—	—	< 2.5
132	6:40:31.9	9:28:31.5	0.50	—	06403194+0928315	2488	3842	—	—	—	< 2.5
133	6:40:32.0	9:28:02.5	1.00	—	—	—	3848	—	—	—	< 2.7
134	6:40:32.2	9:30:04.8	0.50	—	06403216+0930047	—	3856	—	—	—	< 2.3
135	6:40:32.2	9:33:50.0	1.00	—	—	—	3859	—	—	—	< 1.8
136	6:40:32.2	9:27:40.3	1.00	—	—	—	3862	—	—	—	< 2.8
137	6:40:32.3	9:28:37.8	1.00	—	—	—	3865	—	—	—	< 2.5
138	6:40:32.3	9:39:52.0	1.00	—	—	—	3866	—	—	—	< 2.8
139	6:40:32.3	9:40:23.8	1.00	—	—	—	3869	—	—	—	< 3.1
140	6:40:32.4	9:28:37.0	1.00	—	—	—	3875	—	—	—	< 2.5
141	6:40:32.4	9:30:50.7	1.00	—	—	—	3876	—	—	—	< 2.2
142	6:40:32.5	9:27:35.1	1.00	—	—	—	3877	—	—	—	< 2.9
143	6:40:32.5	9:40:15.7	0.50	—	06403253+0940156	2506	3883	—	—	—	< 2.9
144	6:40:32.6	9:39:28.1	1.00	—	—	—	3886	—	—	—	< 2.7
145	6:40:32.6	9:27:28.5	1.00	—	—	—	3888	—	—	—	< 3.4
146	6:40:32.6	9:38:25.6	1.00	—	—	—	3889	—	—	—	< 2.3
147*	6:40:32.6	9:41:52.4	1.00	13	—	—	3892	—	—	—	7.0
148	6:40:32.7	9:34:51.5	0.50	—	06403269+0934515	2509	3897	—	—	—	< 1.8
149	6:40:32.7	9:38:32.5	1.00	—	—	—	3895	—	—	—	< 2.3
150	6:40:32.7	9:31:18.7	1.00	—	—	—	3898	—	—	—	< 2.2
151	6:40:32.7	9:27:19.5	1.00	—	—	—	3901	—	—	—	< 8.3
152	6:40:32.8	9:37:41.0	1.00	—	—	—	3905	—	—	—	< 2.2
153	6:40:32.8	9:35:20.0	0.88	—	06403283+0935199	—	3906	—	—	—	< 1.9
154	6:40:32.9	9:41:35.2	0.50	—	06403285+0941352	—	3914	—	—	—	< 21.4
155	6:40:32.9	9:39:23.0	0.50	—	06403285+0939230	2512	3915	—	—	—	< 2.8
156	6:40:32.9	9:40:39.6	1.00	—	—	—	3913	—	—	—	< 3.1
157	6:40:32.9	9:32:02.0	0.50	—	06403289+0932020	2513	3912	—	—	—	< 1.9
158	6:40:33.0	9:36:18.5	0.50	—	06403298+0936184	—	3921	—	—	—	< 1.9
159	6:40:33.1	9:37:46.5	0.50	—	06403305+0937465	2516	3928	—	—	—	< 2.2
160	6:40:33.1	9:36:49.3	0.50	—	06403306+0936493	2517	3927	—	—	—	< 1.8
161	6:40:33.1	9:32:42.2	0.50	—	06403306+0932421	—	3926	—	—	—	< 1.8
162	6:40:33.1	9:41:40.7	1.00	—	—	—	3929	—	—	—	< 9.9
163	6:40:33.1	9:40:29.9	1.00	—	—	—	3931	—	—	—	< 3.0
164	6:40:33.1	9:42:04.2	1.00	—	—	—	3932	—	—	—	< 7.3
165	6:40:33.2	9:34:48.9	0.50	—	06403315+0934488	—	—	—	—	—	< 1.8
166	6:40:33.2	9:28:24.2	1.00	—	—	—	3936	—	—	—	< 2.4
167	6:40:33.2	9:38:45.8	1.00	—	—	—	3937	—	—	—	< 2.4
168	6:40:33.2	9:40:36.5	1.00	—	—	—	3938	—	—	—	< 3.0
169	6:40:33.2	9:39:48.2	1.00	—	—	—	3939	—	—	—	< 2.9
170	6:40:33.3	9:39:37.0	0.50	—	06403325+0939369	2523	3945	—	—	—	< 2.8
171	6:40:33.3	9:30:45.1	0.50	—	06403327+0930450	—	3943	—	—	—	< 1.9
172	6:40:33.3	9:29:42.6	1.00	—	—	—	3944	—	—	—	< 2.2
173	6:40:33.3	9:30:03.7	0.64	—	06403329+0930037	—	3946	—	—	—	< 2.1
174	6:40:33.4	9:30:48.0	1.00	—	—	—	3950	—	—	—	< 1.9
175	6:40:33.5	9:32:53.0	1.00	—	—	—	3954	—	—	—	< 1.6
176	6:40:33.5	9:40:01.7	1.00	—	—	—	3955	—	—	—	< 3.0
177	6:40:33.5	9:39:11.9	1.00	—	—	—	3957	—	—	—	< 2.8
178	6:40:33.5	9:41:52.0	1.00	—	—	—	3958	—	—	—	< 6.0
179	6:40:33.5	9:41:49.7	0.64	—	06403347+0941497	2529	3963	—	—	—	< 6.0
180	6:40:33.5	9:29:27.4	1.00	—	—	—	3959	—	—	—	< 2.2

Table 3. (Continued)

N	RA [h m s]	Dec. [d m s]	Id. rad. [""]	ACIS	2Mass	Reb.+	Lamm+	Flacc+	W56	Dahm+	Ct. Rate. [$10^{-4} s^{-1}$]
181	6:40:33.5	9:40:29.8	1.00	—	—	—	3960	—	—	—	< 3.0
182	6:40:33.5	9:40:45.9	1.00	—	—	—	3961	—	—	—	< 3.1
183	6:40:33.5	9:29:29.7	1.00	—	—	—	3962	—	—	—	< 2.2
184	6:40:33.5	9:42:55.0	0.50	—	06403349+0942550	2531	3967	—	—	—	< 18.5
185*	6:40:33.5	9:34:58.6	0.50	14	06403350+0934586	2532	3966	—	—	—	7.8
186	6:40:33.5	9:41:45.4	1.00	—	—	—	3970	—	—	—	< 6.0
187	6:40:33.5	9:34:11.6	0.50	—	06403354+0934115	—	3969	—	—	—	< 1.6
188*	6:40:33.6	9:33:36.4	0.50	15	06403357+0933363	2537	3972	—	—	58	4.8
189*	6:40:33.6	9:27:28.3	0.50	—	06403357+0927282	2538	3973	—	—	—	< 3.0
190	6:40:33.6	9:41:28.1	0.50	—	06403360+0941281	2539	3974	—	—	—	< 3.6
191	6:40:33.6	9:33:59.6	0.50	—	06403362+0933595	—	3975	—	—	—	< 1.6
192	6:40:33.6	9:27:20.0	1.00	—	—	—	3977	—	—	—	< 8.6
193	6:40:33.7	9:31:53.9	1.00	—	—	—	3979	—	—	—	< 1.7
194	6:40:33.7	9:30:51.9	0.50	—	06403369+0930518	—	3981	—	—	—	< 1.8
195	6:40:33.7	9:27:24.8	1.00	—	—	—	3982	—	—	—	< 3.3
196	6:40:33.7	9:32:25.0	0.59	—	06403373+0932249	2544	3983	—	—	—	< 1.8
197	6:40:33.8	9:32:57.0	0.50	—	06403376+0932570	2546	3985	—	62	—	< 1.6
198	6:40:33.8	9:40:50.4	1.00	—	—	—	3987	—	—	—	< 3.1
199	6:40:33.8	9:43:11.5	1.00	—	—	—	3989	—	—	—	< 26.4
200	6:40:33.8	9:34:33.1	0.50	—	06403379+0934331	—	3991	—	—	—	< 1.7
201	6:40:33.8	9:41:15.5	0.50	—	06403380+0941154	2553	3996	—	61	—	< 3.3
202	6:40:33.8	9:42:26.9	0.50	—	06403380+0942269	2552	3997	—	—	—	< 4.1
203	6:40:33.8	9:38:45.7	1.00	—	—	—	3995	—	—	—	< 2.3
204	6:40:33.9	9:41:03.8	1.00	—	—	—	4000	—	—	—	< 3.2
205	6:40:33.9	9:30:57.8	1.00	—	—	—	4002	—	—	—	< 1.8
206	6:40:33.9	9:28:13.3	0.50	—	06403394+0928133	—	4004	—	—	—	< 2.4
207	6:40:34.0	9:31:15.0	0.50	—	06403397+0931149	—	4006	—	—	—	< 1.8
208	6:40:34.0	9:27:40.3	1.00	—	—	—	4011	—	—	—	< 2.8
209	6:40:34.0	9:41:51.7	1.00	—	—	—	4012	—	—	—	< 3.7
210	6:40:34.0	9:37:43.9	1.00	—	—	—	4015	—	—	—	< 2.0
211	6:40:34.1	9:35:26.9	0.50	—	06403407+0935269	—	4016	—	—	—	< 1.9
212	6:40:34.1	9:39:52.0	1.00	—	—	—	4018	—	—	—	< 3.0
213	6:40:34.1	9:42:52.1	1.00	—	—	—	4020	—	—	—	< 16.3
214	6:40:34.2	9:41:35.4	1.00	—	—	—	4023	—	—	—	< 3.4
215	6:40:34.2	9:29:17.9	0.50	—	06403416+0929178	2563	4022	—	—	—	< 2.2
216	6:40:34.2	9:30:47.8	0.71	—	06403417+0930477	—	4024	—	—	—	< 1.8
217	6:40:34.2	9:39:23.9	0.69	—	06403423+0939239	—	4029	—	—	—	< 2.5
218	6:40:34.3	9:27:55.6	0.59	—	06403425+0927555	2569	4031	—	—	—	< 2.7
219	6:40:34.3	9:38:51.7	0.50	—	06403430+0938517	2572	4034	—	63	—	< 2.3
220*	6:40:34.3	9:39:17.7	3.20	16	—	—	—	—	—	—	3.4
221	6:40:34.3	9:30:38.4	0.50	—	06403431+0930384	—	4036	—	—	—	< 1.8
222	6:40:34.3	9:33:01.1	0.50	—	06403432+0933011	—	4037	—	—	—	< 1.5
223	6:40:34.4	9:40:40.9	0.78	—	06403436+0940409	2577	4043	—	—	—	< 3.0
224	6:40:34.4	9:37:17.2	1.00	—	—	—	4039	—	—	—	< 1.8
225	6:40:34.4	9:43:58.0	1.00	—	—	—	4041	—	—	—	< 17.0
226	6:40:34.4	9:29:53.5	1.00	—	—	—	4042	—	—	—	< 2.1
227	6:40:34.4	9:42:06.8	1.00	—	—	—	4044	—	—	—	< 3.7
228	6:40:34.4	9:31:07.1	0.50	—	06403442+0931070	2578	4045	—	—	—	< 1.7
229	6:40:34.5	9:31:53.7	1.00	—	—	—	4047	—	—	—	< 1.6
230*	6:40:34.5	9:35:18.3	0.50	17	06403446+0935182	2579	4048	—	—	63	15.6
231	6:40:34.5	9:30:10.0	1.00	—	—	—	4049	—	—	—	< 2.0
232	6:40:34.6	9:42:40.6	1.00	—	—	—	4054	—	—	—	< 4.0
233	6:40:34.6	9:42:22.3	1.00	—	—	—	4056	—	—	—	< 3.7
234	6:40:34.6	9:30:20.9	0.50	—	06403457+0930208	2583	4058	—	—	—	< 1.9
235	6:40:34.6	9:29:14.6	0.50	—	06403458+0929145	2584	4059	—	—	—	< 2.2
236	6:40:34.6	9:39:18.6	1.00	—	—	—	4060	—	—	—	< 2.4
237	6:40:34.6	9:43:04.3	1.00	—	—	—	4061	—	—	—	< 5.0
238	6:40:34.6	9:39:21.7	1.00	—	—	—	4063	—	—	—	< 2.4
239	6:40:34.7	9:28:54.8	1.00	—	—	—	4064	—	—	—	< 2.3
240	6:40:34.7	9:40:15.6	1.00	—	—	—	4065	—	—	—	< 3.2

Table 3. (Continued)

N	RA [h m s]	Dec. [d m s]	Id. rad. ["]	ACIS	2Mass	Reb.+	Lamm+	Flacc+	W56	Dahm+	Ct. Rate. [$10^{-4} s^{-1}$]
241	6:40:34.7	9:37:10.4	1.00	—	—	—	4066	—	—	—	< 1.7
242	6:40:34.8	9:32:46.3	0.50	—	06403479+0932463	—	4068	—	—	—	< 1.5
243	6:40:34.8	9:40:33.1	0.96	—	06403481+0940330	2592	4071	—	—	—	< 3.0
244	6:40:34.9	9:37:26.7	0.68	—	06403492+0937266	—	4080	—	—	—	< 1.8
245	6:40:34.9	9:42:50.5	1.00	—	—	—	4077	—	—	—	< 4.1
246	6:40:35.0	9:33:14.7	0.60	—	06403496+0933146	—	—	—	—	—	< 1.4
247	6:40:35.0	9:27:52.2	0.50	—	06403497+0927521	—	4081	—	—	—	< 2.7
248	6:40:35.0	9:35:30.3	0.50	—	06403499+0935303	—	4083	—	—	—	< 2.4
249*	6:40:35.0	9:39:54.9	4.34	18	—	—	—	—	—	—	3.2
250	6:40:35.1	9:28:58.6	0.50	—	06403508+0928586	—	4088	—	—	—	< 2.2
251	6:40:35.1	9:41:52.4	1.00	—	—	—	4089	—	—	—	< 3.3
252	6:40:35.1	9:41:32.1	1.00	—	—	—	4091	—	—	—	< 3.1
253	6:40:35.1	9:43:55.2	1.00	—	—	—	4092	—	—	—	< 8.2
254	6:40:35.2	9:28:20.7	0.50	—	06403517+0928206	2596	4094	—	—	—	< 2.5
255	6:40:35.2	9:29:56.9	0.50	—	06403519+0929569	2598	4097	—	—	—	< 2.0
256	6:40:35.2	9:38:11.4	0.50	—	06403521+0938113	2600	4100	—	—	—	< 1.8
257	6:40:35.2	9:42:26.2	1.00	—	—	—	4101	—	—	—	< 3.7
258	6:40:35.3	9:41:51.3	1.00	—	—	—	4103	—	—	—	< 3.3
259	6:40:35.3	9:38:08.9	1.00	—	—	—	4106	—	—	—	< 1.8
260	6:40:35.3	9:29:11.4	1.00	—	—	—	4107	—	—	—	< 2.2
261	6:40:35.4	9:37:46.5	1.00	—	—	—	4109	—	—	—	< 1.8
262	6:40:35.4	9:27:30.5	0.50	—	06403541+0927304	2602	4111	—	—	—	< 2.7
263	6:40:35.5	9:39:59.4	1.00	—	—	—	4113	—	—	—	< 3.0
264	6:40:35.5	9:41:41.0	1.00	—	—	—	4114	—	—	—	< 3.2
265	6:40:35.5	9:43:54.2	0.50	—	06403550+0943542	2607	4117	—	—	—	< 11.9
266*	6:40:35.5	9:42:28.2	0.50	—	06403550+0942281	2608	4118	—	—	—	< 3.7
267	6:40:35.5	9:28:45.7	1.00	—	—	—	4119	—	—	—	< 2.3
268	6:40:35.5	9:34:20.1	0.50	—	06403553+0934200	—	—	—	—	—	< 1.4
269	6:40:35.6	9:28:04.6	1.00	—	—	—	4121	—	—	—	< 2.6
270	6:40:35.7	9:28:53.9	1.00	—	—	—	4127	—	—	—	< 2.2
271	6:40:35.7	9:39:47.4	1.00	—	—	—	4129	—	—	—	< 2.8
272	6:40:35.8	9:41:33.8	0.80	—	06403583+0941337	2611	4136	—	—	—	< 3.0
273	6:40:35.9	9:35:33.4	0.50	—	06403585+0935334	—	—	—	—	—	< 3.1
274	6:40:35.9	9:27:46.7	1.00	—	—	—	4137	—	—	—	< 2.7
275	6:40:35.9	9:38:44.5	1.00	—	—	—	4138	—	—	—	< 2.0
276	6:40:35.9	9:27:29.2	1.00	—	—	—	4139	—	—	—	< 2.7
277	6:40:35.9	9:42:28.2	1.00	—	—	—	4143	—	—	—	< 3.7
278	6:40:36.0	9:41:46.0	1.00	—	—	—	4150	—	—	—	< 3.2
279	6:40:36.0	9:42:44.6	1.00	—	—	—	4151	—	—	—	< 4.0
280	6:40:36.0	9:42:50.6	1.00	—	—	—	4152	—	—	—	< 4.0
281	6:40:36.1	9:41:58.4	0.68	—	06403606+0941584	—	4149	—	—	—	< 3.3
282	6:40:36.2	9:27:19.2	1.00	—	—	—	4158	—	—	—	< 2.8
283*	6:40:36.2	9:28:04.2	0.50	20	06403621+0928042	2617	4159	—	—	68	3.3
284*	6:40:36.2	9:40:01.6	0.50	19	06403622+0940015	2618	4161	—	—	69	8.9
285	6:40:36.3	9:40:51.1	0.50	—	06403625+0940510	—	4162	—	—	—	< 3.3
286	6:40:36.3	9:27:08.9	0.89	—	06403628+0927089	—	4163	—	—	—	< 9.4
287*	6:40:36.3	9:40:37.0	8.92	21	—	—	—	—	—	—	3.3
288	6:40:36.3	9:42:58.9	0.50	—	06403633+0942588	2623	4167	—	—	—	< 4.1
289*	6:40:36.4	9:43:08.0	6.61	22	—	—	—	—	—	—	3.0
290	6:40:36.4	9:38:44.3	1.00	—	—	—	4175	—	—	—	< 1.9
291	6:40:36.4	9:28:50.4	1.00	—	—	—	4178	—	—	—	< 2.1
292	6:40:36.5	9:41:18.1	1.00	—	—	—	4179	—	—	—	< 3.1
293	6:40:36.5	9:41:04.2	0.50	—	06403651+0941042	—	4182	—	—	—	< 2.8
294	6:40:36.6	9:40:12.4	1.00	—	—	—	4186	—	—	—	< 3.0
295	6:40:36.6	9:28:52.9	1.00	—	—	—	4187	—	—	—	< 2.0
296	6:40:36.6	9:27:31.0	1.00	—	—	—	4189	—	—	—	< 2.7
297	6:40:36.6	9:28:18.1	1.00	—	—	—	4190	—	—	—	< 2.4
298	6:40:36.7	9:42:15.2	1.00	—	—	—	4194	—	—	—	< 3.4
299	6:40:36.7	9:41:24.7	0.50	—	06403671+0941246	2638	4198	—	—	—	< 3.9
300	6:40:36.7	9:34:54.4	0.50	—	06403673+0934543	—	4199	—	—	—	< 1.4

Table 3. (Continued)

N	RA [h m s]	Dec. [d m s]	Id. rad. [""]	ACIS	2Mass	Reb.+	Lamm+	Flacc+	W56	Dahm+	Ct. Rate. [$10^{-4} s^{-1}$]
301	6:40:36.8	9:29:30.6	0.81	—	06403675+0929306	2639	4200	—	—	—	< 1.9
302	6:40:36.8	9:29:44.5	1.00	—	—	—	4201	—	—	—	< 1.9
303*	6:40:36.8	9:37:30.5	2.55	23	—	—	—	—	—	—	2.0
304	6:40:36.8	9:39:38.2	0.59	—	06403679+0939382	—	4206	—	—	—	< 2.7
305*	6:40:36.8	9:41:04.2	0.50	—	06403679+0941042	—	4207	—	—	—	< 2.7
306	6:40:36.8	9:41:02.8	1.00	—	—	—	4208	—	—	—	< 2.7
307	6:40:36.8	9:43:02.8	0.50	—	06403684+0943027	2641	4209	—	—	—	< 4.1
308*	6:40:36.9	9:32:37.5	1.52	24	—	—	—	—	—	—	1.4
309	6:40:36.9	9:39:29.4	1.00	—	—	—	4214	—	—	—	< 2.5
310	6:40:36.9	9:40:46.1	1.00	—	—	—	4215	—	—	—	< 3.3
311	6:40:36.9	9:27:44.3	0.50	—	06403693+0927442	2645	4217	—	—	—	< 2.7
312*	6:40:37.0	9:39:09.8	0.50	25	06403697+0939097	—	4220	—	—	74	22.1
313	6:40:37.0	9:40:60.0	0.50	—	06403698+0940599	—	4221	—	—	—	< 2.7
314	6:40:37.0	9:41:36.3	1.00	—	—	—	4222	—	—	—	< 3.9
315	6:40:37.0	9:27:09.6	1.00	—	—	—	4227	—	—	—	< 3.7
316*	6:40:37.2	9:31:09.9	0.50	26	06403720+0931098	2665†	4235	20†	—	76	19.4
317	6:40:37.3	9:41:17.0	1.00	28†	—	—	4238	—	—	—	< 3.9
318	6:40:37.3	9:40:20.6	1.00	—	—	—	4242	—	—	—	< 2.7
319	6:40:37.3	9:41:24.0	1.00	28†	—	—	4244	—	—	—	< 3.9
320	6:40:37.3	9:35:42.6	0.50	—	06403732+0935426	—	—	—	69	—	< 2.2
321*	6:40:37.3	9:39:09.4	1.50	—	—	2664	—	—	—	—	< 16.6
322	6:40:37.4	9:29:01.2	0.93	—	06403738+0929012	—	4249	—	—	—	< 2.0
323	6:40:37.4	9:40:30.5	1.00	—	—	—	4248	—	—	—	< 2.7
324	6:40:37.5	9:38:12.8	1.00	—	—	—	4252	—	—	—	< 1.7
325	6:40:37.5	9:40:47.8	1.00	—	—	—	4255	—	—	—	< 2.7
326	6:40:37.5	9:41:20.0	1.00	28†	—	—	4258	—	—	—	< 3.9
327	6:40:37.5	9:36:32.1	1.00	—	—	—	4260	—	—	—	< 1.3
328	6:40:37.5	9:42:33.3	1.00	—	—	—	4261	—	—	—	< 3.5
329	6:40:37.6	9:41:44.2	0.50	—	06403756+0941441	—	4263	—	—	—	< 3.5
330	6:40:37.6	9:42:15.7	0.50	—	06403759+0942156	2660	4266	—	—	—	< 3.3
331	6:40:37.6	9:31:10.4	0.61	—	06403759+0931103	2665†	4262	20†	—	—	< 5.0
332*	6:40:37.7	9:39:39.8	0.50	27	06403768+0939397	2663	4271	—	—	77	11.3
333	6:40:37.7	9:27:58.0	1.00	—	—	—	4270	—	—	—	< 2.5
334	6:40:37.7	9:37:28.5	0.50	—	06403772+0937285	—	4272	—	—	—	< 1.6
335	6:40:37.7	9:41:17.0	1.00	28†	—	—	4273	—	—	—	< 3.9
336	6:40:37.8	9:34:12.9	0.50	—	06403775+0934128	—	4274	—	—	—	< 1.2
337	6:40:37.8	9:40:10.6	0.50	—	06403779+0940105	2678	4278	—	—	—	< 2.6
338	6:40:37.8	9:31:18.8	0.50	—	06403783+0931187	—	4279	—	—	—	< 1.5
339*	6:40:37.9	9:35:56.7	0.50	29	06403786+0935567	—	4280	—	—	—	30.3
340*	6:40:37.9	9:34:54.0	0.50	30	06403787+0934540	—	4282	23	—	79	71.0
341	6:40:37.9	9:29:17.2	1.00	—	—	—	4284	—	—	—	< 1.9
342	6:40:37.9	9:43:21.4	0.50	—	06403788+0943213	—	4285	—	—	—	< 3.9
343	6:40:37.9	9:37:41.5	1.00	—	—	—	4288	—	—	—	< 1.6
344	6:40:37.9	9:40:22.2	0.50	—	06403794+0940222	—	4290	—	—	—	< 2.5
345	6:40:37.9	9:39:24.0	0.50	—	06403794+0939239	2684	4292	—	—	—	< 2.2
346	6:40:38.0	9:30:49.0	1.00	—	—	—	4293	—	—	—	< 1.5
347	6:40:38.0	9:43:04.7	1.00	—	—	—	4294	—	—	—	< 3.9
348	6:40:38.0	9:29:50.7	1.00	—	—	—	4297	—	—	—	< 4.1
349	6:40:38.0	9:32:49.2	0.50	—	06403803+0932491	2686	4300	—	—	—	< 1.3
350*	6:40:38.1	9:31:34.7	1.96	31	—	—	—	—	—	—	1.6
351	6:40:38.1	9:42:22.5	1.00	—	—	—	4305	—	—	—	< 3.4
352	6:40:38.2	9:28:30.5	0.66	—	06403817+0928304	—	4308	—	—	—	< 2.1
353	6:40:38.2	9:39:16.1	1.00	—	—	—	4309	—	—	—	< 2.2
354*	6:40:38.2	9:29:52.5	0.50	32	06403819+0929524	2692	4313	—	—	80	6.8
355	6:40:38.2	9:42:21.3	1.00	—	—	—	4314	—	—	—	< 3.3
356	6:40:38.2	9:27:01.6	1.00	—	—	—	4315	—	—	—	< 4.6
357	6:40:38.2	9:28:19.9	0.50	—	06403823+0928198	2693	4316	—	—	—	< 2.2
358	6:40:38.3	9:42:51.6	1.00	—	—	—	4317	—	—	—	< 3.6
359	6:40:38.3	9:28:59.6	0.71	—	06403829+0928595	—	4321	—	—	—	< 2.0
360	6:40:38.3	9:42:50.3	0.50	—	06403829+0942502	2695	4322	—	—	—	< 3.5

Table 3. (Continued)

N	RA [h m s]	Dec. [d m s]	Id. rad. [""]	ACIS	2Mass	Reb.+	Lamm+	Flacc+	W56	Dahm+	Ct. Rate. [$10^{-4} s^{-1}$]
361	6:40:38.3	9:27:25.0	1.00	—	—	—	4320	—	—	—	< 2.5
362	6:40:38.3	9:29:25.4	1.00	—	—	—	4323	—	—	—	< 1.8
363	6:40:38.3	9:29:26.0	0.50	—	06403834+0929260	2699	4326	—	—	—	< 1.8
364	6:40:38.4	9:41:23.6	1.00	28†	—	—	4328	—	—	—	< 3.9
365	6:40:38.4	9:33:17.1	1.00	—	—	—	4339	—	—	—	< 1.2
366	6:40:38.6	9:30:21.5	0.60	—	06403859+0930215	—	4342	—	—	—	< 1.6
367	6:40:38.6	9:39:50.0	1.00	—	—	—	4343	—	—	—	< 2.4
368*	6:40:38.7	9:36:57.0	0.50	33	06403867+0936569	2709	4349	25	—	81	10.0
369*	6:40:38.7	9:34:34.3	0.50	34	06403868+0934342	—	4348	—	—	—	1.4
370	6:40:38.8	9:38:37.3	1.00	—	—	—	4354	—	—	—	< 1.7
371*	6:40:38.8	9:29:48.1	1.75	35	—	—	—	—	—	—	2.3
372	6:40:38.9	9:40:50.9	0.61	—	06403885+0940508	—	4358	—	—	—	< 2.4
373	6:40:38.9	9:39:46.9	0.50	—	06403890+0939469	—	4362	—	—	—	< 2.3
374	6:40:38.9	9:38:49.0	1.00	—	—	—	4363	—	—	—	< 1.8
375*	6:40:39.0	9:35:60.0	0.50	36	06403902+0935599	2714	4367	—	—	—	15.9
376	6:40:39.1	9:33:15.6	0.50	—	06403913+0933156	—	—	—	—	—	< 1.1
377	6:40:39.1	9:29:36.6	1.00	—	—	—	4372	—	—	—	< 1.8
378	6:40:39.2	9:35:27.3	0.50	—	06403915+0935273	—	—	—	—	—	< 2.4
379	6:40:39.2	9:32:39.9	0.50	—	06403917+0932398	—	—	—	—	—	< 1.2
380	6:40:39.2	9:43:40.9	0.50	—	06403919+0943409	—	4383	—	—	—	< 5.6
381	6:40:39.2	9:41:47.9	0.50	—	06403919+0941479	2720	4381	—	—	—	< 3.0
382	6:40:39.2	9:28:17.7	1.00	—	—	—	4382	—	—	—	< 2.2
383*	6:40:39.2	9:29:30.4	1.91	37	—	—	—	—	—	—	2.2
384	6:40:39.3	9:31:28.1	1.00	—	—	—	4387	—	—	—	< 1.4
385	6:40:39.3	9:36:14.0	0.50	—	06403928+0936140	—	—	—	—	—	< 1.3
386	6:40:39.3	9:40:18.9	1.00	—	—	—	4388	—	—	—	< 2.3
387	6:40:39.3	9:31:29.2	0.50	—	06403933+0931292	2724	4390	—	—	—	< 1.4
388*	6:40:39.3	9:34:45.6	0.50	38	06403934+0934455	2725	4392	—	—	85	3.8
389	6:40:39.4	9:30:34.0	1.00	—	—	—	4395	—	—	—	< 1.5
390	6:40:39.4	9:43:05.1	1.00	—	—	—	4396	—	—	—	< 3.5
391	6:40:39.4	9:42:34.3	1.00	—	—	—	4399	—	—	—	< 3.3
392	6:40:39.5	9:42:56.3	0.50	—	06403947+0942563	2729	4403	—	—	—	< 3.5
393	6:40:39.5	9:40:56.2	0.52	—	06403952+0940561	—	4408	—	—	—	< 2.4
394	6:40:39.5	9:34:11.4	0.53	—	06403953+0934113	—	—	—	—	—	< 1.1
395	6:40:39.5	9:42:20.6	1.00	—	—	—	4410	—	—	—	< 3.2
396	6:40:39.6	9:28:12.4	1.00	—	—	—	4411	—	—	—	< 2.2
397	6:40:39.6	9:29:41.8	0.50	—	06403957+0929417	2733	4413	—	—	—	< 1.8
398	6:40:39.6	9:41:35.1	1.00	—	—	—	4414	—	—	—	< 2.8
399	6:40:39.6	9:27:20.1	1.00	—	—	—	4418	—	—	—	< 2.3
400	6:40:39.7	9:28:37.8	1.00	—	—	—	4420	—	—	—	< 1.9
401	6:40:39.7	9:42:09.7	1.00	—	—	—	4422	—	—	—	< 3.1
402	6:40:39.8	9:28:35.0	1.00	—	—	—	4424	—	—	—	< 1.9
403	6:40:39.8	9:40:10.5	0.50	—	06403983+0940105	2738	4427	—	—	—	< 2.2
404	6:40:40.0	9:35:42.7	0.51	—	06403996+0935426	—	—	—	—	—	< 1.2
405	6:40:40.0	9:27:14.2	1.00	—	—	—	4436	—	—	—	< 2.3
406	6:40:40.0	9:38:31.2	1.00	—	—	—	4437	—	—	—	< 1.6
407	6:40:40.0	9:27:20.7	1.00	—	—	—	4441	—	—	—	< 2.3
408	6:40:40.0	9:42:32.0	1.00	—	—	—	4442	—	—	—	< 3.1
409*	6:40:40.1	9:35:02.9	0.50	39	06404005+0935029	2742	4443	26†	77	87	26.4
410	6:40:40.1	9:42:07.2	1.00	—	—	—	4444	—	—	—	< 3.0
411	6:40:40.1	9:43:47.1	0.50	—	06404006+0943470	—	4446	—	—	—	< 9.5
412	6:40:40.1	9:41:32.9	1.00	—	—	—	4447	—	—	—	< 2.9
413	6:40:40.1	9:28:28.5	1.00	—	—	—	4449	—	—	—	< 2.0
414	6:40:40.2	9:43:41.4	0.50	—	06404016+0943413	2746	4451	—	—	—	< 4.9
415	6:40:40.2	9:41:49.5	0.62	—	06404017+0941495	2747	4450	—	—	—	< 3.0
416	6:40:40.2	9:43:04.3	0.50	—	06404021+0943042	2748	4452	—	—	—	< 3.4
417	6:40:40.3	9:40:41.2	1.00	—	—	—	4455	—	—	—	< 2.3
418	6:40:40.3	9:37:43.0	1.00	—	—	—	4457	—	—	—	< 1.4
419	6:40:40.4	9:39:35.7	0.50	—	06404037+0939357	—	4464	—	—	—	< 1.9
420	6:40:40.4	9:41:19.3	1.00	—	—	—	4467	—	—	—	< 2.7

Table 3. (Continued)

N	RA [h m s]	Dec. [d m s]	Id. rad. [""]	ACIS	2Mass	Reb.+	Lamm+	Flacc+	W56	Dahm+	Ct. Rate. [$10^{-4} s^{-1}$]
421*	6:40:40.4	9:31:34.8	0.50	40	06404043+0931347	2754	4468	—	—	—	1.9
422*	6:40:40.5	9:38:25.7	2.22	42	—	—	—	—	—	—	2.7
423*	6:40:40.5	9:35:05.5	0.50	41	06404050+0935055	—	4474	26†	—	—	2.1
424	6:40:40.5	9:40:17.9	1.00	—	—	—	4476	—	—	—	< 2.2
425*	6:40:40.5	9:35:01.1	0.50	43	06404052+0935011	—	4475	26†	—	—	1.9
426*	6:40:40.5	9:29:19.8	0.50	—	06404052+0929197	2757	4477	—	—	90	< 1.7
427	6:40:40.6	9:27:49.3	0.50	—	06404058+0927492	2758	4480	—	—	—	< 2.3
428	6:40:40.6	9:27:07.3	1.00	—	—	—	4482	—	—	—	< 2.4
429	6:40:40.7	9:30:29.5	0.50	—	06404065+0930295	—	4486	—	—	—	< 1.5
430	6:40:40.7	9:31:11.4	1.00	—	—	—	4488	—	—	—	< 1.4
431	6:40:40.7	9:42:13.2	0.59	—	06404069+0942131	2762	4489	—	—	—	< 3.1
432*	6:40:40.8	9:34:26.9	0.50	44	06404078+0934269	2764	4490	27	—	—	1.3
433	6:40:40.8	9:27:39.0	1.00	—	—	—	4494	—	—	—	< 2.3
434	6:40:40.8	9:40:20.0	1.00	—	—	—	4497	—	—	—	< 2.3
435	6:40:40.9	9:30:40.4	0.60	—	06404085+0930404	—	4496	—	—	—	< 1.4
436	6:40:40.9	9:29:44.8	0.50	—	06404086+0929448	2767	4498	—	—	—	< 1.6
437	6:40:40.9	9:38:27.4	0.71	—	06404088+0938274	—	4499	—	—	—	< 1.6
438	6:40:40.9	9:41:21.7	0.69	—	06404088+0941217	—	4507	—	—	—	< 2.7
439	6:40:40.9	9:42:24.9	1.00	—	—	—	4502	—	—	—	< 3.1
440*	6:40:40.9	9:27:59.5	0.50	45	06404091+0927595	—	4503	—	—	91	17.6
441	6:40:40.9	9:30:08.8	0.50	—	06404093+0930088	—	4504	—	—	—	< 1.5
442*	6:40:41.0	9:27:54.3	0.50	—	06404100+0927543	2771	4511	—	—	92	< 11.2
443	6:40:41.0	9:43:12.7	0.50	—	06404103+0943127	—	4516	—	—	—	< 3.4
444*	6:40:41.1	9:33:57.9	0.50	46	06404114+0933578	2776	4522	—	79	94	1.1
445	6:40:41.2	9:27:23.5	0.50	—	06404118+0927235	—	4534	—	—	—	< 2.3
446*	6:40:41.2	9:31:28.7	0.50	47	06404119+0931287	—	4529	—	—	—	1.5
447	6:40:41.2	9:27:21.1	1.00	—	—	—	4531	—	—	—	< 2.4
448	6:40:41.2	9:30:07.2	0.50	—	06404120+0930072	2779	4533	—	—	—	< 1.5
449	6:40:41.2	9:28:16.3	1.00	—	—	—	4535	—	—	—	< 2.0
450	6:40:41.2	9:38:37.5	1.00	—	—	—	4536	—	—	—	< 1.6
451	6:40:41.3	9:37:53.2	0.50	—	06404130+0937532	—	4539	—	—	—	< 1.3
452*	6:40:41.3	9:39:09.5	2.14	48	—	—	—	—	—	—	3.9
453	6:40:41.4	9:28:04.4	1.00	—	—	—	4548	—	—	—	< 2.2
454	6:40:41.4	9:31:31.5	0.50	—	06404144+0931314	2790	4555	—	—	—	< 1.3
455	6:40:41.5	9:27:30.4	1.00	—	—	—	4556	—	—	—	< 2.4
456	6:40:41.5	9:27:37.1	0.79	—	06404151+0927370	—	4557	—	—	—	< 2.3
457	6:40:41.6	9:40:14.7	0.50	—	06404163+0940146	—	4566	—	—	—	< 2.2
458	6:40:41.6	9:32:20.6	10.12	—	—	—	—	30	—	—	< 1.2
459	6:40:41.6	9:27:19.9	1.00	—	—	—	4565	—	—	—	< 2.4
460*	6:40:41.6	9:31:43.2	0.50	49	06404164+0931431	2793	4568	—	—	102	2.0
461	6:40:41.8	9:26:55.9	0.50	—	06404176+0926559	2800	4572	—	—	—	< 2.8
462*	6:40:41.8	9:41:38.6	0.50	50	06404184+0941386	—	4578	—	—	106	3.7
463	6:40:41.9	9:40:01.4	1.00	—	—	—	4581	—	—	—	< 2.2
464	6:40:41.9	9:42:24.0	0.50	—	06404193+0942240	—	4583	—	—	—	< 2.8
465	6:40:41.9	9:35:48.6	0.57	—	06404193+0935486	2804	4585	—	—	—	< 1.0
466	6:40:42.1	9:31:41.8	0.50	51	06404213+0931418	—	4595	—	—	—	3.1
467	6:40:42.2	9:41:53.1	0.89	—	06404217+0941530	—	4596	—	—	—	< 2.9
468*	6:40:42.2	9:33:37.4	0.50	52	06404218+0933374	2811	4598	—	84	107	19.5
469	6:40:42.2	9:30:57.6	1.00	—	—	—	4599	—	—	—	< 1.3
470*	6:40:42.2	9:40:11.1	0.50	53	06404221+0940110	2817	4602	32†	—	108	55.5
471	6:40:42.2	9:37:01.4	0.50	—	06404222+0937014	—	4603	—	—	—	< 1.2
472	6:40:42.2	9:38:38.9	0.50	—	06404223+0938389	—	—	—	—	—	< 1.6
473	6:40:42.2	9:42:48.4	0.50	—	06404223+0942483	—	—	—	—	—	< 3.1
474*	6:40:42.3	9:39:21.3	0.50	54	06404228+0939212	—	—	31	83	—	75.5
475	6:40:42.3	9:37:57.2	1.00	—	—	—	4608	—	—	—	< 1.2
476*	6:40:42.3	9:34:25.0	0.50	55	06404232+0934250	2819	4610	—	—	109	11.1
477	6:40:42.4	9:32:45.4	0.56	—	06404235+0932454	—	—	—	—	—	< 1.0
478	6:40:42.4	9:27:21.9	0.50	—	06404237+0927218	2820	4613	—	—	—	< 2.3
479*	6:40:42.4	9:32:20.6	0.50	56	06404244+0932206	2822	4615	—	—	110	32.6
480	6:40:42.5	9:31:26.6	0.50	—	06404246+0931266	—	4617	—	—	—	< 1.2

Table 3. (Continued)

N	RA [h m s]	Dec. [d m s]	Id. rad. ['"]	ACIS	2Mass	Reb.+	Lamm+	Flacc+	W56	Dahm+	Ct. Rate. [$10^{-4} s^{-1}$]
481	6:40:42.5	9:41:06.3	1.00	—	—	—	4619	—	—	—	< 2.4
482	6:40:42.6	9:42:50.2	1.00	—	—	—	4623	—	—	—	< 3.1
483	6:40:42.7	9:29:31.5	1.00	—	—	—	4629	—	—	—	< 1.5
484	6:40:42.7	9:42:54.9	1.00	—	—	—	4630	—	—	—	< 3.1
485	6:40:42.7	9:40:07.9	0.83	—	06404270+0940079	—	4634	32†	—	—	< 2.1
486	6:40:42.7	9:27:27.8	1.00	—	—	—	4633	—	—	—	< 2.2
487*	6:40:42.7	9:27:06.8	0.50	—	06404273+0927067	2830	4635	—	—	—	< 2.3
488*	6:40:42.8	9:33:35.1	0.50	57	06404278+0933350	—	4638	—	—	112	2.6
489	6:40:42.8	9:30:36.6	0.50	—	06404280+0930365	2835	4639	—	—	—	< 1.3
490*	6:40:42.8	9:39:05.6	0.54	58	06404280+0939056	—	—	—	—	—	1.7
491	6:40:42.8	9:43:14.9	0.58	—	06404281+0943148	—	4640	—	—	—	< 3.3
492	6:40:42.8	9:29:19.3	1.00	—	—	—	4643	—	—	—	< 1.6
493	6:40:42.9	9:38:51.8	0.50	—	06404294+0938517	—	—	—	—	—	< 1.6
494	6:40:43.1	9:40:29.0	1.00	—	—	—	4650	—	—	—	< 2.2
495	6:40:43.1	9:42:34.5	1.00	—	—	—	4652	—	—	—	< 2.9
496	6:40:43.2	9:40:23.6	1.00	—	—	—	4654	—	—	—	< 2.2
497	6:40:43.2	9:26:49.4	0.68	—	06404316+0926493	2842	4653	—	—	—	< 3.6
498	6:40:43.2	9:26:52.5	1.00	—	—	—	4656	—	—	—	< 2.5
499	6:40:43.2	9:26:57.1	1.00	—	—	—	4657	—	—	—	< 2.4
500	6:40:43.2	9:42:42.6	1.00	—	—	—	4659	—	—	—	< 3.0
501	6:40:43.2	9:29:47.3	1.00	—	—	—	4660	—	—	—	< 1.4
502	6:40:43.2	9:43:44.8	0.50	—	06404321+0943447	2847	4662	—	—	—	< 13.9
503*	6:40:43.2	9:31:15.0	0.50	59	06404323+0931149	2845	4664	—	—	114	35.7
504	6:40:43.3	9:33:59.1	0.50	—	06404330+0933591	—	4670	—	—	—	< 0.9
505	6:40:43.3	9:43:03.3	0.50	—	06404330+0943033	2849	4671	—	—	—	< 3.2
506	6:40:43.4	9:43:14.8	1.00	—	—	—	4678	—	—	—	< 3.3
507	6:40:43.4	9:43:17.0	1.00	—	—	—	4679	—	—	—	< 3.3
508*	6:40:43.4	9:30:34.3	0.50	60	06404340+0930343	—	4680	—	—	116	4.0
509*	6:40:43.4	9:28:40.9	0.50	61	06404342+0928409	2853	4682	—	—	117	17.4
510*	6:40:43.6	9:37:20.5	0.50	62	06404358+0937205	—	4695	—	—	—	2.2
511	6:40:43.6	9:40:42.4	0.50	—	06404360+0940423	—	4696	—	—	—	< 2.1
512	6:40:43.6	9:33:39.9	1.00	—	—	—	4698	—	—	—	< 0.9
513*	6:40:43.6	9:35:11.5	0.50	64	06404363+0935114	2864	4700	—	—	—	3.1
514*	6:40:43.6	9:31:14.4	2.09	63	—	—	—	—	—	—	1.1
515*	6:40:43.7	9:38:35.7	0.50	65	06404365+0938356	—	4703	—	—	119	35.8
516	6:40:43.7	9:30:02.3	0.50	—	06404368+0930023	—	4705	—	—	—	< 1.3
517	6:40:43.7	9:43:14.2	1.00	—	—	—	4706	—	—	—	< 3.3
518	6:40:43.7	9:28:55.1	1.00	—	—	—	4708	—	—	—	< 3.5
519	6:40:43.8	9:39:39.5	0.50	—	06404381+0939395	—	—	—	—	—	< 1.7
520	6:40:43.8	9:38:49.2	1.00	—	—	—	4719	—	—	—	< 1.5
521*	6:40:43.9	9:28:55.2	0.50	66	06404386+0928552	2868	4722	—	—	—	3.9
522	6:40:43.9	9:42:35.1	1.00	—	—	—	4725	—	—	—	< 2.9
523	6:40:44.0	9:28:22.1	1.00	—	—	—	4734	—	—	—	< 1.9
524	6:40:44.0	9:43:39.6	1.00	—	—	—	4735	—	—	—	< 6.7
525	6:40:44.0	9:29:21.8	1.00	—	—	—	4741	—	—	—	< 1.5
526	6:40:44.0	9:29:32.1	1.00	—	—	—	4743	—	—	—	< 1.4
527	6:40:44.1	9:28:05.9	0.50	—	06404411+0928058	—	4748	—	—	—	< 1.8
528	6:40:44.2	9:41:04.0	1.00	—	—	—	4752	—	—	—	< 2.1
529	6:40:44.2	9:43:05.7	0.50	—	06404418+0943056	2877	4754	—	—	—	< 3.2
530*	6:40:44.2	9:36:35.9	1.05	67	—	—	—	—	—	—	1.5
531	6:40:44.4	9:42:25.8	0.50	—	06404440+0942258	2887	4764	—	—	—	< 2.9
532	6:40:44.5	9:40:22.9	1.00	—	—	—	4770	—	—	—	< 1.9
533	6:40:44.5	9:29:43.2	0.50	—	06404452+0929432	2891	4772	—	—	—	< 1.3
534*	6:40:44.6	9:32:26.2	0.50	68	06404459+0932261	2895	4776	36	—	123	6.8
535*	6:40:44.6	9:27:44.0	0.50	—	06404459+0927439	2897	4775	—	—	—	< 1.9
536	6:40:44.7	9:28:04.5	1.00	—	—	—	4785	—	—	—	< 1.8
537	6:40:44.7	9:30:45.9	1.00	—	—	—	4786	—	—	—	< 1.2
538	6:40:44.7	9:30:00.8	0.50	—	06404471+0930008	2899	4788	—	—	—	< 1.2
539*	6:40:44.8	9:34:04.6	1.00	69	—	—	—	—	—	—	1.1
540*	6:40:44.9	9:38:49.8	0.50	70	06404494+0938497	2906	4798	—	—	—	2.4

Table 3. (Continued)

N	RA [h m s]	Dec. [d m s]	Id. rad. [""]	ACIS	2Mass	Reb.+	Lamm+	Flacc+	W56	Dahm+	Ct. Rate. [$10^{-4} s^{-1}$]
541	6:40:45.0	9:30:01.2	0.50	—	06404500+0930011	—	4803	—	—	—	< 1.2
542	6:40:45.0	9:33:22.9	0.50	—	06404502+0933229	2909	4806	—	—	—	< 0.8
543	6:40:45.0	9:27:43.3	1.00	—	—	—	4805	—	—	—	< 1.9
544	6:40:45.1	9:42:06.5	1.00	—	—	—	4813	—	—	—	< 2.8
545	6:40:45.1	9:43:01.7	0.64	—	06404510+0943016	—	4814	—	—	—	< 3.3
546	6:40:45.1	9:41:28.7	0.50	—	06404510+0941287	2912	4816	—	—	—	< 2.2
547	6:40:45.1	9:28:31.6	0.50	—	06404513+0928316	2914	4821	—	—	—	< 1.8
548	6:40:45.2	9:43:11.5	1.00	—	—	—	4824	—	—	—	< 3.4
549*	6:40:45.2	9:28:44.4	0.50	71	06404516+0928444	2915	4826	—	—	130	34.7
550	6:40:45.2	9:43:17.1	0.50	—	06404519+0943170	2917	4827	—	—	—	< 3.4
551	6:40:45.3	9:43:03.4	1.00	—	—	—	4832	—	—	—	< 3.3
552	6:40:45.3	9:35:45.0	0.50	—	06404526+0935450	—	—	—	—	—	< 0.8
553	6:40:45.3	9:42:35.1	1.00	—	—	—	4836	—	—	—	< 3.0
554	6:40:45.3	9:38:20.0	0.95	—	06404530+0938199	—	—	—	—	—	< 1.3
555	6:40:45.3	9:38:47.6	0.50	—	06404534+0938475	—	4838	—	—	—	< 1.6
556	6:40:45.4	9:37:51.5	0.50	—	06404539+0937515	2922	4841	—	—	—	< 1.2
557	6:40:45.4	9:40:29.7	0.50	—	06404540+0940297	2923	4843	—	—	—	< 1.9
558	6:40:45.4	9:43:17.9	1.00	—	—	—	4844	—	—	—	< 3.4
559	6:40:45.5	9:26:56.0	1.50	—	—	2925	—	—	—	—	< 2.2
560	6:40:45.5	9:28:00.5	0.50	—	06404552+0928005	—	—	—	—	—	< 1.7
561	6:40:45.6	9:28:40.0	1.00	—	—	—	4858	—	—	—	< 1.7
562	6:40:45.6	9:28:21.3	1.00	—	—	—	4861	—	—	—	< 1.8
563	6:40:45.8	9:28:02.6	0.50	—	06404576+0928025	2934	4869	—	—	—	< 1.7
564*	6:40:45.9	9:38:44.4	0.50	72	06404587+0938443	2938	4875	—	—	131	1.8
565	6:40:45.9	9:39:19.5	0.69	—	06404590+0939195	—	4877	—	—	—	< 1.7
566*	6:40:45.9	9:26:44.2	5.27	73	—	—	—	—	—	—	1.8
567	6:40:45.9	9:36:37.8	1.00	—	—	2940	4878	—	—	—	< 0.9
568	6:40:46.0	9:30:51.8	1.00	—	—	—	4882	—	—	—	< 1.0
569	6:40:46.1	9:43:15.5	1.00	—	—	—	4888	—	—	—	< 3.4
570	6:40:46.1	9:39:46.4	0.67	—	06404614+0939464	—	4890	—	—	—	< 1.8
571	6:40:46.2	9:42:46.9	1.00	—	—	—	4893	—	—	—	< 3.2
572	6:40:46.2	9:35:12.4	1.00	—	—	—	4895	—	—	—	< 1.7
573	6:40:46.3	9:42:51.5	1.00	—	—	—	4898	—	—	—	< 3.2
574	6:40:46.3	9:43:06.3	1.00	—	—	—	4901	—	—	—	< 3.3
575	6:40:46.4	9:42:26.5	1.00	—	—	—	4903	—	—	—	< 2.8
576	6:40:46.4	9:27:53.7	1.00	—	—	—	4906	—	—	—	< 1.8
577	6:40:46.4	9:41:56.8	0.50	—	06404644+0941568	2947	4908	—	—	—	< 2.5
578	6:40:46.5	9:42:04.5	1.00	—	—	—	4909	—	—	—	< 2.6
579	6:40:46.6	9:33:52.4	0.50	—	06404655+0933523	2950	4913	—	—	—	< 0.8
580*	6:40:46.6	9:42:49.7	0.61	—	06404658+0942497	—	4914	—	—	135	< 3.2
581	6:40:46.6	9:41:54.8	0.50	—	06404663+0941547	—	4919	—	—	—	< 2.5
582	6:40:46.7	9:42:00.8	1.00	—	—	—	4921	—	—	—	< 2.6
583	6:40:46.7	9:37:06.3	0.50	—	06404667+0937062	—	4922	—	—	—	< 1.0
584*	6:40:46.7	9:40:01.4	0.50	—	06404668+0940014	2957	4923	—	—	137	< 1.7
585*	6:40:46.7	9:40:22.3	2.69	74	—	—	—	—	—	—	5.4
586*	6:40:46.8	9:32:57.5	0.50	76	06404677+0932575	—	4928	—	—	—	1.8
587	6:40:46.8	9:42:56.9	0.61	—	06404677+0942568	—	4927	—	—	—	< 3.2
588	6:40:46.8	9:28:44.5	1.00	—	—	—	4929	—	—	—	< 1.6
589	6:40:46.8	9:26:53.9	1.00	—	—	—	4935	—	—	—	< 2.5
590*	6:40:46.9	9:32:30.9	0.50	75	06404686+0932309	2969	4937	40	—	139	10.4
591	6:40:46.9	9:26:39.1	1.00	—	—	—	4938	—	—	—	< 4.9
592	6:40:46.9	9:33:22.3	1.00	—	—	—	4939	—	—	—	< 0.8
593	6:40:47.0	9:38:37.4	0.50	—	06404696+0938374	—	4943	—	—	—	< 1.3
594*	6:40:47.1	9:30:19.7	0.50	77	06404710+0930197	—	4954	—	—	—	1.0
595*	6:40:47.1	9:32:40.1	0.50	78	06404711+0932401	2974	4955	41	95	142	61.6
596*	6:40:47.1	9:42:07.7	0.50	79	06404712+0942077	2975	4956	—	—	143	2.7
597	6:40:47.1	9:28:55.9	0.50	—	06404712+0928558	—	4958	—	—	—	< 1.5
598*	6:40:47.2	9:28:49.9	0.50	—	06404717+0928498	2979	4960	—	—	—	< 1.6
599	6:40:47.2	9:41:55.9	1.00	—	—	—	4961	—	—	—	< 2.7
600*	6:40:47.2	9:31:08.7	0.50	80	06404722+0931086	2981	4967	—	—	145	1.5

Table 3. (Continued)

N	RA [h m s]	Dec. [d m s]	Id. rad. ['"]	ACIS	2Mass	Reb.+	Lamm+	Flacc+	W56	Dahm+	Ct. Rate. [$10^{-4} s^{-1}$]
601	6:40:47.2	9:41:47.5	1.00	—	—	—	4966	—	—	—	< 2.6
602	6:40:47.3	9:29:01.8	1.00	—	—	—	4968	—	—	—	< 1.5
603	6:40:47.3	9:42:41.8	1.00	—	—	—	4969	—	—	—	< 3.2
604	6:40:47.3	9:42:26.8	0.50	—	06404730+0942268	—	4970	—	—	—	< 3.0
605	6:40:47.3	9:27:29.2	1.00	—	—	—	4973	—	—	—	< 2.1
606	6:40:47.4	9:42:42.3	0.59	—	06404737+0942423	—	4978	—	—	—	< 3.3
607	6:40:47.5	9:32:48.6	0.50	—	06404750+0932485	—	4985	—	—	—	< 0.8
608	6:40:47.5	9:42:53.5	0.86	—	06404752+0942534	—	4994	—	—	—	< 3.3
609*	6:40:47.6	9:40:33.1	0.50	81	06404756+0940331	2988	4991	—	—	—	1.9
610	6:40:47.7	9:41:38.1	0.62	—	06404769+0941381	—	4998	—	—	—	< 2.5
611	6:40:47.7	9:43:26.5	1.00	—	—	—	4999	—	—	—	< 4.6
612	6:40:47.7	9:42:10.7	0.50	—	06404771+0942106	2992	5002	—	—	—	< 2.9
613	6:40:47.7	9:29:42.1	0.55	—	06404771+0929421	2994	5001	—	—	—	< 1.2
614	6:40:47.8	9:26:37.4	1.00	—	—	—	5004	—	—	—	< 4.2
615*	6:40:47.8	9:26:45.2	2.62	82	—	—	—	—	—	—	6.2
616	6:40:47.9	9:27:47.4	1.00	—	—	—	5011	—	—	—	< 1.7
617	6:40:47.9	9:29:44.9	1.00	—	—	—	5012	—	—	—	< 1.3
618*	6:40:47.9	9:33:03.1	0.50	83	06404792+0933031	2997	5015	—	—	—	10.5
619	6:40:48.0	9:27:29.5	0.50	—	06404796+0927294	2999	5018	—	—	—	< 2.0
620*	6:40:48.0	9:32:03.7	0.50	84	06404799+0932037	3000	5019	—	—	—	0.8
621	6:40:48.0	9:31:20.9	0.50	—	06404801+0931208	3002	5023	—	—	—	< 0.8
622*	6:40:48.1	9:34:05.5	0.50	85	06404807+0934054	3003	5027	—	—	—	0.8
623	6:40:48.1	9:27:31.2	1.00	—	—	—	5026	—	—	—	< 1.9
624	6:40:48.2	9:26:54.1	1.00	—	—	—	5032	—	—	—	< 2.8
625*	6:40:48.2	9:27:00.8	0.50	86	06404819+0927008	3010	5035	—	—	151	3.9
626	6:40:48.2	9:27:42.6	1.00	—	—	—	5036	—	—	—	< 1.8
627	6:40:48.2	9:36:23.5	1.00	—	—	—	5037	—	—	—	< 0.9
628	6:40:48.3	9:30:54.6	0.50	—	06404825+0930546	—	5040	—	—	—	< 0.9
629*	6:40:48.3	9:36:38.7	0.50	87	06404827+0936386	3013	5041	44	97	152	60.0
630	6:40:48.4	9:42:34.4	1.00	—	—	—	5050	—	—	—	< 3.2
631*	6:40:48.5	9:34:16.8	0.50	88	06404853+0934167	3016	5055	—	—	—	1.5
632	6:40:48.6	9:36:48.1	0.50	—	06404861+0936481	—	—	—	—	—	< 0.9
633*	6:40:48.6	9:32:52.4	0.50	90	06404862+0932524	3018	5063	45	101	155	25.6
634*	6:40:48.6	9:35:57.8	0.50	89	06404862+0935578	3017	5061	—	—	154	15.7
635	6:40:48.6	9:26:55.6	1.00	—	—	—	5062	—	—	—	< 2.4
636	6:40:48.6	9:32:44.1	1.00	—	—	—	5065	—	—	—	< 0.8
637	6:40:48.7	9:39:01.8	0.63	—	06404873+0939017	—	—	—	—	—	< 1.3
638*	6:40:48.8	9:32:42.6	0.50	91	06404875+0932425	3019	5070	—	—	156	18.3
639	6:40:48.8	9:42:01.8	0.61	—	06404882+0942017	—	5072	—	—	—	< 2.7
640	6:40:48.8	9:34:05.8	1.00	—	—	—	5073	—	—	—	< 0.7
641*	6:40:48.8	9:43:25.7	0.50	—	06404884+0943256	3023	5074	—	—	157	< 12.8
642	6:40:48.9	9:31:10.3	0.82	—	06404887+0931103	—	5081	—	—	—	< 0.9
643	6:40:48.9	9:29:16.4	1.00	—	—	—	5077	—	—	—	< 1.3
644	6:40:48.9	9:41:36.3	1.00	—	—	—	5083	—	—	—	< 2.3
645	6:40:48.9	9:30:03.0	1.00	—	—	—	5085	—	—	—	< 1.2
646	6:40:49.0	9:42:39.2	0.50	—	06404896+0942391	3026	5089	—	—	—	< 3.0
647*	6:40:49.0	9:36:55.2	1.99	92	—	—	—	—	—	—	0.9
648	6:40:49.0	9:29:14.3	1.00	—	—	—	5096	—	—	—	< 1.3
649*	6:40:49.1	9:37:36.3	0.50	93	06404912+0937363	—	5099	—	—	158	2.8
650	6:40:49.2	9:37:14.5	0.50	—	06404916+0937145	—	5101	—	—	—	< 0.9
651	6:40:49.2	9:30:51.3	1.00	—	—	—	5102	—	—	—	< 1.0
652	6:40:49.2	9:27:11.3	0.50	—	06404921+0927112	—	5104	—	—	—	< 2.1
653	6:40:49.3	9:33:43.8	0.50	—	06404933+0933437	—	—	—	—	—	< 0.7
654	6:40:49.3	9:31:57.7	1.00	—	—	—	5112	—	—	—	< 0.8
655	6:40:49.4	9:30:54.7	1.00	—	—	—	5113	—	—	—	< 0.9
656	6:40:49.4	9:36:57.1	0.50	—	06404939+0936571	—	—	—	—	—	< 0.9
657*	6:40:49.5	9:31:41.6	1.55	94	—	—	—	—	—	—	2.3
658	6:40:49.5	9:30:32.7	1.00	—	—	—	5119	—	—	—	< 1.1
659	6:40:49.6	9:38:40.4	0.50	—	06404955+0938403	3043	5120	—	—	—	< 1.2
660	6:40:49.6	9:38:39.7	1.00	—	—	—	5124	—	—	—	< 1.2

Table 3. (Continued)

N	RA [h m s]	Dec. [d m s]	Id. rad. [""]	ACIS	2Mass	Reb.+	Lamm+	Flacc+	W56	Dahm+	Ct. Rate. [$10^{-4} s^{-1}$]
661	6:40:49.7	9:41:07.3	1.00	—	—	—	5133	—	—	—	< 2.0
662	6:40:49.9	9:41:49.2	0.50	—	06404986+0941491	—	5139	—	—	—	< 2.5
663*	6:40:49.9	9:36:49.5	0.50	95	06404989+0936494	3051	5143	—	105	167	11.9
664	6:40:50.0	9:42:15.2	1.00	—	—	—	5147	—	—	—	< 2.8
665	6:40:50.0	9:27:27.9	1.00	—	—	—	5151	—	—	—	< 1.8
666	6:40:50.1	9:37:10.7	1.00	—	—	—	5154	—	—	—	< 0.9
667	6:40:50.1	9:35:20.8	1.00	—	—	—	5156	—	—	—	< 0.7
668*	6:40:50.1	9:29:32.5	3.27	96	—	—	—	—	—	—	1.8
669*	6:40:50.1	9:30:39.9	0.50	97	06405010+0930399	3059	5160	—	—	171	14.1
670	6:40:50.1	9:43:00.3	1.00	—	—	—	5162	—	—	—	< 3.3
671	6:40:50.2	9:37:25.5	0.50	—	06405018+0937255	3062	5166	—	106	—	< 0.9
672	6:40:50.2	9:33:49.1	0.54	—	06405018+0933490	3063	5167	—	—	—	< 0.7
673	6:40:50.2	9:30:23.0	0.50	—	06405023+0930229	—	5170	—	—	—	< 1.0
674	6:40:50.3	9:29:36.6	0.50	—	06405025+0929365	—	5171	—	—	—	< 1.8
675	6:40:50.3	9:32:24.2	0.50	—	06405026+0932241	—	5172	—	—	—	< 0.8
676	6:40:50.3	9:27:32.3	0.66	—	06405029+0927323	3070	5175	—	—	—	< 1.7
677	6:40:50.3	9:43:11.8	1.00	—	—	—	5178	—	—	—	< 3.7
678	6:40:50.4	9:35:35.9	0.50	—	06405036+0935359	—	—	—	—	—	< 0.7
679	6:40:50.4	9:36:47.2	0.61	—	06405037+0936471	—	5183	—	—	—	< 0.8
680	6:40:50.4	9:27:58.5	1.00	—	—	—	5182	—	—	—	< 1.5
681*	6:40:50.5	9:32:19.7	1.00	98	—	—	—	—	—	—	10.2
682	6:40:50.5	9:41:50.7	1.00	—	—	—	5191	—	—	—	< 2.4
683	6:40:50.6	9:42:55.0	0.52	—	06405060+0942549	3080	5194	—	—	—	< 3.2
684*	6:40:50.6	9:31:31.5	0.50	99	06405063+0931314	3081	5199	—	—	—	1.2
685	6:40:50.6	9:39:27.8	1.00	—	—	—	5200	—	—	—	< 1.3
686	6:40:50.7	9:42:36.4	0.58	—	06405069+0942364	—	5201	—	—	—	< 2.7
687	6:40:50.8	9:27:26.1	0.80	—	06405076+0927260	—	5206	—	—	—	< 1.8
688	6:40:50.8	9:29:21.1	1.00	—	—	—	5207	—	—	—	< 1.3
689*	6:40:50.8	9:41:55.3	0.50	100	06405078+0941553	3087	5210	—	—	180	3.7
690	6:40:50.8	9:40:09.2	1.00	—	—	—	5211	—	—	—	< 1.6
691	6:40:50.8	9:36:42.4	0.50	—	06405082+0936424	—	—	—	—	—	< 0.8
692	6:40:50.9	9:27:19.5	1.00	—	—	—	5214	—	—	—	< 1.8
693	6:40:50.9	9:43:12.6	1.00	—	—	—	5215	—	—	—	< 3.6
694	6:40:50.9	9:41:09.4	0.77	—	06405091+0941093	—	5220	—	—	—	< 1.9
695	6:40:51.0	9:27:05.2	0.50	—	06405097+0927052	3093	5221	—	—	—	< 1.9
696	6:40:51.0	9:31:32.1	0.50	—	06405101+0931320	—	5224	—	—	—	< 0.8
697	6:40:51.0	9:37:14.8	0.50	—	06405103+0937147	—	5226	—	—	—	< 0.8
698*	6:40:51.0	9:38:52.9	1.49	101	—	—	—	—	—	—	3.3
699	6:40:51.1	9:31:22.7	1.00	—	—	—	5231	—	—	—	< 0.8
700	6:40:51.1	9:39:43.1	0.50	—	06405111+0939431	—	5232	—	—	—	< 1.4
701	6:40:51.2	9:26:25.3	0.67	—	06405116+0926252	—	5234	—	—	—	< 2.9
702	6:40:51.2	9:42:17.8	1.00	—	—	—	5237	—	—	—	< 2.6
703	6:40:51.2	9:27:57.8	0.50	—	06405121+0927578	3099	5238	—	—	—	< 1.5
704	6:40:51.2	9:31:33.4	1.00	—	—	—	5242	—	—	—	< 0.8
705*	6:40:51.3	9:36:39.0	0.50	—	06405130+0936390	3101	5244	—	—	—	< 0.7
706	6:40:51.3	9:26:26.9	1.00	—	—	—	5243	—	—	—	< 2.4
707	6:40:51.3	9:30:20.7	0.50	—	06405133+0930207	—	—	—	—	—	< 1.0
708	6:40:51.3	9:27:06.7	1.00	—	—	—	5248	—	—	—	< 1.8
709	6:40:51.4	9:27:45.0	0.53	—	06405136+0927449	—	5249	—	—	—	< 1.6
710*	6:40:51.4	9:30:13.4	0.50	103	06405137+0930133	3103	5252	—	—	187	2.5
711	6:40:51.4	9:41:21.4	0.50	—	06405142+0941213	3106	5257	—	—	—	< 1.9
712*	6:40:51.5	9:37:14.5	0.50	104	06405146+0937144	3107	5263	—	111	—	8.6
713	6:40:51.5	9:31:46.8	0.50	—	06405146+0931468	3108	5262	—	—	—	< 0.8
714	6:40:51.5	9:26:42.7	1.00	—	—	—	5266	—	—	—	< 2.1
715*	6:40:51.5	9:43:24.2	0.50	102	06405154+0943242	3111	5268	—	—	188	3.6
716*	6:40:51.6	9:28:44.5	0.50	105	06405159+0928445	3112	5274	50	—	189	28.8
717	6:40:51.6	9:26:58.2	0.50	—	06405160+0926581	—	5275	—	—	—	< 1.9
718	6:40:51.6	9:26:42.2	0.50	—	06405164+0926421	3115	5277	—	—	—	< 2.1
719	6:40:51.7	9:26:37.1	1.00	—	—	—	5278	—	—	—	< 2.2
720	6:40:51.7	9:26:22.2	1.00	—	—	—	5279	—	—	—	< 3.9

Table 3. (Continued)

N	RA [h m s]	Dec. [d m s]	Id. rad. ["]	ACIS	2Mass	Reb.+	Lamm+	Flacc+	W56	Dahm+	Ct. Rate. [$10^{-4} s^{-1}$]
721	6:40:51.8	9:39:07.5	0.50	—	06405184+0939074	—	5288	—	112	—	< 1.2
722	6:40:51.8	9:32:52.6	0.50	—	06405184+0932526	—	5287	—	—	—	< 0.7
723	6:40:51.9	9:37:55.9	0.50	—	06405191+0937558	—	5292	—	—	—	< 0.9
724	6:40:52.0	9:41:10.9	1.00	—	—	—	5294	—	—	—	< 1.9
725	6:40:52.0	9:26:25.3	1.00	—	—	—	5295	—	—	—	< 2.3
726	6:40:52.0	9:41:22.6	1.00	—	—	—	5296	—	—	—	< 2.0
727*	6:40:52.1	9:29:13.9	0.50	106	06405210+0929139	3125	5303	—	—	192	12.6
728	6:40:52.3	9:41:27.3	0.50	—	06405228+0941272	—	5309	—	—	—	< 2.0
729	6:40:52.3	9:34:58.7	1.00	—	—	—	5310	—	—	—	< 1.1
730	6:40:52.3	9:39:44.3	1.00	—	—	—	5311	—	—	—	< 1.4
731	6:40:52.3	9:27:41.7	0.50	—	06405233+0927417	3128	5313	—	—	—	< 1.6
732	6:40:52.5	9:33:19.6	0.50	—	06405250+0933196	—	5315	—	—	—	< 0.6
733	6:40:52.6	9:32:16.4	1.00	—	—	—	5324	—	—	—	< 0.7
734	6:40:52.6	9:41:58.3	1.00	—	—	—	5325	—	—	—	< 2.3
735	6:40:52.6	9:26:28.4	1.00	—	—	—	5327	—	—	—	< 2.2
736*	6:40:52.6	9:29:53.5	1.02	107	—	—	—	—	—	—	11.4
737	6:40:52.6	9:26:29.6	1.00	—	—	—	5328	—	—	—	< 2.1
738*	6:40:52.7	9:28:55.4	0.50	—	06405271+0928554	3140	5336	—	—	—	< 1.3
739	6:40:52.7	9:38:16.1	0.50	—	06405271+0938160	—	5337	—	—	—	< 1.0
740*	6:40:52.7	9:28:43.8	0.50	—	06405272+0928437	—	5339	—	—	—	< 1.3
741*	6:40:52.8	9:43:00.4	0.50	—	06405275+0943004	3141	5340	—	—	197	< 3.0
742	6:40:52.8	9:26:30.3	1.00	—	—	—	5341	—	—	—	< 2.1
743	6:40:52.9	9:31:53.5	1.00	—	—	—	5346	—	—	—	< 0.7
744*	6:40:52.9	9:35:15.5	0.50	108	06405293+0935155	—	—	—	—	—	11.2
745	6:40:52.9	9:41:54.1	0.75	—	06405294+0941540	—	5353	—	—	—	< 2.1
746*	6:40:53.0	9:26:25.7	0.50	—	06405295+0926257	3145	5355	—	—	199	< 2.2
747	6:40:53.0	9:39:41.5	1.00	—	—	—	5356	—	—	—	< 1.3
748	6:40:53.0	9:27:19.4	0.50	—	06405299+0927193	—	5357	—	—	—	< 1.7
749*	6:40:53.1	9:30:10.3	0.50	—	06405312+0930103	—	5365	—	—	—	< 1.1
750*	6:40:53.2	9:29:54.1	0.50	109	06405321+0929541	3149	5370	—	—	202	1.4
751	6:40:53.2	9:29:57.1	1.00	—	—	—	5372	—	—	—	< 1.1
752	6:40:53.2	9:42:10.8	1.00	—	—	—	5373	—	—	—	< 2.2
753*	6:40:53.3	9:43:11.6	0.50	—	06405328+0943116	3151	5376	—	—	—	< 5.5
754	6:40:53.4	9:26:27.9	1.00	—	—	—	5377	—	—	—	< 2.2
755	6:40:53.4	9:30:22.6	0.50	—	06405337+0930225	—	5378	—	—	—	< 1.0
756	6:40:53.4	9:32:10.6	0.50	—	06405341+0932105	—	5381	—	—	—	< 0.7
757	6:40:53.4	9:42:12.3	1.00	—	—	—	5382	—	—	—	< 2.2
758	6:40:53.5	9:32:06.0	1.00	—	—	—	5385	—	—	—	< 0.7
759	6:40:53.5	9:30:19.8	1.00	—	—	—	5386	—	—	—	< 1.0
760	6:40:53.6	9:36:46.1	0.50	110	06405362+0936461	3156	5392	—	—	—	1.2
761*	6:40:53.6	9:29:53.3	0.50	—	06405363+0929532	—	5391	—	—	203	< 1.1
762*	6:40:53.6	9:33:24.7	0.50	111	06405363+0933247	3157	5394	54	115	206	37.1
763*	6:40:53.8	9:30:39.0	0.50	112	06405377+0930389	—	5400	55	116	—	22.1
764	6:40:53.9	9:40:03.8	0.50	—	06405391+0940037	—	5405	—	—	—	< 1.5
765*	6:40:53.9	9:38:04.9	1.16	113	—	—	—	—	—	—	1.1
766	6:40:53.9	9:40:32.5	0.50	—	06405393+0940324	—	5406	—	—	—	< 1.6
767	6:40:54.0	9:32:11.0	1.00	—	—	—	5409	—	—	—	< 0.7
768	6:40:54.0	9:37:29.1	0.50	—	06405396+0937290	—	—	—	—	—	< 0.9
769	6:40:54.0	9:42:15.4	0.50	—	06405396+0942153	3163	5410	—	—	—	< 2.3
770	6:40:54.0	9:26:42.7	1.00	—	—	—	5411	—	—	—	< 2.3
771*	6:40:54.1	9:29:51.1	0.50	114	06405411+0929510	3166	5413	57	—	208	83.7
772	6:40:54.1	9:28:17.8	1.00	—	—	—	5415	—	—	—	< 1.4
773	6:40:54.2	9:28:30.4	0.50	—	06405417+0928303	—	5419	—	—	—	< 1.4
774	6:40:54.3	9:42:50.4	1.00	—	—	—	5427	—	—	—	< 2.8
775	6:40:54.3	9:29:60.0	1.00	—	—	—	5428	—	—	—	< 1.1
776	6:40:54.3	9:40:22.7	0.50	—	06405430+0940226	—	5430	—	—	—	< 1.7
777	6:40:54.4	9:27:00.5	0.52	—	06405437+0927005	—	5432	—	—	—	< 2.3
778	6:40:54.4	9:39:50.5	1.00	—	—	—	5434	—	—	—	< 1.5
779	6:40:54.5	9:38:59.4	0.50	—	06405446+0938594	—	—	—	—	—	< 1.1
780	6:40:54.5	9:42:38.2	0.50	—	06405449+0942381	3185	5438	—	—	—	< 2.6

Table 3. (Continued)

N	RA [h m s]	Dec. [d m s]	Id. rad. [""]	ACIS	2Mass	Reb.+	Lamm+	Flacc+	W56	Dahm+	Ct. Rate. [$10^{-4} s^{-1}$]
781	6:40:54.5	9:42:55.3	1.00	—	—	—	5441	—	—	—	< 2.8
782	6:40:54.6	9:31:07.7	0.50	—	06405455+0931076	—	5440	—	—	—	< 0.8
783	6:40:54.6	9:36:25.9	1.00	—	—	—	5444	—	—	—	< 0.7
784	6:40:54.6	9:43:07.6	1.00	—	—	—	5447	—	—	—	< 3.9
785	6:40:54.7	9:39:58.1	1.00	—	—	—	5449	—	—	—	< 1.5
786*	6:40:54.7	9:31:59.0	1.11	115	—	—	—	—	—	—	0.7
787	6:40:54.7	9:42:50.1	0.50	—	06405471+0942500	—	5453	—	—	—	< 2.8
788	6:40:54.8	9:37:58.7	0.50	—	06405480+0937587	—	—	—	—	—	< 0.9
789	6:40:55.0	9:42:11.5	1.00	—	—	—	5469	—	—	—	< 2.3
790	6:40:55.1	9:32:39.6	0.50	—	06405505+0932395	—	5472	—	—	—	< 0.6
791	6:40:55.1	9:42:58.6	1.00	—	—	—	5474	—	—	—	< 2.9
792*	6:40:55.1	9:33:18.7	0.50	116	06405514+0933186	3199	5475	—	—	212	1.2
793*	6:40:55.2	9:30:16.7	1.39	117	—	—	—	—	—	—	1.1
794*	6:40:55.2	9:41:28.9	0.50	—	06405522+0941289	3202	5482	—	—	—	< 2.0
795	6:40:55.3	9:42:36.8	0.50	—	06405526+0942367	—	5484	—	—	—	< 2.6
796*	6:40:55.3	9:33:24.9	0.50	118	06405527+0933249	3206	5486	—	—	—	1.6
797	6:40:55.3	9:30:07.8	0.50	—	06405530+0930078	3208	5490	—	—	215	< 1.0
798*	6:40:55.3	9:39:58.8	0.50	119	06405532+0939588	—	5491	—	—	214	12.1
799	6:40:55.4	9:39:52.1	1.00	—	—	—	5493	—	—	—	< 1.5
800	6:40:55.4	9:26:23.1	1.00	—	—	—	5496	—	—	—	< 3.6
801	6:40:55.4	9:30:18.0	0.50	—	06405540+0930180	—	5497	—	—	—	< 1.0
802*	6:40:55.4	9:37:23.7	0.50	120	06405542+0937237	3211	5498	59	119	217	39.2
803*	6:40:55.5	9:31:21.8	0.50	121	06405548+0931218	3212	5501	—	120	—	1.8
804*	6:40:55.5	9:38:39.6	0.50	122	06405554+0938396	3213	5502	—	—	—	1.4
805	6:40:55.6	9:28:26.5	1.00	—	—	—	5503	—	—	—	< 1.8
806*	6:40:55.6	9:38:24.9	0.50	123	06405561+0938249	3214	5505	—	—	219	2.0
807*	6:40:55.8	9:40:18.2	0.50	124	06405577+0940181	3218	5518	60	—	223	49.3
808	6:40:55.8	9:31:48.0	1.00	—	—	—	5519	—	—	—	< 0.7
809*	6:40:55.8	9:36:06.2	0.50	125	06405579+0936061	—	5520	—	—	—	1.1
810	6:40:55.8	9:26:29.7	1.00	—	—	—	5522	—	—	—	< 2.6
811*	6:40:55.9	9:37:17.8	0.50	126	06405586+0937177	3221	5526	—	—	225	3.4
812	6:40:55.9	9:36:59.0	0.50	—	06405586+0936590	3222	5525	—	—	—	< 0.8
813	6:40:55.9	9:31:32.4	0.50	—	06405590+0931324	—	5528	—	—	—	< 0.7
814	6:40:56.0	9:30:02.4	0.71	—	06405603+0930024	—	5532	63†	—	—	< 1.0
815	6:40:56.0	9:28:12.9	1.00	—	—	—	5531	—	—	—	< 3.5
816	6:40:56.1	9:43:02.6	0.50	—	06405606+0943025	3226	5534	—	—	—	< 3.2
817*	6:40:56.1	9:42:54.1	0.50	—	06405607+0942540	3228	5533	—	—	226	< 2.8
818	6:40:56.1	9:30:16.9	0.67	—	06405614+0930169	—	5537	63†	—	—	< 1.0
819*	6:40:56.2	9:36:30.9	0.50	127	06405616+0936309	—	5538	—	122	227	22.0
820	6:40:56.2	9:32:22.9	0.50	—	06405621+0932229	3232	5540	—	—	—	< 0.6
821	6:40:56.2	9:40:45.4	1.00	—	—	—	5543	—	—	—	< 1.8
822*	6:40:56.2	9:39:32.7	0.50	129	06405624+0939327	3233	5542	—	—	228	2.3
823	6:40:56.2	9:40:37.9	0.50	128	06405625+0940378	3234	5544	—	—	—	1.5
824	6:40:56.3	9:28:27.9	0.71	—	06405626+0928279	—	5547	—	—	—	< 3.5
825	6:40:56.3	9:39:30.5	1.00	—	—	—	5545	—	—	—	< 2.3
826	6:40:56.3	9:37:30.2	0.50	—	06405627+0937302	—	—	—	—	—	< 0.8
827	6:40:56.3	9:34:18.0	0.50	130	06405630+0934180	3236	5548	—	—	229	5.2
828*	6:40:56.4	9:30:50.0	0.50	—	06405638+0930499	—	5550	—	—	—	< 0.8
829*	6:40:56.4	9:35:53.3	0.50	131	06405639+0935533	3240	5551	—	123	230	1.7
830	6:40:56.4	9:34:44.2	0.57	—	06405641+0934442	3241	5552	—	—	—	< 1.2
831	6:40:56.5	9:41:19.3	1.00	—	—	—	5554	—	—	—	< 2.0
832	6:40:56.5	9:34:38.0	1.00	—	—	—	5555	—	—	—	< 1.3
833*	6:40:56.5	9:29:53.9	0.50	132	06405649+0929538	3244	5558	—	—	231	3.7
834	6:40:56.5	9:31:30.9	0.50	—	06405652+0931308	—	5559	—	—	—	< 0.7
835	6:40:56.6	9:39:43.3	0.50	—	06405658+0939432	3248	5560	—	124	—	< 1.5
836	6:40:56.6	9:32:19.6	0.50	—	06405664+0932196	—	5567	—	—	—	< 0.6
837	6:40:56.7	9:30:03.0	0.50	—	06405665+0930029	—	5568	63†	—	—	< 1.0
838	6:40:56.7	9:38:10.2	0.50	—	06405674+0938101	—	5570	—	—	—	< 1.0
839	6:40:56.8	9:41:27.4	0.50	—	06405675+0941273	—	5572	—	—	—	< 2.1
840*	6:40:56.8	9:30:15.1	0.50	133	06405677+0930150	3252	5571	63†	127	232	20.8

Table 3. (Continued)

N	RA [h m s]	Dec. [d m s]	Id. rad. ['"]	ACIS	2Mass	Reb.+	Lamm+	Flacc+	W56	Dahm+	Ct. Rate. [$10^{-4} s^{-1}$]
841*	6:40:56.8	9:29:59.7	0.50	134	06405678+0929596	—	5574	63†	—	233	2.0
842	6:40:56.8	9:30:05.3	0.51	—	06405678+0930052	—	5576	63†	—	—	< 1.1
843*	6:40:56.8	9:37:49.0	0.50	135	06405679+0937490	3253	5575	62	126	234	92.9
844	6:40:56.8	9:28:23.4	1.00	—	—	—	5577	—	—	—	< 2.9
845	6:40:56.8	9:30:14.6	1.00	—	—	—	5579	—	—	—	< 18.5
846	6:40:56.9	9:34:27.2	0.65	—	06405689+0934272	—	5587	—	—	—	< 0.9
847	6:40:56.9	9:31:52.9	0.50	—	06405689+0931528	—	5584	—	—	—	< 0.7
848	6:40:57.0	9:29:38.5	0.50	—	06405699+0929384	3258	5590	—	—	—	< 2.1
849*	6:40:57.0	9:33:01.3	0.50	136	06405699+0933013	3260	5591	—	—	237	14.9
850	6:40:57.1	9:32:27.4	0.50	—	06405708+0932273	—	5595	—	—	—	< 0.6
851	6:40:57.2	9:31:03.0	0.54	—	06405723+0931029	—	5597	—	—	—	< 0.8
852	6:40:57.3	9:26:52.8	0.50	—	06405729+0926527	—	5602	—	—	—	< 2.0
853	6:40:57.4	9:40:42.7	0.50	—	06405740+0940426	—	5606	—	—	—	< 1.9
854*	6:40:57.5	9:29:23.4	0.50	137	06405745+0929234	3268	5612	—	—	238	11.2
855*	6:40:57.5	9:26:17.1	0.50	138	06405745+0926170	3266	5610	—	—	—	2.9
856*	6:40:57.5	9:35:14.7	0.50	—	06405747+0935147	—	5613	—	—	239	< 0.7
857	6:40:57.5	9:40:14.2	1.00	—	—	—	5615	—	—	—	< 1.6
858*	6:40:57.6	9:37:07.5	0.50	139	06405761+0937075	3270	5622	—	—	240	1.5
859*	6:40:57.7	9:31:50.1	0.50	140	06405766+0931501	3272	5624	—	—	241	2.4
860*	6:40:57.7	9:36:08.2	0.50	141	06405767+0936082	—	—	—	—	—	7.8
861	6:40:57.8	9:39:53.8	0.50	—	06405775+0939537	—	—	—	—	—	< 1.4
862*	6:40:57.8	9:30:50.3	0.50	142	06405777+0930502	3276	—	64†	—	242	40.9
863*	6:40:57.8	9:41:20.2	0.50	143	06405783+0941201	3278	—	—	129	244	6.5
864*	6:40:57.9	9:27:09.0	3.41	144	—	—	—	—	—	—	1.8
865*	6:40:58.0	9:36:39.3	1.10	145	—	—	—	—	—	—	0.9
866	6:40:58.0	9:36:15.1	1.00	—	—	—	—	—	—	—	< 0.7
867*	6:40:58.0	9:41:31.4	0.50	—	06405799+0941314	3282	—	—	—	245	< 2.2
868	6:40:58.0	9:40:49.3	0.50	—	06405803+0940493	—	—	—	—	—	< 1.8
869*	6:40:58.1	9:36:53.4	0.50	146	06405809+0936533	3284	—	—	—	246	2.4
870	6:40:58.3	9:42:34.7	0.69	—	06405832+0942347	—	—	—	—	—	< 2.7
871*	6:40:58.3	9:37:56.8	0.50	147	06405834+0937567	—	—	—	—	—	3.5
872*	6:40:58.4	9:27:25.0	0.50	148	06405839+0927250	3289	—	—	—	250	6.5
873	6:40:58.4	9:28:46.9	0.50	—	06405840+0928468	—	—	—	—	—	< 1.5
874	6:40:58.4	9:30:58.0	0.66	—	06405842+0930579	—	—	64†	—	—	< 1.9
875	6:40:58.4	9:37:44.5	0.50	—	06405843+0937445	—	—	—	—	—	< 0.9
876	6:40:58.4	9:34:52.5	0.50	—	06405843+0934525	—	—	—	—	—	< 0.6
877	6:40:58.5	9:42:08.3	0.50	—	06405845+0942083	—	—	—	—	—	< 2.4
878*	6:40:58.5	9:33:31.7	0.50	149	06405851+0933317	—	—	65	132	—	324.0
879	6:40:58.6	9:32:22.9	0.50	—	06405859+0932229	—	—	—	—	—	< 0.6
880*	6:40:58.6	9:36:39.4	0.50	150	06405861+0936393	—	—	—	—	—	1.0
881*	6:40:58.7	9:36:13.3	0.50	151	06405867+0936132	3302	—	—	—	251	77.0
882	6:40:58.7	9:30:43.9	0.50	—	06405874+0930439	—	—	—	—	—	< 1.5
883	6:40:58.7	9:38:05.8	1.50	—	—	3303	—	—	—	—	< 1.0
884	6:40:58.7	9:37:45.5	1.50	—	—	3304	—	—	—	—	< 0.8
885*	6:40:58.8	9:34:05.4	1.00	152	—	—	—	—	—	—	1.8
886*	6:40:58.8	9:39:18.8	0.50	155	06405882+0939187	3300	—	66	—	252	20.4
887*	6:40:58.8	9:30:57.3	0.50	154	06405884+0930573	3307	—	—	—	253	43.2
888*	6:40:58.9	9:36:46.3	0.50	156	06405886+0936462	—	—	—	—	—	3.1
889*	6:40:58.9	9:42:25.5	0.50	153	06405888+0942255	3298	—	—	—	—	2.0
890*	6:40:58.9	9:28:52.8	0.50	157	06405891+0928528	3305	—	—	—	254	6.6
891	6:40:58.9	9:36:01.1	0.75	—	06405892+0936011	—	—	—	—	—	< 0.7
892	6:40:58.9	9:42:15.5	0.50	—	06405893+0942155	3299	—	—	—	—	< 2.4
893	6:40:58.9	9:26:33.5	0.50	—	06405894+0926335	—	—	—	—	—	< 2.1
894*	6:40:59.1	9:33:22.2	0.50	158	06405905+0933222	—	—	—	—	257	1.0
895	6:40:59.1	9:33:01.9	0.50	—	06405906+0933019	—	—	—	—	—	< 0.7
896	6:40:59.1	9:36:15.1	1.00	—	—	—	—	—	—	—	< 0.7
897	6:40:59.2	9:35:45.3	0.50	—	06405915+0935452	—	—	—	—	—	< 0.7
898	6:40:59.2	9:37:28.1	0.50	—	06405919+0937281	—	—	—	—	—	< 0.8
899*	6:40:59.2	9:31:50.3	0.50	159	06405923+0931503	3317	—	—	—	—	3.2
900*	6:40:59.3	9:33:25.0	0.50	160	06405926+0933250	—	—	—	—	258	0.9

Table 3. (Continued)

N	RA [h m s]	Dec. [d m s]	Id. rad. [""]	ACIS	2Mass	Reb.+	Lamm+	Flacc+	W56	Dahm+	Ct. Rate. [$10^{-4} s^{-1}$]
901*	6:40:59.3	9:35:52.4	0.50	161	06405930+0935523	3320	—	—	—	—	16.3
902	6:40:59.3	9:33:58.3	0.50	—	06405930+0933583	—	—	—	—	—	< 0.6
903	6:40:59.3	9:42:40.3	0.50	—	06405931+0942402	—	—	—	—	—	< 2.7
904*	6:40:59.3	9:35:56.9	1.00	162	—	—	—	—	—	—	6.8
905*	6:40:59.4	9:33:33.4	0.50	163	06405936+0933333	—	—	—	—	—	21.1
906*	6:40:59.4	9:30:59.6	0.50	—	06405940+0930595	—	5627	—	—	—	< 0.9
907*	6:40:59.4	9:27:53.5	0.50	—	06405942+0927534	3326	5628	—	—	—	< 1.6
908*	6:40:59.5	9:29:51.7	0.50	164	06405949+0929517	3329	5630	—	—	262	4.6
909*	6:40:59.5	9:36:10.5	0.50	165	06405952+0936105	—	—	—	—	—	12.8
910	6:40:59.5	9:27:31.9	0.50	—	06405953+0927319	—	5629	—	—	—	< 1.9
911	6:40:59.5	9:34:43.7	1.00	—	—	—	5631	—	—	—	< 0.7
912*	6:40:59.5	9:35:10.9	0.50	167	06405954+0935109	3330	5633	71	136	260	107.2
913*	6:40:59.6	9:35:51.7	1.00	168	—	—	—	—	—	—	1.3
914*	6:40:59.6	9:39:06.3	0.50	166	06405955+0939063	3331	—	—	—	261	1.4
915*	6:40:59.6	9:36:57.6	0.50	169	06405962+0936575	3333	5634	—	—	263	1.0
916*	6:40:59.7	9:28:43.8	0.50	170	06405968+0928438	3336	5638	73†	—	265	2.7
917	6:40:59.7	9:28:49.8	1.00	—	—	—	5639	—	—	—	< 41.2
918	6:40:59.7	9:34:22.3	0.50	—	06405972+0934222	—	5640	—	—	—	< 1.2
919	6:40:59.8	9:27:29.2	1.00	—	—	—	5644	—	—	—	< 1.9
920	6:40:59.8	9:35:59.2	0.50	—	06405975+0935592	—	5643	—	—	—	< 0.7
921	6:40:59.8	9:36:33.3	0.50	—	06405981+0936332	—	—	—	—	—	< 0.7
922	6:40:59.8	9:42:06.1	1.00	—	—	—	5646	—	—	—	< 2.3
923	6:40:59.9	9:35:17.2	1.00	—	—	—	5649	—	—	—	< 0.6
924	6:40:60.0	9:35:01.0	0.50	171	06405998+0935009	—	5652	—	—	—	0.9
925*	6:41:00.0	9:28:50.0	0.50	172	06405999+0928500	3343	5653	73†	—	268	122.9
926	6:41:00.0	9:32:23.3	0.65	—	06410002+0932233	—	—	—	—	—	< 1.3
927	6:41:00.2	9:42:37.3	1.00	—	—	—	5656	—	—	—	< 2.6
928	6:41:00.2	9:39:07.0	0.50	—	06410022+0939070	3349	5657	—	—	269	< 1.2
929*	6:41:00.3	9:36:31.2	0.50	173	06410025+0936311	—	5659	—	—	—	0.9
930*	6:41:00.3	9:28:34.1	0.50	—	06410028+0928341	—	5661	—	—	270	< 1.6
931*	6:41:00.3	9:35:59.1	0.50	174	06410028+0935591	—	—	—	—	—	3.7
932*	6:41:00.3	9:34:24.3	0.50	—	06410030+0934243	—	5663	—	—	—	< 1.9
933	6:41:00.3	9:30:16.9	0.50	—	06410032+0930169	3356	5664	—	—	—	< 0.9
934*	6:41:00.4	9:41:15.3	0.50	175	06410040+0941153	—	5667	—	—	—	1.8
935	6:41:00.4	9:41:29.3	0.50	—	06410041+0941293	—	5669	—	—	—	< 1.9
936*	6:41:00.4	9:41:20.2	0.50	—	06410044+0941201	—	5672	—	—	—	< 1.9
937*	6:41:00.5	9:29:16.0	0.50	176	06410051+0929159	3359	5677	75†	—	271	97.9
938	6:41:00.5	9:41:44.4	0.50	—	06410054+0941444	—	5678	—	—	—	< 2.0
939*	6:41:00.5	9:36:12.6	1.00	177	—	3362	5679	—	—	—	2.5
940*	6:41:00.6	9:36:10.3	0.50	178	06410063+0936103	—	5680	—	—	—	11.7
941	6:41:00.8	9:28:39.9	1.00	—	—	—	5688	—	—	—	< 1.5
942*	6:41:00.8	9:30:14.2	0.50	—	06410082+0930142	3371	5690	—	—	275	< 0.9
943*	6:41:01.0	9:32:44.4	0.50	179	06410098+0932444	3373	5692	78	139	276	83.4
944*	6:41:01.0	9:29:37.5	1.17	180	—	—	—	—	—	—	1.2
945	6:41:01.1	9:27:32.7	1.00	—	—	—	5695	—	—	—	< 1.8
946*	6:41:01.1	9:34:52.2	0.50	181	06410111+0934522	—	5696	79†	—	277	28.0
947	6:41:01.1	9:29:15.7	0.50	—	06410114+0929157	—	5697	75†	—	—	< 1.3
948	6:41:01.2	9:41:47.7	0.50	—	06410116+0941476	—	5698	—	—	—	< 2.0
949*	6:41:01.2	9:36:09.5	0.50	182	06410123+0936095	—	—	—	—	—	6.7
950*	6:41:01.3	9:34:52.6	0.50	183	06410133+0934526	—	5701	79†	—	278	23.3
951	6:41:01.4	9:34:07.8	1.00	—	—	—	—	—	—	—	< 57.6
952	6:41:01.4	9:27:41.4	1.00	—	—	—	5702	—	—	—	< 1.8
953*	6:41:01.4	9:34:08.1	0.50	184	06410141+0934081	3378	5704	80	—	—	63.5
954	6:41:01.4	9:38:50.6	0.50	—	06410144+0938506	—	—	—	—	—	< 1.1
955	6:41:01.5	9:40:10.5	0.50	—	06410146+0940104	—	—	—	—	—	< 1.5
956*	6:41:01.6	9:28:13.1	0.50	185	06410155+0928130	—	5709	—	145	—	27.7
957	6:41:01.6	9:34:33.0	0.50	—	06410156+0934329	—	5710	—	—	—	< 2.7
958	6:41:01.6	9:28:41.2	0.50	—	06410158+0928411	—	5712	—	—	—	< 1.4
959	6:41:01.6	9:41:39.4	0.50	—	06410159+0941394	—	5713	—	—	—	< 2.1
960*	6:41:01.6	9:37:28.8	0.50	—	06410160+0937287	3386	5714	—	—	279	< 0.8

Table 3. (Continued)

Table 3. (Continued)

Table 3. (Continued)

N	RA [h m s]	Dec. [d m s]	Id. rad. [""]	ACIS	2Mass	Reb.+	Lamm+	Flacc+	W56	Dahm+	Ct. Rate. [$10^{-4} s^{-1}$]
1081*	6:41:05.0	9:42:15.4	2.44	230	—	—	—	—	—	—	3.3
1082	6:41:05.0	9:29:39.1	1.00	—	—	—	5875	—	—	—	< 1.2
1083	6:41:05.0	9:38:56.8	0.54	—	06410504+0938567	—	—	—	—	—	< 3.0
1084*	6:41:05.1	9:33:00.3	0.50	231	06410505+0933002	—	5876	—	—	324	20.9
1085	6:41:05.2	9:34:10.3	1.00	—	—	—	—	—	—	—	< 1.6
1086*	6:41:05.2	9:36:31.5	1.01	232	—	—	—	—	—	—	1.1
1087*	6:41:05.2	9:38:08.8	1.78	233	—	—	—	—	—	—	1.6
1088	6:41:05.2	9:35:35.8	0.50	—	06410522+0935358	—	—	—	—	—	< 0.7
1089	6:41:05.2	9:35:46.1	1.00	—	—	—	5886	—	—	—	< 0.7
1090	6:41:05.2	9:40:17.7	1.00	—	—	—	5887	—	—	—	< 2.5
1091	6:41:05.3	9:31:01.0	1.00	—	—	—	5889	—	—	—	< 0.9
1092*	6:41:05.3	9:28:12.5	0.50	—	06410533+0928124	3497	5890	—	—	332	< 1.7
1093	6:41:05.4	9:34:13.3	0.50	—	06410535+0934133	—	—	—	—	—	< 1.5
1094*	6:41:05.4	9:33:13.4	0.50	234	06410536+0933134	3500	5894	98	160	333	301.3
1095*	6:41:05.4	9:36:30.9	0.50	235	06410538+0936309	—	—	—	—	—	11.4
1096	6:41:05.4	9:33:23.5	1.00	—	—	—	—	—	—	—	< 0.7
1097	6:41:05.4	9:34:09.5	0.50	237†	06410542+0934095	3502	5895	—	—	—	< 2.2
1098*	6:41:05.5	9:36:26.5	1.00	236	—	—	—	—	—	—	1.8
1099	6:41:05.5	9:34:11.7	1.00	—	—	—	—	—	—	—	< 1.4
1100	6:41:05.5	9:34:36.9	1.00	—	—	—	—	—	—	—	< 0.7
1101	6:41:05.5	9:35:01.4	1.00	—	—	—	—	—	—	—	< 0.7
1102*	6:41:05.5	9:31:40.5	0.50	238	06410554+0931405	—	5897	99†	—	335	24.6
1103	6:41:05.6	9:34:08.1	1.00	—	—	—	—	—	—	—	< 2.0
1104	6:41:05.6	9:34:05.9	0.50	237†	06410561+0934058	—	—	—	—	—	< 2.2
1105	6:41:05.6	9:33:54.9	0.50	—	06410562+0933549	—	5898	—	—	—	< 0.7
1106*	6:41:05.6	9:35:44.5	0.50	239	06410563+0935445	—	—	—	—	—	3.1
1107	6:41:05.7	9:37:43.0	0.50	—	06410571+0937430	—	—	—	—	—	< 0.9
1108	6:41:05.7	9:34:06.3	1.00	—	—	—	—	—	—	—	< 1.4
1109*	6:41:05.7	9:31:01.3	0.50	240	06410574+0931012	3514	5902	100†	162	337	63.0
1110	6:41:05.7	9:33:48.3	1.00	—	—	—	5901	—	—	—	< 0.7
1111	6:41:05.8	9:33:00.5	1.00	—	—	—	—	—	—	—	< 0.7
1112*	6:41:05.8	9:36:32.0	0.50	241	06410576+0936319	—	5903	—	—	—	5.3
1113*	6:41:05.8	9:35:29.6	0.50	242	06410577+0935295	—	—	—	—	—	18.8
1114*	6:41:05.8	9:31:07.3	0.50	243	06410579+0931072	—	5906	100†	—	—	2.2
1115	6:41:05.9	9:34:52.8	1.00	—	—	—	—	—	—	—	< 0.7
1116*	6:41:05.9	9:34:45.9	1.00	244	—	—	—	—	—	—	81.6
1117	6:41:05.9	9:41:25.3	0.52	—	06410590+0941253	—	5913	—	—	—	< 2.6
1118	6:41:05.9	9:34:04.9	1.00	—	—	—	—	—	—	—	< 1.4
1119	6:41:05.9	9:35:03.2	1.00	—	—	—	—	—	—	—	< 0.7
1120*	6:41:05.9	9:27:17.4	0.50	245	06410593+0927174	3519	5912	—	—	340	14.2
1121	6:41:06.0	9:34:39.8	1.00	—	—	—	—	—	—	—	< 0.7
1122*	6:41:06.0	9:31:39.8	0.50	246	06410596+0931398	—	5914	99†	—	—	19.0
1123*	6:41:06.0	9:39:14.2	0.50	—	06410597+0939142	3520	5915	—	—	341	< 1.5
1124	6:41:06.0	9:34:11.5	0.50	—	06410598+0934115	—	—	—	—	—	< 1.5
1125*	6:41:06.0	9:35:51.3	0.50	247	06410599+0935513	3522	5916	—	—	—	1.9
1126	6:41:06.0	9:34:46.2	0.50	248	06410604+0934461	—	5920	—	—	—	8.5
1127	6:41:06.0	9:27:08.5	0.50	—	06410604+0927084	—	5919	—	—	—	< 2.6
1128*	6:41:06.1	9:29:26.4	0.50	—	06410614+0929263	—	5922	103†	—	—	< 1.3
1129	6:41:06.2	9:34:08.9	1.00	—	—	—	—	—	—	—	< 1.5
1130*	6:41:06.2	9:36:23.0	0.50	249	06410620+0936229	3525	5924	101	164	342	228.2
1131*	6:41:06.2	9:33:08.8	0.50	250	06410623+0933087	3527	5927	—	—	343	11.1
1132	6:41:06.2	9:40:09.1	1.00	—	—	—	5928	—	—	—	< 3.0
1133*	6:41:06.3	9:29:40.5	0.50	251	06410626+0929404	—	5929	103†	—	—	3.3
1134	6:41:06.3	9:33:49.7	0.50	—	06410629+0933496	—	—	—	—	—	< 0.7
1135*	6:41:06.3	9:29:31.0	1.00	252	—	3528	5932	103†	—	345	13.3
1136	6:41:06.3	9:40:10.6	0.50	—	06410634+0940105	3531	5934	—	—	346	< 2.7
1137	6:41:06.3	9:34:15.3	1.00	—	—	—	—	—	—	—	< 1.4
1138*	6:41:06.4	9:37:08.6	0.50	253	06410637+0937085	—	—	—	—	—	2.2
1139	6:41:06.4	9:35:06.1	0.50	—	06410640+0935061	—	5937	—	—	—	< 0.7
1140	6:41:06.4	9:30:33.7	1.00	—	—	—	5940	—	—	—	< 1.0

Table 3. (Continued)

N	RA [h m s]	Dec. [d m s]	Id. rad. ["]	ACIS	2Mass	Reb.+	Lamm+	Flacc+	W56	Dahm+	Ct. Rate. [10^{-4}s^{-1}]
1141	6:41:06.4	9:34:10.0	0.50	—	06410642+0934099	—	—	—	—	—	< 1.5
1142*	6:41:06.4	9:28:38.8	0.50	254	06410642+0928388	3534	5941	—	—	348	9.7
1143*	6:41:06.4	9:26:58.7	0.50	255	06410643+0926587	—	5939	—	—	—	153.9
1144	6:41:06.4	9:33:43.3	1.00	—	—	—	—	—	—	—	< 0.7
1145*	6:41:06.4	9:38:37.1	0.50	256	06410644+0938371	—	—	—	—	—	2.5
1146*	6:41:06.5	9:36:05.5	0.50	257	06410647+0936055	—	—	—	—	—	39.3
1147	6:41:06.5	9:35:54.1	1.00	—	—	—	—	—	—	—	< 0.8
1148	6:41:06.5	9:30:05.1	1.00	—	—	—	5944	—	—	—	< 1.2
1149	6:41:06.6	9:35:45.2	0.50	258	06410659+0935451	3538	5945	—	—	—	2.0
1150	6:41:06.6	9:35:00.3	1.00	—	—	—	—	—	—	—	< 0.7
1151	6:41:06.6	9:35:02.1	1.00	—	—	—	—	—	—	—	< 0.7
1152	6:41:06.6	9:34:21.1	1.00	—	—	—	—	—	—	—	< 0.9
1153	6:41:06.7	9:33:57.7	0.50	—	06410665+0933576	—	—	—	—	—	< 1.0
1154	6:41:06.7	9:34:26.5	1.00	—	—	—	—	—	—	—	< 0.7
1155	6:41:06.7	9:33:30.0	1.00	—	—	—	—	—	—	—	< 0.7
1156	6:41:06.7	9:41:46.6	1.00	—	—	—	5947	—	—	—	< 4.2
1157*	6:41:06.7	9:33:54.3	1.00	259	—	—	—	—	—	—	0.7
1158	6:41:06.7	9:34:38.0	1.00	—	—	—	—	—	—	—	< 0.7
1159	6:41:06.7	9:34:31.9	1.00	—	—	—	—	—	—	—	< 0.7
1160*	6:41:06.7	9:34:45.9	0.50	260	06410673+0934459	3541	5949	—	166	349	7.8
1161	6:41:06.7	9:34:59.3	1.00	—	—	—	—	—	—	—	< 0.7
1162	6:41:06.7	9:34:53.9	1.00	—	—	—	—	—	—	—	< 0.7
1163	6:41:06.8	9:33:34.7	1.00	—	—	—	—	—	—	—	< 0.7
1164*	6:41:06.8	9:27:32.3	0.50	261	06410682+0927322	3543	5952	104†	—	351	168.7
1165	6:41:06.8	9:35:02.5	1.00	—	—	—	—	—	—	—	< 0.7
1166	6:41:06.9	9:41:46.1	0.50	—	06410687+0941460	3544	5954	—	—	—	< 4.5
1167*	6:41:06.9	9:29:24.0	0.50	263	06410689+0929240	3546	5956	—	—	352	8.7
1168	6:41:07.0	9:35:55.8	0.50	—	06410696+0935557	—	5957	—	—	—	< 0.8
1169*	6:41:07.0	9:40:54.5	0.50	262	06410696+0940544	3548	5958	—	—	353	3.1
1170	6:41:07.1	9:38:11.2	0.50	—	06410705+0938112	—	5961	—	—	—	< 1.1
1171	6:41:07.1	9:30:37.5	0.50	—	06410706+0930375	—	5960	—	—	—	< 3.4
1172	6:41:07.1	9:38:23.6	0.74	—	06410706+0938235	—	5962	—	—	—	< 1.1
1173	6:41:07.1	9:34:42.3	1.00	—	—	—	—	—	—	—	< 0.7
1174	6:41:07.1	9:27:09.8	1.00	—	—	—	5965	—	—	—	< 2.7
1175	6:41:07.1	9:34:44.9	1.00	—	—	—	—	—	—	—	< 0.7
1176*	6:41:07.1	9:25:54.9	1.00	—	—	—	5966	—	—	356	< 42.2
1177*	6:41:07.2	9:30:36.7	1.00	264	—	—	—	—	—	—	5.2
1178*	6:41:07.2	9:27:48.0	0.50	265	06410715+0927479	3552	5968	105	—	355	67.2
1179*	6:41:07.2	9:27:29.4	0.50	—	06410715+0927294	—	5967	104†	—	354	< 132.5
1180	6:41:07.2	9:34:24.3	0.50	—	06410719+0934242	—	—	—	—	—	< 0.7
1181*	6:41:07.2	9:42:25.6	0.50	266	06410721+0942256	3554	5969	—	—	—	6.2
1182	6:41:07.2	9:34:41.3	1.00	—	—	—	—	—	—	—	< 0.7
1183	6:41:07.2	9:36:59.3	1.00	267	—	—	5970	—	—	—	1.0
1184*	6:41:07.3	9:31:18.1	0.50	268	06410729+0931180	3556	5973	107	—	—	11.2
1185*	6:41:07.3	9:25:55.0	0.50	269	06410734+0925549	3559	5974	106	—	359	53.2
1186	6:41:07.3	9:34:40.5	1.00	—	—	—	—	—	—	—	< 0.7
1187	6:41:07.4	9:35:20.8	0.50	—	06410739+0935207	—	5975	—	—	—	< 0.7
1188*	6:41:07.4	9:31:11.1	0.50	271	06410740+0931110	3563	5976	—	—	360	5.0
1189*	6:41:07.4	9:34:55.0	0.50	270	06410740+0934549	—	—	—	—	—	0.8
1190*	6:41:07.4	9:34:33.6	0.50	272	06410744+0934335	3565	5978	—	—	361	0.7
1191	6:41:07.4	9:30:00.9	1.00	—	—	—	5979	—	—	—	< 8.5
1192*	6:41:07.5	9:33:36.9	0.50	—	06410748+0933369	3566	5980	—	—	—	< 0.7
1193*	6:41:07.6	9:41:33.6	0.50	—	06410755+0941335	3568	5982	—	—	362	< 4.2
1194*	6:41:07.6	9:30:00.5	0.50	273	06410755+0930004	3569	5983	—	—	—	9.9
1195	6:41:07.6	9:30:29.2	0.50	—	06410757+0930292	—	—	—	—	—	< 1.2
1196*	6:41:07.7	9:34:19.2	1.00	274	—	—	—	—	—	—	28.7
1197*	6:41:07.7	9:41:26.4	0.50	—	06410770+0941264	3573	5985	—	—	363	< 3.4
1198	6:41:07.7	9:29:13.7	0.50	—	06410773+0929136	—	—	—	—	—	< 1.5
1199*	6:41:07.8	9:41:14.9	0.50	275	06410776+0941149	3574	5987	—	170	—	9.0
1200*	6:41:07.8	9:28:13.5	0.50	276	06410776+0928134	3575	5986	—	—	364	41.8

Table 3. (Continued)

N	RA [h m s]	Dec. [d m s]	Id. rad. [""]	ACIS	2Mass	Reb.+	Lamm+	Flacc+	W56	Dahm+	Ct. Rate. [$10^{-4} s^{-1}$]
1201	6:41:07.8	9:41:29.5	0.50	—	06410781+0941294	—	5991	—	—	—	< 3.3
1202*	6:41:07.8	9:26:24.7	0.50	—	06410781+0926247	3579	5990	—	—	—	< 2.5
1203	6:41:07.9	9:33:33.9	1.00	—	—	—	—	—	—	—	< 0.7
1204	6:41:07.9	9:34:27.9	1.00	—	—	—	—	—	—	—	< 0.7
1205	6:41:07.9	9:34:33.7	1.00	—	—	—	—	—	—	—	< 0.7
1206	6:41:08.0	9:34:16.4	1.00	—	—	—	—	—	—	—	< 1.0
1207*	6:41:08.0	9:34:47.0	0.50	277	06410798+0934469	3580	5992	—	—	—	2.3
1208*	6:41:08.0	9:30:40.3	0.50	278	06410801+0930403	3582	5994	109	175	365	25.8
1209	6:41:08.0	9:27:56.0	1.00	—	—	—	5995	—	—	—	< 2.3
1210	6:41:08.1	9:33:13.6	1.00	—	—	—	5996	—	—	—	< 0.7
1211	6:41:08.1	9:34:30.1	1.00	—	—	—	—	—	—	—	< 0.7
1212	6:41:08.1	9:34:16.1	1.00	—	—	—	—	—	—	—	< 1.0
1213*	6:41:08.2	9:30:03.9	0.50	—	06410817+0930038	—	6000	—	—	—	< 1.3
1214*	6:41:08.2	9:30:08.0	0.50	279	06410818+0930079	—	—	—	—	—	9.8
1215*	6:41:08.2	9:36:56.2	0.50	280	06410820+0936561	3588	6001	—	—	—	33.1
1216*	6:41:08.2	9:34:09.5	0.50	281	06410821+0934094	3591	6002	—	—	367	1.9
1217*	6:41:08.2	9:38:30.4	0.50	282	06410821+0938303	3590	6003	—	—	366	46.9
1218*	6:41:08.3	9:30:22.8	0.50	—	06410827+0930228	—	6004	—	—	368	< 1.2
1219	6:41:08.3	9:34:06.7	1.00	—	—	—	—	—	—	—	< 1.7
1220	6:41:08.3	9:38:14.3	0.50	—	06410828+0938143	3592	6005	—	171	—	< 1.1
1221	6:41:08.3	9:34:25.8	1.00	—	—	—	—	—	—	—	< 0.7
1222*	6:41:08.3	9:29:39.6	0.50	283	06410833+0929395	—	—	—	—	—	2.1
1223*	6:41:08.4	9:40:36.2	0.50	284	06410837+0940361	3594	6007	—	—	369	4.4
1224*	6:41:08.4	9:37:52.5	0.50	285	06410843+0937525	3595	6008	—	—	370	7.4
1225	6:41:08.5	9:25:59.6	0.50	—	06410849+0925595	—	—	—	—	—	< 3.1
1226*	6:41:08.5	9:31:10.7	1.00	286	—	—	—	—	—	—	1.4
1227	6:41:08.5	9:32:50.8	0.50	—	06410854+0932508	—	6010	—	—	—	< 0.8
1228*	6:41:08.5	9:34:13.2	0.50	287	06410854+0934132	—	—	—	—	—	9.4
1229	6:41:08.6	9:31:05.9	0.50	—	06410857+0931058	—	6012	—	—	—	< 0.9
1230	6:41:08.6	9:34:08.1	1.00	—	—	—	—	—	—	—	< 1.6
1231	6:41:08.6	9:35:42.1	1.00	—	—	—	—	—	—	—	< 0.7
1232	6:41:08.6	9:28:13.8	1.00	—	—	—	6015	—	—	—	< 2.0
1233*	6:41:08.6	9:30:03.6	0.50	288	06410859+0930036	—	6014	—	—	372	1.4
1234	6:41:08.6	9:36:03.4	0.55	—	06410863+0936033	—	—	—	—	—	< 0.8
1235*	6:41:08.6	9:40:13.3	0.50	—	06410864+0940133	3599	6019	—	—	—	< 1.7
1236	6:41:08.7	9:39:11.4	1.00	—	—	—	6018	—	—	—	< 1.3
1237*	6:41:08.7	9:38:25.3	1.79	289	—	—	—	—	—	—	1.3
1238	6:41:08.7	9:29:56.8	0.50	—	06410871+0929567	—	—	—	—	—	< 1.4
1239	6:41:08.7	9:31:13.9	0.76	—	06410872+0931139	—	—	—	—	—	< 0.9
1240	6:41:08.8	9:29:51.7	0.59	—	06410880+0929516	—	—	—	—	—	< 1.4
1241	6:41:08.8	9:27:53.3	0.50	—	06410880+0927533	—	6021	—	—	—	< 2.4
1242	6:41:08.9	9:29:55.1	0.59	—	06410889+0929550	—	—	—	—	—	< 1.4
1243	6:41:08.9	9:29:45.1	0.50	—	06410890+0929451	—	6028	—	—	—	< 1.5
1244*	6:41:08.9	9:41:14.8	0.50	290	06410891+0941147	3608	6031	112	174	—	48.9
1245	6:41:08.9	9:29:29.2	0.50	—	06410892+0929291	—	6029	—	—	—	< 1.6
1246	6:41:08.9	9:29:56.8	0.50	—	06410894+0929568	—	—	—	—	—	< 1.4
1247*	6:41:09.0	9:33:46.0	0.50	291	06410896+0933460	3611	6032	—	—	374	1.7
1248	6:41:09.0	9:29:21.7	0.50	—	06410896+0929217	—	6030	—	—	—	< 1.6
1249*	6:41:09.0	9:31:08.9	0.50	—	06410899+0931088	—	6033	—	—	375	< 0.9
1250*	6:41:09.1	9:29:07.2	0.50	292	06410905+0929072	—	6036	—	—	—	14.3
1251	6:41:09.1	9:29:19.1	0.75	—	06410907+0929190	—	—	—	—	—	< 1.6
1252*	6:41:09.1	9:30:09.1	0.50	293	06410908+0930090	—	6039	—	—	376	7.4
1253	6:41:09.1	9:29:43.1	1.00	—	—	—	6038	—	—	—	< 1.5
1254	6:41:09.2	9:26:40.2	0.61	—	06410916+0926402	—	6040	—	—	—	< 2.5
1255	6:41:09.2	9:26:50.7	0.50	—	06410922+0926507	—	6044	—	—	—	< 2.5
1256	6:41:09.2	9:29:04.5	1.00	—	—	—	6047	—	—	—	< 6.9
1257	6:41:09.3	9:30:25.7	0.50	—	06410928+0930257	—	—	—	—	—	< 1.1
1258	6:41:09.5	9:29:59.6	0.61	—	06410946+0929595	—	6053	—	—	—	< 1.3
1259	6:41:09.5	9:27:45.9	1.00	—	—	—	6056	—	—	—	< 128.2
1260*	6:41:09.5	9:35:25.5	0.50	294	06410951+0935254	3620	6057	—	—	—	6.5

Table 3. (Continued)

N	RA [h m s]	Dec. [d m s]	Id. rad. ["]	ACIS	2Mass	Reb.+	Lamm+	Flacc+	W56	Dahm+	Ct. Rate. [10^{-4}s^{-1}]
1261*	6:41:09.5	9:29:36.8	1.98	295	—	—	—	—	—	—	3.5
1262*	6:41:09.5	9:29:25.1	0.50	296	06410954+0929250	—	—	—	—	—	49.7
1263*	6:41:09.6	9:27:57.5	0.50	297	06410959+0927574	—	—	113	—	—	9.1
1264	6:41:09.6	9:29:46.7	0.54	—	06410960+0929466	—	—	—	—	—	< 1.5
1265*	6:41:09.6	9:36:29.1	0.50	298	06410962+0936291	—	6061	—	—	—	3.2
1266	6:41:09.6	9:29:40.2	0.50	—	06410964+0929402	—	—	—	—	—	< 3.1
1267	6:41:09.7	9:29:20.7	0.50	—	06410965+0929207	—	—	—	—	—	< 1.7
1268	6:41:09.8	9:29:36.7	0.54	—	06410976+0929366	—	—	—	—	—	< 3.1
1269*	6:41:09.8	9:29:15.4	1.25	299	—	—	—	—	—	—	2.6
1270*	6:41:09.8	9:27:12.2	0.50	300	06410982+0927122	3625	6067	114	—	379	71.1
1271	6:41:09.9	9:29:45.9	0.50	—	06410986+0929458	—	6068	—	—	—	< 1.5
1272	6:41:09.9	9:35:41.1	1.00	—	—	—	—	—	—	—	< 0.8
1273	6:41:09.9	9:29:36.8	1.00	—	—	—	6070	—	—	—	< 6.9
1274*	6:41:09.9	9:30:20.2	0.50	301	06410992+0930202	—	6071	—	—	—	22.0
1275	6:41:09.9	9:29:34.7	0.50	—	06410992+0929347	—	—	—	—	—	< 6.9
1276	6:41:09.9	9:29:43.2	0.50	—	06410994+0929431	—	—	—	—	—	< 1.5
1277*	6:41:10.0	9:27:46.1	0.50	302	06410999+0927460	—	—	115	—	—	311.3
1278	6:41:10.0	9:40:37.9	0.50	—	06410999+0940379	—	—	—	—	—	< 1.8
1279	6:41:10.0	9:29:35.2	1.00	—	—	—	6073	—	—	—	< 6.9
1280*	6:41:10.1	9:29:28.6	1.59	303	—	—	—	—	—	—	1.5
1281	6:41:10.1	9:25:34.1	1.00	—	—	—	6074	—	—	—	< 4.9
1282	6:41:10.1	9:29:27.0	0.59	—	06411011+0929270	—	—	—	—	—	< 1.7
1283	6:41:10.1	9:33:42.8	0.50	—	06411011+0933427	3634	6075	—	—	—	< 0.8
1284*	6:41:10.1	9:31:28.5	0.50	304	06411013+0931285	3635	6078	—	—	381	4.4
1285*	6:41:10.2	9:29:33.6	0.50	305	06411015+0929336	—	6076	—	—	—	7.4
1286	6:41:10.2	9:31:22.4	0.57	—	06411016+0931223	—	6077	—	—	—	< 0.9
1287*	6:41:10.2	9:30:31.1	1.00	306	—	—	6079	—	—	380	2.5
1288	6:41:10.2	9:41:10.5	0.50	—	06411021+0941105	3636	6080	—	—	—	< 2.2
1289	6:41:10.2	9:29:29.6	0.50	—	06411023+0929296	—	—	—	—	—	< 1.7
1290*	6:41:10.3	9:33:25.1	0.50	307	06411027+0933250	3639	6081	—	—	382	5.4
1291*	6:41:10.3	9:34:22.0	0.50	308	06411029+0934219	—	—	—	—	—	2.6
1292	6:41:10.3	9:29:26.6	0.50	—	06411029+0929265	—	—	—	—	—	< 1.7
1293*	6:41:10.3	9:28:33.5	1.00	309	—	—	6083	—	—	383	3.0
1294	6:41:10.4	9:42:06.2	0.50	—	06411040+0942062	3643	6086	—	—	—	< 2.7
1295*	6:41:10.4	9:34:18.7	0.50	310	06411042+0934186	—	—	—	—	—	1.7
1296	6:41:10.4	9:41:41.0	0.50	—	06411044+0941410	3644	6087	—	—	—	< 2.5
1297	6:41:10.5	9:39:45.2	0.50	—	06411053+0939452	—	—	—	—	—	< 1.5
1298	6:41:10.8	9:35:14.8	0.50	—	06411082+0935148	—	6096	—	—	—	< 0.8
1299	6:41:10.9	9:34:08.3	0.50	—	06411093+0934082	—	—	—	—	—	< 1.0
1300	6:41:11.0	9:40:44.1	0.50	—	06411096+0940440	—	—	—	—	—	< 1.8
1301	6:41:11.0	9:25:59.4	0.57	—	06411096+0925593	—	6101	—	—	—	< 3.0
1302*	6:41:11.0	9:35:55.7	0.50	311	06411099+0935556	3660	6102	—	—	387	19.7
1303	6:41:11.0	9:36:32.4	0.50	—	06411101+0936323	—	—	—	—	—	< 0.9
1304	6:41:11.0	9:37:43.8	0.50	—	06411102+0937438	—	6104	—	—	—	< 1.1
1305*	6:41:11.0	9:34:24.6	1.00	313	—	—	—	—	—	—	0.9
1306	6:41:11.1	9:34:12.3	0.50	—	06411106+0934123	—	6105	—	—	—	< 0.8
1307*	6:41:11.1	9:42:08.4	0.50	312	06411106+0942083	3662	6107	—	—	—	3.4
1308	6:41:11.2	9:30:23.5	0.50	—	06411121+0930235	3667	6112	—	—	—	< 1.2
1309	6:41:11.3	9:29:40.8	0.51	—	06411125+0929408	—	—	—	—	—	< 1.6
1310	6:41:11.3	9:27:00.1	1.00	—	—	—	6114	—	—	—	< 2.6
1311*	6:41:11.3	9:30:50.8	0.50	—	06411132+0930508	—	6115	—	—	—	< 1.1
1312*	6:41:11.4	9:29:24.9	1.43	314	—	—	—	—	—	—	1.5
1313*	6:41:11.4	9:26:38.1	0.50	—	06411139+0926380	3672	6117	—	—	388	< 8.2
1314*	6:41:11.4	9:28:13.8	0.50	—	06411144+0928137	—	6119	—	—	—	< 2.0
1315	6:41:11.5	9:35:07.4	1.00	—	—	—	6121	—	—	—	< 0.8
1316*	6:41:11.6	9:29:09.8	2.52	315	—	—	—	—	—	—	1.8
1317*	6:41:11.8	9:31:12.3	0.50	316	06411180+0931123	3677	6125	—	—	—	2.6
1318	6:41:11.8	9:35:23.1	0.50	—	06411184+0935230	—	—	—	—	—	< 0.8
1319*	6:41:11.8	9:35:31.3	0.50	317	06411184+0935313	—	—	—	—	—	2.5
1320*	6:41:11.9	9:26:31.4	0.50	318	06411185+0926314	3679	6127	116	183	391	40.0

Table 3. (Continued)

N	RA [h m s]	Dec. [d m s]	Id. rad. [""]	ACIS	2Mass	Reb.+	Lamm+	Flacc+	W56	Dahm+	Ct. Rate. [$10^{-4} s^{-1}$]
1321*	6:41:11.9	9:30:26.7	0.50	—	06411185+0930267	3680	6128	—	—	—	< 1.2
1322*	6:41:11.9	9:37:43.9	0.50	319	06411190+0937438	3681	6129	—	—	—	1.7
1323	6:41:12.0	9:29:09.0	0.50	—	06411196+0929089	3683	6132	—	—	—	< 1.9
1324	6:41:12.0	9:29:55.4	0.50	—	06411197+0929553	—	—	—	—	—	< 3.7
1325	6:41:12.1	9:35:30.5	0.50	—	06411206+0935305	—	—	—	—	—	< 0.8
1326*	6:41:12.1	9:29:52.1	0.50	320	06411212+0929521	3687	6136	—	—	392	6.4
1327	6:41:12.2	9:35:29.5	0.50	—	06411219+0935294	—	—	—	—	—	< 0.8
1328*	6:41:12.2	9:29:14.8	2.40	321	—	—	—	—	—	—	2.2
1329*	6:41:12.2	9:40:12.1	0.50	322	06411224+0940121	3691	6139	—	—	—	2.0
1330	6:41:12.3	9:27:57.6	1.00	—	—	—	6141	—	—	—	< 2.3
1331	6:41:12.4	9:39:26.5	0.50	—	06411236+0939264	3692	6143	—	185	—	< 1.5
1332	6:41:12.5	9:29:09.2	0.50	—	06411245+0929092	—	—	—	—	—	< 2.0
1333*	6:41:12.5	9:35:08.8	0.50	323	06411251+0935088	—	6146	—	—	—	2.8
1334*	6:41:12.6	9:29:04.8	0.50	324	06411259+0929048	—	—	—	—	—	7.8
1335	6:41:12.6	9:27:57.7	1.00	—	—	—	6149	—	—	—	< 2.3
1336	6:41:12.7	9:29:10.2	0.50	—	06411274+0929102	—	—	—	—	—	< 44.0
1337*	6:41:12.8	9:32:28.0	0.50	—	06411275+0932280	3701	6154	—	—	395	< 0.9
1338	6:41:12.8	9:29:15.3	0.50	—	06411283+0929153	—	—	—	—	—	< 21.2
1339*	6:41:12.9	9:26:14.9	0.50	—	06411286+0926148	3706	6159	120†	—	397	< 116.2
1340*	6:41:12.9	9:35:49.9	0.50	325	06411293+0935499	—	—	—	187	—	2.8
1341*	6:41:13.0	9:35:32.3	0.50	326	06411295+0935322	—	6162	—	—	—	9.4
1342*	6:41:13.0	9:29:08.7	1.37	327	—	—	—	—	—	—	50.2
1343*	6:41:13.0	9:27:39.3	0.50	328	06411300+0927393	—	6163	118†	—	398	31.3
1344*	6:41:13.0	9:27:31.9	0.50	329	06411303+0927319	—	6164	118†	189	—	106.3
1345*	6:41:13.1	9:31:38.2	0.50	—	06411306+0931382	3714	6166	—	—	399	< 1.0
1346*	6:41:13.1	9:31:06.7	0.50	330	06411311+0931066	3717	6168	—	—	401	4.5
1347*	6:41:13.1	9:28:59.3	0.50	331	06411314+0928593	3718	6170	—	—	402	1.8
1348	6:41:13.2	9:29:20.6	0.54	—	06411315+0929206	—	—	—	—	—	< 1.9
1349*	6:41:13.2	9:26:10.3	0.50	332	06411320+0926103	3719	6172	120†	—	403	160.3
1350	6:41:13.3	9:35:47.4	0.50	—	06411326+0935473	—	6174	—	—	—	< 0.9
1351*	6:41:13.3	9:31:50.3	0.50	333	06411329+0931503	3722	6175	—	—	405	19.1
1352	6:41:13.3	9:30:11.9	0.50	—	06411330+0930119	—	6176	—	—	—	< 1.3
1353*	6:41:13.3	9:28:07.5	0.50	334	06411333+0928074	3726	6179	124	—	407	19.9
1354*	6:41:13.4	9:38:13.8	0.50	335	06411336+0938137	—	6181	—	—	—	3.0
1355*	6:41:13.4	9:30:23.8	0.50	—	06411340+0930237	3727	6182	—	—	—	< 1.3
1356	6:41:13.4	9:33:33.0	0.50	—	06411340+0933329	—	—	—	—	—	< 0.9
1357*	6:41:13.4	9:27:36.2	0.50	—	06411341+0927362	—	6183	118†	—	—	< 50.0
1358	6:41:13.4	9:40:43.7	1.00	—	—	—	6184	—	—	—	< 2.0
1359	6:41:13.5	9:28:39.3	0.65	—	06411352+0928393	—	6185	—	—	—	< 2.0
1360	6:41:13.7	9:25:42.8	1.00	—	—	—	6187	—	—	—	< 3.5
1361*	6:41:13.8	9:29:32.1	1.00	—	—	3729	6190	—	—	—	< 1.6
1362*	6:41:13.8	9:28:42.6	1.82	337	—	—	—	—	—	—	2.8
1363*	6:41:13.9	9:40:42.4	4.74	336	—	—	—	—	—	—	2.3
1364*	6:41:14.1	9:26:40.6	0.50	338	06411413+0926405	3733	6201	—	—	408	39.2
1365	6:41:14.2	9:38:20.0	1.00	—	—	—	6202	—	—	—	< 1.4
1366*	6:41:14.2	9:33:21.6	1.00	—	—	—	6203	—	—	—	< 1.0
1367*	6:41:14.4	9:26:58.3	0.50	339	06411441+0926582	3737	6207	—	—	410	4.4
1368*	6:41:14.5	9:33:21.4	0.50	340	06411446+0933214	3738	6209	126	191	411	67.1
1369	6:41:14.5	9:32:05.9	0.50	—	06411447+0932058	—	—	—	—	—	< 1.0
1370*	6:41:14.5	9:37:14.3	0.50	341	06411448+0937143	3739	6210	125	—	412	77.9
1371	6:41:14.6	9:38:06.9	0.50	—	06411464+0938069	—	6212	—	—	—	< 1.4
1372*	6:41:14.8	9:34:13.5	0.50	342	06411475+0934134	3743	6216	—	—	413	1.2
1373	6:41:14.8	9:31:49.9	0.50	—	06411477+0931498	—	—	—	—	—	< 1.1
1374	6:41:14.8	9:37:32.0	1.00	—	—	—	6217	—	—	—	< 1.3
1375*	6:41:14.8	9:32:35.9	0.50	343	06411484+0932358	3746	6220	127	—	415	36.2
1376*	6:41:14.9	9:25:55.1	0.50	—	06411485+0925550	—	6219	—	—	414	< 3.9
1377	6:41:14.9	9:26:13.5	0.50	—	06411488+0926135	—	6222	—	—	—	< 4.8
1378	6:41:15.0	9:35:41.3	0.50	—	06411502+0935412	—	—	—	—	—	< 1.0
1379	6:41:15.1	9:39:47.2	0.50	—	06411506+0939471	3752	6226	—	—	—	< 1.9
1380*	6:41:15.1	9:26:44.3	0.50	344	06411511+0926443	3755	6228	—	—	416	17.4

Table 3. (Continued)

N	RA [h m s]	Dec. [d m s]	Id. rad. [""]	ACIS	2Mass	Reb.+	Lamm+	Flacc+	W56	Dahm+	Ct. Rate. [10^{-4}s^{-1}]
1381*	6:41:15.1	9:30:17.0	0.50	346	06411514+0930170	3758	6229	—	—	—	1.4
1382*	6:41:15.2	9:37:57.7	0.50	345	06411521+0937576	—	6232	—	—	417	10.0
1383	6:41:15.3	9:31:22.2	0.50	—	06411528+0931222	—	—	—	—	—	< 1.1
1384*	6:41:15.3	9:31:16.4	0.50	347	06411530+0931163	—	—	—	193	—	6.3
1385*	6:41:15.4	9:25:16.8	0.50	—	06411537+0925167	3761	6236	—	—	419	< 11.8
1386	6:41:15.5	9:40:12.6	0.50	—	06411547+0940125	3763	6240	—	—	—	< 2.0
1387*	6:41:15.5	9:26:33.5	1.00	—	—	—	6242	—	—	—	< 25.3
1388*	6:41:15.6	9:26:33.4	0.50	348	06411563+0926334	3765	6245	—	—	420	38.9
1389	6:41:15.7	9:27:52.7	0.50	—	06411570+0927526	—	—	—	—	—	< 2.4
1390*	6:41:15.7	9:38:18.3	0.50	349	06411571+0938182	3768	6247	—	194	—	5.8
1391*	6:41:15.7	9:26:16.8	0.50	350	06411574+0926168	3769	6248	129†	—	421	294.0
1392*	6:41:15.9	9:30:37.4	0.50	351	06411587+0930373	—	6249	—	—	—	1.6
1393*	6:41:16.0	9:26:09.5	0.50	—	06411599+0926094	3775	6251	129†	—	422	< 199.1
1394*	6:41:16.1	9:26:43.6	0.50	—	06411610+0926435	—	6255	—	—	—	< 3.9
1395	6:41:16.1	9:38:16.7	0.50	—	06411613+0938166	—	6257	—	—	—	< 1.5
1396	6:41:16.2	9:27:10.6	0.50	—	06411618+0927105	—	—	—	—	—	< 3.1
1397	6:41:16.3	9:26:32.0	8.10	—	—	—	—	130	—	—	< 11.6
1398	6:41:16.4	9:39:54.2	0.50	—	06411642+0939542	—	—	—	—	—	< 1.9
1399	6:41:16.5	9:35:22.4	1.00	—	—	—	6264	—	—	—	< 1.1
1400*	6:41:16.5	9:26:08.3	0.50	—	06411650+0926082	—	6263	—	—	423	< 4.1
1401	6:41:16.5	9:33:49.8	0.50	—	06411653+0933498	—	6266	—	—	—	< 1.8
1402*	6:41:16.7	9:29:52.3	0.50	352	06411668+0929522	3789	6270	131	—	424	41.6
1403*	6:41:16.8	9:27:30.2	0.50	353	06411678+0927301	3794	6273	—	—	425	26.2
1404	6:41:16.8	9:30:22.5	0.50	—	06411679+0930225	—	6274	—	—	—	< 1.5
1405*	6:41:16.8	9:36:20.6	0.50	354	06411684+0936206	3795	6276	132	—	—	25.6
1406	6:41:16.9	9:38:50.7	1.00	—	—	—	6278	—	—	—	< 1.6
1407	6:41:16.9	9:27:32.5	1.00	—	—	—	6279	—	—	—	< 21.7
1408*	6:41:17.1	9:32:52.3	0.50	355	06411705+0932523	3802	6285	—	—	426	6.4
1409	6:41:17.1	9:34:33.5	0.50	—	06411706+0934335	—	6287	—	—	—	< 1.1
1410	6:41:17.1	9:26:23.7	0.50	—	06411706+0926236	—	—	—	—	—	< 3.8
1411	6:41:17.1	9:26:19.1	0.50	—	06411707+0926191	—	—	—	—	—	< 3.9
1412*	6:41:17.1	9:29:04.9	0.50	—	06411714+0929048	—	6291	—	—	—	< 2.1
1413*	6:41:17.1	9:30:12.3	0.50	356	06411714+0930123	3808	6293	—	—	—	5.2
1414	6:41:17.2	9:36:23.2	0.50	—	06411718+0936231	—	6296	—	—	—	< 1.2
1415	6:41:17.2	9:35:43.1	0.50	—	06411723+0935430	—	6297	—	—	—	< 1.1
1416	6:41:17.3	9:30:58.5	0.50	—	06411725+0930584	—	—	—	—	—	< 1.4
1417	6:41:17.3	9:26:59.9	0.50	—	06411727+0926598	—	—	—	—	—	< 3.4
1418	6:41:17.4	9:31:52.0	0.51	—	06411736+0931519	—	6302	—	—	—	< 1.4
1419*	6:41:17.4	9:37:15.1	0.69	358	06411737+0937151	—	6307	—	—	—	1.1
1420	6:41:17.4	9:35:55.9	0.50	—	06411738+0935559	—	6306	—	—	—	< 1.2
1421	6:41:17.4	9:35:39.6	1.00	—	—	—	6305	—	—	—	< 1.1
1422*	6:41:17.4	9:30:28.7	0.50	357	06411744+0930287	3816	6308	—	—	—	1.6
1423	6:41:17.5	9:35:48.9	1.00	—	—	—	6309	—	—	—	< 1.1
1424*	6:41:17.5	9:28:06.3	0.50	—	06411750+0928063	—	6312	—	—	429	< 2.4
1425	6:41:17.6	9:29:58.9	0.50	—	06411760+0929588	—	—	—	—	—	< 1.8
1426*	6:41:17.7	9:29:26.2	0.50	359	06411771+0929261	3820	6316	133	—	430	41.0
1427	6:41:17.7	9:40:39.6	0.50	—	06411773+0940396	—	—	—	—	—	< 2.1
1428	6:41:17.7	9:34:22.0	0.50	—	06411774+0934219	—	6317	—	—	—	< 1.1
1429	6:41:17.9	9:41:47.3	1.00	—	—	—	6323	—	—	—	< 2.8
1430	6:41:17.9	9:38:20.4	0.50	—	06411791+0938204	—	6328	—	—	—	< 11.4
1431*	6:41:17.9	9:29:01.1	0.50	361	06411792+0929011	3826	6326	—	—	431	7.5
1432*	6:41:17.9	9:33:37.0	0.50	360	06411792+0933370	3827	6327	134†	198	432	62.7
1433	6:41:18.0	9:39:16.7	0.71	—	06411797+0939167	—	6331	—	—	—	< 1.8
1434	6:41:18.1	9:36:41.0	0.50	—	06411806+0936409	—	6333	—	—	—	< 1.3
1435*	6:41:18.1	9:38:25.4	0.50	362	06411808+0938253	3831	6334	—	—	433	13.1
1436	6:41:18.1	9:40:05.6	0.50	—	06411809+0940056	—	—	—	—	—	< 2.1
1437	6:41:18.2	9:39:02.0	0.53	—	06411817+0939019	—	—	—	—	—	< 1.7
1438*	6:41:18.2	9:28:03.1	0.50	363	06411820+0928031	—	—	—	—	—	4.0
1439	6:41:18.2	9:33:44.9	0.50	—	06411822+0933448	—	6337	134†	—	434	< 2.0
1440*	6:41:18.3	9:33:53.6	0.50	364	06411827+0933535	3836	6339	135	199	435	29.3

Table 3. (Continued)

N	RA [h m s]	Dec. [d m s]	Id. rad. [""]	ACIS	2Mass	Reb.+	Lamm+	Flacc+	W56	Dahm+	Ct. Rate. [$10^{-4} s^{-1}$]
1441*	6:41:18.3	9:28:33.0	0.50	365	06411829+0928330	3837	6340	–	–	436	13.0
1442*	6:41:18.3	9:29:32.4	0.50	366	06411830+0929323	–	–	–	–	–	8.3
1443*	6:41:18.4	9:39:41.1	0.50	367	06411837+0939411	3839	6345	137†	–	437	12.6
1444*	6:41:18.4	9:31:29.6	0.50	368	06411839+0931296	3840	6344	136	–	–	16.9
1445	6:41:18.5	9:27:11.6	0.50	–	06411849+0927116	–	–	–	–	–	< 6.2
1446	6:41:18.7	9:32:51.9	0.78	–	06411870+0932519	–	6355	–	–	–	< 1.2
1447	6:41:18.7	9:34:25.6	1.00	–	–	–	6356	–	–	–	< 1.2
1448	6:41:18.8	9:36:48.2	1.00	–	–	–	6357	–	–	–	< 1.4
1449	6:41:18.8	9:35:19.1	1.00	–	–	–	6359	–	–	–	< 1.1
1450*	6:41:18.8	9:30:19.9	0.50	369	06411882+0930199	3847	6362	–	–	–	1.6
1451	6:41:18.9	9:39:44.0	0.50	–	06411889+0939440	3848	6365	137†	–	–	< 2.0
1452*	6:41:18.9	9:35:54.2	0.50	371	06411890+0935541	3849	6364	–	–	–	1.6
1453*	6:41:18.9	9:27:15.8	0.50	370	06411893+0927157	3850	6366	–	–	438	14.5
1454	6:41:19.0	9:32:56.1	0.83	–	06411896+0932560	–	6367	–	–	–	< 1.2
1455*	6:41:19.1	9:26:29.4	0.50	–	06411911+0926294	3853	6376	–	–	439	< 3.0
1456	6:41:19.1	9:33:37.0	0.50	–	06411911+0933369	–	6377	–	–	–	< 2.7
1457	6:41:19.1	9:33:26.3	1.00	–	–	–	6378	–	–	–	< 2.3
1458	6:41:19.1	9:35:53.5	1.00	–	–	–	6379	–	–	–	< 1.6
1459	6:41:19.2	9:38:18.6	1.00	–	–	–	6380	–	–	–	< 1.8
1460	6:41:19.2	9:33:06.6	0.69	–	06411921+0933066	–	6384	–	–	–	< 1.2
1461	6:41:19.2	9:34:49.1	0.50	–	06411921+0934491	–	6381	–	–	–	< 1.2
1462*	6:41:19.3	9:30:48.8	0.50	372	06411926+0930487	3856	6383	–	–	440	1.9
1463*	6:41:19.3	9:38:07.1	0.50	373	06411928+0938071	3857	6387	–	–	–	1.6
1464*	6:41:19.5	9:30:28.6	0.50	374	06411945+0930286	3862	6390	–	–	–	1.8
1465	6:41:19.5	9:34:08.9	1.00	–	–	–	6392	–	–	–	< 1.2
1466	6:41:19.5	9:39:38.1	0.65	–	06411952+0939380	–	6395	–	–	–	< 2.0
1467	6:41:19.6	9:37:50.8	1.00	–	–	–	6394	–	–	–	< 1.6
1468	6:41:19.6	9:27:24.8	0.50	–	06411957+0927247	3864	–	–	203	–	< 3.1
1469*	6:41:19.6	9:31:44.4	0.50	375	06411963+0931443	3865	6399	138†	–	441	127.6
1470	6:41:19.7	9:31:54.2	0.52	–	06411967+0931542	–	6401	–	–	–	< 1.6
1471	6:41:19.7	9:36:24.0	1.00	–	–	–	6402	–	–	–	< 1.3
1472	6:41:19.7	9:26:49.4	0.50	–	06411969+0926493	–	–	–	–	–	< 3.4
1473*	6:41:19.8	9:31:38.2	1.98	376	–	–	–	138†	–	–	1.9
1474*	6:41:19.8	9:27:04.8	0.50	377	06411984+0927048	3869	6407	–	–	442	3.5
1475	6:41:20.0	9:28:45.7	1.00	–	–	–	6411	–	–	–	< 2.3
1476*	6:41:20.0	9:32:07.4	2.75	378	–	–	–	–	–	–	1.2
1477	6:41:20.1	9:36:12.0	1.00	–	–	–	6414	–	–	–	< 1.4
1478	6:41:20.1	9:28:34.8	0.50	–	06412006+0928347	–	–	–	–	–	< 2.4
1479	6:41:20.1	9:34:07.3	1.00	–	–	–	6418	–	–	–	< 1.3
1480	6:41:20.1	9:35:36.1	0.50	–	06412012+0935360	3872	6420	–	–	–	< 1.4
1481	6:41:20.4	9:39:52.9	1.00	–	–	–	6431	–	–	–	< 2.2
1482	6:41:20.5	9:36:29.7	0.60	–	06412052+0936297	–	6437	–	–	–	< 1.4
1483*	6:41:20.6	9:38:10.3	3.55	379	–	–	–	–	–	–	1.5
1484	6:41:20.7	9:35:17.0	0.50	–	06412067+0935169	–	6450	–	–	–	< 1.3
1485*	6:41:20.7	9:28:45.3	0.50	–	06412070+0928452	3886	6451	–	–	444	< 2.3
1486	6:41:20.7	9:31:40.7	0.50	–	06412072+0931407	–	6452	–	–	–	< 1.7
1487*	6:41:20.7	9:32:00.7	2.04	380	–	–	–	–	–	–	3.0
1488*	6:41:20.7	9:30:12.0	0.50	381	06412074+0930119	3887	6455	–	–	–	23.3
1489	6:41:20.8	9:26:47.7	1.00	–	–	–	6458	–	–	–	< 3.2
1490*	6:41:20.9	9:34:44.8	0.50	–	06412085+0934448	3888	6461	–	–	446	< 1.3
1491	6:41:20.9	9:34:39.4	0.50	–	06412090+0934394	–	6463	–	–	–	< 1.3
1492*	6:41:20.9	9:34:18.1	0.59	–	06412093+0934181	3891	6464	–	–	445	< 1.3
1493*	6:41:21.0	9:33:36.2	0.50	383	06412100+0933361	3893	6467	141	204	447	54.7
1494	6:41:21.0	9:36:59.7	0.50	–	06412102+0936596	3894	6469	–	–	–	< 1.5
1495*	6:41:21.0	9:32:41.7	0.50	382	06412104+0932417	3895	6468	–	–	–	1.7
1496*	6:41:21.2	9:32:14.6	0.50	384	06412119+0932146	–	6476	142	–	448	15.5
1497	6:41:21.2	9:28:31.3	0.50	–	06412124+0928312	–	–	–	–	–	< 2.4
1498	6:41:21.3	9:39:39.6	1.00	–	–	–	6479	–	–	–	< 2.2
1499	6:41:21.3	9:33:32.8	1.00	–	–	–	6481	–	–	–	< 2.6
1500	6:41:21.3	9:35:24.5	0.50	–	06412131+0935244	–	6485	–	–	–	< 1.3

Table 3. (Continued)

N	RA [h m s]	Dec. [d m s]	Id. rad. ["]	ACIS	2Mass	Reb.+	Lamm+	Flacc+	W56	Dahm+	Ct. Rate. [$10^{-4} s^{-1}$]
1501	6:41:21.5	9:35:52.2	1.00	—	—	—	6492	—	—	—	< 1.4
1502	6:41:21.8	9:34:59.6	1.00	—	—	—	6505	—	—	—	< 1.4
1503*	6:41:21.8	9:30:40.0	2.90	385	—	—	—	—	—	—	1.5
1504	6:41:22.0	9:40:00.5	0.65	—	06412196+0940004	—	6512	—	—	—	< 2.4
1505	6:41:22.0	9:35:09.0	0.50	—	06412199+0935089	—	6516	—	—	—	< 1.4
1506	6:41:22.0	9:32:23.7	1.00	—	—	—	6514	—	—	—	< 1.5
1507	6:41:22.0	9:34:29.0	1.00	—	—	—	6515	—	—	—	< 1.4
1508	6:41:22.0	9:33:49.1	0.58	—	06412202+0933491	—	6518	—	—	—	< 1.5
1509	6:41:22.2	9:35:24.2	0.50	—	06412215+0935241	—	6526	—	—	—	< 1.4
1510	6:41:22.2	9:30:52.8	1.00	—	—	—	6529	—	—	—	< 1.9
1511	6:41:22.2	9:37:30.4	1.00	—	—	—	6532	—	—	—	< 1.8
1512	6:41:22.4	9:31:21.5	1.00	—	—	—	6539	—	—	—	< 1.7
1513	6:41:22.5	9:34:33.7	1.00	—	—	—	6542	—	—	—	< 1.5
1514	6:41:22.5	9:38:01.3	1.00	—	—	—	6544	—	—	—	< 2.0
1515	6:41:22.5	9:35:36.2	1.00	—	—	—	6546	—	—	—	< 1.4
1516	6:41:22.5	9:38:12.7	1.00	—	—	—	6547	—	—	—	< 2.1
1517	6:41:22.5	9:29:12.9	0.50	—	06412253+0929129	3923	6549	—	—	—	< 2.2
1518	6:41:22.6	9:25:24.4	0.50	—	06412259+0925243	—	—	—	—	—	< 3.6
1519	6:41:22.7	9:30:43.1	1.00	—	—	—	6558	—	—	—	< 2.0
1520	6:41:22.7	9:39:09.7	1.00	—	—	—	6560	—	—	—	< 2.2
1521	6:41:22.7	9:32:32.6	1.00	—	—	—	6563	—	—	—	< 1.6
1522	6:41:22.7	9:40:15.0	1.00	—	—	—	6564	—	—	—	< 2.6
1523	6:41:22.7	9:40:54.5	1.00	—	—	—	6565	—	—	—	< 2.9
1524	6:41:22.8	9:32:14.8	1.00	—	—	—	6571	—	—	—	< 1.7
1525*	6:41:22.8	9:32:39.4	0.50	—	06412277+0932394	3926	6572	—	—	—	< 1.6
1526*	6:41:22.8	9:29:38.9	0.50	386	06412280+0929389	3927	6573	—	—	—	19.3
1527	6:41:22.8	9:36:10.8	0.50	—	06412282+0936108	3928	6574	—	—	—	< 1.5
1528*	6:41:23.0	9:29:30.8	0.50	387	06412297+0929307	—	6577	—	—	—	2.9
1529*	6:41:23.0	9:27:26.7	0.50	388	06412303+0927266	3935	6580	146	208	—	162.3
1530	6:41:23.1	9:33:03.9	0.50	—	06412305+0933039	—	6583	—	—	—	< 1.7
1531	6:41:23.1	9:31:25.3	0.50	—	06412313+0931253	3941	6588	—	—	—	< 1.9
1532*	6:41:23.1	9:37:33.9	0.50	389	06412313+0937338	3940	6589	—	—	452	13.4
1533*	6:41:23.2	9:35:22.7	0.50	390	06412316+0935226	3942	6592	—	—	—	1.9
1534*	6:41:23.2	9:30:36.4	0.50	391	06412320+0930364	3944	6595	—	—	453	37.6
1535	6:41:23.2	9:39:46.9	0.59	—	06412322+0939469	—	6603	—	—	—	< 2.4
1536	6:41:23.2	9:38:46.5	0.50	—	06412323+0938464	3945	6602	—	—	—	< 2.1
1537	6:41:23.2	9:40:14.8	1.00	—	—	—	6600	—	—	—	< 2.8
1538	6:41:23.2	9:38:39.8	1.00	—	—	—	6601	—	—	—	< 2.0
1539	6:41:23.3	9:33:31.7	1.00	—	—	—	6604	—	—	—	< 2.2
1540	6:41:23.3	9:32:30.3	1.00	—	—	—	6607	—	—	—	< 1.7
1541	6:41:23.3	9:40:01.0	0.50	—	06412333+0940010	—	6611	—	—	—	< 2.6
1542*	6:41:23.3	9:38:04.4	0.50	392	06412333+0938044	3948	6610	—	—	—	4.4
1543	6:41:23.4	9:27:57.0	0.71	—	06412338+0927570	—	6620	—	—	—	< 2.7
1544	6:41:23.4	9:34:48.6	1.00	—	—	—	6612	—	—	—	< 1.6
1545	6:41:23.4	9:37:40.2	1.00	—	—	—	6613	—	—	—	< 5.3
1546	6:41:23.4	9:38:42.6	0.50	—	06412343+0938425	—	6619	—	—	—	< 2.0
1547	6:41:23.4	9:36:33.1	1.00	—	—	—	6618	—	—	—	< 1.6
1548	6:41:23.5	9:37:25.7	1.00	—	—	—	6621	—	—	—	< 2.0
1549*	6:41:23.5	9:41:39.1	7.75	393	—	—	—	—	—	—	4.9
1550	6:41:23.5	9:33:27.1	1.00	—	—	—	6628	—	—	—	< 2.9
1551	6:41:23.5	9:41:10.5	1.00	—	—	—	6630	—	—	—	< 3.0
1552	6:41:23.6	9:30:12.5	0.50	—	06412355+0930125	—	6632	—	—	—	< 2.3
1553	6:41:23.6	9:40:09.3	1.00	—	—	—	6640	—	—	—	< 2.8
1554	6:41:23.6	9:33:49.7	0.50	—	06412363+0933497	—	6639	—	—	456	< 1.6
1555	6:41:23.6	9:32:40.0	0.50	—	06412363+0932399	—	6641	—	—	—	< 1.7
1556*	6:41:23.8	9:33:56.5	0.50	394	06412378+0933565	—	6648	—	209	—	4.0
1557	6:41:23.8	9:40:21.3	0.50	—	06412381+0940212	—	6651	—	—	—	< 3.0
1558	6:41:23.9	9:27:39.3	0.50	—	06412390+0927393	—	6654	—	—	—	< 3.3
1559	6:41:23.9	9:38:25.4	1.00	—	—	—	6655	—	—	—	< 2.0
1560	6:41:24.0	9:37:50.1	0.50	—	06412397+0937501	—	6659	—	—	—	< 2.3

Table 3. (Continued)

N	RA [h m s]	Dec. [d m s]	Id. rad. [""]	ACIS	2Mass	Reb.+	Lamm+	Flacc+	W56	Dahm+	Ct. Rate. [$10^{-4} s^{-1}$]
1561	6:41:24.0	9:36:44.8	0.50	—	06412397+0936447	3962	6661	—	—	—	< 1.6
1562	6:41:24.0	9:35:01.7	0.50	—	06412399+0935016	—	6663	—	—	—	< 1.7
1563*	6:41:24.0	9:26:52.5	0.50	—	06412402+0926525	—	6668	—	—	—	< 3.4
1564	6:41:24.2	9:38:17.8	0.60	—	06412415+0938178	—	6677	—	—	—	< 2.1
1565	6:41:24.2	9:37:13.2	1.00	—	—	—	6675	—	—	—	< 2.1
1566	6:41:24.2	9:39:50.7	1.00	—	—	—	6676	—	—	—	< 2.5
1567	6:41:24.2	9:38:35.7	0.50	—	06412423+0938357	—	6686	—	—	—	< 2.0
1568	6:41:24.2	9:32:29.6	1.00	—	—	—	6684	—	—	—	< 1.7
1569*	6:41:24.3	9:31:54.2	0.50	395	06412425+0931541	3969	6685	—	—	—	40.0
1570	6:41:24.3	9:40:30.7	1.00	—	—	—	6687	—	—	—	< 3.1
1571	6:41:24.3	9:34:46.1	0.50	—	06412434+0934461	—	6693	—	—	—	< 1.7
1572*	6:41:24.5	9:32:45.1	0.50	396	06412445+0932451	3977	6699	148†	—	459	26.9
1573	6:41:24.5	9:35:02.0	1.00	—	—	—	6703	—	—	—	< 1.7
1574*	6:41:24.5	9:37:35.5	0.50	397	06412454+0937355	3980	6706	—	—	460	14.2
1575	6:41:24.6	9:34:39.9	1.00	—	—	—	6707	—	—	—	< 1.7
1576	6:41:24.6	9:32:49.3	0.50	—	06412459+0932493	—	6709	148†	—	—	< 23.0
1577	6:41:24.6	9:38:28.6	1.00	—	—	—	6710	—	—	—	< 2.1
1578	6:41:24.7	9:32:39.0	1.00	—	—	—	6713	—	—	—	< 1.7
1579*	6:41:24.7	9:26:23.4	0.50	398	06412473+0926233	3982	6716	—	210	—	3.1
1580	6:41:24.8	9:39:50.2	0.50	—	06412475+0939502	—	6720	—	—	—	< 2.5
1581	6:41:24.8	9:41:40.0	1.00	—	—	—	6718	—	—	—	< 14.3
1582	6:41:24.8	9:39:36.4	1.00	—	—	—	6719	—	—	—	< 2.5
1583	6:41:24.8	9:31:19.1	1.00	—	—	—	6721	—	—	—	< 2.1
1584	6:41:24.8	9:32:21.2	0.50	—	06412480+0932211	—	6725	—	—	—	< 1.8
1585	6:41:24.9	9:38:39.0	1.00	—	—	—	6730	—	—	—	< 2.2
1586	6:41:24.9	9:36:16.6	1.00	—	—	—	6732	—	—	—	< 1.8
1587	6:41:25.0	9:39:47.5	0.50	—	06412498+0939475	3984	6735	—	—	—	< 2.5
1588	6:41:25.0	9:31:58.4	1.00	—	—	—	6737	—	—	—	< 2.0
1589	6:41:25.1	9:30:54.0	1.00	—	—	—	6740	—	—	—	< 2.2
1590	6:41:25.1	9:35:07.4	1.00	—	—	—	6741	—	—	—	< 1.8
1591*	6:41:25.1	9:36:00.2	0.50	399	06412508+0936001	3987	6743	—	—	—	4.5
1592	6:41:25.1	9:38:42.6	1.00	—	—	—	6745	—	—	—	< 2.3
1593	6:41:25.2	9:39:35.9	1.00	—	—	—	6749	—	—	—	< 2.5
1594	6:41:25.2	9:40:28.8	1.00	—	—	—	6750	—	—	—	< 3.1
1595	6:41:25.2	9:32:39.4	1.00	—	—	—	6755	—	—	—	< 1.8
1596	6:41:25.3	9:38:23.9	1.00	—	—	—	6759	—	—	—	< 2.2
1597	6:41:25.4	9:32:25.3	1.00	—	—	—	6762	—	—	—	< 2.0
1598	6:41:25.4	9:36:54.3	1.00	—	—	—	6763	—	—	—	< 1.8
1599	6:41:25.4	9:30:22.9	1.00	—	—	—	6766	—	—	—	< 2.3
1600	6:41:25.4	9:32:50.4	0.50	—	06412543+0932503	—	6770	—	—	—	< 1.9
1601	6:41:25.4	9:39:27.7	1.00	—	—	—	6773	—	—	—	< 2.5
1602	6:41:25.5	9:31:00.9	0.50	—	06412548+0931008	3994	6776	—	—	—	< 2.1
1603	6:41:25.5	9:26:20.1	0.50	—	06412549+0926200	—	6775	—	—	—	< 3.6
1604	6:41:25.5	9:33:12.7	1.00	—	—	—	6777	—	—	—	< 3.5
1605	6:41:25.5	9:34:54.9	1.00	—	—	—	6778	—	—	—	< 1.9
1606*	6:41:25.6	9:34:43.0	0.50	400	06412562+0934429	3995	6784	149†	—	461	10.3
1607	6:41:25.6	9:37:46.7	1.00	—	—	—	6782	—	—	—	< 2.3
1608	6:41:25.6	9:31:23.1	1.00	—	—	—	6785	—	—	—	< 2.2
1609	6:41:25.6	9:40:16.6	1.00	—	—	—	6786	—	—	—	< 2.9
1610	6:41:25.7	9:31:56.8	1.00	—	—	—	6788	—	—	—	< 2.2
1611	6:41:25.7	9:36:40.0	0.50	—	06412569+0936400	3999	6792	—	211	—	< 1.9
1612*	6:41:25.8	9:40:36.5	3.09	401	—	—	—	—	—	—	4.1
1613	6:41:25.8	9:33:16.7	1.00	—	—	—	6795	—	—	—	< 3.5
1614	6:41:25.8	9:41:16.7	1.00	—	—	—	6797	—	—	—	< 3.2
1615	6:41:25.9	9:41:00.8	1.00	—	—	—	6799	—	—	—	< 3.2
1616	6:41:25.9	9:36:07.5	1.00	—	—	—	6803	—	—	—	< 1.9
1617	6:41:25.9	9:36:47.9	1.00	—	—	—	6804	—	—	—	< 1.9
1618*	6:41:25.9	9:30:26.1	0.50	—	06412593+0930260	4001	6805	—	—	—	< 2.3
1619	6:41:26.0	9:33:46.3	1.00	—	—	—	6812	—	—	—	< 1.8
1620	6:41:26.1	9:27:44.4	0.55	—	06412607+0927443	—	—	—	—	—	< 3.0

Table 3. (Continued)

N	RA [h m s]	Dec. [d m s]	Id. rad. ["]	ACIS	2Mass	Reb.+	Lamm+	Flacc+	W56	Dahm+	Ct. Rate. [$10^{-4} s^{-1}$]
1621	6:41:26.1	9:32:44.1	1.00	—	—	—	6814	—	—	—	< 2.1
1622	6:41:26.1	9:31:48.0	1.00	—	—	—	6815	—	—	—	< 2.1
1623	6:41:26.1	9:29:59.2	1.00	—	—	—	6816	—	—	—	< 2.5
1624	6:41:26.2	9:35:06.9	1.00	—	—	—	6818	—	—	—	< 1.9
1625	6:41:26.2	9:41:38.7	1.00	—	—	—	6819	—	—	—	< 15.8
1626	6:41:26.2	9:37:09.1	0.50	—	06412618+0937090	—	6822	—	—	—	< 2.0
1627	6:41:26.2	9:38:24.1	1.00	—	—	—	6820	—	—	—	< 2.3
1628	6:41:26.2	9:36:24.1	1.00	—	—	—	6826	—	—	—	< 2.0
1629	6:41:26.2	9:31:34.4	0.50	—	06412624+0931343	4009	6827	—	—	—	< 2.0
1630	6:41:26.3	9:34:48.3	0.50	—	06412628+0934482	4010	6834	149†	—	—	< 2.0
1631	6:41:26.3	9:32:05.6	1.00	—	—	—	6833	—	—	—	< 2.1
1632	6:41:26.3	9:35:42.6	1.02	—	06412634+0935425	—	6836	—	—	—	< 1.8
1633	6:41:26.4	9:40:17.2	1.00	—	—	—	6839	—	—	—	< 3.0
1634	6:41:26.4	9:38:32.7	1.00	—	—	—	6841	—	—	—	< 2.3
1635	6:41:26.5	9:37:37.6	0.81	—	06412651+0937375	—	6849	—	—	—	< 2.2
1636	6:41:26.5	9:33:09.5	1.00	—	—	—	6848	—	—	—	< 4.0
1637	6:41:26.5	9:24:57.0	0.50	—	06412653+0924569	—	—	—	—	—	< 5.8
1638	6:41:26.5	9:32:14.3	1.00	—	—	—	6850	—	—	—	< 2.1
1639	6:41:26.6	9:39:24.8	1.00	—	—	—	6854	—	—	—	< 2.7
1640	6:41:26.6	9:34:12.5	0.50	—	06412658+0934125	—	6860	—	—	—	< 1.9
1641	6:41:26.6	9:35:30.3	1.00	—	—	—	6863	—	—	—	< 1.9
1642	6:41:26.7	9:31:24.8	0.76	—	06412669+0931248	—	6868	—	—	—	< 2.1
1643	6:41:26.7	9:32:04.4	1.00	—	—	—	6869	—	—	—	< 2.6
1644	6:41:26.8	9:33:38.4	1.00	—	—	—	6870	—	—	—	< 1.9
1645	6:41:26.8	9:27:54.0	0.50	—	06412676+0927540	—	6871	—	—	—	< 3.1
1646	6:41:26.8	9:37:44.3	1.00	—	—	—	6875	—	—	—	< 2.2
1647*	6:41:26.8	9:27:04.5	0.50	404	06412682+0927044	—	6876	—	—	—	6.3
1648	6:41:26.9	9:35:23.4	0.50	—	06412688+0935234	4022	6879	—	—	—	< 2.0
1649	6:41:26.9	9:26:42.2	1.00	—	—	—	6878	—	—	—	< 4.0
1650	6:41:26.9	9:38:32.1	1.00	—	—	—	6882	—	—	—	< 2.6
1651*	6:41:27.0	9:38:40.2	0.50	402	06412696+0938401	4024	6889	—	—	—	2.3
1652	6:41:27.0	9:38:39.1	1.00	—	—	—	6885	—	—	—	< 2.7
1653	6:41:27.0	9:30:52.7	0.50	—	06412699+0930526	4026	6888	—	—	—	< 2.2
1654*	6:41:27.0	9:30:13.2	0.50	403	06412700+0930131	4027	6887	—	—	462	7.8
1655	6:41:27.1	9:33:05.2	0.50	—	06412710+0933052	4030	6893	—	—	—	< 4.3
1656	6:41:27.1	9:41:32.7	1.00	—	—	—	6894	—	—	—	< 8.6
1657*	6:41:27.2	9:35:06.1	0.50	405	06412715+0935061	4032	6899	150	—	—	94.4
1658*	6:41:27.2	9:26:29.4	0.51	—	06412716+0926294	4033	6902	—	—	—	< 3.7
1659	6:41:27.2	9:30:59.0	1.00	—	—	—	6903	—	—	—	< 2.2
1660	6:41:27.2	9:31:32.6	1.00	—	—	—	6905	—	—	—	< 2.2
1661	6:41:27.3	9:28:07.3	0.50	—	06412727+0928073	—	6908	—	—	—	< 3.1
1662*	6:41:27.3	9:32:06.5	0.50	406	06412730+0932064	4038	6913	—	—	463	3.8
1663	6:41:27.3	9:26:07.6	0.50	—	06412733+0926076	—	6916	—	—	—	< 3.9
1664	6:41:27.4	9:32:40.2	1.00	—	—	—	6918	—	—	—	< 2.2
1665	6:41:27.4	9:40:41.5	1.00	—	—	—	6921	—	—	—	< 3.1
1666	6:41:27.4	9:30:13.8	1.00	—	—	—	6923	—	—	—	< 5.1
1667	6:41:27.5	9:36:51.8	0.62	—	06412747+0936517	—	6926	—	—	—	< 2.1
1668	6:41:27.5	9:39:46.1	1.00	—	—	—	6929	—	—	—	< 3.7
1669	6:41:27.5	9:31:03.6	1.00	—	—	—	6933	—	—	—	< 2.2
1670	6:41:27.5	9:40:14.0	0.50	—	06412754+0940140	4043	6935	—	—	—	< 3.1
1671	6:41:27.5	9:38:05.4	1.00	—	—	—	6934	—	—	—	< 2.4
1672	6:41:27.6	9:31:55.8	0.50	—	06412756+0931558	4045	6938	—	—	—	< 2.2
1673	6:41:27.6	9:41:06.4	0.82	—	06412756+0941063	—	6940	—	—	—	< 3.2
1674	6:41:27.6	9:30:58.4	1.00	—	—	—	6937	—	—	—	< 2.2
1675	6:41:27.6	9:25:39.5	0.50	—	06412758+0925395	—	6941	—	—	—	< 7.5
1676	6:41:27.7	9:31:42.2	1.00	—	—	—	6947	—	—	—	< 2.3
1677	6:41:27.7	9:34:22.9	0.50	—	06412772+0934228	4048	6952	—	—	—	< 2.1
1678	6:41:27.7	9:37:00.6	0.89	—	06412772+0937006	4050	6953	—	—	—	< 2.2
1679	6:41:27.7	9:32:26.4	0.50	—	06412773+0932264	4049	6951	—	—	—	< 2.3
1680	6:41:27.8	9:28:07.4	1.00	—	—	—	6956	—	—	—	< 3.1

Table 3. (Continued)

N	RA [h m s]	Dec. [d m s]	Id. rad. [""]	ACIS	2Mass	Reb.+	Lamm+	Flacc+	W56	Dahm+	Ct. Rate. [$10^{-4} s^{-1}$]
1681	6:41:27.8	9:31:32.4	0.50	—	06412779+0931323	—	6960	—	—	—	< 2.3
1682	6:41:27.8	9:39:41.5	0.50	—	06412780+0939415	—	6962	—	—	—	< 3.9
1683	6:41:27.8	9:36:07.3	1.00	—	—	—	6963	—	—	—	< 2.0
1684	6:41:27.9	9:31:45.0	1.00	—	—	—	6967	—	—	—	< 2.3
1685	6:41:27.9	9:31:20.8	1.00	—	—	—	6968	—	—	—	< 2.2
1686	6:41:27.9	9:31:56.6	0.50	—	06412794+0931566	—	6972	—	—	—	< 2.3
1687	6:41:27.9	9:38:08.9	1.00	—	—	—	6970	—	—	—	< 2.6
1688	6:41:28.0	9:34:35.8	0.65	—	06412795+0934358	—	6975	—	—	—	< 2.3
1689	6:41:28.0	9:30:53.7	1.00	—	—	—	6974	—	—	—	< 2.3
1690	6:41:28.0	9:40:52.8	0.64	—	06412797+0940527	—	6977	—	—	—	< 3.2
1691	6:41:28.0	9:31:08.5	1.00	—	—	—	6979	—	—	—	< 2.2
1692*	6:41:28.1	9:32:49.9	0.50	407	06412808+0932498	4059	6987	—	—	—	11.4
1693	6:41:28.1	9:32:34.1	1.00	—	—	—	6986	—	—	—	< 2.4
1694	6:41:28.2	9:28:15.0	1.00	—	—	—	6991	—	—	—	< 3.1
1695	6:41:28.2	9:35:58.8	1.00	—	—	—	6993	—	—	—	< 2.0
1696	6:41:28.2	9:37:26.3	1.00	—	—	—	6994	—	—	—	< 2.3
1697*	6:41:28.2	9:32:53.3	0.50	—	06412819+0932533	—	6996	—	—	—	< 10.4
1698	6:41:28.2	9:37:42.0	0.73	—	06412823+0937420	—	7000	—	—	—	< 2.3
1699	6:41:28.3	9:34:28.7	0.50	—	06412826+0934286	4060	7002	—	—	—	< 2.2
1700	6:41:28.3	9:40:42.2	0.50	—	06412826+0940421	4061	7003	—	—	—	< 3.2
1701	6:41:28.3	9:39:30.1	0.50	—	06412827+0939300	—	7004	152†	—	—	< 4.1
1702	6:41:28.3	9:40:03.1	0.50	—	06412829+0940031	4062	7009	—	—	—	< 3.9
1703	6:41:28.3	9:34:60.0	0.50	—	06412829+0934599	4063	7010	—	—	—	< 2.4
1704	6:41:28.3	9:34:56.5	1.00	—	—	—	7008	—	—	—	< 2.4
1705	6:41:28.3	9:32:27.0	1.00	—	—	—	7011	—	—	—	< 2.4
1706	6:41:28.3	9:34:29.9	1.00	—	—	—	7012	—	—	—	< 2.1
1707	6:41:28.3	9:30:54.9	1.00	—	—	—	7013	—	—	—	< 2.3
1708	6:41:28.3	9:37:20.2	1.00	—	—	—	7014	—	—	—	< 2.3
1709	6:41:28.4	9:31:21.0	1.00	—	—	—	7016	—	—	—	< 2.3
1710	6:41:28.4	9:33:29.6	1.00	—	—	—	7019	—	—	—	< 2.0
1711	6:41:28.4	9:32:42.5	1.00	—	—	—	7021	—	—	—	< 6.3
1712	6:41:28.5	9:33:17.4	1.00	—	—	—	7023	—	—	—	< 2.4
1713	6:41:28.5	9:32:13.1	1.00	—	—	—	7024	—	—	—	< 2.3
1714	6:41:28.5	9:27:14.7	1.00	—	—	—	7026	—	—	—	< 11.4
1715	6:41:28.5	9:33:37.5	1.00	—	—	—	7028	—	—	—	< 2.1
1716	6:41:28.5	9:39:17.6	1.00	—	—	—	7029	—	—	—	< 3.8
1717	6:41:28.5	9:37:30.4	1.00	—	—	—	7030	—	—	—	< 2.3
1718	6:41:28.6	9:40:53.7	1.00	—	—	—	7032	—	—	—	< 3.3
1719	6:41:28.6	9:28:05.8	1.00	—	—	—	7036	—	—	—	< 3.2
1720	6:41:28.7	9:32:34.3	1.00	—	—	—	7042	—	—	—	< 2.4
1721*	6:41:28.7	9:27:10.8	0.50	409	06412874+0927107	4069	7044	—	—	464	20.5
1722	6:41:28.8	9:26:11.2	0.50	—	06412875+0926112	4070	7043	—	—	—	< 23.3
1723	6:41:28.8	9:28:15.8	1.02	—	06412876+0928158	—	—	—	—	—	< 3.1
1724	6:41:28.8	9:38:01.6	1.00	—	—	—	7046	—	—	—	< 2.4
1725*	6:41:28.8	9:38:38.8	0.50	408	06412878+0938388	4072	7049	153	213	—	48.5
1726	6:41:28.8	9:32:08.8	0.50	—	06412879+0932087	4073	7051	—	—	—	< 2.3
1727*	6:41:28.8	9:34:54.1	0.50	410	06412884+0934540	4075	7057	—	—	—	2.6
1728	6:41:28.8	9:34:00.6	1.00	—	—	—	7055	—	—	—	< 2.1
1729	6:41:28.9	9:31:44.2	0.57	—	06412888+0931441	—	7060	—	—	—	< 2.3
1730	6:41:28.9	9:31:46.1	1.00	—	—	—	7058	—	—	—	< 2.3
1731	6:41:28.9	9:31:49.4	0.50	—	06412892+0931494	—	7061	—	—	—	< 2.3
1732	6:41:29.0	9:34:21.0	1.00	—	—	—	7063	—	—	—	< 2.1
1733	6:41:29.0	9:29:42.1	1.00	—	—	—	7064	—	—	—	< 2.6
1734	6:41:29.0	9:31:11.8	1.00	—	—	—	7065	—	—	—	< 2.3
1735	6:41:29.0	9:33:56.3	0.50	—	06412901+0933563	—	7066	—	—	—	< 2.1
1736	6:41:29.0	9:41:06.4	1.00	—	—	—	7069	—	—	—	< 3.5
1737*	6:41:29.1	9:39:50.4	2.72	411	—	—	—	—	—	—	8.9
1738	6:41:29.1	9:34:21.9	1.00	—	—	—	7072	—	—	—	< 2.1
1739	6:41:29.2	9:28:48.2	0.50	—	06412915+0928481	—	7075	—	—	—	< 2.7
1740*	6:41:29.2	9:39:36.0	0.50	412	06412918+0939359	4081	7076	152†	214	—	96.0

Table 3. (Continued)

N	RA [h m s]	Dec. [d m s]	Id. rad. ["]	ACIS	2Mass	Reb.+	Lamm+	Flacc+	W56	Dahm+	Ct. Rate. [$10^{-4} s^{-1}$]
1741	6:41:29.2	9:39:15.4	1.00	—	—	—	7078	—	—	—	< 8.9
1742	6:41:29.3	9:30:12.2	1.00	—	—	—	7081	—	—	—	< 2.6
1743	6:41:29.3	9:34:52.3	1.00	—	—	—	7082	—	—	—	< 2.4
1744	6:41:29.3	9:30:19.5	1.00	—	—	—	7084	—	—	—	< 2.5
1745	6:41:29.3	9:28:27.7	0.62	—	06412927+0928276	—	7086	—	—	—	< 3.1
1746	6:41:29.3	9:34:26.8	1.00	—	—	—	7087	—	—	—	< 2.1
1747	6:41:29.3	9:31:10.1	1.00	—	—	—	7089	—	—	—	< 2.4
1748	6:41:29.3	9:29:53.4	0.50	—	06412933+0929534	4082	7091	—	—	—	< 2.6
1749	6:41:29.4	9:31:58.3	1.00	—	—	—	7093	—	—	—	< 2.3
1750	6:41:29.4	9:36:22.7	1.00	—	—	—	7098	—	—	—	< 2.3
1751	6:41:29.4	9:32:03.1	0.59	—	06412943+0932030	4083	7097	—	—	—	< 2.3
1752*	6:41:29.4	9:39:18.2	0.50	413	06412944+0939181	4084	7103	152†	—	—	14.4
1753	6:41:29.4	9:32:51.3	1.00	—	—	—	7100	—	—	—	< 3.3
1754	6:41:29.4	9:41:23.7	1.00	—	—	—	7101	—	—	—	< 4.9
1755	6:41:29.5	9:39:48.4	0.69	—	06412945+0939483	—	7099	—	—	—	< 4.9
1756	6:41:29.5	9:32:13.3	0.77	—	06412952+0932132	—	7109	—	—	—	< 2.3
1757	6:41:29.5	9:26:44.7	0.50	—	06412954+0926447	—	7108	—	—	—	< 6.4
1758	6:41:29.6	9:40:22.4	1.00	—	—	—	7111	—	—	—	< 3.2
1759	6:41:29.6	9:29:13.0	0.50	—	06412957+0929129	—	7114	—	—	—	< 2.7
1760	6:41:29.7	9:33:58.6	1.00	—	—	—	7118	—	—	—	< 2.2
1761	6:41:29.7	9:40:05.6	1.00	—	—	—	7119	—	—	—	< 3.7
1762	6:41:29.7	9:33:04.4	0.61	—	06412969+0933044	—	7123	—	—	—	< 4.3
1763	6:41:29.8	9:38:42.2	1.00	—	—	—	7130	—	—	—	< 3.6
1764	6:41:29.9	9:31:11.2	1.00	—	—	—	7136	—	—	—	< 2.4
1765	6:41:29.9	9:37:14.5	1.00	—	—	—	7137	—	—	—	< 2.6
1766	6:41:29.9	9:34:38.9	1.00	—	—	—	7138	—	—	—	< 2.2
1767	6:41:30.0	9:39:13.5	0.50	—	06412995+0939135	—	7141	152†	—	—	< 8.7
1768	6:41:30.0	9:41:06.7	1.00	—	—	—	7143	—	—	—	< 3.4
1769	6:41:30.0	9:36:45.5	1.00	—	—	—	7145	—	—	—	< 2.5
1770	6:41:30.0	9:38:30.9	1.00	—	—	—	7146	—	—	—	< 3.3
1771	6:41:30.0	9:34:39.5	0.50	—	06413004+0934394	—	7150	—	—	—	< 2.3
1772	6:41:30.1	9:33:13.4	1.00	—	—	—	7148	—	—	—	< 2.6
1773	6:41:30.1	9:37:02.1	0.52	—	06413007+0937020	4096	7152	—	—	—	< 2.7
1774	6:41:30.1	9:39:08.4	1.00	—	—	—	7151	—	—	—	< 4.0
1775	6:41:30.1	9:31:00.6	1.00	—	—	—	7155	—	—	—	< 2.5
1776	6:41:30.1	9:34:11.1	1.00	—	—	—	7156	—	—	—	< 2.3
1777	6:41:30.1	9:31:45.8	0.50	—	06413014+0931458	4097	7163	—	—	—	< 2.5
1778	6:41:30.2	9:28:38.8	1.00	—	—	—	7165	—	—	—	< 5.8
1779	6:41:30.3	9:32:06.6	1.00	—	—	—	7169	—	—	—	< 2.5
1780	6:41:30.3	9:32:42.5	1.00	—	—	—	7170	—	—	—	< 2.5
1781	6:41:30.3	9:33:52.2	1.00	—	—	—	7173	—	—	—	< 2.3
1782	6:41:30.4	9:38:24.7	1.00	—	—	—	7177	—	—	—	< 3.3
1783	6:41:30.4	9:38:30.1	0.50	—	06413038+0938300	4104	7180	—	—	—	< 3.4
1784	6:41:30.4	9:36:56.6	1.00	—	—	—	7179	—	—	—	< 2.7
1785	6:41:30.4	9:28:41.5	1.00	—	—	—	7181	—	—	—	< 5.9
1786	6:41:30.5	9:38:05.8	1.00	—	—	—	7187	—	—	—	< 3.1
1787	6:41:30.5	9:30:55.8	0.71	—	06413050+0930557	4105	7184	—	—	—	< 2.6
1788	6:41:30.5	9:36:07.1	1.00	—	—	—	7188	—	—	—	< 2.3
1789	6:41:30.6	9:28:18.4	0.50	—	06413058+0928184	4106	7191	—	—	—	< 13.7
1790	6:41:30.6	9:30:30.3	1.00	—	—	—	7192	—	—	—	< 2.7
1791	6:41:30.6	9:30:48.4	1.00	—	—	—	7193	—	—	—	< 2.7
1792	6:41:30.6	9:40:40.0	1.00	—	—	—	7197	—	—	—	< 3.3
1793	6:41:30.7	9:37:12.9	1.00	—	—	—	7199	—	—	—	< 2.8
1794	6:41:30.7	9:41:24.7	1.00	—	—	—	7200	—	—	—	< 6.3
1795	6:41:30.7	9:38:32.0	1.00	—	—	—	7202	—	—	—	< 3.5
1796	6:41:30.7	9:31:09.9	0.50	—	06413070+0931098	—	7203	—	—	—	< 2.5
1797	6:41:30.7	9:32:14.4	1.00	—	—	—	7205	—	—	—	< 2.6
1798	6:41:30.7	9:32:16.0	1.00	—	—	—	7207	—	—	—	< 2.6
1799	6:41:30.8	9:33:45.1	1.00	—	—	—	7210	—	—	—	< 2.3
1800	6:41:30.8	9:29:50.2	1.00	—	—	—	7211	—	—	—	< 2.9

Table 3. (Continued)

N	RA [h m s]	Dec. [d m s]	Id. rad. [""]	ACIS	2Mass	Reb.+	Lamm+	Flacc+	W56	Dahm+	Ct. Rate. [$10^{-4} s^{-1}$]
1801	6:41:30.8	9:32:47.4	0.50	—	06413077+0932474	4109	7215	—	—	—	< 3.2
1802	6:41:30.8	9:30:08.4	0.50	—	06413078+0930083	4110	7214	—	—	—	< 2.8
1803*	6:41:30.8	9:39:00.7	3.08	414	—	—	—	—	—	—	13.7
1804	6:41:30.9	9:30:25.0	0.72	—	06413088+0930250	—	7222	—	—	—	< 2.8
1805*	6:41:31.0	9:35:25.3	2.75	415	—	—	—	—	—	—	5.8
1806	6:41:31.0	9:41:22.6	1.00	—	—	—	7228	—	—	—	< 5.9
1807	6:41:31.1	9:33:44.9	1.00	—	—	—	7232	—	—	—	< 2.3
1808	6:41:31.1	9:32:14.8	0.54	—	06413109+0932148	—	7239	—	—	—	< 2.6
1809	6:41:31.2	9:29:39.6	0.50	—	06413123+0929396	—	7256	—	—	—	< 3.6
1810	6:41:31.2	9:34:27.6	0.65	—	06413123+0934275	—	7250	—	—	—	< 2.4
1811	6:41:31.3	9:29:16.4	1.00	—	—	—	7255	—	—	—	< 3.5
1812	6:41:31.3	9:37:03.2	1.00	—	—	—	7261	—	—	—	< 2.9
1813*	6:41:31.3	9:32:57.3	1.00	—	—	—	—	—	—	466	< 4.6
1814	6:41:31.3	9:31:16.4	1.00	—	—	—	7264	—	—	—	< 2.5
1815	6:41:31.3	9:41:05.3	1.00	—	—	—	7265	—	—	—	< 3.5
1816	6:41:31.3	9:40:54.2	1.00	—	—	—	7267	—	—	—	< 3.4
1817	6:41:31.3	9:35:12.0	0.50	—	06413132+0935120	—	7272	—	—	—	< 2.6
1818	6:41:31.3	9:33:14.0	1.00	—	—	—	7270	—	—	—	< 2.6
1819	6:41:31.3	9:40:35.9	1.00	—	—	—	7271	—	—	—	< 3.3
1820	6:41:31.3	9:40:03.8	1.00	—	—	4123	7274	—	—	—	< 3.3
1821	6:41:31.3	9:38:43.6	1.00	—	—	—	7273	—	—	—	< 3.6
1822	6:41:31.4	9:32:42.9	1.00	—	—	—	7275	—	—	—	< 2.9
1823	6:41:31.4	9:40:39.5	1.00	—	—	—	7276	—	—	—	< 3.2
1824	6:41:31.4	9:35:28.3	0.50	—	06413136+0935282	4124	7279	—	—	—	< 4.5
1825	6:41:31.4	9:38:50.5	0.50	—	06413141+0938504	4126	7281	—	—	—	< 3.7
1826	6:41:31.5	9:36:50.5	0.50	—	06413146+0936505	4128	7288	—	—	—	< 2.8
1827	6:41:31.5	9:39:44.6	1.00	—	—	—	7285	—	—	—	< 3.5
1828	6:41:31.5	9:32:22.8	0.74	—	06413150+0932228	—	7292	—	—	—	< 2.5
1829	6:41:31.5	9:34:39.7	1.00	—	—	—	7291	—	—	—	< 2.4
1830	6:41:31.6	9:39:29.6	0.69	—	06413156+0939296	4130	7294	—	—	—	< 3.4
1831	6:41:31.6	9:36:12.7	1.00	—	—	—	7295	—	—	—	< 2.4
1832	6:41:31.6	9:36:53.2	1.00	—	—	—	7296	—	—	—	< 2.8
1833	6:41:31.6	9:30:24.7	1.00	—	—	—	7302	—	—	—	< 2.9
1834*	6:41:31.7	9:31:54.3	0.50	416	06413168+0931543	4133	7303	—	—	—	5.9
1835	6:41:31.7	9:30:00.6	0.50	—	06413171+0930006	4134	7305	—	—	—	< 8.4
1836	6:41:31.7	9:39:42.2	1.00	—	—	—	7306	—	—	—	< 3.3
1837	6:41:32.0	9:36:46.9	0.50	—	06413197+0936468	4141	7328	—	—	—	< 2.9
1838	6:41:32.1	9:34:40.3	1.00	—	—	—	7337	—	—	—	< 2.5
1839	6:41:32.1	9:32:25.1	0.50	—	06413205+0932251	—	7341	—	—	—	< 2.5
1840	6:41:32.1	9:36:15.5	1.00	—	—	—	7338	—	—	—	< 2.6
1841	6:41:32.1	9:37:57.0	1.00	—	—	—	7342	—	—	—	< 18.8
1842	6:41:32.1	9:30:02.7	1.00	—	—	—	7343	—	—	—	< 17.3
1843	6:41:32.1	9:34:30.1	1.00	—	—	—	7344	—	—	—	< 2.5
1844	6:41:32.1	9:37:51.0	1.00	—	—	—	7346	—	—	—	< 3.4
1845	6:41:32.1	9:31:19.8	0.83	—	06413214+0931197	—	—	—	—	—	< 2.6
1846	6:41:32.2	9:37:42.9	0.65	—	06413216+0937428	—	—	—	—	—	< 3.2
1847	6:41:32.2	9:39:53.1	0.50	—	06413220+0939530	4149	—	—	—	—	< 3.6
1848	6:41:32.2	9:39:25.6	0.50	—	06413223+0939256	4151	—	—	—	—	< 3.4
1849	6:41:32.5	9:37:16.3	0.50	—	06413245+0937163	4153	—	—	—	—	< 2.9
1850*	6:41:32.5	9:38:07.4	0.50	417	06413250+0938074	4155	—	156	—	—	64.4
1851	6:41:32.5	9:33:10.5	0.50	—	06413251+0933104	4156	—	—	—	—	< 3.4
1852	6:41:32.7	9:35:02.2	0.50	—	06413272+0935021	—	—	—	—	—	< 2.6
1853	6:41:32.8	9:40:32.5	0.54	—	06413278+0940324	4165	—	—	—	—	< 3.5
1854	6:41:32.9	9:32:12.1	0.50	—	06413289+0932121	4168	—	—	—	—	< 2.9
1855	6:41:33.2	9:36:07.8	0.63	—	06413323+0936077	—	—	—	—	—	< 2.7
1856	6:41:33.4	9:40:12.8	0.50	—	06413341+0940128	4174	—	—	219	—	< 3.6
1857	6:41:33.7	9:36:02.2	0.50	—	06413372+0936022	—	—	—	—	—	< 2.8
1858	6:41:33.7	9:36:14.4	0.50	—	06413372+0936143	—	—	—	—	—	< 3.0
1859	6:41:33.8	9:35:21.5	0.50	—	06413375+0935214	—	—	—	—	—	< 3.2
1860	6:41:33.8	9:41:12.4	0.50	—	06413379+0941123	4181	—	—	—	—	< 6.7

Table 3. (Continued)

N	RA [h m s]	Dec. [d m s]	Id. rad. [""]	ACIS	2Mass	Reb.+	Lamm+	Flacc+	W56	Dahm+	Ct. Rate. [10^{-4} s^{-1}]
1861	6:41:33.9	9:32:45.4	1.00	—	—	7364	—	—	—	—	< 8.7
1862	6:41:33.9	9:38:48.3	0.50	—	06413390+0938482	4184	—	—	—	—	< 3.6
1863	6:41:34.0	9:39:46.8	1.00	—	—	—	7372	—	—	—	< 4.0
1864	6:41:34.0	9:39:15.5	1.00	—	—	4190	7374	—	—	—	< 3.8
1865	6:41:34.1	9:34:24.4	1.00	—	—	—	7376	—	—	—	< 3.1
1866	6:41:34.2	9:36:08.5	0.50	—	06413416+0936084	4194	7382	—	—	—	< 3.2
1867	6:41:34.2	9:36:49.3	1.00	—	—	—	7384	—	—	—	< 3.3
1868	6:41:34.2	9:35:07.1	0.50	—	06413420+0935071	—	7387	—	—	—	< 3.4
1869	6:41:34.2	9:33:45.8	1.00	—	—	—	7391	—	—	—	< 3.1
1870	6:41:34.3	9:34:42.4	0.50	—	06413426+0934423	4197	7393	—	—	—	< 3.2
1871	6:41:34.3	9:38:52.5	0.62	—	06413431+0938525	—	—	—	—	—	< 3.6
1872	6:41:34.4	9:39:09.7	1.00	—	—	—	7402	—	—	—	< 4.0
1873	6:41:34.4	9:39:51.6	1.00	—	—	—	7403	—	—	—	< 4.2
1874	6:41:34.4	9:41:04.2	1.00	—	—	—	7405	—	—	—	< 4.6
1875	6:41:34.5	9:35:41.5	0.50	—	06413447+0935414	—	7411	—	—	—	< 3.6
1876	6:41:34.5	9:39:49.6	1.00	—	—	—	7412	—	—	—	< 4.2
1877	6:41:34.5	9:36:11.7	1.00	—	—	—	7417	—	—	—	< 3.7
1878*	6:41:34.6	9:36:32.5	0.50	418	06413455+0936325	4204	7418	—	—	470	11.5
1879	6:41:34.6	9:34:46.5	0.50	—	06413455+0934465	—	7422	—	—	—	< 3.2
1880	6:41:34.6	9:33:45.6	0.50	—	06413456+0933455	—	7421	—	—	—	< 3.2
1881	6:41:34.6	9:37:16.1	1.00	—	—	—	7432	—	—	—	< 3.0
1882	6:41:34.7	9:40:38.4	1.00	—	—	—	7434	—	—	—	< 3.9
1883	6:41:34.7	9:39:18.2	1.00	—	—	—	7438	—	—	—	< 4.1
1884	6:41:34.8	9:41:02.5	1.00	—	—	—	7441	—	—	—	< 9.1
1885	6:41:34.8	9:33:59.3	1.00	—	—	—	7442	—	—	—	< 3.2
1886	6:41:34.9	9:35:18.7	0.50	—	06413485+0935187	—	7452	—	—	—	< 3.7
1887	6:41:34.9	9:40:53.6	1.00	—	—	—	7454	—	—	—	< 4.3
1888	6:41:35.0	9:40:50.7	1.00	—	—	—	7460	—	—	—	< 4.2
1889	6:41:35.0	9:37:19.8	1.00	—	—	—	7464	—	—	—	< 3.3
1890	6:41:35.1	9:39:06.5	0.50	—	06413506+0939065	4222	—	—	—	—	< 4.2
1891	6:41:35.1	9:40:38.2	0.50	—	06413513+0940382	—	7473	—	—	—	< 4.1
1892	6:41:35.2	9:38:28.1	0.50	—	06413518+0938280	4226	7478	—	—	—	< 3.7
1893	6:41:35.2	9:40:29.0	1.00	—	—	—	7484	—	—	—	< 4.3
1894	6:41:35.3	9:36:55.3	1.00	—	—	—	7490	—	—	—	< 3.8
1895	6:41:35.3	9:34:58.6	1.00	—	—	—	7494	—	—	—	< 4.3
1896	6:41:35.5	9:34:41.7	1.00	—	—	—	7508	—	—	—	< 27.2
1897	6:41:35.5	9:40:54.7	1.00	—	—	—	7512	—	—	—	< 7.0
1898	6:41:35.7	9:38:53.3	0.66	—	06413570+0938533	—	—	—	—	—	< 4.1
1899	6:41:35.8	9:34:50.1	0.50	—	06413577+0934500	4245	7546	—	—	—	< 37.5
1900	6:41:35.8	9:40:14.2	1.00	—	—	—	7551	—	—	—	< 4.2
1901	6:41:35.9	9:34:40.4	0.50	—	06413585+0934403	4249	7554	—	—	—	< 51.6
1902	6:41:35.9	9:40:42.0	0.50	—	06413589+0940419	—	7557	—	—	—	< 4.2
1903	6:41:35.9	9:40:53.1	1.00	—	—	—	7559	—	—	—	< 6.6
1904	6:41:35.9	9:39:46.3	0.50	—	06413594+0939462	4251	7564	—	—	—	< 4.4
1905	6:41:36.0	9:41:00.4	1.00	—	—	—	7568	—	—	—	< 18.7
1906	6:41:36.0	9:37:37.8	1.00	—	—	—	7571	—	—	—	< 3.9
1907	6:41:36.1	9:39:41.5	1.00	—	—	—	7580	—	—	—	< 4.6
1908	6:41:36.1	9:40:07.5	1.00	—	—	—	7588	—	—	—	< 4.2
1909	6:41:36.2	9:40:45.1	0.50	—	06413619+0940451†	4260	7592†	—	—	—	< 4.5
1910	6:41:36.2	9:40:45.1	0.50	—	06413619+0940451†	4261	7592†	—	—	—	< 4.5
1911*	6:41:36.2	9:39:20.4	0.50	419	06413623+0939204	4263	7597	—	—	471	14.1
1912	6:41:36.3	9:40:15.3	0.50	—	06413629+0940153	—	7602	—	—	—	< 4.3
1913	6:41:36.3	9:38:48.0	1.00	—	—	—	7606	—	—	—	< 4.1
1914	6:41:36.4	9:39:42.0	1.00	—	—	4270	7618	—	—	—	< 4.7
1915	6:41:36.5	9:39:07.2	1.00	—	—	—	7621	—	—	—	< 10.6
1916	6:41:36.5	9:39:17.0	0.50	—	06413653+0939169	—	7628	—	—	—	< 11.7
1917	6:41:36.6	9:39:18.7	1.00	—	—	—	7630	—	—	—	< 11.7
1918	6:41:36.6	9:37:00.6	0.56	—	06413657+0937006	—	7629	—	—	—	< 4.0
1919	6:41:36.6	9:37:56.3	0.50	—	06413660+0937563	4275	7634	—	—	—	< 4.1
1920	6:41:36.7	9:39:27.5	0.50	—	06413668+0939274	—	7640	—	—	—	< 11.7

Table 3. (Continued)

N	RA [h m s]	Dec. [d m s]	Id. rad. [""]	ACIS	2Mass	Reb.+	Lamm+	Flacc+	W56	Dahm+	Ct. Rate. [$10^{-4} s^{-1}$]
1921	6:41:36.7	9:38:30.3	0.50	—	06413668+0938303	4281	7641	—	—	—	< 4.1
1922	6:41:36.8	9:40:15.2	1.00	—	—	—	7655	—	—	—	< 4.3
1923	6:41:36.8	9:36:36.8	1.00	—	—	—	7656	—	—	—	< 4.3
1924	6:41:36.8	9:40:59.0	1.00	—	—	—	7662	—	—	—	< 25.4
1925	6:41:36.9	9:36:12.0	1.00	—	—	—	7671	—	—	—	< 37.9
1926	6:41:36.9	9:40:22.1	1.00	—	—	—	7677	—	—	—	< 4.4
1927	6:41:37.0	9:40:27.7	0.50	—	06413697+0940277	—	7680	—	—	—	< 4.3
1928	6:41:37.0	9:38:13.7	1.00	—	—	—	7687	—	—	—	< 4.1
1929	6:41:37.1	9:37:07.2	0.50	—	06413712+0937072	4298	7699	—	—	—	< 4.7
1930	6:41:37.2	9:38:14.0	1.00	—	—	—	7705	—	—	—	< 4.1
1931	6:41:37.3	9:39:12.4	0.76	—	06413727+0939124	—	7710	—	—	—	< 5.4
1932	6:41:37.3	9:36:42.7	1.00	—	—	—	7719	—	—	—	< 5.2
1933	6:41:37.4	9:37:28.1	0.50	—	06413743+0937280	4305	7732	—	—	—	< 19.4
1934	6:41:37.4	9:37:14.0	1.00	—	—	—	7733	—	—	—	< 8.9
1935	6:41:37.5	9:39:25.8	0.50	—	06413745+0939258	4307	7734	—	—	—	< 5.6
1936	6:41:37.5	9:40:26.6	1.00	—	—	—	7739	—	—	—	< 5.0
1937	6:41:37.5	9:40:58.2	0.50	—	06413752+0940582	—	7742	—	—	—	< 24.1
1938	6:41:37.5	9:40:40.8	0.50	—	06413754+0940407	4309	7745	—	—	—	< 5.2
1939	6:41:37.6	9:40:29.8	0.71	—	06413764+0940298	4313	7759	—	—	—	< 5.2
1940	6:41:37.8	9:37:52.2	1.00	—	—	—	7773	—	—	—	< 5.4
1941	6:41:38.0	9:39:53.4	0.50	—	06413797+0939534	4328	7783	—	—	—	< 4.8
1942	6:41:38.4	9:39:15.2	1.00	—	—	—	7825	—	—	—	< 9.4
1943	6:41:38.4	9:40:47.6	1.00	—	—	—	7826	—	—	—	< 17.2
1944	6:41:38.4	9:38:18.3	1.00	—	—	—	7829	—	—	—	< 5.0
1945	6:41:38.4	9:40:59.2	1.00	—	—	—	7837	—	—	—	< 22.2
1946	6:41:38.5	9:39:50.0	1.00	—	—	—	7844	—	—	—	< 4.8
1947	6:41:38.5	9:37:56.3	0.50	—	06413848+0937563	4343	7842	—	—	—	< 9.4
1948	6:41:38.5	9:39:20.4	0.50	—	06413849+0939203	4344	7843	—	—	—	< 6.9
1949	6:41:38.5	9:39:38.6	1.00	—	—	—	7846	—	—	—	< 4.8
1950	6:41:38.5	9:40:29.0	0.75	—	06413852+0940290	—	7847	—	—	—	< 32.2
1951	6:41:38.7	9:38:35.8	0.54	—	06413866+0938358	4346	7865	—	—	—	< 22.2
1952	6:41:38.7	9:40:10.3	0.50	—	06413874+0940102	—	7870	—	—	—	< 9.7
1953	6:41:38.9	9:38:52.1	0.50	—	06413894+0938520	4352	—	—	—	—	< 4.6
1954	6:41:39.0	9:40:20.7	1.00	—	—	—	7895	—	—	—	< 32.2
1955	6:41:39.1	9:39:54.8	1.00	—	—	—	7902	—	—	—	< 6.1
1956	6:41:39.2	9:40:13.2	1.00	—	—	—	7922	—	—	—	< 32.2
1957	6:41:39.4	9:39:10.9	1.00	—	—	—	7942	—	—	—	< 35.8
1958	6:41:39.5	9:39:22.9	0.72	—	06413949+0939228	4374	7952	—	—	—	< 25.9
1959	6:41:39.5	9:39:44.5	1.00	—	—	—	7949	—	—	—	< 5.4
1960	6:41:39.5	9:40:09.5	1.00	—	—	—	7950	—	—	—	< 40.2
1961	6:41:39.6	9:40:12.1	1.00	—	—	—	7962	—	—	—	< 44.2
1962*	6:41:39.8	9:40:27.9	0.50	420	06413974+0940279	4382	7974	159	—	475	38.5
1963	6:41:40.0	9:40:55.5	1.00	—	—	—	8001	—	—	—	< 25.2
1964	6:41:40.1	9:40:15.5	1.00	—	—	—	8012	—	—	—	< 32.2
1965	6:41:40.2	9:40:39.0	0.64	—	06414024+0940389	—	8027	—	—	—	< 32.2
1966	6:41:40.4	9:40:46.9	1.00	—	—	—	8036	—	—	—	< 14.9
1967	6:41:40.7	9:40:43.6	0.79	—	06414070+0940435	—	8070	—	—	—	< 24.4

*: A likely NGC 2264 member;

†: Entry also present in another row.

Table 4. Optical/NIR properties of X-ray sources.

N	I	R-I	J	H	K	Sp.T.	Av	Av(JHK)	$\log T_{eff}$ [K]	$\log L_{bol}$ [L_{\odot}]	Mass [M_{\odot}]	LogAge [yr.]	P_{rot} [d]
1	17.97	2.10	15.92	14.17	13.37	—	—	9.96	—	—	—	—	—
2	15.68	1.25	14.27	13.54	13.29	M2.5	0.00	0.62	3.54	-0.80	0.34	6.63	1.23
3	15.88	1.33	14.44	13.70	13.50	M3	0.00	0.00	3.53	-0.87	0.30	6.63	12.09
4	14.14	1.03	12.79	12.07	11.85	M0	0.62	0.41	3.59	-0.06	0.57	6.11	4.55
5	13.26	0.86	11.81	11.30	10.75	K4	1.61	0.00	3.66	0.51	1.57	6.19	7.49
6	15.15	1.33	13.66	12.97	12.78	M3	0.00	0.00	3.53	-0.57	0.32	6.33	0.76
7	19.86	1.74	—	—	—	—	—	—	—	—	—	—	—
8	14.39	0.86	12.69	11.51	10.67	K1	1.92	2.39	3.71	0.15	1.30	7.10	12.09
9	13.82	0.83	12.57	11.90	11.62	K6	0.58	0.00	3.62	0.01	0.92	6.38	1.98
10	17.06	1.70	15.42	14.85	14.60	—	—	0.00	—	—	—	—	—
11	14.74	1.30	13.15	12.41	12.17	—	—	0.63	—	—	—	—	12.58
12	—	—	—	—	—	—	—	—	—	—	—	—	—
13	21.35	—	—	—	—	—	—	—	—	—	—	—	—
14	15.92	1.27	14.51	13.79	13.57	M3	0.00	0.00	3.53	-0.88	0.30	6.65	0.76
15	16.02	1.48	14.41	13.73	13.47	—	—	0.00	—	—	—	—	16.69
16	—	—	—	—	—	—	—	—	—	—	—	—	—
17	15.00	1.26	13.55	12.82	12.53	M2	0.45	0.85	3.55	-0.43	0.39	6.28	3.88
18	—	—	—	—	—	—	—	—	—	—	—	—	—
19	16.25	1.55	14.57	—	13.64	—	—	—	—	—	—	—	—
20	16.10	1.76	14.51	13.98	13.67	—	—	0.00	—	—	—	—	—
21	—	—	—	—	—	—	—	—	—	—	—	—	—
22	—	—	—	—	—	—	—	—	—	—	—	—	—
23	—	—	—	—	—	—	—	—	—	—	—	—	—
24	—	—	—	—	—	—	—	—	—	—	—	—	—
25	15.76	1.21	13.88	13.02	12.59	M1	0.85	2.45	3.57	-0.65	0.47	6.69	—
26	14.81	1.35	13.33	12.55	12.33	—	—	1.00	—	—	—	—	1.15
27	15.07	0.86	14.00	13.27	13.14	K7	0.45	0.00	3.61	-0.53	0.81	7.07	5.82
28	—	—	—	—	—	—	—	—	—	—	—	—	—
29	15.09	1.12	—	—	—	—	—	—	—	—	—	—	—
30	14.45	1.18	12.91	12.19	11.83	M3	0.00	0.00	3.53	-0.29	0.32	6.12	—
31	—	—	—	—	—	—	—	—	—	—	—	—	—
32	15.23	1.11	13.93	13.19	12.89	M1	0.40	0.98	3.57	-0.54	0.48	6.57	—
33	14.96	1.35	13.43	12.81	12.55	M3	0.00	0.00	3.53	-0.50	0.32	6.27	1.32
34	16.60	2.00	14.63	14.01	13.58	—	—	0.00	—	—	—	—	1.18
35	—	—	—	—	—	—	—	—	—	—	—	—	—
36	14.56	0.92	—	12.56	—	M0	0.13	—	3.59	-0.35	0.58	6.47	4.55
37	—	—	—	—	—	—	—	—	—	—	—	—	—
38	14.50	1.26	12.65	11.14	9.95	K6	2.50	4.26	3.62	0.21	0.91	6.11	—
39	13.28	0.61	12.24	11.58	11.25	K4	0.49	0.00	3.66	0.23	1.41	6.55	4.50
40	17.28	1.75	15.61	15.02	14.75	—	—	0.00	—	—	—	—	1.89
41	15.94	1.41	—	—	—	—	—	—	—	—	—	—	2.55
42	—	—	—	—	—	—	—	—	—	—	—	—	—
43	15.62	1.89	—	12.78	—	—	—	—	—	—	—	—	2.46
44	17.70	2.03	15.61	15.13	14.84	—	—	0.00	—	—	—	—	0.62
45	15.23	1.55	13.74	13.05	12.87	M5	0.00	0.00	3.49	-0.47	0.22	5.85	1.22
46	14.66	0.83	13.12	12.25	11.45	K7:	—	0.00	—	—	—	—	—
47	18.60	2.50	—	—	—	—	—	—	—	—	—	—	—
48	—	—	—	—	—	—	—	—	—	—	—	—	—
49	17.54	2.05	15.67	15.08	14.69	M5	0.67	0.00	3.49	-1.23	0.15	6.72	0.60
50	15.90	1.43	14.35	13.66	13.46	—	—	0.00	—	—	—	—	—
51	20.30	2.19	16.64	15.57	14.91	—	—	0.00	—	—	—	—	—
52	11.43	0.31	10.76	10.28	9.84	G0	0.00	0.00	3.78	0.88	1.67	6.97	—
53	14.19	0.85	12.86	12.14	11.80	M0	0.00	1.08	3.59	-0.23	0.57	6.31	6.97
54	—	—	8.25	8.34	8.37	—	—	0.00	—	—	—	—	—
55	15.74	1.41	14.27	13.48	13.35	—	—	0.00	—	—	—	—	7.09
56	14.17	0.63	13.23	12.64	12.52	K4	0.58	0.00	3.66	-0.10	1.17	7.02	14.81
57	15.13	1.05	—	13.00	12.67	K7	1.29	—	3.61	-0.34	0.79	6.77	2.50
58	—	—	—	—	—	—	—	—	—	—	—	—	—
59	15.00	1.50	13.49	12.83	12.57	M3	0.58	0.00	3.53	-0.37	0.32	6.17	8.46
60	15.55	1.29	13.97	13.11	12.39	M0	1.78	0.00	3.59	-0.34	0.58	6.45	—

Table 4. (Continued)

N	I	R-I	J	H	K	Sp.T.	Av	Av(JHK)	$\log T_{eff}$ [K]	$\log L_{bol}$ [L_{\odot}]	Mass [M_{\odot}]	LogAge [yr.]	P_{rot} [d]
61	14.54	1.10	13.23	12.50	12.36	M0	0.94	0.00	3.59	-0.14	0.57	6.20	9.25
62	16.51	1.86	14.65	14.03	13.80	—	—	0.00	—	—	—	—	0.55
63	—	—	—	—	—	—	—	—	—	—	—	—	—
64	16.84	1.86	14.82	14.02	13.88	—	—	0.00	—	—	—	—	1.96
65	16.15	1.50	14.57	13.94	13.71	—	—	0.00	—	—	—	—	1.29
66	16.32	1.80	14.47	13.89	13.50	—	—	0.00	—	—	—	—	—
67	—	—	—	—	—	—	—	—	—	—	—	—	—
68	15.62	1.42	14.05	13.34	12.98	M3	0.22	0.00	3.53	-0.71	0.31	6.46	—
69	—	—	—	—	—	—	—	—	—	—	—	—	—
70	17.43	2.44	14.90	—	—	—	—	—	—	—	—	—	—
71	13.30	0.62	12.39	11.67	11.35	K2	0.67	0.97	3.69	0.27	1.50	6.80	—
72	15.17	1.94	13.22	12.61	12.34	—	—	0.00	—	—	—	—	—
73	—	—	—	—	—	—	—	—	—	—	—	—	—
74	—	—	—	—	—	—	—	—	—	—	—	—	—
75	15.23	1.49	13.73	13.02	12.77	M3.5	0.00	0.00	3.52	-0.58	0.29	6.31	13.68
76	20.45	—	16.28	14.41	13.50	—	—	11.24	—	—	—	—	—
77	17.70	2.14	15.66	15.20	14.88	—	—	0.00	—	—	—	—	1.59
78	14.10	0.94	12.77	12.00	11.69	M1	0.00	1.19	3.57	-0.19	0.47	6.13	—
79	15.24	1.17	13.86	13.07	12.84	M2	0.04	1.00	3.55	-0.62	0.38	6.49	5.51
80	16.35	1.74	14.53	13.38	12.61	M4.5	0.00	2.60	3.50	-0.96	0.20	6.55	9.71
81	17.02	1.77	15.21	14.46	14.45	—	—	0.00	—	—	—	—	1.57
82	—	—	—	—	—	—	—	—	—	—	—	—	—
83	15.88	1.29	14.41	13.73	13.47	—	—	0.00	—	—	—	—	2.57
84	17.37	2.04	15.32	14.82	14.37	—	—	0.00	—	—	—	—	—
85	17.51	1.83	15.86	15.20	14.77	—	—	0.00	—	—	—	—	—
86	15.30	1.47	13.88	13.14	12.93	M5	0.00	0.51	3.49	-0.50	0.22	5.99	3.09
87	14.34	1.13	12.92	12.17	11.95	M1	0.49	0.64	3.57	-0.17	0.47	6.10	1.67
88	16.45	1.51	14.95	14.23	13.94	—	—	0.00	—	—	—	—	—
89	16.84	1.84	14.38	12.20	10.60	—	—	10.30	—	—	—	—	—
90	14.99	0.97	13.69	13.04	12.80	K8	0.65	0.00	3.60	-0.42	0.70	6.74	—
91	14.48	0.88	13.28	12.60	12.40	K4	1.70	0.00	3.66	0.05	1.30	6.81	6.77
92	—	—	—	—	—	—	—	—	—	—	—	—	—
93	15.06	1.39	13.69	12.79	12.26	—	—	1.06	—	—	—	—	—
94	—	—	—	—	—	—	—	—	—	—	—	—	—
95	13.81	0.77	12.40	11.61	11.16	K4	1.20	0.00	3.66	0.19	1.40	6.61	7.64
96	—	—	—	—	—	—	—	—	—	—	—	—	—
97	16.38	1.79	14.31	13.26	12.88	M5	0.00	3.61	3.49	-0.93	0.18	6.53	2.16
98	—	—	—	—	—	—	—	—	—	—	—	—	—
99	16.04	1.94	14.15	13.57	13.20	—	—	0.00	—	—	—	—	—
100	16.15	1.65	14.35	13.78	13.56	—	—	0.00	—	—	—	—	—
101	—	—	—	—	—	—	—	—	—	—	—	—	—
102	13.20	0.63	12.36	11.62	11.16	K4	0.58	0.00	3.66	0.28	1.48	6.49	—
103	15.43	1.50	13.87	13.19	12.97	M5	0.00	0.00	3.49	-0.55	0.21	6.23	—
104	14.97	0.94	13.72	12.99	12.87	M1	0.00	0.00	3.57	-0.54	0.48	6.56	9.04
105	14.31	0.82	12.99	12.20	11.79	K4	1.43	0.00	3.66	0.05	1.30	6.81	—
106	16.21	1.63	14.15	13.34	12.85	M4	0.00	0.00	3.51	-0.94	0.23	6.60	7.22
107	—	—	—	—	—	—	—	—	—	—	—	—	—
108	—	—	—	—	13.61	—	—	—	—	—	—	—	—
109	15.95	1.43	14.50	13.78	13.54	—	—	0.00	—	—	—	—	—
110	17.81	1.80	15.94	15.24	14.92	—	—	0.00	—	—	—	—	—
111	13.47	0.60	12.35	11.68	11.32	K1	0.76	0.00	3.71	0.24	1.41	7.00	2.38
112	11.14	0.31	10.61	10.34	10.25	F5	0.18	1.00	3.81	1.09	1.81	6.90	—
113	—	—	—	—	—	—	—	—	—	—	—	—	—
114	15.22	1.13	13.81	13.12	12.95	—	—	0.00	—	—	—	—	9.95
115	—	—	—	—	—	—	—	—	—	—	—	—	—
116	16.92	1.60	15.35	14.59	14.49	M5	0.00	0.00	3.49	-1.15	0.15	6.67	1.47
117	—	—	—	—	—	—	—	—	—	—	—	—	—
118	16.88	1.75	15.11	14.50	14.45	—	—	0.00	—	—	—	—	1.55
119	15.67	1.65	13.68	12.96	12.59	M3	1.25	0.00	3.53	-0.48	0.32	6.25	7.64
120	13.97	0.87	12.70	12.02	11.80	K6	0.76	0.00	3.62	-0.00	0.93	6.41	—

Table 4. (Continued)

Table 4. (Continued)

N	I	R-I	J	H	K	Sp.T.	Av	Av(JHK)	$\log T_{eff}$ [K]	$\log L_{bol}$ [L_{\odot}]	Mass [M_{\odot}]	LogAge [yr.]	P_{rot} [d]
181	14.71	—	—	—	—	—	—	—	—	—	—	—	—
182	—	—	—	14.53	13.01	—	—	—	—	—	—	—	—
183	15.25	1.03	—	—	—	—	—	—	—	—	—	—	—
184	13.36	0.69	12.35	11.71	11.55	K5	0.27	0.00	3.64	0.13	1.12	6.41	0.91
185	10.56	0.11	10.45	10.40	10.36	A0	0.49	0.00	3.98	1.68	2.50	6.64	—
186	—	—	—	—	—	—	—	—	—	—	—	—	—
187	13.30	0.71	12.24	11.61	11.38	K4	0.94	0.00	3.66	0.33	1.49	6.42	—
188	17.20	2.30	—	—	13.63	—	—	—	—	—	—	—	—
189	14.15	0.73	—	—	—	—	—	—	—	—	—	—	5.15
190	13.30	0.60	12.36	11.82	11.65	K0	0.94	1.86	3.72	0.36	1.47	6.99	—
191	16.42	1.85	14.34	13.53	13.14	—	—	0.00	—	—	—	—	—
192	18.10	2.77	—	—	—	—	—	—	—	—	—	—	—
193	13.90	0.71	12.85	12.23	12.05	K5	0.36	0.00	3.64	-0.07	1.09	6.70	4.26
194	19.89	—	—	—	—	—	—	—	—	—	—	—	—
195	—	—	—	15.07	13.66	—	—	—	—	—	—	—	—
196	—	—	9.28	9.27	9.28	—	—	0.00	—	—	—	—	—
197	15.77	1.70	13.28	11.89	11.16	M1	3.03	7.33	3.57	-0.11	0.48	6.08	—
198	—	—	—	—	—	—	—	—	—	—	—	—	—
199	—	—	16.88	14.14	12.63	—	—	19.84	—	—	—	—	—
200	15.53	1.18	—	—	13.31	M0	1.29	—	3.59	-0.45	0.59	6.62	3.63
201	16.99	2.34	14.44	13.76	13.36	—	—	0.00	—	—	—	—	3.11
202	15.75	1.68	—	12.26	—	M3	1.38	—	3.53	-0.48	0.32	6.25	—
203	14.17	0.87	12.93	12.24	12.07	M1	0.00	0.00	3.57	-0.22	0.47	6.16	0.91
204	14.50	1.37	12.97	12.27	12.02	M2:	—	0.00	—	—	—	—	1.31
205	16.76	2.11	14.54	13.75	13.38	—	—	0.00	—	—	—	—	1.13
206	11.95	0.42	11.39	11.04	10.95	G3	0.27	0.00	3.77	0.73	1.57	7.01	2.16
207	14.68	1.75	12.81	12.03	11.69	—	—	1.43	—	—	—	—	9.71
208	16.80	1.74	—	—	—	—	—	—	—	—	—	—	—
209	—	—	—	14.79	13.30	—	—	—	—	—	—	—	—
210	15.24	1.30	13.86	13.03	12.76	M1	1.25	1.41	3.57	-0.34	0.47	6.29	—
211	16.22	1.23	—	—	—	—	—	—	—	—	—	—	—
212	14.45	0.84	13.34	12.67	12.49	K4	1.52	0.00	3.66	0.01	1.28	6.86	4.35
213	17.18	1.97	14.00	12.37	11.65	—	—	8.92	—	—	—	—	8.84
214	16.21	1.79	14.52	13.87	13.58	—	—	0.00	—	—	—	—	—
215	18.74	2.67	15.20	13.81	—	—	—	—	—	—	—	—	4.95
216	14.41	1.17	13.02	12.34	12.10	M2.5	0.00	0.00	3.54	-0.29	0.36	6.13	7.49
217	17.29	2.37	14.78	14.20	13.70	—	—	0.00	—	—	—	—	1.12
218	17.33	1.81	15.60	14.93	14.55	—	—	0.00	—	—	—	—	1.71
219	16.43	1.72	14.67	13.98	13.84	—	—	0.00	—	—	—	—	—
220	18.77	2.27	16.19	15.02	14.40	M	—	5.30	—	—	—	—	1.66
221	15.87	1.56	14.25	13.60	13.30	M3	0.85	0.00	3.53	-0.65	0.32	6.41	1.30
222	—	—	—	—	—	—	—	—	—	—	—	—	—
223	15.84	1.40	14.41	13.71	13.49	—	—	0.00	—	—	—	—	1.11
224	17.00	0.95	—	—	—	—	—	—	—	—	—	—	—
225	15.58	1.24	13.93	13.11	12.64	—	—	0.00	—	—	—	—	—
226	15.48	1.45	13.97	13.21	13.03	M	—	0.00	—	—	—	—	0.90
227	16.05	1.42	14.62	13.91	13.71	M3	0.22	0.00	3.53	-0.88	0.30	6.65	5.66
228	—	—	—	—	—	—	—	—	—	—	—	—	—
229	10.89	0.09	10.64	10.51	10.44	A0	0.40	0.00	3.98	1.52	2.46	6.75	—
230	—	—	—	—	—	—	—	—	—	—	—	—	—
231	15.60	1.27	14.13	13.37	13.16	M2	0.49	0.72	3.55	-0.66	0.38	6.53	7.49
232	—	—	—	—	—	—	—	—	—	—	—	—	—
233	—	—	—	—	—	—	—	—	—	—	—	—	—
234	13.72	0.88	12.48	11.85	11.64	K5	1.12	0.00	3.64	0.19	1.11	6.31	—
235	—	—	—	—	—	—	—	—	—	—	—	—	—
236	—	—	—	—	—	—	—	—	—	—	—	—	—
237	—	—	—	—	—	—	—	—	—	—	—	—	—
238	15.19	1.53	13.13	12.36	12.07	M3	0.71	1.07	3.53	-0.42	0.32	6.20	1.90
239	—	—	—	—	14.12	—	—	—	—	—	—	—	—
240	13.55	0.96	12.37	11.59	11.30	K5	1.47	1.13	3.64	0.35	1.12	6.11	12.88

Table 4. (Continued)

N	I	R-I	J	H	K	Sp.T.	Av	Av(JHK)	$\log T_{eff}$ [K]	$\log L_{bol}$ [L_{\odot}]	Mass [M_{\odot}]	LogAge [yr.]	P_{rot} [d]
241	16.51	1.58	14.86	14.18	—	—	—	—	—	—	—	—	4.35
242	—	—	16.26	12.73	10.56	—	—	24.90	—	—	—	—	—
243	17.25	2.20	—	—	—	—	—	—	—	—	—	—	1.50
244	—	—	—	—	—	—	—	—	—	—	—	—	—
245	13.85	1.50	12.27	11.54	11.31	M3	0.58	0.56	3.53	0.09	0.32	5.17	—
246	16.22	1.43	—	13.42	13.06	—	—	—	—	—	—	—	11.73
247	13.01	0.44	12.37	11.90	11.79	—	—	0.00	—	—	—	—	—
248	20.41	-1.09	—	—	—	—	—	—	—	—	—	—	—
249	12.52	0.48	11.64	11.02	10.55	G5	0.49	0.00	3.76	0.55	1.40	7.14	3.00
250	16.16	1.86	14.11	13.35	13.05	M5	0.00	1.10	3.49	-0.85	0.19	6.42	2.55
251	18.56	3.06	14.78	13.27	12.43	—	—	8.40	—	—	—	—	—
252	15.10	1.67	12.93	12.09	11.68	M3	1.34	0.00	3.53	-0.23	0.32	6.07	3.16
253	—	—	—	—	14.91	—	—	—	—	—	—	—	—
254	15.15	1.12	13.85	13.12	12.98	M1.5	0.13	0.00	3.56	-0.57	0.42	6.49	—
255	17.73	2.48	14.12	12.36	11.53	—	—	10.15	—	—	—	—	—
256	—	—	—	—	15.04	—	—	—	—	—	—	—	—
257	—	—	—	—	14.33	—	—	—	—	—	—	—	—
258	13.39	0.37	12.81	12.50	12.44	G5	0.00	0.00	3.76	0.09	1.14	7.82	—
259	—	—	—	—	—	—	—	—	—	—	—	—	—
260	13.59	1.22	11.76	10.28	9.23	G6:	—	5.05	—	—	—	—	—
261	11.64	0.72	10.43	9.53	8.86	G	—	0.00	—	—	—	—	—
262	15.33	1.62	13.57	12.84	12.59	—	—	0.65	—	—	—	—	1.07
263	15.47	1.18	13.41	12.55	11.93	M0	1.29	0.00	3.59	-0.43	0.59	6.59	3.14
264	—	—	—	—	—	—	—	—	—	—	—	—	—
265	13.33	0.89	12.20	11.54	11.36	M0	0.00	0.00	3.59	0.11	0.56	5.92	9.48
266	16.93	1.65	15.30	14.65	14.54	—	—	0.00	—	—	—	—	1.73
267	19.57	2.22	—	—	—	—	—	—	—	—	—	—	—
268	15.36	1.32	13.96	13.39	13.13	—	—	0.00	—	—	—	—	—
269	13.71	0.84	12.59	11.95	11.68	K4	1.52	0.00	3.66	0.31	1.50	6.46	0.88
270	—	—	—	14.30	12.10	—	—	—	—	—	—	—	—
271	15.46	1.36	14.03	13.42	13.21	M2.5	0.42	0.00	3.54	-0.61	0.35	6.42	—
272	16.88	1.65	15.15	14.47	—	M4	0.09	—	3.51	-1.19	0.21	6.81	1.81
273	18.08	2.50	14.18	12.39	11.16	—	—	7.83	—	—	—	—	—
274	—	—	—	—	—	—	—	—	—	—	—	—	—
275	14.04	0.94	12.81	12.04	11.85	M0	0.22	0.00	3.59	-0.12	0.57	6.17	1.97
276	14.35	1.12	13.11	12.34	12.18	M1.5	0.13	0.00	3.56	-0.25	0.43	6.14	2.67
277	16.30	1.59	13.98	12.69	12.12	—	—	5.77	—	—	—	—	—
278	14.23	0.70	13.26	12.64	12.48	K4	0.89	0.00	3.66	-0.05	1.20	6.94	3.88
279	—	—	—	—	—	—	—	—	—	—	—	—	—
280	16.91	2.06	13.60	12.09	11.31	—	—	8.33	—	—	—	—	6.01
281	15.16	1.69	12.97	11.90	11.50	—	—	3.64	—	—	—	—	—
282	16.56	1.93	13.63	12.31	11.55	—	—	5.18	—	—	—	—	—
283	—	—	—	—	—	—	—	—	—	—	—	—	—
284	16.10	1.48	14.54	13.86	13.65	—	—	0.00	—	—	—	—	—
285	16.70	2.03	14.62	13.98	13.69	—	—	0.00	—	—	—	—	1.32
286	—	—	—	—	—	—	—	—	—	—	—	—	—
287	—	—	—	—	11.82	—	—	—	—	—	—	—	—
288	17.20	1.97	15.44	14.40	—	M6	0.00	—	3.48	-1.20	0.11	6.61	1.59
289	—	—	—	—	—	—	—	—	—	—	—	—	—
290	13.85	0.63	12.90	12.28	12.17	K5	0.00	0.00	3.64	-0.13	1.11	6.82	3.92
291	14.72	1.57	12.96	12.14	—	M3	0.89	—	3.53	-0.18	0.33	6.04	0.80
292	17.07	2.49	13.72	12.25	11.23	—	—	4.97	—	—	—	—	—
293	14.44	1.05	12.94	11.96	11.54	K7	1.29	3.12	3.61	-0.07	0.77	6.33	5.83
294	13.83	1.11	12.44	11.67	11.52	M2	0.00	0.00	3.55	-0.07	0.39	5.92	0.86
295	—	—	—	—	—	—	—	—	—	—	—	—	—
296	—	—	15.10	—	—	—	—	—	—	—	—	—	—
297	—	—	7.66	7.81	7.87	—	—	0.00	—	—	—	—	—
298	19.66	—	15.62	13.72	12.88	—	—	11.63	—	—	—	—	—
299	—	—	—	—	—	—	—	—	—	—	—	—	—
300	12.78	0.89	11.54	10.88	10.64	K5	1.16	0.00	3.64	0.58	1.15	5.85	2.93

Table 4. (Continued)

N	I	R-I	J	H	K	Sp.T.	Av	Av(JHK)	$\log T_{eff}$ [K]	$\log L_{bol}$ [L_{\odot}]	Mass [M_{\odot}]	LogAge [yr.]	P_{rot} [d]
301	15.36	1.16	13.98	13.30	—	—	—	—	—	—	—	—	—
302	—	—	9.61	9.40	9.32	—	—	0.00	—	—	—	—	—
303	—	—	—	—	—	—	—	—	—	—	—	—	—
304	15.12	1.52	13.48	12.79	12.61	M3.5	0.09	0.00	3.52	-0.51	0.29	6.25	—
305	17.28	0.98	—	7.64	4.92	—	—	—	—	—	—	—	—
306	15.83	1.89	—	—	—	—	—	—	—	—	—	—	5.22
307	15.07	1.38	13.52	12.80	12.56	M3	0.04	0.49	3.53	-0.53	0.32	6.29	0.68
308	—	—	—	—	—	—	—	—	—	—	—	—	—
309	16.45	0.76	—	—	—	K5	0.58	—	3.64	-1.03	—	—	—
310	—	—	—	14.23	—	—	—	—	—	—	—	—	—
311	15.15	1.25	13.36	12.23	11.50	K7	2.19	2.56	3.61	-0.13	0.80	6.44	9.04
312	17.25	1.90	15.34	14.66	14.16	M4	1.20	0.00	3.51	-1.06	0.22	6.70	—
313	—	—	—	—	—	—	—	—	—	—	—	—	—
314	—	—	—	—	—	—	—	—	—	—	—	—	—
315	—	—	—	—	—	—	—	—	—	—	—	—	—
316	18.47	2.55	15.54	14.84	14.54	—	—	0.00	—	—	—	—	3.60
317	—	—	—	15.15	12.22	—	—	—	—	—	—	—	—
318	13.43	0.93	12.21	11.52	11.26	K7	0.76	0.48	3.61	0.20	0.74	6.04	—
319	16.91	1.68	14.66	13.36	12.57	—	—	4.70	—	—	—	—	—
320	15.29	1.55	—	—	—	—	—	—	—	—	—	—	2.25
321	—	—	—	—	—	—	—	—	—	—	—	—	—
322	16.47	1.74	14.74	14.10	13.70	—	—	0.00	—	—	—	—	1.61
323	15.88	1.78	14.11	13.56	13.25	—	—	0.00	—	—	—	—	1.05
324	—	—	—	14.79	—	—	—	—	—	—	—	—	—
325	—	—	9.37	9.40	9.38	—	—	0.00	—	—	—	—	—
326	14.62	1.16	—	12.43	12.28	—	—	—	—	—	—	—	1.43
327	—	—	—	—	—	—	—	—	—	—	—	—	—
328	14.65	1.26	—	—	—	—	—	—	—	—	—	—	2.09
329	10.71	0.34	10.30	9.98	9.90	—	—	0.00	—	—	—	—	—
330	16.21	1.76	14.39	13.67	13.39	M6	0.00	0.72	3.48	-0.80	0.14	5.70	1.09
331	16.57	1.71	—	—	—	M4	0.36	—	3.51	-1.00	0.23	6.65	—
332	12.86	0.81	11.61	10.81	10.34	K5	0.80	0.00	3.64	0.46	1.13	5.98	1.76
333	14.64	1.69	12.74	12.03	11.68	M4	0.27	0.00	3.51	-0.25	0.27	5.67	4.17
334	14.59	0.94	13.42	12.73	12.55	K5	1.38	0.00	3.64	-0.09	1.11	6.74	5.75
335	15.76	1.69	13.48	12.31	11.77	—	—	4.90	—	—	—	—	2.38
336	—	—	—	—	—	—	—	—	—	—	—	—	—
337	—	—	—	—	—	—	—	—	—	—	—	—	—
338	14.50	1.02	13.22	12.52	12.33	M1	0.00	0.00	3.57	-0.35	0.47	6.31	1.44
339	14.58	1.58	13.03	12.33	12.11	M3.5	0.36	0.00	3.52	-0.23	0.29	5.98	3.06
340	13.74	0.82	12.60	11.94	11.72	K5	0.85	0.00	3.64	0.12	1.12	6.42	11.07
341	15.19	1.06	13.88	13.19	12.95	—	—	0.00	—	—	—	—	0.84
342	15.30	1.14	13.87	12.70	11.80	K8.5	1.26	1.92	3.59	-0.38	0.64	6.59	—
343	14.26	1.49	12.52	11.69	11.43	M3	0.54	1.35	3.53	-0.09	0.32	5.79	1.37
344	14.44	1.12	13.00	12.06	11.60	M0.5	0.74	3.08	3.58	-0.15	0.53	6.16	8.28
345	15.02	1.05	13.72	12.99	12.70	M1	0.13	0.81	3.57	-0.53	0.47	6.52	—
346	16.30	1.44	14.96	14.13	13.73	—	—	0.00	—	—	—	—	—
347	—	—	9.39	9.28	9.23	A7	—	0.00	3.89	—	—	—	—
348	14.43	1.24	12.71	11.93	11.61	M3.5	0.00	1.32	3.52	-0.26	0.29	6.03	0.61
349	12.39	0.33	11.88	11.61	11.56	—	—	0.00	—	—	—	—	—
350	12.31	0.79	11.31	10.67	10.44	K5	0.71	0.00	3.64	0.66	1.16	5.77	6.30
351	19.82	—	16.26	14.57	13.79	—	—	9.46	—	—	—	—	—
352	13.34	1.06	11.27	10.50	10.07	K5	1.92	0.00	3.64	0.54	1.14	5.89	—
353	13.64	0.69	12.65	11.88	11.50	K4	0.85	0.00	3.66	0.17	1.40	6.64	5.20
354	15.07	1.45	13.53	12.86	12.62	M3.5	0.00	0.00	3.52	-0.51	0.29	6.26	0.44
355	15.82	1.32	14.27	13.59	13.36	M2.5	0.25	0.00	3.54	-0.79	0.34	6.63	—
356	16.60	1.87	13.74	11.99	11.36	—	—	10.13	—	—	—	—	2.71
357	16.88	1.62	14.36	12.75	11.87	—	—	9.28	—	—	—	—	0.97
358	19.17	2.55	16.08	15.65	15.27	—	—	0.00	—	—	—	—	1.38
359	13.53	1.18	12.12	11.35	11.14	M3	0.00	0.95	3.53	0.07	0.32	5.20	2.43
360	13.77	0.87	12.63	11.97	11.78	M0	0.00	0.00	3.59	-0.07	0.56	6.10	6.51

Table 4. (Continued)

N	I	R-I	J	H	K	Sp.T.	Av	Av(JHK)	$\log T_{eff}$ [K]	$\log L_{bol}$ [L_{\odot}]	Mass [M_{\odot}]	LogAge [yr.]	P_{rot} [d]
361	15.43	1.62	13.33	12.30	11.85	M2.5	1.58	3.58	3.54	-0.31	0.36	6.14	2.91
362	15.65	1.70	13.92	13.31	13.07	M3	1.47	0.00	3.53	-0.41	0.32	6.20	0.96
363	—	—	—	16.31	13.15	—	—	—	—	—	—	—	—
364	13.57	0.68	12.49	11.84	11.61	K4	0.80	0.00	3.66	0.19	1.40	6.61	—
365	15.75	1.35	14.33	13.63	13.38	M0	2.05	0.00	3.59	-0.35	0.58	6.47	1.45
366	—	—	—	—	—	—	—	—	—	—	—	—	—
367	14.69	1.01	13.41	12.65	12.46	M1	0.00	0.00	3.57	-0.43	0.47	6.40	11.32
368	15.79	1.48	14.31	13.74	13.45	—	—	0.00	—	—	—	—	0.71
369	16.65	1.65	15.04	14.41	14.03	—	—	0.00	—	—	—	—	5.15
370	14.75	1.63	13.12	12.47	12.19	M5	0.00	0.00	3.49	-0.28	0.23	5.28	—
371	16.20	1.47	14.54	13.76	13.51	—	—	0.00	—	—	—	—	—
372	16.58	1.87	14.83	14.14	13.84	M5	0.00	0.00	3.49	-1.01	0.17	6.58	0.91
373	17.25	2.32	14.16	12.82	12.08	—	—	6.87	—	—	—	—	2.65
374	12.94	0.45	12.29	11.84	11.79	K5	0.00	0.00	3.64	0.23	1.12	6.27	—
375	13.01	0.76	11.93	11.28	11.11	K5	0.58	0.00	3.64	0.34	1.12	6.12	2.50
376	—	—	—	—	—	—	—	—	—	—	—	—	—
377	15.39	1.48	13.92	13.21	13.01	M5	0.00	0.00	3.49	-0.54	0.22	6.19	1.18
378	—	—	—	—	—	—	—	—	—	—	—	—	—
379	—	—	—	—	—	—	—	—	—	—	—	—	—
380	—	—	—	—	—	—	—	—	—	—	—	—	—
381	14.95	1.17	13.54	12.90	12.64	—	—	0.00	—	—	—	—	8.53
382	17.36	2.14	15.25	14.72	14.43	—	—	0.00	—	—	—	—	—
383	13.56	0.82	12.43	11.63	11.19	K6	0.54	0.00	3.62	0.10	0.91	6.25	—
384	15.48	1.27	14.08	13.40	13.19	M2.5	0.02	0.00	3.54	-0.71	0.34	6.53	8.46
385	—	—	—	—	—	—	—	—	—	—	—	—	—
386	14.53	0.62	13.72	13.12	12.94	K5	0.00	1.93	3.64	-0.41	0.90	7.20	1.07
387	16.47	1.22	15.17	14.57	—	—	—	—	—	—	—	—	5.08
388	11.69	0.46	11.11	10.70	10.64	—	—	0.00	—	—	—	—	—
389	15.48	1.27	13.86	13.04	12.60	M1	1.12	0.00	3.57	-0.47	0.47	6.45	—
390	17.04	1.96	15.03	14.46	14.18	—	—	0.00	—	—	—	—	0.67
391	15.32	1.19	13.92	13.20	13.03	M1	0.76	0.00	3.57	-0.49	0.48	6.50	4.30
392	17.04	1.68	15.35	14.72	14.71	—	—	0.00	—	—	—	—	1.89
393	—	—	—	—	—	—	—	—	—	—	—	—	—
394	10.92	0.21	10.60	10.47	10.47	—	—	0.00	—	—	—	—	—
395	14.01	0.71	13.05	12.40	12.25	—	—	0.00	—	—	—	—	7.95
396	14.43	1.27	—	12.27	—	M5	0.00	—	3.49	-0.15	0.23	5.13	0.78
397	14.95	1.32	13.47	12.72	12.56	M3	0.00	0.00	3.53	-0.49	0.32	6.26	—
398	12.53	0.42	12.04	11.69	11.65	—	—	0.00	—	—	—	—	—
399	15.63	1.59	14.03	13.38	13.08	—	—	0.00	—	—	—	—	—
400	14.33	0.92	13.06	12.39	12.10	M0	0.13	0.49	3.59	-0.26	0.58	6.35	9.48
401	—	—	—	—	—	—	—	—	—	—	—	—	—
402	17.07	1.71	14.83	14.18	13.81	—	—	0.00	—	—	—	—	—
403	15.20	1.23	13.81	13.07	12.88	M1	0.94	0.55	3.57	-0.40	0.48	6.38	5.08
404	21.05	—	—	15.70	15.01	—	—	—	—	—	—	—	—
405	13.15	0.58	12.32	11.73	11.59	K2	0.49	0.00	3.69	0.29	1.54	6.79	1.54
406	15.72	1.72	14.02	13.35	13.15	M3:	—	0.00	—	—	—	—	0.61
407	16.58	1.75	14.32	13.67	13.58	—	—	0.00	—	—	—	—	3.22
408	12.87	0.55	12.10	11.55	11.39	—	—	1.61	—	—	—	—	5.92
409	15.08	1.36	13.63	12.90	12.69	—	—	0.47	—	—	—	—	1.17
410	15.23	1.22	13.92	13.17	12.90	—	—	0.88	—	—	—	—	—
411	—	—	—	—	—	—	—	—	—	—	—	—	—
412	12.19	0.52	11.41	10.98	10.85	G5	0.67	1.24	3.76	0.73	1.60	6.99	—
413	15.06	1.02	13.78	13.09	12.90	M0	0.58	0.00	3.59	-0.44	0.58	6.60	4.13
414	—	—	—	—	—	—	—	—	—	—	—	—	—
415	—	—	—	—	—	—	—	—	—	—	—	—	—
416	15.27	1.14	13.97	13.21	13.00	M2	0.00	0.69	3.55	-0.65	0.38	6.52	2.79
417	13.26	0.74	12.27	11.63	11.47	K6	0.18	0.00	3.62	0.14	0.91	6.21	—
418	15.13	1.05	13.71	13.00	12.81	M1	0.13	0.00	3.57	-0.57	0.47	6.58	15.32
419	14.82	0.82	13.66	12.91	12.82	K7	0.27	0.00	3.61	-0.47	0.79	6.97	6.57
420	12.57	0.66	11.34	10.57	10.07	K4	0.71	0.00	3.66	0.57	1.59	6.12	0.88

Table 6. Spectral properties of ACIS sources with more than 50 counts.

N	Mod	n_H (Ref)	P_{null}	n_H [10^{22}cm^{-2}]	kT_1 [keV]	n_1	kT_2 [keV]	n_2	F_X [a] [ergs/s/cm^2]	F_X [u] [ergs/s/cm^2]
2	1T	Av	0.40	0.00	$0.86^{1.07}_{0.72}$	$-5.23^{5.14}_{3.33}$	--	--	-14.35	-14.35
4	1T	Av	0.62	0.10	$1.29^{1.12}_{0.30}$	$-4.58^{4.65}_{3.51}$	--	--	-13.78	-13.69
5	2T	Av	0.14	0.26	$0.26^{0.22}_{0.22}$	$-3.63^{1.34}_{3.77}$	$1.23^{1.15}_{1.15}$	$-3.88^{3.84}_{3.92}$	-13.07	-12.74
6	1T	Av	0.85	0.00	$1.13^{1.39}_{0.92}$	$-5.00^{5.09}_{4.49}$	--	--	-14.12	-14.12
8	1T	X	0.41	$0.62^{0.99}_{0.36}$	$9.64^{64.00}_{3.36}$	$-4.67^{4.79}_{4.79}$	--	--	-13.62	-13.48
9	2T	Av	0.92	0.09	$0.31^{0.25}_{0.40}$	$-4.32^{4.51}_{4.51}$	$1.26^{1.53}_{1.12}$	$-4.40^{4.34}_{4.48}$	-13.43	-13.31
11	1T	JHK	0.17	0.10	$0.98^{1.13}_{0.86}$	$-4.63^{4.70}_{3.80}$	--	--	-13.86	-13.75
13	1T	X	0.99	$1.66^{2.96}_{0.82}$	$1.63^{5.07}_{0.85}$	$-4.38^{4.38}_{4.38}$	--	--	-13.98	-13.45
14	1T	Av	0.51	0.00	$0.80^{1.07}_{0.63}$	$-5.30^{5.21}_{5.43}$	--	--	-14.43	-14.43
17	2T	Av	0.14	0.07	$0.09^{0.92}_{0.92}$	$-3.48^{1.55}_{4.26}$	$0.95^{1.21}_{0.80}$	$-4.93^{4.86}_{5.08}$	-13.97	-13.82
19	1T	X	0.37	$0.00^{0.25}_{0.00}$	$0.99^{1.20}_{0.74}$	$-5.20^{5.31}_{4.63}$	--	--	-14.31	-14.31
25	1T	Av	0.48	0.14	$1.52^{2.09}_{1.13}$	$-4.69^{4.63}_{4.75}$	--	--	-13.88	-13.77
26	2T	JHK	0.19	0.16	$0.38^{0.61}_{0.24}$	$-4.75^{4.52}_{5.08}$	$1.36^{64.00}_{1.00}$	$-5.02^{4.87}_{5.34}$	-14.01	-13.80
27	1T	Av	0.75	0.07	$1.32^{2.02}_{1.02}$	$-5.08^{5.00}_{5.18}$	--	--	-14.25	-14.18
29	2T	X	0.35	$0.00^{0.08}_{0.00}$	$1.09^{1.41}_{0.89}$	$-4.85^{4.68}_{5.04}$	$64.00^{64.00}_{5.26}$	$-4.80^{4.68}_{5.12}$	-13.51	-13.51
30	1T	Av	0.22	0.00	$1.62^{1.85}_{1.85}$	$-4.26^{4.23}_{4.29}$	--	--	-13.33	-13.33
33	1T	Av	0.77	0.00	$0.84^{1.05}_{0.72}$	$-5.10^{5.02}_{5.19}$	--	--	-14.22	-14.22
36	1T	Av	0.71	0.02	$0.79^{1.01}_{0.69}$	$-4.93^{4.87}_{5.01}$	--	--	-14.09	-14.06
39	1T	X	0.23	$0.00^{0.11}_{0.00}$	$0.95^{1.05}_{0.79}$	$-4.68^{4.62}_{4.73}$	--	--	-13.80	-13.80
45	1T	Av	0.90	0.00	$1.47^{1.19}_{1.19}$	$-4.96^{4.90}_{5.04}$	--	--	-14.05	-14.05
52	1T	Av	0.21	0.00	$0.77^{0.86}_{0.62}$	$-4.86^{4.80}_{4.93}$	--	--	-13.99	-13.99
53	1T	Av	0.34	0.00	$1.33^{1.62}_{1.23}$	$-4.41^{4.37}_{4.45}$	--	--	-13.51	-13.51
54	2T	JHK	0.39	0.00	$0.79^{1.05}_{0.65}$	$-4.73^{4.59}_{4.95}$	$2.88^{3.84}_{1.96}$	$-4.49^{4.37}_{4.62}$	-13.30	-13.30
55	1T	JHK	0.84	0.00	$1.00^{1.65}_{1.65}$	$-5.16^{5.08}_{5.08}$	--	--	-14.28	-14.28
56	2T	Av	0.95	0.09	$0.34^{0.77}_{0.41}$	$-4.52^{4.37}_{4.76}$	$1.29^{2.00}_{1.03}$	$-4.81^{4.70}_{4.91}$	-13.74	-13.61
59	2T	Av	0.88	0.09	$0.32^{0.41}_{0.41}$	$-4.38^{4.27}_{4.27}$	$2.90^{64.00}_{1.55}$	$-4.85^{4.70}_{5.02}$	-13.60	-13.49
61	1T	X	0.24	$0.00^{0.11}_{0.00}$	$1.16^{1.35}_{0.26}$	$-4.92^{4.88}_{4.99}$	--	--	-14.03	-14.03
65	2T	JHK	0.34	0.00	$1.03^{1.33}_{1.33}$	$-4.89^{4.84}_{4.84}$	$4.32^{64.00}_{1.99}$	$-4.91^{4.66}_{5.31}$	-13.58	-13.58
68	1T	Av	0.39	0.04	$1.00^{0.87}_{0.87}$	$-5.31^{5.31}_{5.31}$	--	--	-14.46	-14.42
71	1T	X	1.00	$1.93^{2.57}_{1.43}$	$6.38^{23.58}_{2.24}$	$-4.17^{5.37}_{4.29}$	--	--	-13.28	-13.00
75	1T	Av	0.39	0.00	$0.83^{1.27}_{1.27}$	$-5.17^{5.09}_{5.27}$	--	--	-14.30	-14.30
78	2T	Av	0.27	0.00	$0.30^{0.48}_{0.23}$	$-4.70^{5.33}_{5.00}$	$1.48^{1.69}_{1.26}$	$-4.41^{4.36}_{4.46}$	-13.40	-13.40
83	1T	JHK	0.43	0.00	$2.51^{5.33}_{5.33}$	$-5.18^{5.09}_{5.09}$	--	--	-14.16	-14.16
87	1T	X	0.47	$0.00^{0.03}_{0.00}$	$1.55^{1.38}_{1.38}$	$-4.34^{4.34}_{4.34}$	--	--	-13.42	-13.42
89	1T	JHK	0.29	1.65	$2.22^{3.22}_{3.22}$	$-4.35^{4.48}_{4.48}$	--	--	-13.77	-13.35
90	2T	Av	0.56	0.10	$0.34^{0.85}_{0.23}$	$-4.71^{4.53}_{4.53}$	$1.26^{2.07}_{1.01}$	$-4.77^{4.67}_{5.58}$	-13.80	-13.67
91	1T	Av	0.28	0.27	$0.70^{0.81}_{0.81}$	$-4.60^{4.51}_{4.51}$	--	--	-14.07	-13.74
95	1T	Av	0.25	0.19	$1.04^{1.33}_{0.89}$	$-4.91^{4.88}_{4.99}$	--	--	-14.21	-14.02
97	1T	X	0.97	$0.22^{0.47}_{0.13}$	$4.74^{2.78}_{2.78}$	$-4.94^{4.76}_{4.76}$	--	--	-13.90	-13.81
98	1T	X	0.92	$2.68^{4.51}_{1.71}$	$10.84^{64.00}_{2.78}$	$-4.63^{5.24}_{4.76}$	--	--	-13.72	-13.43
102	1T	Av	0.91	0.09	$1.04^{1.30}_{1.30}$	$-4.90^{4.82}_{4.82}$	--	--	-14.11	-14.01
104	2T	Av	0.32	0.00	$0.46^{0.76}_{0.30}$	$-5.35^{5.13}_{5.89}$	$1.36^{64.00}_{0.91}$	$-5.49^{5.27}_{6.16}$	-14.30	-14.30
105	1T	Av	0.33	0.23	$0.62^{0.71}_{0.56}$	$-4.35^{4.29}_{4.43}$	--	--	-13.82	-13.52
106	2T	Av	0.10	0.00	$0.94^{1.30}_{0.74}$	$-5.52^{5.26}_{5.97}$	$64.00^{64.00}_{4.71}$	$-5.27^{5.09}_{5.73}$	-14.03	-14.03
107	1T	X	0.27	$2.86^{4.54}_{2.18}$	$64.00^{64.00}_{3.93}$	$-4.51^{4.42}_{4.66}$	--	--	-13.64	-13.40
108	1T	X	0.76	$2.80^{4.04}_{1.89}$	$2.56^{6.68}_{6.68}$	$-4.35^{3.92}_{3.92}$	--	--	-13.81	-13.33
111	2T	Av	0.15	0.12	$0.12^{0.20}_{0.01}$	$-3.76^{1.65}_{4.51}$	$0.87^{0.97}_{0.83}$	$-4.48^{4.44}_{4.55}$	-13.62	-13.40
112	2T	Av	0.21	0.03	$0.76^{0.89}_{0.65}$	$-4.92^{4.81}_{5.09}$	$4.96^{64.00}_{1.42}$	$-5.45^{5.03}_{5.84}$	-13.89	-13.86
114	2T	JHK	0.91	0.00	$0.72^{0.83}_{0.59}$	$-4.70^{4.57}_{4.89}$	$2.06^{2.47}_{1.69}$	$-4.40^{4.31}_{4.51}$	-13.28	-13.28
119	1T	Av	0.80	0.20	$1.00^{1.27}_{0.85}$	$-4.86^{4.94}_{4.94}$	--	--	-14.17	-13.97
120	2T	Av	0.23	0.12	$0.28^{0.40}_{0.21}$	$-4.48^{4.30}_{4.72}$	$1.26^{1.87}_{1.09}$	$-4.56^{4.49}_{4.61}$	-13.64	-13.48
124	2T	Av	0.49	0.00	$0.42^{0.66}_{0.26}$	$-5.09^{4.84}_{5.47}$	$32.94^{64.00}_{9.75}$	$-4.53^{4.43}_{4.61}$	-13.33	-13.33
127	1T	X	0.56	$0.90^{1.30}_{0.59}$	$3.46^{10.11}_{2.00}$	$-4.47^{4.26}_{4.66}$	--	--	-13.63	-13.39
133	1T	X	0.23	$0.00^{0.06}_{0.00}$	$1.44^{1.13}_{1.13}$	$-4.82^{4.77}_{4.88}$	--	--	-13.91	-13.91
135	2T	Av	0.12	0.11	$0.81^{0.96}_{0.76}$	$-4.37^{4.29}_{4.49}$	$3.74^{7.28}_{2.58}$	$-4.48^{4.34}_{4.61}$	-13.22	-13.13
136	1T	Av	0.07	0.29	$1.81^{2.54}_{1.53}$	$-4.77^{4.71}_{4.86}$	--	--	-14.01	-13.82
141	1T	X	0.72	$2.62^{4.34}_{1.51}$	$2.04^{6.91}_{1.91}$	$-4.42^{4.32}_{4.82}$	--	--	-13.99	-13.44
142	1T	Av	0.78	0.21	$1.24^{1.09}_{0.99}$	$-4.32^{4.27}_{4.37}$	--	--	-13.60	-13.42
149	2T	JHK	0.38	0.00	$1.90^{1.17}_{1.52}$	$-3.86^{4.37}_{4.45}$	$34.45^{64.00}_{9.12}$	$-3.96^{3.85}_{4.10}$	-12.55	-12.55
151	1T	Av	0.80	0.04	$1.98^{1.72}_{1.72}$	$-4.19^{4.23}_{4.23}$	--	--	-13.25	-13.22

Table 6. (Continued)

N	Mod	n_H (Ref)	P_{null}	n_H [10^{22}cm^{-2}]	kT_1 [keV]	n_1	kT_2 [keV]	n_2	$F_X[\text{a}]$ [ergs/s/cm^2]	$F_X[\text{u}]$ [ergs/s/cm^2]
154	2T	Av	0.20	0.09	$0.75^{0.91}_{0.60}$	$-4.57^{-4.47}_{-4.74}$	$64.00^{64.00}_{1.99}$	$-4.71^{-4.53}_{-5.12}$	-13.41	-13.35
155	1T	X	0.56	$0.00^{0.04}_{0.00}$	$1.48^{1.23}_{0.81}$	$-4.77^{-4.83}_{-4.89}$	--	--	-13.85	-13.85
161	1T	JHK	0.48	2.37	$8.35^{34.16}_{4.54}$	$-4.48^{-4.56}_{-3.56}$	--	--	-13.58	-13.29
162	1T	X	0.58	$2.73^{4.43}_{1.61}$	$1.27^{3.63}_{0.58}$	$-4.29^{-3.31}_{-3.31}$	--	--	-14.19	-13.39
163	1T	JHK	0.48	0.30	$1.80^{2.33}_{0.43}$	$-4.60^{-4.54}_{-4.67}$	--	--	-13.84	-13.65
165	1T	X	0.73	$3.02^{4.30}_{2.09}$	$2.09^{4.66}_{1.11}$	$-4.14^{-3.67}_{-3.67}$	--	--	-13.72	-13.15
167	2T	Av	0.49	0.30	$0.97^{1.23}_{0.77}$	$-4.28^{-4.16}_{-4.53}$	$3.48^{6.19}_{2.48}$	$-4.17^{-4.03}_{-4.39}$	-13.08	-12.91
172	2T	Av	0.45	0.05	$0.95^{1.04}_{0.83}$	$-4.29^{-4.53}_{-4.44}$	$3.57^{6.07}_{2.56}$	$-4.35^{-4.21}_{-4.51}$	-13.06	-13.02
176	1T	X	0.33	$0.23^{0.29}_{0.17}$	$2.54^{3.24}_{2.11}$	$-4.03^{-3.98}_{-3.98}$	--	--	-13.13	-13.00
178	1T	X	0.85	$0.35^{0.74}_{0.12}$	$10.84^{64.00}_{3.01}$	$-4.96^{-4.75}_{-5.07}$	--	--	-13.85	-13.75
179	2T	JHK	0.82	0.13	$0.97^{1.20}_{0.80}$	$-4.50^{-4.36}_{-4.75}$	$4.47^{7.49}_{2.84}$	$-4.39^{-4.25}_{-4.53}$	-13.19	-13.10
181	1T	X	0.64	$0.00^{0.11}_{0.00}$	$1.01^{1.26}_{0.87}$	$-4.68^{-4.75}_{-4.75}$	--	--	-13.80	-13.80
182	1T	X	0.89	$2.97^{6.67}_{1.71}$	$1.11^{2.36}_{0.59}$	$-4.09^{-3.74}_{-3.74}$	--	--	-14.14	-13.20
183	2T	X	0.31	$0.04^{0.68}_{0.00}$	$0.14^{0.24}_{0.02}$	$-4.08^{-2.70}_{-4.84}$	$0.90^{7.42}_{0.20}$	$-4.93^{-3.72}_{-5.13}$	-13.79	-13.70
184	2T	Av	0.32	0.04	$0.74^{0.85}_{0.61}$	$-4.46^{-4.33}_{-4.58}$	$1.85^{6.10}_{1.12}$	$-4.68^{-5.47}_{-5.13}$	-13.40	-13.35
185	2T	Av	0.40	0.08	$0.31^{0.42}_{0.23}$	$-4.68^{-4.59}_{-4.97}$	$1.28^{1.48}_{1.42}$	$-4.81^{-4.71}_{-4.92}$	-13.80	-13.70
187	2Tab ^a	X	0.09	$0.00^{0.12}_{0.00}$	$0.64^{0.78}_{0.51}$	$-5.50^{-5.04}_{-5.04}$	$1.69^{2.78}_{1.31}$	$-4.92^{-4.68}_{-5.33}$	-13.62	-13.62
189	1T	X	0.41	$0.19^{0.33}_{0.06}$	$0.67^{0.79}_{0.57}$	$-4.58^{-4.36}_{-4.82}$	--	--	-13.94	-13.70
190	1T	X	0.35	$0.00^{0.03}_{0.00}$	$1.30^{0.44}_{1.21}$	$-4.27^{-4.23}_{-4.30}$	--	--	-13.37	-13.37
192	1T	X	0.61	$2.17^{3.11}_{1.48}$	$1.51^{2.36}_{0.98}$	$-3.55^{-3.20}_{-3.20}$	--	--	-13.26	-12.63
193	2T	Av	0.85	0.06	$0.76^{0.85}_{0.63}$	$-4.36^{-4.26}_{-4.51}$	$3.34^{5.83}_{2.33}$	$-4.28^{-4.17}_{-4.41}$	-13.07	-13.02
194	1T	X	0.92	$2.57^{3.69}_{1.72}$	$2.39^{4.75}_{1.52}$	$-3.74^{-3.59}_{-3.59}$	--	--	-13.21	-12.72
196	1T	JHK	0.95	0.00	$1.22^{1.86}_{0.90}$	$-5.17^{-5.09}_{-5.27}$	--	--	-14.24	-14.24
197	1T	Av	0.18	0.49	$10.07^{10.05}_{64.00}$	$-5.09^{1.21}_{1.21}$	--	--	-14.02	-13.89
199	1T	JHK	0.59	3.17	$2.04^{2.68}_{1.65}$	$-3.83^{3.23}_{3.23}$	--	--	-13.44	-12.85
200	1T	Av	0.32	0.21	$1.23^{1.00}_{1.00}$	$-4.78^{-4.71}_{-4.86}$	--	--	-14.07	-13.89
202	1T	Av	0.87	0.22	$2.57^{6.15}_{1.68}$	$-4.96^{-4.86}_{-5.08}$	--	--	-14.05	-13.93
203	1T	Av	0.25	0.00	$2.46^{5.07}_{1.32}$	$-5.07^{-5.08}_{-5.17}$	--	--	-14.05	-14.05
204	1T	JHK	0.74	0.00	$1.46^{1.30}_{1.30}$	$-4.70^{-4.66}_{-4.76}$	--	--	-13.79	-13.79
205	1T	JHK	0.71	0.00	$5.43^{64.00}_{2.09}$	$-5.40^{-5.30}_{-5.51}$	--	--	-14.24	-14.24
206	2T	Av	0.41	0.04	$0.64^{0.76}_{0.55}$	$-4.31^{-4.31}_{-4.52}$	$1.44^{1.58}_{1.32}$	$-3.87^{-3.82}_{-3.93}$	-12.89	-12.84
207	1T	JHK	0.75	0.23	$0.68^{0.84}_{0.58}$	$-4.67^{-4.78}_{-4.59}$	--	--	-14.11	-13.82
208	1T	X	0.85	$1.18^{1.75}_{0.66}$	$0.68^{1.21}_{0.41}$	$-4.42^{-4.78}_{-4.76}$	--	--	-14.49	-13.56
212	2T	Av	0.28	0.24	$0.19^{0.26}_{0.02}$	$-4.12^{-3.90}_{-4.55}$	$0.95^{1.36}_{0.77}$	$-4.65^{-4.48}_{-4.82}$	-13.85	-13.45
216	2T	Av	0.98	0.00	$0.64^{0.78}_{0.26}$	$-4.87^{-4.75}_{-4.97}$	$1.70^{2.60}_{1.22}$	$-4.97^{-4.80}_{-5.29}$	-13.73	-13.73
226	1T	JHK	0.81	0.00	$0.98^{1.50}_{0.79}$	$-5.13^{-5.05}_{-5.05}$	--	--	-14.24	-14.24
227	1T	Av	0.95	0.04	$1.65^{2.41}_{1.31}$	$-4.99^{-4.92}_{-5.07}$	--	--	-14.08	-14.05
228	1T	X	0.42	$6.18^{8.14}_{4.48}$	$4.64^{27.03}_{2.63}$	$-3.86^{-3.56}_{-4.10}$	--	--	-13.24	-12.72
229	2T	Av	0.13	0.06	$0.43^{0.58}_{0.31}$	$-4.61^{-4.44}_{-4.82}$	$1.13^{1.28}_{1.01}$	$-4.51^{-4.44}_{-4.61}$	-13.52	-13.44
231	1T	Av	0.35	0.08	$1.25^{1.46}_{1.11}$	$-4.75^{-4.69}_{-4.81}$	--	--	-13.93	-13.85
234	2Tab ^b	X	0.02	$0.06^{0.08}_{0.02}$	$0.80^{1.60}_{0.66}$	$-4.86^{-4.59}_{-5.14}$	$2.98^{3.34}_{2.64}$	$-3.76^{-3.70}_{-3.82}$	-12.64	-12.60
235	1T	X	0.45	$4.79^{4.42}_{2.96}$	$1.99^{6.68}_{1.10}$	$-3.98^{-3.35}_{-3.35}$	--	--	-13.71	-13.00
238	1T	Av	0.35	0.11	$1.53^{1.97}_{1.28}$	$-4.66^{-4.61}_{-4.71}$	--	--	-13.83	-13.74
240	2T	Av	0.23	0.24	$0.24^{0.30}_{0.21}$	$-3.69^{-3.57}_{-3.87}$	$1.64^{2.40}_{1.37}$	$-4.43^{-4.35}_{-4.54}$	-13.39	-13.01
241	1T	X	0.17	$0.33^{0.65}_{0.00}$	$0.60^{0.84}_{0.38}$	$-4.95^{-4.34}_{-4.34}$	--	--	-14.54	-14.12
242	1T	JHK	0.48	3.98	$1.33^{1.63}_{1.11}$	$-3.61^{-3.48}_{-3.75}$	--	--	-13.60	-12.71
244	1T	X	0.76	$2.22^{2.59}_{1.89}$	$4.61^{7.17}_{3.39}$	$-3.71^{-3.60}_{-3.81}$	--	--	-12.90	-12.57
245	1T	Av	0.87	0.09	$0.73^{0.85}_{0.60}$	$-4.89^{-4.82}_{-4.98}$	--	--	-14.15	-14.03
246	1T	X	0.86	$0.17^{0.45}_{0.05}$	$1.56^{2.13}_{1.13}$	$-4.70^{-4.52}_{-4.82}$	--	--	-13.91	-13.78
248	1T	X	0.94	$2.30^{3.36}_{1.59}$	$1.82^{2.70}_{1.40}$	$-4.20^{-3.77}_{-3.77}$	--	--	-13.80	-13.24
249	2T	Av	0.75	0.08	$1.03^{0.91}_{0.91}$	$-4.10^{-3.86}_{-4.09}$	$3.80^{13.95}_{2.86}$	$-3.99^{-3.89}_{-4.29}$	-12.77	-12.72
250	1T	Av	0.44	0.00	$1.26^{2.00}_{0.92}$	$-5.15^{-5.25}_{-5.25}$	--	--	-14.26	-14.26
252	1T	Av	0.49	0.21	$1.01^{1.25}_{0.83}$	$-4.88^{-4.98}_{-4.98}$	--	--	-14.20	-13.99
254	1T	Av	0.65	0.02	$1.12^{1.40}_{0.89}$	$-5.21^{-5.32}_{-5.32}$	--	--	-14.35	-14.32
255	1T	X	0.89	$0.95^{1.11}_{0.81}$	$5.57^{7.89}_{7.89}$	$-3.67^{-3.72}_{-3.72}$	--	--	-12.71	-12.51
257	1T	X	0.02	$3.82^{7.9}_{3.15}$	$4.82^{10.94}_{2.74}$	$-3.89^{-3.65}_{-4.05}$	--	--	-13.16	-12.75
260	1T	JHK	0.35	0.81	$4.21^{16.23}_{2.28}$	$-5.01^{-4.88}_{-4.88}$	--	--	-14.10	-13.89
261	2T	JHK	0.67	0.00	$0.94^{1.03}_{0.83}$	$-4.23^{-4.38}_{-4.38}$	$2.75^{4.18}_{2.12}$	$-4.21^{-4.09}_{-4.36}$	-12.94	-12.94
263	1T	Av	0.25	0.21	$1.30^{3.28}_{1.04}$	$-5.13^{-5.25}_{-5.04}$	--	--	-14.41	-14.24
265	1T	Av	0.44	0.00	$1.24^{1.32}_{1.15}$	$-4.35^{-4.39}_{-4.39}$	--	--	-13.46	-13.46

Table 6. (Continued)

N	Mod	n_H (Ref)	P_{null}	n_H [10^{22}cm^{-2}]	kT_1 [keV]	n_1	kT_2 [keV]	n_2	$F_X[\text{a}]$ [ergs/s/cm^2]	$F_X[\text{u}]$ [ergs/s/cm^2]
268	1T	JHK	0.38	0.00	$0.79^{+0.07}_{-0.04}$	$-5.15^{+5.07}_{-4.18}$	--	--	-14.28	-14.28
269	1T	Av	0.60	0.24	$0.97^{+0.04}_{-0.04}$	$-4.22^{+4.22}_{-4.20}$	--	--	-13.58	-13.34
273	1T	JHK	0.87	1.25	$1.32^{+0.04}_{-0.04}$	$-4.50^{+4.63}_{-4.63}$	--	--	-14.15	-13.60
274	1T	X	0.94	$8.92^{+11.55}_{-7.33}$	$63.98^{+64.00}_{-63.96}$	$-3.79^{+3.71}_{-3.89}$	--	--	-13.10	-12.68
275	1T	Av	0.12	0.04	$1.62^{+2.29}_{-1.26}$	$-5.26^{+5.16}_{-5.39}$	--	--	-14.36	-14.33
276	1T	Av	0.91	0.02	$1.23^{+1.35}_{-1.12}$	$-4.50^{+4.46}_{-4.55}$	--	--	-13.63	-13.61
278	2T	Av	0.78	0.14	$0.24^{+0.34}_{-0.18}$	$-4.35^{+4.14}_{-4.05}$	$1.29^{+1.68}_{-1.07}$	$-4.78^{+4.69}_{-4.90}$	-13.79	-13.56
279	1T	X	0.63	$2.66^{+4.36}_{-1.62}$	$2.02^{+5.57}_{-0.98}$	$-4.41^{+3.75}_{-3.75}$	--	--	-13.99	-13.43
280	1T	JHK	0.15	1.33	$2.24^{+2.87}_{-1.78}$	$-4.10^{+4.02}_{-4.19}$	--	--	-13.49	-13.11
282	1T	JHK	0.66	0.83	$3.63^{+4.70}_{-2.84}$	$-4.17^{+4.11}_{-4.23}$	--	--	-13.31	-13.07
285	1T	JHK	0.68	0.00	$1.45^{+2.45}_{-0.97}$	$-5.32^{+5.23}_{-5.44}$	--	--	-14.41	-14.41
287	1T	X	0.71	$2.79^{+4.55}_{-1.52}$	$1.13^{+2.76}_{-0.97}$	$-3.99^{+3.08}_{-3.08}$	--	--	-14.00	-13.10
290	1T	Av	0.40	0.00	$1.87^{+1.54}_{-1.54}$	$-4.44^{+4.40}_{-4.49}$	--	--	-13.49	-13.49
292	1T	JHK	0.74	0.80	$2.13^{+3.31}_{-1.57}$	$-4.63^{+4.54}_{-4.76}$	--	--	-13.95	-13.64
293	1T	Av	0.90	0.21	$2.13^{+3.18}_{-1.18}$	$-5.14^{+5.04}_{-5.28}$	--	--	-14.28	-14.15
294	1T	Av	0.62	0.00	$0.96^{+1.44}_{-0.74}$	$-5.40^{+5.30}_{-5.52}$	--	--	-14.52	-14.52
296	1T	X	0.87	$1.92^{+2.36}_{-1.55}$	$4.80^{+6.63}_{-3.02}$	$-3.94^{+3.78}_{-4.07}$	--	--	-13.11	-12.80
297	1T	JHK	0.95	0.00	$0.39^{+3.56}_{-0.32}$	$-4.89^{+4.76}_{-5.12}$	--	--	-14.22	-14.22
300	2Tab ^c	Av	0.10	0.19	$0.32^{+0.40}_{-0.26}$	$-4.67^{+4.52}_{-5.05}$	$1.46^{+1.68}_{-1.27}$	$-4.47^{+4.28}_{-4.58}$	-13.40	-13.20
301	1T	X	0.74	$0.00^{+0.13}_{-0.00}$	$0.74^{+0.83}_{-0.62}$	$-4.82^{+4.63}_{-4.88}$	--	--	-13.95	-13.95
302	2T	JHK	0.80	0.00	$0.81^{+0.97}_{-0.72}$	$-4.16^{+3.98}_{-4.30}$	$1.61^{+1.73}_{-1.46}$	$-3.82^{+3.76}_{-3.98}$	-12.75	-12.75
305	1T	X	0.65	$4.84^{+8.95}_{-3.26}$	$64.00^{+64.00}_{-54.00}$	$-4.64^{+4.39}_{-4.39}$	--	--	-13.82	-13.51
307	1T	Av	0.87	0.01	$0.95^{+1.24}_{-0.74}$	$-5.36^{+5.26}_{-5.26}$	--	--	-14.48	-14.47
311	1T	Av	0.33	0.35	$3.03^{+3.14}_{-2.14}$	$-4.67^{+4.58}_{-4.77}$	--	--	-13.77	-13.61
318	1T	X	0.57	$0.00^{+0.04}_{-0.04}$	$2.35^{+3.31}_{-2.31}$	$-4.60^{+4.55}_{-4.60}$	--	--	-13.59	-13.59
324	1T	X	0.44	$3.49^{+5.34}_{-2.97}$	$21.64^{+34.00}_{-24.00}$	$-4.53^{+4.48}_{-4.48}$	--	--	-13.59	-13.30
326	1T	X	0.78	$0.00^{+0.77}_{-0.00}$	$0.94^{+1.15}_{-0.23}$	$-5.21^{+5.03}_{-5.31}$	--	--	-14.33	-14.33
327	1T	X	0.38	$5.78^{+7.06}_{-4.63}$	$3.22^{+6.16}_{-2.20}$	$-3.53^{+3.29}_{-3.78}$	--	--	-13.00	-12.42
328	2T	X	0.41	$0.00^{+0.10}_{-0.00}$	$0.95^{+1.18}_{-0.57}$	$-4.81^{+4.61}_{-5.17}$	$10.85^{+64.00}_{-2.12}$	$-4.94^{+4.63}_{-5.23}$	-13.44	-13.44
329	1T	X	0.32	$0.15^{+0.21}_{-0.08}$	$0.74^{+0.79}_{-0.64}$	$-4.03^{+3.88}_{-4.12}$	--	--	-13.27	-13.08
332	1T	X	0.28	$0.05^{+0.08}_{-0.02}$	$1.87^{+1.55}_{-1.07}$	$-3.86^{+3.80}_{-3.80}$	--	--	-12.94	-12.90
333	1T	Av	0.37	0.04	$1.30^{+1.78}_{-1.11}$	$-4.84^{+4.78}_{-4.91}$	--	--	-13.98	-13.94
334	1T	X	0.40	$0.00^{+0.09}_{-0.00}$	$1.15^{+1.32}_{-0.97}$	$-4.87^{+4.80}_{-4.94}$	--	--	-13.98	-13.98
338	2T	Av	0.63	0.00	$0.99^{+1.17}_{-0.84}$	$-4.78^{+4.64}_{-5.06}$	$5.12^{+31.58}_{-2.34}$	$-4.97^{+4.72}_{-5.22}$	-13.56	-13.56
340	1T	X	0.21	$0.00^{+0.03}_{-0.00}$	$1.47^{+1.83}_{-1.29}$	$-4.30^{+4.26}_{-4.33}$	--	--	-13.38	-13.38
341	2T	JHK	0.44	0.00	$0.89^{+1.07}_{-0.78}$	$-4.70^{+4.48}_{-4.98}$	$2.19^{+3.84}_{-1.67}$	$-4.47^{+4.35}_{-4.72}$	-13.31	-13.31
343	1T	Av	0.87	0.09	$1.74^{+2.13}_{-1.54}$	$-4.48^{+4.44}_{-4.53}$	--	--	-13.61	-13.54
344	1T	Av	0.25	0.12	$6.21^{+26.92}_{-2.99}$	$-4.99^{+4.91}_{-5.07}$	--	--	-13.85	-13.80
345	1T	Av	0.89	0.02	$0.93^{+1.12}_{-0.70}$	$-5.16^{+5.08}_{-5.26}$	--	--	-14.30	-14.28
348	1T	X	0.31	$0.11^{+0.22}_{-0.04}$	$1.47^{+1.71}_{-1.27}$	$-4.43^{+4.35}_{-4.51}$	--	--	-13.60	-13.50
350	2T	Av	0.48	0.11	$0.80^{+0.98}_{-0.70}$	$-4.10^{+3.98}_{-4.25}$	$1.64^{+1.90}_{-1.49}$	$-3.75^{+3.68}_{-3.90}$	-12.78	-12.67
352	1T	X	0.46	$0.02^{+0.10}_{-0.00}$	$1.91^{+1.53}_{-1.53}$	$-4.51^{+4.43}_{-4.57}$	--	--	-13.56	-13.55
353	2T	Av	0.10	0.14	$0.27^{+0.39}_{-0.19}$	$-4.66^{+4.39}_{-5.00}$	$3.00^{+4.76}_{-2.09}$	$-4.79^{+4.69}_{-4.90}$	-13.71	-13.58
354	1T	Av	0.41	0.00	$1.66^{+1.04}_{-1.04}$	$-4.68^{+4.63}_{-4.73}$	--	--	-13.75	-13.75
359	2T	Av	0.24	0.00	$0.40^{+0.61}_{-0.05}$	$-5.24^{+4.85}_{-6.08}$	$1.50^{+1.84}_{-1.33}$	$-4.61^{+4.54}_{-4.69}$	-13.64	-13.64
360	1T	Av	0.37	0.00	$1.32^{+1.68}_{-1.18}$	$-4.05^{+4.01}_{-4.10}$	--	--	-13.16	-13.16
361	1T	Av	0.32	0.25	$1.97^{+2.51}_{-0.91}$	$-5.15^{+5.02}_{-5.35}$	--	--	-14.34	-14.18
362	1T	X	0.25	$0.00^{+0.09}_{-0.00}$	$1.24^{+1.58}_{-0.92}$	$-5.02^{+5.10}_{-5.10}$	--	--	-14.12	-14.12
364	1T	Av	0.60	0.13	$0.81^{+0.91}_{-0.74}$	$-4.49^{+4.49}_{-4.55}$	--	--	-13.78	-13.62
365	2T	Av	0.25	0.33	$0.80^{+0.99}_{-0.26}$	$-4.89^{+4.77}_{-5.07}$	$64.00^{+64.00}_{-2.54}$	$-5.35^{+5.06}_{-5.92}$	-14.04	-13.81
366	1T	X	0.74	$4.15^{+6.44}_{-2.71}$	$2.00^{+1.93}_{-0.70}$	$-4.16^{+3.36}_{-4.05}$	--	--	-13.85	-13.19
367	2T	Av	0.18	0.00	$0.29^{+0.19}_{-0.18}$	$-5.05^{+4.85}_{-5.53}$	$1.54^{+12.24}_{-1.05}$	$-5.23^{+5.10}_{-5.53}$	-14.09	-14.09
368	1T	JHK	0.37	0.00	$0.97^{+1.27}_{-0.78}$	$-4.93^{+3.87}_{-5.00}$	--	--	-14.05	-14.05
370	2T	Av	0.17	0.00	$0.65^{+1.38}_{-0.25}$	$-5.41^{+5.09}_{-5.99}$	$8.38^{+64.00}_{-1.10}$	$-5.24^{+5.04}_{-5.47}$	-13.94	-13.94
375	1T	X	0.24	$0.00^{+0.02}_{-0.00}$	$1.30^{+1.24}_{-1.24}$	$-4.03^{+4.05}_{-4.05}$	--	--	-13.10	-13.10
381	1T	JHK	0.77	0.00	$1.17^{+1.31}_{-1.03}$	$-4.75^{+4.69}_{-4.80}$	--	--	-13.85	-13.85
383	2T	Av	0.34	0.09	$0.40^{+0.78}_{-0.28}$	$-4.44^{+4.25}_{-4.68}$	$1.55^{+5.22}_{-1.18}$	$-4.48^{+4.37}_{-4.94}$	-13.44	-13.34
384	1T	Av	0.27	0.00	$0.99^{+0.36}_{-0.89}$	$-4.96^{+4.88}_{-5.03}$	--	--	-14.08	-14.07
386	1T	Av	0.22	0.00	$1.52^{+1.11}_{-1.06}$	$-4.94^{+4.87}_{-5.01}$	--	--	-13.97	-13.97
388	2T	JHK	0.10	0.00	$0.99^{+0.85}_{-0.85}$	$-4.14^{+4.06}_{-4.32}$	$2.72^{+3.81}_{-1.77}$	$-4.44^{+4.19}_{-4.69}$	-13.02	-13.02

Table 6. (Continued)

N	Mod	n_H (Ref)	P_{null}	n_H [10^{22}cm^{-2}]	kT_1 [keV]	n_1	kT_2 [keV]	n_2	F_X [a] [ergs/s/cm^2]	F_X [u] [ergs/s/cm^2]
389	1T	Av	0.95	0.18	$6.84^{+25.05}_{-3.62}$	$-5.02^{+4.95}_{-3.10}$	--	--	-13.91	-13.84
391	1T	X	0.26	$0.00^{+0.03}_{-0.00}$	$1.92^{+2.50}_{-1.38}$	$-4.57^{+4.52}_{-4.47}$	--	--	-13.60	-13.60
395	1T	JHK	0.79	0.00	$1.25^{+1.13}_{-1.13}$	$-4.51^{+4.56}_{-4.64}$	--	--	-13.62	-13.62
396	1T	Av	0.50	0.00	$1.29^{+1.15}_{-1.29}$	$-4.69^{+4.75}_{-4.75}$	--	--	-13.79	-13.79
397	1T	Av	0.52	0.00	$1.03^{+0.88}_{-0.88}$	$-5.01^{+4.95}_{-5.11}$	--	--	-14.13	-14.13
400	1T	Av	0.27	0.02	$1.09^{+0.90}_{-0.64}$	$-5.20^{+5.30}_{-4.75}$	--	--	-14.34	-14.31
403	1T	Av	0.90	0.15	$0.46^{+0.32}_{-0.32}$	$-4.99^{+4.75}_{-5.21}$	--	--	-14.49	-14.25
405	1T	Av	0.41	0.08	$1.33^{+1.31}_{-1.26}$	$-4.10^{+4.07}_{-4.13}$	--	--	-13.28	-13.20
407	1T	JHK	0.64	0.00	$1.27^{+1.03}_{-0.97}$	$-5.15^{+5.07}_{-5.26}$	--	--	-14.26	-14.26
408	2T	JHK	0.09	0.26	$0.91^{+1.01}_{-0.78}$	$-4.31^{+4.25}_{-4.38}$	$64.00^{+64.00}_{-3.22}$	$-4.97^{+4.75}_{-5.46}$	-13.49	-13.29
409	1T	JHK	0.28	0.08	$1.00^{+0.76}_{-0.76}$	$-4.84^{+4.78}_{-4.92}$	--	--	-14.04	-13.96
411	1T	X	0.52	$0.73^{+1.86}_{-0.34}$	$34.26^{+64.00}_{-2.50}$	$-4.80^{+4.65}_{-4.97}$	--	--	-13.75	-13.62
412	1T	Av	0.71	0.11	$0.96^{+1.01}_{-0.91}$	$-4.05^{+4.03}_{-4.03}$	--	--	-13.27	-13.15
413	1T	Av	0.82	0.09	$0.98^{+0.91}_{-0.81}$	$-4.91^{+4.84}_{-5.00}$	--	--	-14.13	-14.03
414	1T	X	0.77	$1.49^{+2.33}_{-0.97}$	$13.66^{+64.00}_{-3.63}$	$-4.59^{+4.37}_{-4.70}$	--	--	-13.61	-13.40
417	1T	Av	0.53	0.03	$1.14^{+1.23}_{-1.02}$	$-4.28^{+4.25}_{-4.31}$	--	--	-13.42	-13.39
418	1T	Av	0.38	0.02	$1.18^{+1.09}_{-0.99}$	$-5.19^{+5.09}_{-5.31}$	--	--	-14.32	-14.30
419	1T	Av	0.68	0.04	$1.00^{+1.20}_{-0.84}$	$-5.03^{+4.95}_{-5.13}$	--	--	-14.20	-14.15
420	1T	Av	0.22	0.11	$1.97^{+3.14}_{-1.42}$	$-4.48^{+4.42}_{-4.55}$	--	--	-13.59	-13.51

a) Abund.= $1.43^{5.00}_{-0.42}$; b) Abund.= $0.84^{1.26}_{-0.50}$; c) Abund.= $0.94^{2.69}_{-0.38}$;